A role of SUMOylation in proteostasis, centromere integrity and the DNA damage response

Liebelt, F.

A Role for SUMOylation in Proteostasis, Centromere Integrity and the DNA Damage Response

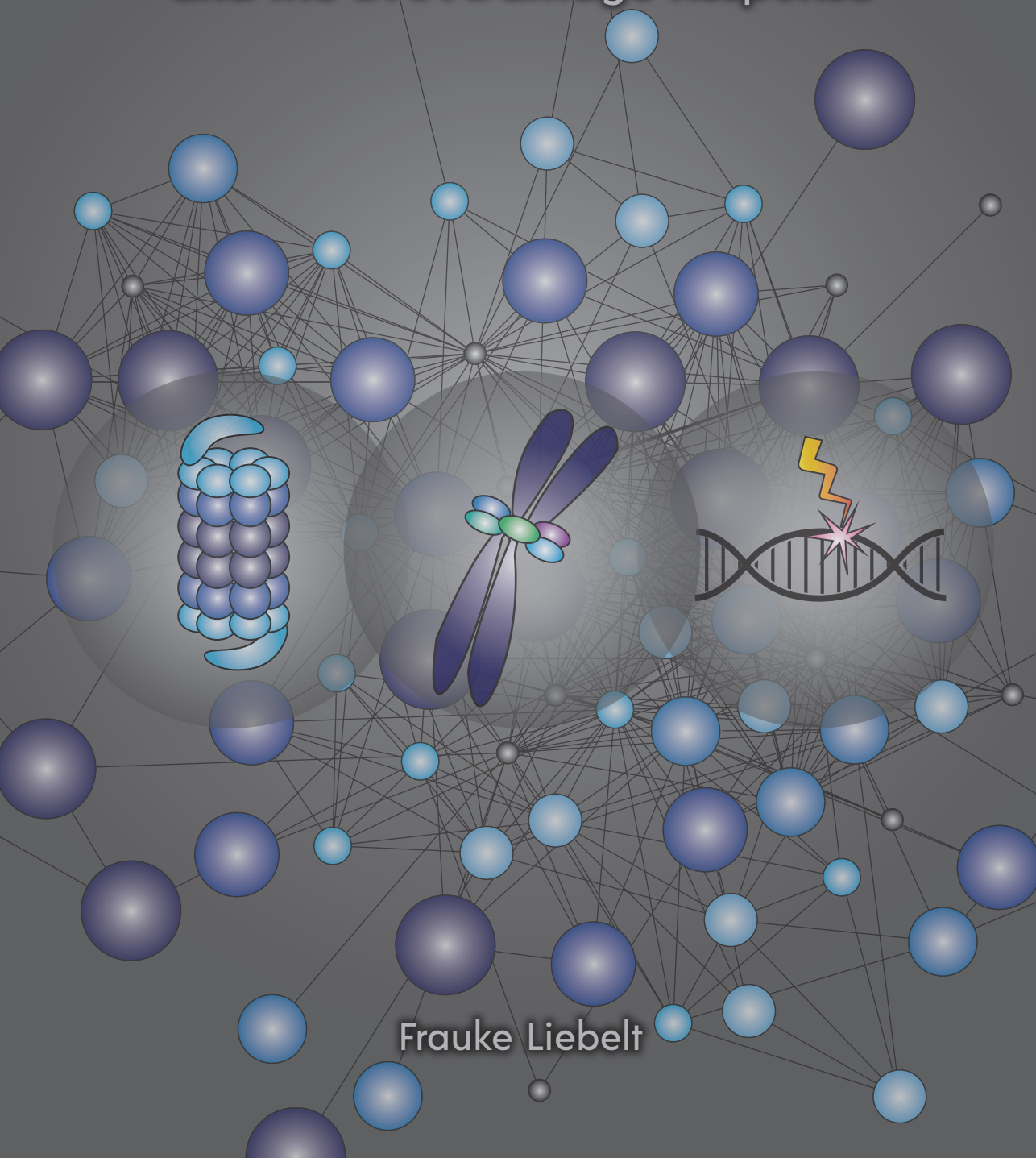

Frauke Liebelt

A Role for SUMOylation in Proteostasis, Centromere Integrity and the DNA Damage Response

Frauke Liebelt

PhD Thesis, Leiden University, 2019.

The research described in this thesis was performed at Leiden University Medical Center, Department of Cell and Chemical Biology, The Netherlands

Cover design & layout by Frauke Liebelt

Printed by: ProefschriftMaken// www.Proefschriftmaken.nl

ISBN: 978-94-6380-633-6

A Role for SUMOylation in Proteostasis, Centromere Integrity and the DNA Damage Response

Proefschrift

ter verkrijging van

de graad van Doctor aan de Universiteit Leiden,

op gezag van Rector Magnificus prof.mr. C.J.J.M. Stolker,

volgens besluit van het College voor Promoties

te verdedigen op donderdag 9 januari 2020

klokke 13.45 uur

door

Frauke Liebelt

geboren te Bad Kreuznach, Duitsland

in 1987

Promotores:	Prof. dr. A.C.O. Vertegaal Prof. dr. P. ten Dijke
Leden Promotiecommissie:	Prof. dr. J.J.C. Neefjes Prof. dr. G.J.P.L. Kops, Hubrecht institute, Utrecht Prof. dr. W. Vermeulen, Erasmus MC, Rotterdam Dr. A.M. Cleton-Jansen

Da steh ich nun, ich armer Tor,
Und bin so klug als wie zuvor!

Johann Wolfgang von Goethe (1808)

TABLE OF CONTENTS

OUTLINE OF THIS THESIS

Chapter 1 contains a general overview of the post-translation modification SUMOylation. The enzymes and proteins involved in SUMOylation and biological processes regulated by SUMO are introduced with a focus on SUMO chain formation, SUMO specific proteases and the role of SUMOylation during nucleotide excision repair.

In **Chapter 2** we review literature about how SUMOylation is involved in and regulates proteostasis with or without cross-talk with ubiquitin. Neurodegenerative diseases are often characterized by an unbalanced proteostasis and accumulation of disease associated proteins. Here we discuss how SUMOylation can influence aggregation or solubility of these disease-associated proteins. Also, we review studies that highlight the neuroprotective role of SUMOylation during oxygen and nutrient deprivation as consequence of ischemia.

In **Chapter 3** we aim to identify how SUMOylation is linked to proteostasis. We observe that SUMOylation dynamics upon heat-shock are altered when the proteostatic transcriptional regulator HSF1 is inhibited. We identify that most SUMOylated proteins are targeted for ubiquitin-mediated degradation upon heat shock and that molecular chaperones, transcribed by HSF1, specifically facilitate the degradation of co-modified proteins. We propose that SUMO quickly solubilizes denatured proteins to prevent formation of toxic aggregates and enables chaperone-facilitated degradation.

In **Chapter 4** we use mass spectrometry to identify SUMOylated proteins that are regulated by the SUMO chain editing protease SENP6. We show that multiple groups or proteins are simultaneously regulated including the majority of members of the constitutive centromere-associated network (CCAN). We show that multiple CCAN proteins fail to localize to the centromere upon SENP6 knockdown. We exclude the possibility of SUMO chain-induced RNF4-dependent ubiquitination and degradation and suggest a model in which SUMO chains could interfere with the assembly of the complex at the centromere.

In **Chapter 5** we identify proteins that are regulated by SUMOylation upon ionizing radiation (IR) and ultraviolet (UV) irradiation. The most dynamically SUMOylated protein upon UV irradiation is Cockayne syndrome B (CSB), a protein highly important for the repair of UV induced DNA damage within actively transcribed genomic regions. Those lesions are repaired by transcription coupled nucleotide excision repair (TC-NER) and CSB is one of the first proteins that is recruited to the site of the damage. We identify that the SUMOylation of CSB enhances the recruitment and stabilization of CSB at the damage site as well as the overall efficiency of TC-NER. Furthermore, we show that Cockayne Syndrome A (CSA) regulates the stability of SUMOylated CSB and the ubiquitination of RNA polymerase II (RNApolII).

In **Chapter 6**, I discuss the scientific findings described in this thesis in light of the published literature. Furthermore, this chapter deliberates on new concepts and future perspectives in the field of SUMOylation.

CHAPTER 1

General Introduction

Frauke Liebelt[1]

[1]Department of Cell and Chemical biology, Leiden University Medical Center, 2300 RC Leiden, The Netherlands.

POST-TRANSLATIONAL MODIFICATIONS

The average adult human body consists of approximately 37.2 trillion cells[1]. All that we are and everything that we do is orchestrated within and between them. Each cell carries an elaborate manual that is essential for everything. The manual, our genetic material or deoxyribonucleic acid (DNA), describes how to build other macromolecules that form the actual workforce of the cell. An important group of macromolecules, which are encoded by our DNA are polypeptides, also called proteins. To build a protein, the DNA of a particular gene, which is the entity of the DNA that carries the instructions for the synthesis of one particular protein, must first be transcribed into messenger ribonucleic acid (mRNA), which is subsequently translated into a protein[2-4]. Due to processes like alternative promotors, alternative splicing or RNA editing, the transcription of around 20,000 genes of the human genome result in about 100,000 different mRNAs[5-10]. After or during the time when a protein is translated it can be altered by the covalent attachment of small chemical entities or other proteins. These processes are called co-translational and post-translational protein modification (PTM), respectively, but are often collectively referred to as PTMs[11,12]. PTMs further increase the complexity and functionality of the proteome[13,14]. As PTMs are reversible they are ideal for fast and transient signal transductions for example when the cell has to rapidly adapt to changing environments. PTMs can be divided into two major classes. The first class of PTMs comprises the covalent attachment of small chemical groups to a substrate protein. The best studied and most abundant chemical PTM is phosphorylation, by which a small phosphoryl group is added to a serine, threonine or tyrosine residue within the substrate by enzymes called kinases[15,16]. Protein phosphatases are responsible for the reversibility of this PTM as they can remove the phosphoryl group from their substrates[17]. Thus far it is estimated that 230,000 phosphorylation sites exist on around 8-10,000 substrate proteins within the human proteome, including substrate proteins involved in most of the cellular signalling pathways[18]. Other abundant chemical modifications include acetylation, methylation and glycosylation, which are all conjugated and deconjugated via specific sets of enzymes[19-21].

The second class of PTMs consist of the covalent attachment of small proteins to a substrate protein[22]. Here, the best studied and most abundant modification is the attachment of ubiquitin to lysine residues, a process referred to as ubiquitination[23,24]. After the discovery of ubiquitin, a whole class of structurally related small proteins were identified, which share not only the structural component of a globular β- grasp fold, called the ubiquitin fold, but are also used for covalent attachment to lysine residues in substrate proteins utilizing their C-terminal Glycine-Glycine motif (di-Gly). This class of ubiquitin-like proteins (UbLs) include the Small Ubiquitin-like Modifiers (SUMOs), Nedd8, Isg15, Fat10, Fub1, Ufm1, Urm1, Atg12 and Atg8[25-35]. Like other PTMs the addition of ubiquitin and UbLs to target proteins is mediated by specialized enzymes. Three distinct groups of enzymes act sequentially to form the enzymatic cascade resulting in the conjugation of ubiquitin and UbLs to a substrate protein. The E1 activating enzymes, the E2 conjugating enzymes and the E3 ligases[36-39]. Modification specific proteases are used to remove the small protein entities from the substrate once the aim of the modification is fulfilled. Despite the structural similarity to each other and the resemblance of the mechanisms used to attach and remove them from substrates, ubiquitin and UbLs all have different primary sequences, different surface charge distributions, different sets of E1, E2 and E3 enzymes and diverse biological significances and consequences[40].

SUMOYLATION

SUMO paralogues

The small ubiquitin-like modifiers, SUMOs, structurally differ from other Ubls due to their flexible N-terminus, which also contains the major site for SUMO chain formation. All eukaryotes express at least one SUMO paralogue, like yeast, C. elegans and Drosophila. Mammals express four SUMO paralogues, SUMO1-4. SUMO2 and SUMO3 share 97% of sequence identity and are thus far not distinguishable by antibodies and often referred to as SUMO2/3. SUMO1 has 47% sequence identity with SUMO2. It is still questionable if the SUMO4 precursor can be processed to expose the C-terminal diGly motif needed for the conjugation to substrate proteins, as none of the known SUMO proteases seem to be able to do so[41]. The mature version of SUMO4 was however identified in lysates of serum starved cells, suggesting possible unknown SUMO proteases that are specifically expressed under these circumstances[42].

All SUMO paralogues are structurally very similar, but differ in expression levels. SUMO2 is the most abundant SUMO family member and knockout of SUMO2 is embryonic lethal in mice, while SUMO1 and SUMO3 knockout mice show only mild phenotypes, possibly due to the ability of SUMO2 to compensate for the loss of either SUMO1 or SUMO3[43,44]. Also, the different family members have different susceptibilities to SUMO specific isopeptidases for both, processing of the precursors and deconjugation[45]. Another difference between SUMO1 and SUMO2/3 is their ability to form SUMO chains. SUMO2 and SUMO3 harbour a lysine residue at position 11 (K11) within their flexible N-terminus that is located in a sequence motif that is preferentially targeted for SUMOylation and referred to as SUMO consensus motif[46]. This enables SUMO2/3 to polymerize[47]. Although the main site of SUMO chain formation seems to be K11, site-specific mass spectrometry approaches have identified several other SUMO acceptor lysines within SUMO2, SUMO3 and even SUMO1[48]. SUMO1 possesses an N-terminal lysine at position 7 that is located in an inverted SUMO consensus motif and low efficiency SUMO1 chain formation was demonstrated in vitro and by site-specific mass spectrometry in vivo, although the biological relevance and stoichiometry of SUMO1 chains remain to be established [48-51]. Rather than forming a chain itself, SUMO1 was suggested to function as a capping factor, terminating SUMO2/3 chain formation[47,52,53].

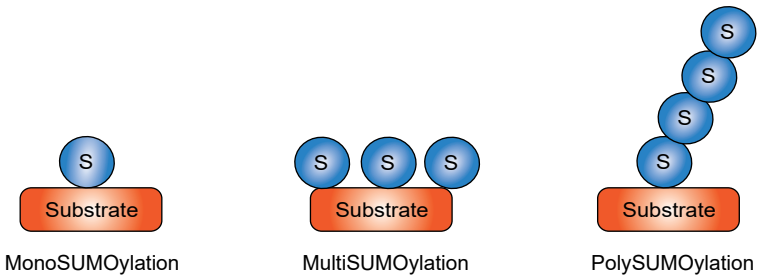

Figure 1. Possibilities of SUMO modification. SUMO substrates can be modified by a single SUMO moiety on a single lysine (mono-SUMOylation). Or single SUMO moieties can be conjugated to multiple lysines within the same substrate (multi-SUMOylation). A substrate can also be modified by a SUMO chain (poly-SUMOylation).

The SUMO conjugation cycle

SUMO can be conjugated to a single lysine within a substrate protein as single moiety (mono-SUMOylation), target multiple lysines within the substrate (multi-SUMOylation) or form a SUMO chain on a lysine residue (poly-SUMOylation) (Figure 1). The SUMO paralogues are translated into premature proteins (pre-SUMO), which have to be matured by the activity of a group of SUMO specific isoeptidases (SENPs). The SENPs remove a couple of C-terminal amino acids to expose the C-terminal di-Gly motif, which is needed for the conjugation to target lysine residues of the substrate. Conjugation and deconjugation of SUMO to a substrate is achieved via the activity of an enzymatic cascade involving SUMO specific E1, E2 and E3 enzymes and isopeptidases (Figure 2). The heterodimeric SUMO E1 enzyme consists of the SUMO-activating enzyme subunit 1 (SAE1) and subunit 2 (SAE2, also called UbA2). In an ATP-dependent two-step process, the mature C-terminus of SUMO is first adenylated, followed by the formation of a SAE2~SUMO thioester bond[36,54]. The single known SUMO E2 conjugating enzyme, Ubc9 renamed as UbE2I, is able to bind the SAE2s ubiquitin fold and this interaction stimulates the transfer of SUMO to Ubc9[55]. Unlike E2 enzymes involved in ubiquitin conjugation, Ubc9 has the unique ability to directly contribute to SUMO substrate selection[56]. Ubc9 has a low affinity to a so-called SUMO consensus motif, which is present in many substrate proteins and defined by a hydrophobic residues (ψ) upstream of the target lysine followed by any amino acid and an acidic residue downstream of the modification site (ψKx(D/E))[57,58]. In vitro a high concentration of Ubc9 together with the E1 enzyme is often sufficient to SUMOylate a substrate, given the presence of a SUMO consensus motif within the target protein[49,57,59]. In vivo, however, most substrates seem to require the presence of a SUMO E3 ligase for efficient SUMOylation.

Bona fide SUMO E3 ligases facilitate the transfer of SUMO to its target lysine by enhancing the interaction between the SUMO-charged Ubc9 and the substrate and by positioning the SUMO-Ubc9 in an orientation ideal for the nucleophilic attack by the target lysine[60]. Compared to the ubiquitin system in which hundreds of E3 ligases have been identified, only a few SUMO E3 ligases have been discovered thus far. The majority of SUMO E3 ligases belong to a family of proteins that carry a SP-RING (Siz/Pias -Really Interesting New Gene) domain that binds to Ubc9[61]. In humans this group consists of six members, the protein inhibitor of activated STAT (PIAS) 1, PIASxα, PIASxβ, PIAS3, PIAS4 (also known as PIASγ) and Nse2[55,62]. In contrast to the ubiquitin E3 ligases, which confer substrate specificity to the ubiquination system, the SUMO E3 ligases seem to exhibit a significant redundancy exemplified by knockout studies in mice[63,64]. The nuclear pore complex (NPC) component RanBP2, another unrelated, well studied SUMO E3 ligase, does not harbour a SP-RING domain but instead carries different motifs that bind SUMO and Ubc9. RanBP2 is involved in nuclear export/import as well as having a critical role during mitosis[49,65]. Additional to the SP-RING family and RanBP2, a third group of E3 ligases was recently discovered. The vertebrate- and SUMO2/3 paralogue- specific ZNF451 family comprised of ZNF451-1 and ZNF451-2, which are very similar, the more distinct isoform ZNF451-3 and the primate-specific KIAA1586, which shares a nearly identical N-terminus, including catalytic tandem-SUMO interaction motifs (SIMs), with the other family members[66,67]. Thus far the ZNF451 family has been implicated in SUMO chain formation and could be of particular importance during stress-induced SUMO conjugation after proteasome inhibition or DNA damage[66].

Additional proteins have been suggested to be E3 ligases as they are able to enhance SUMOylation of one or more substrates. These include the human polycomb protein Pc2/CBX4[68], the topoisomerase I-binding RING finger protein Topors[69], the transcription factor

Krox20[70], the tumour suppressor p14/Arf[71], the histone deacetylase HDAC4[72] and the Ras homologue enriched in striatum (Rhes)[73]. Whether they are bona fide SUMO E3 ligases must further be evaluated.

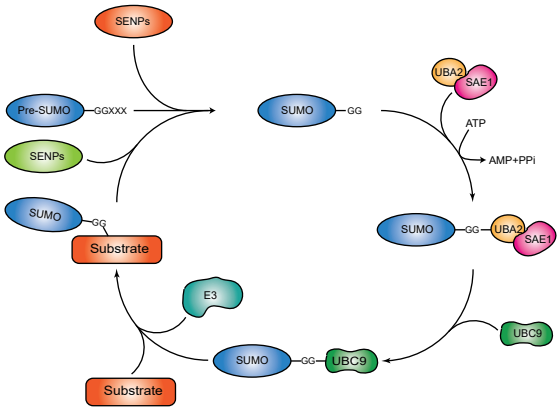

Figure 2. The SUMO conjugation cycle. SUMO is attached to lysine residues within a substrate by an enzymatic cascade comprised of the heterodimeric SUMO E1 activating enzyme, SAE1 and UbA2, the single SUMO E2 conjugation enzyme, Ubc9, and a handful of SUMO E3 ligases. SUMO specific proteases, SENPs, are responsible for the maturation of pre-SUMO and the deconjugation of SUMO from the substrate. SUMO and substrate can re-enter the cycle.

SUMO chains

The discovery of the SUMO chain-stimulating E3 ligase ZNF451 supports the notion of a specific physiological role of poly-SUMOylation, although knowledge about SUMO chain signalling remains limited compared to ubiquitin chain signalling. Ubiquitin has seven internal lysine residues that can be used for ubiquitin conjugation, resulting in different chain linkages with distinct biological consequences[74].

It is considered that the predominant SUMO chain linkage in vivo is via the lysine at position[11], although site specific mass spectrometry has identified multiple additional SUMO acceptor lysines, which could result in different linkages or branched SUMO chains[48]. However, so far there has been no indication that different SUMO chain linkages fulfil distinct roles within the cell. The main consequence of SUMO conjugation is the alteration of binding surfaces of the substrate, which can either hinder or promote intra- or intermolecular interaction. The same holds true for poly-SUMOylation. SUMO is able to promote molecular interaction due to its affinity to SUMO-interacting motifs, which are short peptide sequences mostly located in unstructured regions of the modified protein itself or interacting proteins. The sequences of SIMs consist of a stretch of conserved large hydrophobic amino acids that are either preceded or followed by an acidic patch or phosphorylation sites[75]. Proteins possessing multiple adjacent SIMs can bind to poly-SUMOylated proteins with enhanced affinity.

For example, the mammalian kinetochore protein CENP-E harbours multiple SIMs and its critical localization at the kinetochore during mitosis depends on the SUMOylation of unknown substrates at the kinetochore. SENP2 overexpression, as well as Ubc9 depletion resulted in incorrect CENP-E localization and consequently cell cycle arrest. Although CENP-E preferably binds SUMO2/3 chains in vitro, the necessity for poly-SUMOylation rather than multi-SUMOylation in vivo has not been confirmed with certainty[76]. A more direct need for poly-SUMOylation has however been demonstrated for the accurate localization of the yeast protein Zip1. Zip1 is a subunit of the synaptonemal complex (SC), which bridges homologues chromosomes during meiosis. Depleting the ability of the yeast SUMO paralogue Smt3 to form SUMO chains resulted in a lower sporulation efficiency, which was due to the mislocalization of Zip1 and deformation of the SC. Interestingly, as in the case of CENP-E,

the actual responsible poly-SUMOylated protein remains unidentified[77]. Other proteins that bind SUMO chains are SUMO-targeted ubiquitin ligases and they will be discussed in more detail below. Interestingly, cellular stressors such as DNA damage or heat shock induce global SUMO2/3 modification and most likely the formation of SUMO chains[78-80], hinting towards a global function of poly-SUMOylation during the response to such stressors[81-84].

SUMO-targeted ubiquitin ligases

SUMO chains on target substrates can be a signal for the recruitment of SUMO-targeted ubiquitin ligases (STUbLs). The STUbLs thus far identified all contain a RING domain and SIMS, which are responsible for the interaction with ubiquitin E2 conjugating enzymes and promote the preference of STUbLs for SUMOylated proteins, respectively. Due to the presence of multiple adjacent SIMs, STUbls prefer poly-SUMOylated substrates[85,86]. The most extensively studied human STUbL is the RING-finger protein 4 (RNF4). RNF4 possesses at least three closely spaced SIMs and shows a clear preference for substrates that are modified by a SUMO chain of at least three SUMO moieties[86]. RNF4 thus binds poly-SUMOylated substrates and mediates their ubiquitination by K48- or K63-linked ubiquitin chains, which signal for proteasomal degradation or recruitment of ubiquitin-binding motif-containing proteins, respectively. This mechanism has thus far been implicated in a variety of cellular processes including promyelocytic leukemia (PML) nuclear body (NB) integrity, mitosis and the DNA damage response[86-89]. The second known human STUbL RNF111 (also called Arkadia) was discovered by a bioinformatics approach, screening ubiquitin ligases for potential SIMs[90]. Its ubiquitin ligase activity was previously described in the context of TGF-β signalling but whether RNF111 functions as a STUbL in this signalling pathway is not certain. Like RNF4, RNF111 is preferably recruited to poly-SUMOylated proteins and also targets the nuclear body component PML, suggesting an overlapping pool of SUMO substrates targeted by RNF4 and RNF111[90,91]. How only some poly-SUMOylated proteins are targeted by STUbLs, whether RNF4 and RNF111 have target preferences and if more as yet unidentified STUbLs exist are most certainly interesting topics for future studies.

SUMO Group modification

A major conundrum in the SUMOylation field is the observation that hundreds of proteins have been identified to be SUMOylated but only a relatively small number of SUMO pathway enzymes have been identified. This led to the question of how specificity is achieved within the SUMO system compared to the ubiquitin system, which contains hundreds of different E3 ligases and deubiquitinating enzymes that confer specificity to the system. Another observation is that SUMOylation-deficiency of a single substrate often lacks an observable phenotype, although SUMOylation in general is essential for cell survival[92,93]. The concept of SUMO group modification might explain both of the above mentioned observations[94-96]. It is the idea that multiple proteins within a protein complex or functionally connected pathway are modified by SUMOylation and other proteins carrying SIMs interact with enhanced affinity to the SUMOylated proteins. Since this would result in multiple SUMO-SIM interactions, disrupting one single SUMO-SIM interaction can be easily compensated for by others. Also, the SUMO modification would not need to be extremely specific and therefore locally targeting one of the few SUMO ligases or SUMO proteases to the physically or functionally associated protein group would be sufficient, explaining the limited number of these enzymes. The concept was first proposed by Psakhye and Jentsch in 2012 who showed that in yeast DNA double-strand break (DSB) induction leads to the SUMOylation

of multiple proteins involved in homologues recombination (HR) by the E3 ligase Siz2. Site-directed mutation of single SUMOylation sites did not result in any observable phenotype. Only the mutation of several SUMO acceptor lysines in multiple physically connected HR proteins resulted in reduced repair efficiency[96].
Despite the novelty of the idea that SUMO targeting protein groups is a general mechanism of SUMOylation, observations of multiple SUMO substrates within a protein complex were observed earlier. For example, in yeast three of the five septins, components of a ring structured protein complex located at the bud neck of mitotic yeast cells, are SUMOylated during mitosis by the E3 ligase Siz1, which localizes to the septin ring prior to mitosis[95,97,98]. Additional examples promoting the SUMO group-modification hypothesis can be found in this thesis as in chapter 5 UV irradiation stimulates SUMOylation of multiple subunits of the transcription initiation TFIID complex or in chapter 4, where we demonstrate that SENP6 targets multiple members of the constitutive centromere-associated network (CCAN) for deSUMOylation.

SUMO proteases
SUMOylation of target substrates can be reversed by the activity of SUMO specific proteases. But their role is not limited to deconjugation. Certain SUMO proteases have a dual function within the SUMO cycle and are additionally responsible for the maturation of the SUMO precursor. All up to now identified SUMO proteases are cysteine isopeptidases but they all differ in their preference for SUMO paralogues and for maturation or deconjugation (Figure 3). The known mammalian SUMO proteases can be divided into three main groups. The first group and the largest group is the family of Sentrin (SUMO)-specific proteases (SENPs). The second group that comprises only one member is the recently discovered Ubiquitin-specific protease-like 1 (USPL1). And the third group contains the two related deSUMOylation isopeptidases (DeSIs).

The Ulp/SENP family
The first identified SUMO protease was the yeast protein UbL-specific protease 1 (Ulp1). Based on sequence similarities to Ulp1 the second yeast SUMO protease Ulp2 and the six mammalian SUMO proteases SENP1, 2, 3, 5, 6 and 7 were identified. The Ulp/SENP family shares a conserved catalytic domain located at the C-terminus of the proteins, with their active-site cysteine embedded in the catalytic triad His- Asp- Cys. The mammalian SENP1, 2, 3 and 5 are closer related to yeast Ulp1, whereas SENP6 and SENP7 more closely resemble Ulp2. Furthermore, SENP1 is closest related to SENP2, SENP3 is closest related to SENP5 and SENP6 and SENP7 share the highest sequence identity with each other and their catalytic domains diverge from the remaining SENP family members. The catalytic domains of SENP6 and SENP7 are interrupted by four conserved loop insertions, of which Loop1 protrudes out to make contact with residues in SUMO2 and SUMO3 that are absent in SUMO1, explaining the enzymes SUMO paralogue specificity.
Target specificity of the Ulp/SENP family is thought to be mainly determined by cellular localization that is mediated by their N-termini. Although a small fraction of some SENPs can be found in the cytoplasm, the majority of the enzymes are located within the nucleus, which is also the main site of SUMO conjugation and deconjungation. The yeast SUMO protease Ulp1 and the mammalian SUMO proteases SENP1 and SENP2 are concentrated at the nuclear pore during interphase, while they relocate to the kinetochore during mitosis[99-101]. The major localization site of SENP3 and SENP5 is the nucleolus[102,103]. SENP6

and SENP7 are diffusely localized throughout the nucleoplasm[104,105]. SENP1, SENP2 and catalytically inactive SENP6 are also reported to accumulate in nuclear foci, partly but not exclusively co-occurring with PML bodies[99,106].
SENP1, 2 and 5 have demonstrated SUMO precursor processing activity and show a considerable paralogue specificity based on how well the amino acids C-terminal of the di-Gly motif of the premature SUMO can be placed into the binding pockets of the SUMO proteases. SENP1 prefers SUMO1 for precursor processing as well as for deconjugation in vivo, while in vitro SENP1 deconjugates SUMO1,2 and 3 with equal efficiency[107-110]. SENP2 deconjugates and processes SUMO2 more efficiently than SUMO1 or SUMO3[111-113]. The precursor activity of SENP3 remains to be evaluated. The precursor processing activity of SENP5 is higher for SUMO3 than for the other paralogues and SENP6 and SENP7 do not possess the ability to process precursor SUMOs[114,115]. SENP6 and SENP7 also show a very limited activity towards deconjugating a single SUMO moiety from a target protein, whereas they are very efficient in disassembling SUMO chains[115-117] (Figure 3).

Biological functions of SENP1, SENP2, SENP3 and SENP5
SENP1 has been demonstrated to regulate multiple important transcription factors including ELK1, STAT5, IRF8, Bcl11b and Hif1α[118-122]. For example, the deSUMOylation of Hif1α by SENP1 is crucial for erythropoiesis in early murine embryonic development as it stabilizes the transcription factor and therefore promotes the expression of Hif1α target genes during hypoxic conditions[122]. Interestingly, SENP1 seems to be regulated by a positive feedback loop as its transcription increases upon hypoxia depended on Hif1α activity[123]. Transcription factors are however not the only reported targets of SENP1, as for example it was demonstrated that SENP1 activity at the kinetochore during mitosis is important for faithful sister chromatid separation[99].
SENP2 plays a role during early cardiac development in mice. Here SENP2 deSUMOylates the polycomb transcriptional repression complex subunit PRC1, which reverses the repressive effect of PRC1 on GATA4 and GATA6 expression, important genes for cardiac development[124]. SENP2 activity has also been implicated in the response to DNA damage upon which SENP2 deSUMOylates the Nuclear Factor κ B (NFκB) essential modulator NEMO, which leads to the restriction of NFκB regulated pro-survival genes transcription[125].
SENP3 and SENP5 have been implicated in the regulation if ribosome biogenesis by multiple studies, which fits with their nucleolar localization[102,126,127]. Additionally, SENP3 was shown to colocalize with and deSUMOylate Borealin, a component of the chromosomal passenger complex, in the nucleolus during interphase. SUMOylated Borealin is found at the centromeres during mitosis indicating a role for SENP3 in cell cycle regulation[128]. SENP5 seems to additionally be involved in the regulation of mitochondrial fission and fusion during mitosis[129,130].

SUMO chain regulation by SENP6
As SUMO can modify itself, a multitude of SUMO substrates are targets for poly-SUMOylation. The SUMO specific proteases SENP6 and SENP7 have a preference for deconjugating SUMO chains and are therefore tightly connected to pathways that are regulated by poly-SUMOylation. Thus far poly-SUMOylation is mainly reported to indirectly signal for protein degradation due to the recruitment of STUbLs.
SUMO chain deconjugation by SENP6 to prevent the recruitment of the mammalian STUbL RNF4 has been reported in multiple studies (Figure 4A). For example, the kinetochore

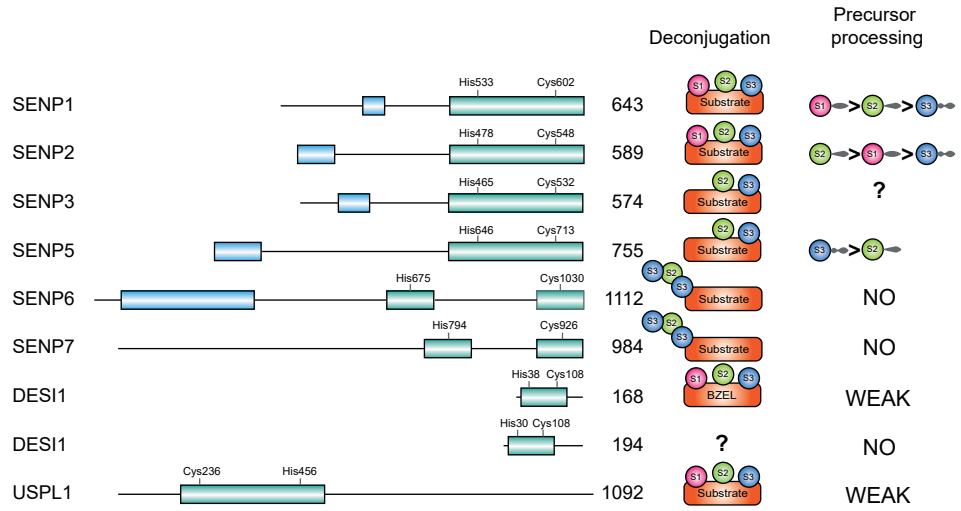

Figure 3. Mammalian SUMO specific proteases. Mammals express six SUMO proteases that belong to the family of Sentrin-specific proteases (SENPs). SENP1, 2 and SENP5 have the additional ability to process pre-SUMO. SENP6 and SENP7 are unique as their catalytic domain has conserved insertions and they have a preference for the deconjugation of SUMO chains. Recently discovered DeSI proteases and USPL1 show no pre-SUMO processing activity but have no SUMO paralogue preference for deconjugation. Blue rectangles indicate position of regulatory N-terminal domains. Green rectangles represent catalytic domains containing indicated catalytic residues. BZEL (ZBTB46) is the only identified target of DeSI1.

proteins CENP-I and Mis18BP1 are deSUMOylated by SENP6, and it has been suggested that accumulation of SUMO chains due to SENP6 depletion stimulates RNF4-mediated ubiquitination and degradation of CENP-I and Mis18BP1 with the consequence of incoherent chromosome congression during metaphase and the delocalization of the epigenetic centromere marker and histone variant CENP-A, respectively[88,131]. Another example of the counterbalancing relationship between SENP6 and RNF4 is their regulation of the Fanconi anemia ID complex (FANCI and FANCD2). Here, SENP6 and RNF4 seem to balance the level of DNA loaded ID complex and the subsequent nuclease activity upon the induction of replication fork-stalling lesions[132]. And finally, it was shown that SENP6 depletion in osteochondroprogenitor cells (OCPs) of mice, led to accumulation of SUMOylated TRIM28 and reduction of TRIM28 total levels, which together with an earlier report that identified TRIM28 as a RNF4 target, suggest SUMO chain induced- and RNF4-mediated degradation of TRIM28[133,134]. As co-repressor TRIM28 negatively controls P53 signalling and SENP6 depletion consequently leads to hyperactive P53 signalling, enhanced senescence and apoptosis of OCPs, which causes the observed premature aging phenotype in adult mice upon SENP6 depletion[134]. Interestingly, SENP6 also deSUMOylates proteins that are known RNF4 targets but SENP6 deficiency does not appear to induce RNF4- dependent degradation, like in the case of the promyolocytic leukemia protein (PML)[86,87,106]. This observation might suggest that not all SUMO chains that are targeted by SENP6 also recruit RNF4 and that chains with different properties might be present on the same protein. Whether these different properties are encoded by different architecture of SUMO chains remains to be investigated. However, STUbLs are not the only effector proteins that can be recruited to SENP6-regulated SUMO chains. For example, the replication protein RPA70 is usually deSUMOylated by

SENP6 during S-phase but upon replication stress-induced DNA damage, the interaction of SENP6 with RPA70 is disrupted. As a consequence, SUMO chains accumulate on RPA70 that subsequently recruit factors that are necessary for DNA damage repair[135] (Figure 4B).
Yet another mechanism of SENP6 regulation is exemplified by the role of SENP6 during Toll-like receptor (TLR) signalling. Here, the SUMOylation of NEMO, a negative regulator of NFκB, interferes with the binding and activity of the deUbiquitinase CYLD, which is needed to activate NEMO and inhibit NFκB signalling. By deSUMOylating NEMO, SENP6 allows CYLD binding and subsequent NEMO activation and attenuation of NFκB signalling[136] (Figure 4C).

The biological functions of SENP7
The closest relative to SENP6 is SENP7 and they share the preference for deconjugating poly-SUMOylated substrates. SENP7 plays an important role in the regulation of chromatin. For example, SENP7 stimulates homologous recombination after DNA damage by deSUMOylating the chromatin associated protein KAP1. SUMOylated KAP1 is able to recruit proteins that induce chromatin condensation. In contrast, deSUMOylation of KAP1 leads to relaxation of chromatin and improved accessibility for DNA damage repair factors[137]. Furthermore, SENP7 is involved in regulating the integrity of pericentric DNA regions, although this might be independent of its protease activity[138,139]. SENP7 was also recently implicated in innate immunity due to SENP7s regulation of the cytoplasmic DNA-sensor cGAS. Here, SUMOylation of cGAS inhibited its activation by DNA located in the cytoplasm. SENP7 reverses this inhibition and therefore stimulates cGAS activity, which ultimately leads to the transcriptional activation of interferon genes[140].

USPL1
USPL1 distantly resembles deubiquitylating enzymes (DUbs) but has SUMO-specific deconjugation activity[141]. USPL1 is the only SUMO protease that localizes to Cajal bodies within the nucleus. Its broad deSUMOylation activity in-vitro suggests that its specificity is conferred by its localization as its prime in-vivo function seems to be in Cajal body integrity[142]. Interestingly, knockdown of USPL1 results in impaired cell growth but as this phenotype can be rescued by exogenous USPL1 without protease activity it is likely that USPL1 has SUMO protease-independent functions as well[141].

DeSI
The SUMO proteases DeSI1 and DeSI2 were discovered in 2012. They belong to the permuted papain fold peptidases of double-stranded RNA viruses and eukaryotes (PPPDE) class of proteases[143]. The DeSI proteases seem to function as homodimers and their active site is formed by the catalytic dyad of Cys-His[144]. DeSI1 and DeSI2 are diffusely located throughout the cytoplasm and the nucleus and specifically deSUMOylate the transcriptional repressor BZEL (BTB-ZF protein expressed in lymphocytes)[143,144]. No other targets have been identified thus far and DeSIs therefore are the only highly specific SUMO proteases.

SUMO and DNA damage
SUMOylation is involved in most nuclear processes. It plays an important role in the regulation of transcription, mitosis, RNA biogenesis and also the cellular response to DNA damage[145-149]. The integrity of our DNA is constantly challenged by endogenous and exogenous DNA insults. Cells are equipped with complex machineries to repair damaged DNA and thereby prevent either cell death or DNA mutations that could lead to diseases

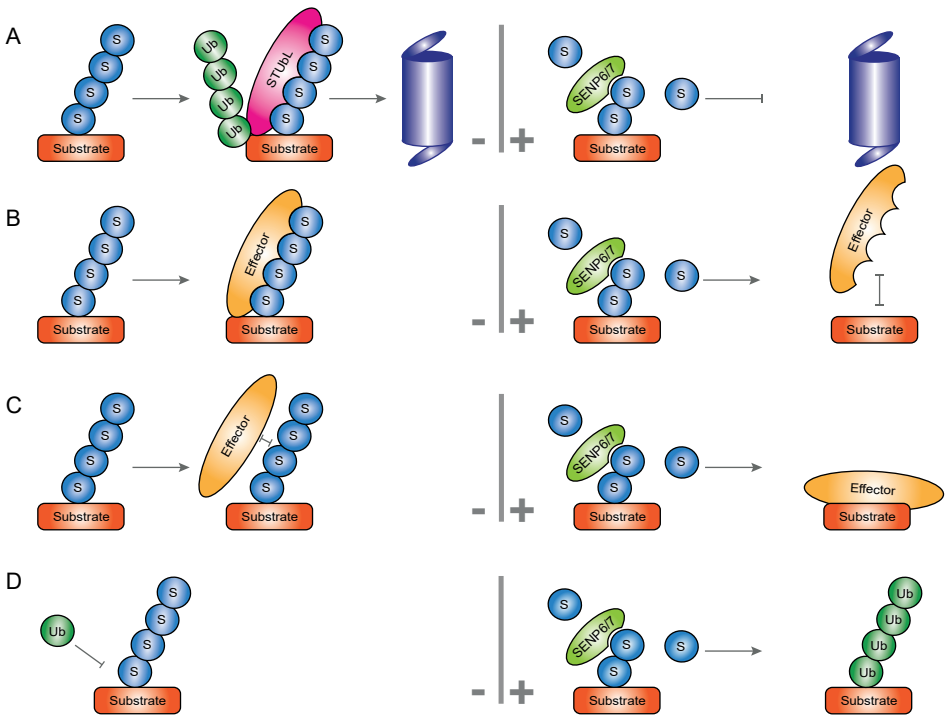

Figure 4. Mechanisms of SUMO chain regulation without (-) and with (+) SENP6. (**A**) SUMO chains can recruit STUbLs, which ubiquitinate and target the substrate to the 26S proteasome for degradation. SENP6 can stabilize the substrate by deconjugation. (**B**) SUMO chains can recruit other effector proteins. SENP6 can inhibit effector binding to the substrate by deconjugation. (**C**) SUMO chains can prevent binding of effector proteins. SENP6 can facilitate binding of the effector protein to the substrate by deconjugation. (**D**) SUMO chains can compete with ubiquitin for the same target lysine, thereby preventing ubiquitination of the substrate. SENP6 can stimulate substrate ubiquitination or any other lysine-targeting PTM by deconjugation.

such as cancer[150]. Different DNA lesions activate different DNA repair pathways. Oxidized, alkylated or deaminated bases are removed by Base-excision repair (BER). Highly cytotoxic double-strand breaks (DSB) can be repaired via several mechanism including homologous recombination (HR), non-homologous end-joining (NHEJ) or alternative NHEJ pathways. UV irradiation-induced cyclobutane pyrimidine dimers (CPDs) or 6-4 photoproducts (6-4 PPs) and other bulky helix-distorting DNA lesions are repaired by nucleotide excision repair (NER)[151]. PTMs, including SUMOylation, play an important role in regulating these pathways.

Base Excision Repair

The first link between SUMO and DNA damage repair was the discovery that the Base-excision repair (BER) protein Thymine-DNA glycosylase (TDG) is SUMOylated. TDG recognises G:T and G:U mismatches and subsequently removes the incorrect base. The resulting abasic site is then further processed by AP endonucleases, DNA polymerases and ligases. The SUMOylation of TDG stimulates an intramolecular interaction between the covalently attached SUMO1 and a SIM. This interaction leads to a conformational change that results in the dissociation of TDG from the established abasic site. This dissociation is needed in order to allow the endonuclease activity of APE1, which is the subsequent step of BER[152,153].

Double-Strand Break break repair

Further, SUMOylation has been implicated to play an important role during the repair of DNA double-strand breaks (DSB). DSBs are the most toxic DNA lesion and functional repair mechanisms are essential to ensure survival of cells. In mammalian cells, several components of the SUMO machinery are recruited to DSB sites, including SUMO1, SUMO2/3, Ubc9, PIAS1 and PIAS4. The SUMO E3 ligases PIAS1 and PIAS4 were shown to be important for the accumulation of crucial DNA repair factors at the DNA damage site, including the pivotal ubiquitin E3 ligase RNF168[154,155]. Upon DNA damage, RNF168 is recruited by ubiquitination events that are mediated by RNF8, another ubiquitin E3 ligase[156]. Together RNF8 and RNF168 create a ubiquitination wave along the sites of DSBs, which is necessary for the accumulation of multiple highly important repair proteins, such as 53BP1 and BRCA1[157]. Consequently, knockdown of PIAS1 and PIAS4 led to a reduced DSB repair efficiency and sensitized cells to various DSB-inducing agents[154]. The STUbL RNF4 is also recruited to DSBs, most likely by the SUMOylation of substrates by PIAS1 and PIAS4. RNF4 recruitment to DSBs results in the K48-linked ubiquitination of SUMOylated proteins and their subsequent proteasomal degradation[158]. In conclusion, SUMOylation regulates both recruitment and degradation of important DNA damage response factors during the repair of DSBs.

Nucleotide Excision Repair

UV-induced DNA lesions and other bulky DNA adducts are repaired by NER. The NER pathway can be divided into two sub-pathways. Global genome NER (GG-NER) removes UV-induced lesions throughout the entire genome while transcription-coupled NER (TC-NER) selectively repairs lesions located within actively transcribed genes. SUMOylation as well as ubiquitination modify and regulate important proteins of both sub-pathways[151,159,160].

GG-NER is activated by the binding of the protein Xeroderma pigmentosum group C (XPC) to the bulky DNA lesion 161. In contrast to 6-4PPs, CPDs, which are the most common UV-induced photolesions, only mildly disturb the DNA helix and are therefore not efficiently recognized by XPC alone[162-166]. UV-radiation DNA damage-binding protein 2 (DDB2) supports XPC in the recognition of CPDs and 6-4PPs[167,168]. DDB2 also forms the substrate recognition subunit of a ubiquitin E3 ligase complex, together with the adaptor DDB1, the scaffold Cullin4A and the RING protein Roc1 (CRL4 complex)[169]. This E3 ligase complex is also called the UV-DDB complex. After lesion recognition by DDB2, UV-DDB targets XPC, the core histones H2A, H3 and H4 as well as DDB2 itself for ubiquitination[170-175]. While ubiquitinated DDB2 is targeted for degradation, the ubiquitination of XPC enhances its DNA binding[171,176]. XPC is highly regulated by PTMs including SUMOylation upon UV damage. This SUMOylation triggers the STUbL RNF111 to add K63-linked ubiquitin chains to XPC, which seems essential for the release of DDB2 from the lesion site and the subsequent hand-over to downstream GG-NER factors[177-180].

The binding of XPC to the lesion recruits the transcription initiation factor IIH (TFIIH) complex. TFIIH contains 10 subunits, including the ATPase XPB and the DNA helicase XPD, which separate the complementary DNA strands around the lesion to create an open repair 'bubble'[181,182]. Subsequently the repair bubble is stabilized by XPA and RPA before the short stretch of DNA containing the lesion is excised by the endonucleases XPF-ERCC1 and XPG and the gap is closed by the joined activity of DNA polymerases and DNA ligases[181,183-185] (Figure5).

TC-NER relies on a different strategy to recognize UV-induced lesion. In actively transcribed

genes, UV-induced lesions will block the elongating RNA polymerases, which is the initial trigger for the recruitment of the proteins Cockayne-Syndrome B (CSB) and CSA. Lesion-bound CSB and CSA are necessary to recruit TFIIH for subsequent repair steps, which are common to both GG-NER and TC-NER 186 (Figure 5). Interestingly, analogous to DDB2, CSA is a substrate adaptor of a ubiquitin E3 ligase, containing DDB1, Cullin4A and Roc1 (CRL)[187]. Targets of the CSA-CRL complex, however, remain scarce and debated. CSB has been suggested to be targeted for ubiquitination by CSA-CRL complex and subsequently be degraded by the proteasome[187]. Recently, a new player in TC-NER has been identified, the UV stimulated scaffold protein A (UVSSA)[188-191]. It was suggested that UVSSA is responsible for the recruitment of the deubiquitinase USP7 to the site of the UV-induced lesion. Subsequently, USP7 deubiquitinates and stabilizes CSB and therefore counteracts the proposed activity of CSA[188,190].

Interestingly, analogous to the GG-NER damage recogniser XPC, CSB has also been identified to be SUMOylated upon UV irradiation. The SUMOylation of CSB is important for TC-NER efficiency, but detailed insight into the function of this SUMOylation event is missing[159] (this thesis chapter 5).

Additional to the SUMOylation and ubiquitination of CSB, the ubiquitination of RNA polymerase II (RNAPII) plays a pivotal role during TC-NER. The lesion stalled RNAPII covers approximately 35 nucleotides and therefore blocks access of downstream repair factors to the lesion[192]. Multiple mechanisms were suggested explaining how the stalled RNAPII is regulated to allow DNA repair. These mechanisms include dissociation of RNAPII from the damaged DNA, which may or may not be followed by proteasomal degradation, or RNAPII backtracking, a known process common in transcriptional proofreading and transcriptional pausing[193,194].

Polyubiquitination and proteasomal degradation of RPB1, the major catalytic subunit of RNAPII, is considered to be a last resort only when TC-NER fails to repair the lesion[193,195]. The ubiquitination of RPB1 involves a two-step mechanism with multiple layers of regulation. Initially, the ubiquitin E3 ligase NEDD4 mediates the monoubiquitination of RNAPII[196,197]. This monoubiquitination event was suggested to subsequently facilitate the polyubiquitination and proteasomal degradation of RPB1. Multiple ubiquitin E3 ligases were proposed to be responsible for the polyubiquitination of RPB1. The Elongin A/B/C complex together with Cullin 5 (CUL5) and RING-box protein 2 (RBX2) form a ubiquitin E3 ligase that selectively modifies monoubiquitinated RPB1 with K48-linked ubiquitin chains[197]. Additionally, the pVHL-ElonginB/C-Cul2-Rbx1 ubiquitin E3 ligase was able to bind and ubiquitinate RPB1[198]. Besides the Elongin containing complexes, the DNA damage associated ubiquitin E3 ligase BRCA1, and the CSA contain E3 ligase complex were suggested to be involved in polyubiquitination of RPB1[199-202]. However, reduced ubiquitination of RPB1, specifically observed during later time points after UV irradiation, in cells depleted of CSA could alternatively be explained by a drastic decrease of transcription upon UV damage in those cells and the consequent absence of new RNAPII molecules encountering the damage lesions[196]. Although the possibility that CSA directly targets RPB1 for ubiquitination at a later time point after damage induction is not convincingly excluded and remains a subject of active discussion.

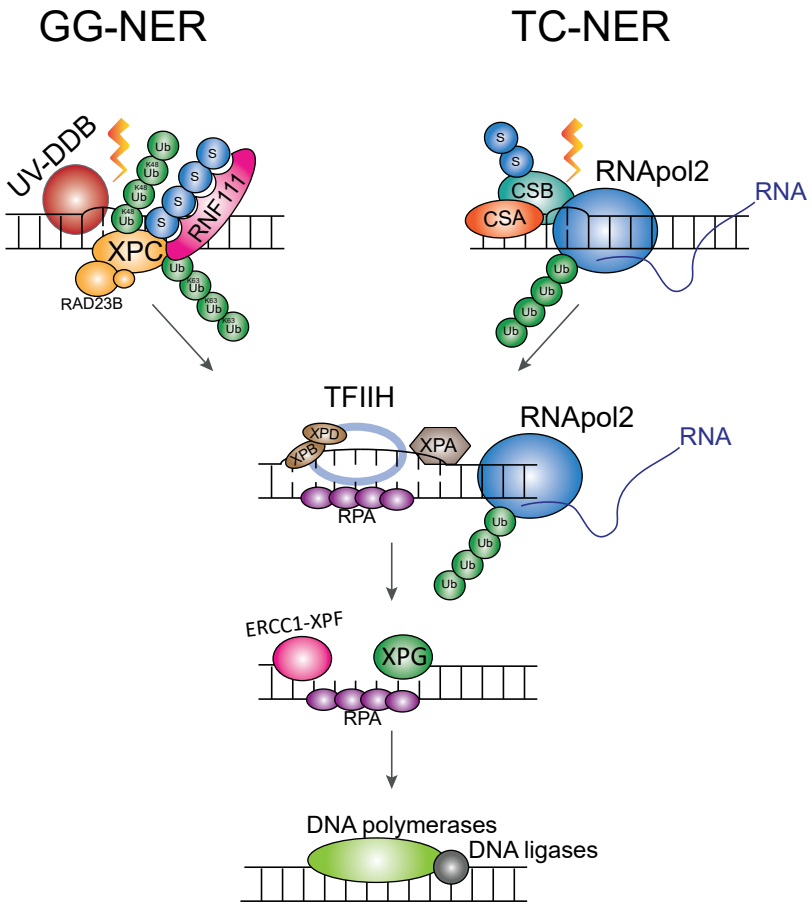

Figure 5. Nucleotide excision repair is regulated by PTMs. Nucleotide excision repair (NER) can be subdivided into two pathways. Global genome (GG) - NER relies on the activity of XPC and UV-DDB to recognise the UV-induced lesion. UV-DDB adds K48-linked ubiquitin chains to XPC. XPC s also SUMOylated, which recruits the STUbL RNF111, which adds K63-linked ubiquitin chains to XPC. In TC-NER the UV-lesion is recognised by the stalling of the processing RNA polymerase 2 (RNApol2) at the lesion. CSA and CSB are recruited to the stalled RNApol2 and are responsible to facilitate the subsequent steps of the pathway. CSB is SUMOylated upon UV damage and RNApol2 is ubiquitinated. Subsequent repair steps include the unwinding of the DNA by the TFIIH subunits XPB and XPD, the stabilization of the unwound DNA by XPA and RPA, the excision of the damaged DNA by the endonucleases ERCC1-XPF and XPG and the closing of the DNA gap by DNA polymerases and DNA ligases.

STUDYING SUMOYLATION

To study how SUMO regulates cellular processes, we first have to identify the proteins in the cell that are targeted for SUMOylation. Mass spectrometry offers an ideal tool to gain a system-wide overview of SUMOylation substrates. During the past decade huge advances in the development of SUMO proteomics were made and multiple hurdles were crossed. However, some challenges remain unsolved.

The identification of SUMO substrates in a complex protein sample is hampered by the low stoichiometry of this modification. Several strategies have been developed to enrich for SUMOylated proteins before identifying them by mass spectrometry, each with their own advantages and disadvantages. Especially the identification of endogenous SUMOylation targets continues to be challenging. Antibodies against SUMO do exist and were used to immunoprecipitate SUMOylated proteins from cell extracts, but due to the mild buffer conditions needed to ensure the integrity of the antibody, the background remains high and the yield poor[203]. In another approach researchers purified endogenous poly-SUMOylated proteins by using a RNF4 fragment including its four SIMs, which has affinity to polySUMOylated but not monoSUMOylated proteins. Here, the structural integrity of the RNF4 fragment was also of high importance for the purification and non-denaturing conditions had to be used and resulted in a co-purification of proteins merely interacting with polySUMOylated proteins that bound to the immobilized RNF4 SIM fragment[204].

Mild buffer conditions might not only lead to high background but also do allow SUMO proteases to deconjugate SUMO from its substrates during the lysis. The inclusion of cysteine protease inhibitors like N-Ethylmaleimide or Iodoacetamide inhibits SUMO proteases and helps to retain SUMOylated species. Additionally, methods have been developed that purify SUMOylated proteins under highly denaturing conditions, reducing non-specific background and maximizing yield. The drawback of these purification methods is that they are all based on the exogenous expression of an epitope tagged SUMO, which can lead to non-physiologically relevant SUMOylated proteins and restrict the identification of SUMOylated proteins to model systems that allow such exogenous protein expression. Multiple different epitope tags have been used including FLAG, TAP, Strep, His6 and His10 epitopes. These purification methods followed by mass spectrometry enabled the identification of hundreds of SUMOylated substrates.

The technique used throughout this thesis, is based on the exogenous expression of a His10-tagged SUMO2. This tagged SUMO is conjugated to substrate proteins and low expression levels of the exogenous His10-SUMO2 reduced possible overexpression artefacts. Although background binding is low, including a parental cell line not harbouring the His10-SUMO2 construct and identifying background binders is an important aspect of the identification of putative SUMO substrates, as only proteins that are highly enriched within the purified sample compared to the background binder control qualify.

Two different methods have been employed in connection to SUMO proteomics to gain quantitative information. Stable isotope labelling by amino acids in cell culture (SILAC) was used in multiple studies but allows a maximum of three experimental conditions to be compared. The recent development in robust computational label-free quantification allows an unlimited number of experimental conditions to be compared and consistent relative quantifications to be obtained[48,205].

However, direct mass spectrometry-based proof that a protein is truly SUMOylated can only be achieved by the identification of the SUMO conjugated peptides of substrate proteins. This, however, presents quite a challenge. For shot-gun proteomics, proteins are routinely digested by proteases, resulting in peptides that can be resolved and identified by mass spectrometry. The most common proteases used are lysyl endopeptidase (Lys-C), which cleaves C-terminal of lysines and trypsin, which cleaves C-terminal of arginines and lysines. If digested with trypsin, mammalian SUMO2/3 leaves behind a 32 amino acid long C-terminal peptide conjugated to the remaining peptide of the target substrate. This tryptic remnant cannot efficiently be resolved and identified by the mass spectrometer. Multiple approaches

were established to overcome this problem. Introduction of an additional cleavage site for trypsin by site-specific mutations of residues close to the C-terminus of SUMO (Q87R or T90R) shortened the tryptic remnants but, without purification of the SUMOylated peptides, resulted in the identification of only a few SUMO acceptor sites[206,207].

An increased number of SUMOylation sites were identified by expressing a His tagged SUMO mutant with all lysines mutated to arginines in combination with the Q87R mutation. This protected the His-tagged SUMO from being digested with Lys-C and enabled post-digestion purification of the SUMOylated peptides, thereby decreasing sample complexity and enhancing the identification of acceptor sites. Subsequently, multiple strategies were developed that combined the expression of SUMO mutants, highly efficient enrichment of SUMOylated proteins prior to tailored enzymatic digestion and re-purification of SUMOylated peptides, leading to the identification of thousands of SUMO acceptor lysines[48].

SUMO proteomics is now a widely used tool to study global SUMOylation events in the cell under specific circumstances and is also the starting point of each chapter within this thesis. It enabled us to have a system-wide look at dynamics and regulations and helps us to study how groups of proteins are simultaneously regulated by SUMO.

References

1. Bianconi, E., Piovesan, A., Facchin, F. et al. An estimation of the number of cells in the human body Annals of human biology 40, 463-471, (2013).
2. CRICK, F. H. On protein synthesis. Symp. Soc. Exp. Biol 12, 138-163, (1958).
3. Davidson, E. H. and Britten, R. J. Organization, transcription, and regulation in the animal genome. Q. Rev. Biol 48, 565-613, (1973).
4. Hershey, J. W. Translational control in mammalian cells. Annu. Rev. Biochem 60, 717-755, (1991).
5. Ayoubi, T. A. andVan de Ven, W. J. Regulation of gene expression by alternative promoters. FASEB J 10, 453-460, (1996).
6. Tischer, E., Mitchell, R., Hartman, T. et al. The human gene for vascular endothelial growth factor. Multiple protein forms are encoded through alternative exon splicing. J. Biol. Chem 266, 11947-11954, (1991).
7. Ota, T., Suzuki, Y., Nishikawa, T. et al. Complete sequencing and characterization of 21,243 full-length human cDNAs. Nat. Genet 36, 40-45, (2004).
8. Hiesel, R., Wissinger, B., Schuster, W. and Brennicke, A. RNA editing in plant mitochondria. Science 246, 1632-1634, (1989).
9. Pan, Q., Shai, O., Lee, L. J., Frey, B. J. and Blencowe, B. J. Deep surveying of alternative splicing complexity in the human transcriptome by high-throughput sequencing. Nat. Genet 40, 1413-1415, (2008).
10. Carninci, P., Kasukawa, T., Katayama, S. et al. The transcriptional landscape of the mammalian genome. Science 309, 1559-1563, (2005).
11. Uy, R. and Wold, F. Posttranslational covalent modification of proteins. Science 198, 890-896, (1977).
12. Wold, F. In vivo chemical modification of proteins (post-translational modification). Annu. Rev. Biochem 50, 783-814, (1981).
13. Jensen, O. N. Modification-specific proteomics: characterization of post-translational modifications by mass spectrometry. Curr. Opin. Chem. Biol 8, 33-41, (2004).
14. Walsh, C. T., Garneau-Tsodikova, S. and Gatto, G. J., Jr. Protein posttranslational modifications: the chemistry of proteome diversifications. Angew. Chem. Int. Ed Engl 44, 7342-7372, (2005).
15. Kruger, R., Kubler, D., Pallisse, R., Burkovski, A. and Lehmann, W. D. Protein and proteome phosphorylation stoichiometry analysis by element mass spectrometry. Analytical chemistry 78, 1987- 1994, (2006).
16. Ubersax, J. A. and Ferrell, J. E., Jr. Mechanisms of specificity in protein phosphorylation. Nature reviews. Molecular cell biology 8, 530-541, (2007).
17. Barford, D., Das, A. K. and Egloff, M. P. The structure and mechanism of protein phosphatases: insights into catalysis and regulation. Annual review of biophysics and biomolecular structure 27, 133-164, (1998).
18. Vlastaridis, P., Kyriakidou, P., Chaliotis, A. et al. Estimating the total number of phosphoproteins and phosphorylation sites in eukaryotic proteomes. GigaScience 6, 1-11, (2017).
19. Drazic, A., Myklebust, L. M., Ree, R. and Arnesen, T. The world of protein acetylation. Biochimica et biophysica acta 1864, 1372-1401, (2016).
20. Murn, J. and Shi, Y. The winding path of protein methylation research: milestones and new frontiers. Nature reviews. Molecular cell biology 18, 517-527, (2017).
21. Ohtsubo, K. and Marth, J. D. Glycosylation in cellular mechanisms of health and disease. Cell 126, 855-867, (2006).
22. Kerscher, O., Felberbaum, R. and Hochstrasser, M. Modification of proteins by ubiquitin and ubiquiin-like proteins. Annu. Rev. Cell Dev. Biol 22, 159-180, (2006).
23. Hochstrasser, M. Ubiquitin-dependent protein degradation. Annu. Rev. Genet 30, 405-439, (1996).
24. Pickart, C. M. Mechanisms underlying ubiquitination. Annu. Rev. Biochem 70, 503-533, (2001).
25. Mahajan, R., Delphin, C., Guan, T., Gerace, L. and Melchior, F. A small ubiquitin-related polypeptide involved in targeting RanGAP1 to nuclear pore complex protein RanBP2. Cell 88, 97-107, (1997).
26. Matunis, M. J., Coutavas, E. and Blobel, G. A novel ubiquitin-like modification modulates the partitioning of the Ran-GTPase-activating protein RanGAP1 between the cytosol and the nuclear pore complex. J. Cell Biol 135, 1457-1470, (1996).
27. Muller, S., Hoege, C., Pyrowolakis, G. and Jentsch, S. SUMO, ubiquitin's mysterious cousin. Nat. Rev. Mol. Cell Biol 2, 202-210, (2001).

28. Liakopoulos, D., Doenges, G., Matuschewski, K. and Jentsch, S. A novel protein modification pathway related to the ubiquitin system. EMBO J 17, 2208-2214, (1998).
29. D'Cunha, J., Jr, K. E., Haas, A. L., Truitt, R. L. and Borden, E. C. Immunoregulatory properties of ISG15, an interferon-induced cytokine. Proc. Natl. Acad. Sci. U. S. A 93, 211-215, (1996).
30. Liu, Y. C., Pan, J., Zhang, C. et al. A MHC-encoded ubiquitin-like protein (FAT10) binds noncovalently to the spindle assembly checkpoint protein MAD2. Proc. Natl. Acad. Sci. U. S. A 96, 4313- 4318, (1999).
31. Michiels, L., Van der Rauwelaert, E., Van, H. F., Kas, K. and Merregaert, J. fau cDNA encodes a ubiquitin-like-S30 fusion protein and is expressed as an antisense sequence in the Finkel-Biskis-Reilly murine sarcoma virus. Oncogene 8, 2537-2546, (1993).
32. Komatsu, M., Chiba, T., Tatsumi, K. et al. A novel protein-conjugating system for Ufm1, a ubiquitin-fold modifier. EMBO J 23, 1977-1986, (2004).
33. Van der Veen, A. G., Schorpp, K., Schlieker, C. et al. Role of the ubiquitin-like protein Urm1 as a noncanonical lysine-directed protein modifier. Proc. Natl. Acad. Sci. U. S. A 108, 1763-1770, (2011).
34. Hochstrasser, M. Biochemistry. All in the ubiquitin family. Science 289, 563-564, (2000).
35. Vierstra, R. D. The expanding universe of ubiquitin and ubiquitin-like modifiers. Plant Physiol 160, 2-14, (2012).
36. Schulman, B. A. and Harper, J. W. Ubiquitin-like protein activation by E1 enzymes: the apex for downstream signalling pathways. Nat. Rev. Mol. Cell Biol 10, 319-331, (2009).
37. Wenzel, D. M., Stoll, K. E. and Klevit, R. E. E2s: structurally economical and functionally replete. The Biochemical journal 433, 31-42, (2011).
38. van Wijk, S. J. and Timmers, H. T. The family of ubiquitin-conjugating enzymes (E2s): deciding between life and death of proteins. FASEB J 24, 981-993, (2010).
39. Nagy, V. and Dikic, I. Ubiquitin ligase complexes: from substrate selectivity to conjugational specificity. Biol. Chem 391, 163-169, (2010).
40. Van der Veen, A. G. and Ploegh, H. L. Ubiquitin-like proteins. Annu. Rev. Biochem 81, 323-357, (2012).
41. Owerbach, D., McKay, E. M., Yeh, E. T., Gabbay, K. H. and Bohren, K. M. A proline-90 residue unique to SUMO-4 prevents maturation and sumoylation. Biochem. Biophys. Res. Commun 337, 517-520, (2005).
42. Guo, D., Han, J., Adam, B. L. et al. Proteomic analysis of SUMO4 substrates in HEK293 cells under serum starvation-induced stress. Biochem. Biophys. Res. Commun 337, 1308-1318, (2005).
43. Evdokimov, E., Sharma, P., Lockett, S. J., Lualdi, M. and Kuehn, M. R. Loss of SUMO1 in mice affects RanGAP1 localization and formation of PML nuclear bodies, but is not lethal as it can be compensated by SUMO2 or SUMO3. J. Cell Sci 121, 4106-4113, (2008).
44. Wang, L., Wansleeben, C., Zhao, S. et al. SUMO2 is essential while SUMO3 is dispensable for mouse embryonic development. EMBO Rep 15, 878-885, (2014).
45. Hickey, C. M., Wilson, N. R. and Hochstrasser, M. Function and regulation of SUMO proteases. Nat. Rev. Mol. Cell Biol 13, 755-766, (2012).
46. Rodriguez, M. S., Dargemont, C. and Hay, R. T. SUMO-1 conjugation in vivo requires both a consensus modification motif and nuclear targeting. J. Biol. Chem 276, 12654-12659, (2001).
47. Tatham, M. H., Jaffray, E., Vaughan, O. A. et al. Polymeric chains of SUMO-2 and SUMO-3 are conjugated to protein substrates by SAE1/SAE2 and Ubc9. J. Biol. Chem 276, 35368-35374, (2001).
48. Hendriks, I. A. and Vertegaal, A. C. A comprehensive compilation of SUMO proteomics. Nat. Rev. Mol. Cell Biol 17, 581-595, (2016).
49. Pichler, A., Gast, A., Seeler, J. S., Dejean, A. and Melchior, F. The nucleoporin RanBP2 has SUMO1 E3 ligase activity. Cell 108, 109-120, (2002).
50. Yang, M., Hsu, C. T., Ting, C. Y., Liu, L. F. and Hwang, J. Assembly of a polymeric chain of SUMO1 on human topoisomerase I in vitro. J. Biol. Chem 281, 8264-8274, (2006).
51. Pedrioli, P. G., Raught, B., Zhang, X. D. et al. Automated identification of SUMOylation sites using mass spectrometry and SUMmOn pattern recognition software. Nat. Methods 3, 533-539, (2006).
52. Chung, T. L., Hsiao, H. H., Yeh, Y. Y. et al. In vitro modification of human centromere protein CENP-C fragments by small ubiquitin-like modifier (SUMO) protein: definitive identification of the modification sites by tandem mass spectrometry analysis of the isopeptides. J. Biol. Chem 279, 39653-39662, (2004).
53. Vertegaal, A. C., Ogg, S. C., Jaffray, E. et al. A proteomic study of SUMO-2 target proteins. J. Biol. Chem 279, 33791-33798, (2004).

54. Dye, B. T. and Schulman, B. A. Structural mechanisms underlying posttranslational modification by ubiquitin-like proteins. Annu. Rev. Biophys. Biomol. Struct 36, 131-150, (2007).

55. Flotho, A. and Melchior, F. Sumoylation: a regulatory protein modification in health and disease. Annu. Rev. Biochem 82, 357-385, (2013).

56. Pichler, A., Fatouros, C., Lee, H. and Eisenhardt, N. SUMO conjugation - a mechanistic view. Biomol. Concepts 8, 13-36, (2017).

57. Bernier-Villamor, V., Sampson, D. A., Matunis, M. J. and Lima, C. D. Structural basis for E2-mediated SUMO conjugation revealed by a complex between ubiquitin-conjugating enzyme Ubc9 and RanGAP1. Cell 108, 345-356, (2002).

58. Yunus, A. A. and Lima, C. D. Lysine activation and functional analysis of E2-mediated conjugation in the SUMO pathway. Nat. Struct. Mol. Biol 13, 491-499, (2006).

59. Okuma, T., Honda, R., Ichikawa, G., Tsumagari, N. and Yasuda, H. In vitro SUMO-1 modification requires two enzymatic steps, E1 and E2. Biochem. Biophys. Res. Commun 254, 693-698, (1999).

60. Reverter, D. and Lima, C. D. Insights into E3 ligase activity revealed by a SUMO-RanGAP1-Ubc9-Nup358 complex. Nature 435, 687-692, (2005).

61. Yunus, A. A. and Lima, C. D. Structure of the Siz/PIAS SUMO E3 ligase Siz1 and determinants required for SUMO modification of PCNA. Mol. Cell 35, 669-682, (2009).

62. Andrews, E. A., Palecek, J., Sergeant, J. et al. Nse2, a component of the Smc5-6 complex, is a SUMO ligase required for the response to DNA damage. Mol. Cell Biol 25, 185-196, (2005).

63. Roth, W., Sustmann, C., Kieslinger, M. et al. PIASy-deficient mice display modest defects in IFN and Wnt signaling. J. Immunol 173, 6189-6199, (2004).

64. Wong, K. A., Kim, R., Christofk, H. et al. Protein inhibitor of activated STAT Y (PIASy) and a splice variant lacking exon 6 enhance sumoylation but are not essential for embryogenesis and adult life. Mol. Cell Biol 24, 5577-5586, (2004).

65. Dawlaty, M. M., Malureanu, L., Jeganathan, K. B. et al. Resolution of sister centromeres requires RanBP2-mediated SUMOylation of topoisomerase IIalpha. Cell 133, 103-115, (2008).

66. Eisenhardt, N., Chaugule, V. K., Koidl, S. et al. A new vertebrate SUMO enzyme family reveals insights into SUMO-chain assembly. Nat. Struct. Mol. Biol 22, 959-967, (2015).

67. Abascal, F., Tress, M. L. and Valencia, A. Alternative splicing and co-option of transposable elements: the case of TMPO/LAP2alpha and ZNF451 in mammals. Bioinformatics 31, 2257-2261, (2015).

68. Kagey, M. H., Melhuish, T. A. and Wotton, D. The polycomb protein Pc2 is a SUMO E3. Cell 113, 127-137, (2003).

69. Weger, S., Hammer, E. and Heilbronn, R. Topors acts as a SUMO-1 E3 ligase for p53 in vitro and in vivo. FEBS Lett 579, 5007-5012, (2005).

70. Garcia-Gutierrez, P., Juarez-Vicente, F., Gallardo-Chamizo, F., Charnay, P. and Garcia-Dominguez, M. The transcription factor Krox20 is an E3 ligase that sumoylates its Nab coregulators. EMBO Rep 12, 1018-1023, (2011).

71. Tago, K., Chiocca, S. and Sherr, C. J. Sumoylation induced by the Arf tumor suppressor: a p53-independent function. Proc. Natl. Acad. Sci. U. S. A 102, 7689-7694, (2005).

72. Zhao, X., Sternsdorf, T., Bolger, T. A., Evans, R. M. and Yao, T. P. Regulation of MEF2 by histone deacetylase 4- and SIRT1 deacetylase-mediated lysine modifications. Mol. Cell Biol 25, 8456-8464, (2005).

73. Subramaniam, S., Mealer, R. G., Sixt, K. M. et al. Rhes, a physiologic regulator of sumoylation, enhances cross-sumoylation between the basic sumoylation enzymes E1 and Ubc9. J. Biol. Chem 285, 20428-20432, (2010).

74. Komander, D., Clague, M. J. and Urbe, S. Breaking the chains: structure and function of the deubiquitinases. Nat. Rev. Mol. Cell Biol 10, 550-563, (2009).

75. Vogt, B. and Hofmann, K. Bioinformatical detection of recognition factors for ubiquitin and SUMO. Methods Mol. Biol 832, 249-261, (2012).

76. Zhang, X. D., Goeres, J., Zhang, H. et al. SUMO-2/3 modification and binding regulate the association of CENP-E with kinetochores and progression through mitosis. Mol. Cell 29, 729-741, (2008).

77. Cheng, C. H., Lo, Y. H., Liang, S. S. et al. SUMO modifications control assembly of synaptonemal complex and polycomplex in meiosis of Saccharomyces cerevisiae. Genes Dev 20, 2067-2081, (2006).

78. Golebiowski, F., Matic, I., Tatham, M. H. et al. System-wide changes to SUMO modifications in response to heat shock. Sci. Signal 2, ra24, (2009).
79. Xiao, Z., Chang, J. G., Hendriks, I. A. et al. System-wide analysis of SUMOylation dynamics in response to replication stress reveals novel SUMO target proteins and acceptor lysines relevant for genome stability. Mol. Cell Proteomics 14, 1419-1434, (2015).
80. Hendriks, I. A., D'Souza, R. C., Yang, B. et al. Uncovering global SUMOylation signaling networks in a site-specific manner. Nat. Struct. Mol. Biol 21, 927-936, (2014).
81. Srikumar, T., Lewicki, M. C., Costanzo, M. et al. Global analysis of SUMO chain function reveals multiple roles in chromatin regulation. J. Cell Biol 201, 145-163, (2013).
82. Zhou, W., Ryan, J. J. and Zhou, H. Global analyses of sumoylated proteins in Saccharomyces cerevisiae. Induction of protein sumoylation by cellular stresses. J. Biol. Chem 279, 32262-32268, (2004).
83. Skilton, A., Ho, J. C., Mercer, B., Outwin, E. and Watts, F. Z. SUMO chain formation is required for response to replication arrest in S. pombe. PLoS One 4, e6750, (2009).
84. Saitoh, H. and Hinchey, J. Functional heterogeneity of small ubiquitin-related protein modifiers SUMO-1 versus SUMO-2/3. J. Biol. Chem 275, 6252-6258, (2000).
85. Uzunova, K., Gottsche, K., Miteva, M. et al. Ubiquitin-dependent proteolytic control of SUMO conjugates. J. Biol. Chem 282, 34167-34175, (2007).
86. Tatham, M. H., Geoffroy, M. C., Shen, L. et al. RNF4 is a poly-SUMO-specific E3 ubiquitin ligase required for arsenic-induced PML degradation. Nat. Cell Biol 10, 538-546, (2008).
87. Lallemand-Breitenbach, V., Jeanne, M., Benhenda, S. et al. Arsenic degrades PML or PML-RARalpha through a SUMO-triggered RNF4/ubiquitin-mediated pathway. Nat. Cell Biol 10, 547-555, (2008).
88. Mukhopadhyay, D., Arnaoutov, A. and Dasso, M. The SUMO protease SENP6 is essential for inner kinetochore assembly. J. Cell Biol 188, 681-692, (2010).
89. Yin, Y., Seifert, A., Chua, J. S. et al. SUMO-targeted ubiquitin E3 ligase RNF4 is required for the response of human cells to DNA damage. Genes Dev 26, 1196-1208, (2012).
90. Sun, H. and Hunter, T. Poly-small ubiquitin-like modifier (PolySUMO)-binding proteins identified through a string search. J. Biol. Chem 287, 42071-42083, (2012).
91. Erker, Y., Neyret-Kahn, H., Seeler, J. S. et al. Arkadia, a novel SUMO-targeted ubiquitin ligase involved in PML degradation. Mol. Cell Biol 33, 2163-2177, (2013).
92. Hayashi, T., Seki, M., Maeda, D. et al. Ubc9 is essential for viability of higher eukaryotic cells. Exp. Cell Res 280, 212-221, (2002).
93. Nacerddine, K., Lehembre, F., Bhaumik, M. et al. The SUMO pathway is essential for nuclear integrity and chromosome segregation in mice. Dev. Cell 9, 769-779, (2005).
94. Cremona, C. A., Sarangi, P., Yang, Y. et al. Extensive DNA damage-induced sumoylation contributes to replication and repair and acts in addition to the mec1 checkpoint. Mol. Cell 45, 422-432, (2012).
95. Johnson, E. S. and Blobel, G. Cell cycle-regulated attachment of the ubiquitin-related protein SUMO to the yeast septins. J. Cell Biol 147, 981-994, (1999).
96. Psakhye, I. and Jentsch, S. Protein group modification and synergy in the SUMO pathway as exemplified in DNA repair. Cell 151, 807-820, (2012).
97. Johnson, E. S. and Gupta, A. A. An E3-like factor that promotes SUMO conjugation to the yeast septins. Cell 106, 735-744, (2001).
98. Reindle, A., Belichenko, I., Bylebyl, G. R. et al. Multiple domains in Siz SUMO ligases contribute to substrate selectivity. J. Cell Sci 119, 4749-4757, (2006).
99. Cubenas-Potts, C., Goeres, J. D. and Matunis, M. J. SENP1 and SENP2 Affect Spatial and Temporal Control of Sumoylation in Mitosis. Mol. Biol. Cell 24, 3483-3495, (2013).
100. Leisner, C., Kammerer, D., Denoth, A. et al. Regulation of mitotic spindle asymmetry by SUMO and the spindle-assembly checkpoint in yeast. Curr. Biol 18, 1249-1255, (2008).
101. Takahashi, Y., Mizoi, J., Toh, E. and Kikuchi, Y. Yeast Ulp1, an Smt3-specific protease, associates with nucleoporins. J. Biochem 128, 723-725, (2000).
102. Haindl, M., Harasim, T., Eick, D. and Muller, S. The nucleolar SUMO-specific protease SENP3 reverses SUMO modification of nucleophosmin and is required for rRNA processing. EMBO Rep 9, 273-279, (2008).

103. Gong, L. and Yeh, E. T. Characterization of a family of nucleolar SUMO-specific proteases with preference for SUMO-2 or SUMO-3. J. Biol. Chem 281, 15869-15877, (2006).

104. Mukhopadhyay, D., Ayaydin, F., Kolli, N. et al. SUSP1 antagonizes formation of highly SUMO2/3-conjugated species. J. Cell Biol 174, 939-949, (2006).

105. Shen, L. N., Geoffroy, M. C., Jaffray, E. G. and Hay, R. T. Characterization of SENP7, a SUMO-2/3-specific isopeptidase. Biochem. J 421, 223-230, (2009).

106. Hattersley, N., Shen, L., Jaffray, E. G. and Hay, R. T. The SUMO protease SENP6 is a direct regulator of PML nuclear bodies. Mol. Biol. Cell 22, 78-90, (2011).

107. Reverter, D. and Lima, C. D. A basis for SUMO protease specificity provided by analysis of human Senp2 and a Senp2-SUMO complex. Structure 12, 1519-1531, (2004).

108. Shen, L. N., Dong, C., Liu, H., Naismith, J. H. and Hay, R. T. The structure of SENP1-SUMO-2 complex suggests a structural basis for discrimination between SUMO paralogues during processing. Biochem. J 397, 279-288, (2006).

109. Shen, L., Tatham, M. H., Dong, C. et al. SUMO protease SENP1 induces isomerization of the scissile peptide bond. Nat. Struct. Mol. Biol 13, 1069-1077, (2006).

110. Sharma, P., Yamada, S., Lualdi, M., Dasso, M. and Kuehn, M. R. Senp1 is essential for desumoylating Sumo1-modified proteins but dispensable for Sumo2 and Sumo3 deconjugation in the mouse embryo. Cell Rep 3, 1640-1650, (2013).

111. Reverter, D. and Lima, C. D. Structural basis for SENP2 protease interactions with SUMO precursors and conjugated substrates. Nat. Struct. Mol. Biol 13, 1060-1068, (2006).

112. Bekes, M., Prudden, J., Srikumar, T. et al. The dynamics and mechanism of SUMO chain deconjugation by SUMO-specific proteases. J. Biol. Chem 286, 10238-10247, (2011).

113. Mikolajczyk, J., Drag, M., Bekes, M. et al. Small ubiquitin-related modifier (SUMO)-specific proteases: profiling the specificities and activities of human SENPs. J. Biol. Chem 282, 26217-26224, (2007).

114. Di, B. A., Ouyang, J., Lee, H. Y. et al. The SUMO-specific protease SENP5 is required for cell division. Mol. Cell Biol 26, 4489-4498, (2006).

115. Lima, C. D. and Reverter, D. Structure of the human SENP7 catalytic domain and poly-SUMO deconjugation activities for SENP6 and SENP7. J. Biol. Chem 283, 32045-32055, (2008).

116. Kolli, N., Mikolajczyk, J., Drag, M. et al. Distribution and paralogue specificity of mammalian deSUMOylating enzymes. Biochem. J 430, 335-344, (2010).

117. Drag, M., Mikolajczyk, J., Krishnakumar, I. M., Huang, Z. and Salvesen, G. S. Activity profiling of human deSUMOylating enzymes (SENPs) with synthetic substrates suggests an unexpected specificity of two newly characterized members of the family. Biochem. J 409, 461-469, (2008).

118. Witty, J., Aguilar-Martinez, E. and Sharrocks, A. D. SENP1 participates in the dynamic regulation of Elk-1 SUMOylation. Biochem. J 428, 247-254, (2010).

119. Van, N. T., Angkasekwinai, P., Dou, H. et al. SUMO-specific protease 1 is critical for early lymphoid development through regulation of STAT5 activation. Mol. Cell 45, 210-221, (2012).

120. Chang, T. H., Xu, S., Tailor, P., Kanno, T. and Ozato, K. The small ubiquitin-like modifier-deconjugating enzyme sentrin-specific peptidase 1 switches IFN regulatory factor 8 from a repressor to an activator during macrophage activation. J. Immunol 189, 3548-3556, (2012).

121. Zhang, L. J., Vogel, W. K., Liu, X. et al. Coordinated regulation of transcription factor Bcl11b activity in thymocytes by the mitogen-activated protein kinase (MAPK) pathways and protein sumoylation. J. Biol. Chem 287, 26971-26988, (2012).

122. Cheng, J., Kang, X., Zhang, S. and Yeh, E. T. SUMO-specific protease 1 is essential for stabilization of HIF1alpha during hypoxia. Cell 131, 584-595, (2007).

123. Xu, Y., Zuo, Y., Zhang, H. et al. Induction of SENP1 in endothelial cells contributes to hypoxia-driven VEGF expression and angiogenesis. J. Biol. Chem 285, 36682-36688, (2010).

124. Kang, X., Qi, Y., Zuo, Y. et al. SUMO-specific protease 2 is essential for suppression of polycomb group protein-mediated gene silencing during embryonic development. Mol. Cell 38, 191-201, (2010).

125. Lee, M. H., Mabb, A. M., Gill, G. B., Yeh, E. T. and Miyamoto, S. NF-kappaB induction of the SUMO protease SENP2: A negative feedback loop to attenuate cell survival response to genotoxic stress. Mol. Cell 43, 180-191, (2011).

126. Yun, C., Wang, Y., Mukhopadhyay, D. et al. Nucleolar protein B23/nucleophosmin regulates the vertebrate SUMO pathway through SENP3 and SENP5 proteases. J. Cell Biol 183, 589-595, (2008).
127. Finkbeiner, E., Haindl, M. and Muller, S. The SUMO system controls nucleolar partitioning of a novel mammalian ribosome biogenesis complex. EMBO J 30, 1067-1078, (2011).
128. Klein, U. R., Haindl, M., Nigg, E. A. and Muller, S. RanBP2 and SENP3 function in a mitotic SUMO2/3 conjugation-deconjugation cycle on Borealin. Mol. Biol. Cell 20, 410-418, (2009).
129. Zunino, R., Schauss, A., Rippstein, P., Andrade-Navarro, M. and McBride, H. M. The SUMO protease SENP5 is required to maintain mitochondrial morphology and function. J. Cell Sci 120, 1178-1188, (2007).
130. Zunino, R., Braschi, E., Xu, L. and McBride, H. M. Translocation of SenP5 from the nucleoli to the mitochondria modulates DRP1-dependent fission during mitosis. J. Biol. Chem 284, 17783-17795, (2009).
131. Fu, H., Liu, N., Dong, Q. et al. SENP6-mediated M18BP1 deSUMOylation regulates CENP-A centromeric localization. Cell Res 29, 254-257, (2019).
132. Gibbs-Seymour, I., Oka, Y., Rajendra, E. et al. Ubiquitin-SUMO Circuitry Controls Activated Fanconi Anemia ID Complex Dosage in Response to DNA Damage. Mol. Cell 57, 150-164, (2015).
133. Kuo, C. Y., Li, X., Kong, X. Q. et al. An arginine-rich motif of ring finger protein 4 (RNF4) oversees the recruitment and degradation of the phosphorylated and SUMOylated Kruppel-associated box domain-associated protein 1 (KAP1)/TRIM28 protein during genotoxic stress. J. Biol. Chem 289, 20757-20772, (2014).
134. Li, J., Lu, D., Dou, H. et al. Desumoylase SENP6 maintains osteochondroprogenitor homeostasis by suppressing the p53 pathway. Nat Commun 9, 143, (2018).
135. Dou, H., Huang, C., Singh, M., Carpenter, P. B. and Yeh, E. T. Regulation of DNA repair through deSUMOylation and SUMOylation of replication protein A complex. Mol. Cell 39, 333-345, (2010).
136. Liu, X., Chen, W., Wang, Q., Li, L. and Wang, C. Negative regulation of TLR inflammatory signaling by the SUMO-deconjugating enzyme SENP6. PLoS Pathog 9, e1003480, (2013).
137. Garvin, A. J., Densham, R. M., Blair-Reid, S. A. et al. The deSUMOylase SENP7 promotes chromatin relaxation for homologous recombination DNA repair. EMBO Rep 14, 975-983, (2013).
138. Romeo, K., Louault, Y., Cantaloube, S. et al. The SENP7 SUMO-Protease Presents a Module of Two HP1 Interaction Motifs that Locks HP1 Protein at Pericentric Heterochromatin. Cell Rep 10, 771-782, (2015).
139. Maison, C., Romeo, K., Bailly, D. et al. The SUMO protease SENP7 is a critical component to ensure HP1 enrichment at pericentric heterochromatin. Nat. Struct. Mol. Biol 19, 458-460, (2012).
140. Cui, Y., Yu, H., Zheng, X. et al. SENP7 Potentiates cGAS Activation by Relieving SUMO-Mediated Inhibition of Cytosolic DNA Sensing. PLoS Pathog 13, e1006156, (2017).
141. Schulz, S., Chachami, G., Kozaczkiewicz, L. et al. Ubiquitin-specific protease-like 1 (USPL1) is a SUMO isopeptidase with essential, non-catalytic functions. EMBO Rep 13, 930-938, (2012).
142. Hutten, S., Chachami, G., Winter, U., Melchior, F. and Lamond, A. I. A role for the Cajal-body-associated SUMO isopeptidase USPL1 in snRNA transcription mediated by RNA polymerase II. J. Cell Sci 127, 1065-1078, (2014).
143. Shin, E. J., Shin, H. M., Nam, E. et al. DeSUMOylating isopeptidase: a second class of SUMO protease. EMBO Rep 13, 339-346, (2012).
144. Suh, H. Y., Kim, J. H., Woo, J. S. et al. Crystal structure of DeSI-1, a novel deSUMOylase belonging to a putative isopeptidase superfamily. Proteins 80, 2099-2104, (2012).
145. Verger, A., Perdomo, J. and Crossley, M. Modification with SUMO. A role in transcriptional regulation. EMBO Rep 4, 137-142, (2003).
146. Dasso, M. Emerging roles of the SUMO pathway in mitosis. Cell Div 3, 5, (2008).
147. Cuijpers, S. A. G. and Vertegaal, A. C. O. Guiding Mitotic Progression by Crosstalk between Post-translational Modifications. Trends in biochemical sciences 43, 251-268, (2018).
148. Finkbeiner, E., Haindl, M., Raman, N. and Muller, S. SUMO routes ribosome maturation. Nucleus 2, 527-532, (2011).
149. Jackson, S. P. and Durocher, D. Regulation of DNA damage responses by ubiquitin and SUMO. Mol. Cell 49, 795-807, (2013).
150. Jackson, S. P. and Bartek, J. The DNA-damage response in human biology and disease. Nature 461, 1071-1078, (2009).
151. Marteijn, J. A., Lans, H., Vermeulen, W. and Hoeijmakers, J. H. Understanding nucleotide excision repair and its roles in cancer and ageing. Nat Rev Mol Cell Biol 15, 465-481, (2014).

152. Baba, D., Maita, N., Jee, J. G. et al. Crystal structure of thymine DNA glycosylase conjugated to SUMO-1. Nature 435, 979-982, (2005).

153. Steinacher, R. and Schar, P. Functionality of human thymine DNA glycosylase requires SUMO-regulated changes in protein conformation. Curr. Biol 15, 616-623, (2005).

154. Galanty, Y., Belotserkovskaya, R., Coates, J. et al. Mammalian SUMO E3-ligases PIAS1 and PIAS4 promote responses to DNA double-strand breaks. Nature 462, 935-939, (2009).

155. Morris, J. R., Boutell, C., Keppler, M. et al. The SUMO modification pathway is involved in the BRCA1 response to genotoxic stress. Nature 462, 886-890, (2009).

156. Bekker-Jensen, S. and Mailand, N. Assembly and function of DNA double-strand break repair foci in mammalian cells. DNA repair 9, 1219-1228, (2010).

157. Lukas, J., Lukas, C. and Bartek, J. More than just a focus: The chromatin response to DNA damage and its role in genome integrity maintenance. Nature cell biology 13, 1161-1169, (2011).

158. Galanty, Y., Belotserkovskaya, R., Coates, J. and Jackson, S. P. RNF4, a SUMO-targeted ubiquitin E3 ligase, promotes DNA double-strand break repair. Genes Dev 26, 1179-1195, (2012).

159. Sin, Y., Tanaka, K. and Saijo, M. The C-terminal Region and SUMOylation of Cockayne Syndrome Group B Protein Play Critical Roles in Transcription-coupled Nucleotide Excision Repair. J. Biol. Chem 291, 1387-1397, (2016).

160. Puumalainen, M. R., Ruthemann, P., Min, J. H. and Naegeli, H. Xeroderma pigmentosum group C sensor: unprecedented recognition strategy and tight spatiotemporal regulation. Cellular and molecular life sciences : CMLS 73, 547-566, (2016).

161. Sugasawa, K., Ng, J. M., Masutani, C. et al. Xeroderma pigmentosum group C protein complex is the initiator of global genome nucleotide excision repair. Molecular cell 2, 223-232, (1998).

162. Kim, J. K., Soni, S. D., Arakali, A. V., Wallace, J. C. and Alderfer, J. L. Solution structure of a nucleic acid photoproduct of deoxyfluorouridylyl-(3'-5')-thymidine monophosphate (d-FpT) determined by NMR and restrained molecular dynamics: structural comparison of two sequence isomer photoadducts (d-U5p5T and d-T5p5U). Nucleic acids research 23, 1810-1815, (1995).

163. Jing, Y., Kao, J. F. and Taylor, J. S. Thermodynamic and base-pairing studies of matched and mismatched DNA dodecamer duplexes containing cis-syn, (6-4) and Dewar photoproducts of TT. Nucleic acids research 26, 3845-3853, (1998).

164. McAteer, K., Jing, Y., Kao, J., Taylor, J. S. and Kennedy, M. A. Solution-state structure of a DNA dodecamer duplex containing a Cis-syn thymine cyclobutane dimer, the major UV photoproduct of DNA. Journal of molecular biology 282, 1013-1032, (1998).

165. Sugasawa, K., Okamoto, T., Shimizu, Y. et al. A multistep damage recognition mechanism for global genomic nucleotide excision repair. Genes & development 15, 507-521, (2001).

166. Reardon, J. T. and Sancar, A. Recognition and repair of the cyclobutane thymine dimer, a major cause of skin cancers, by the human excision nuclease. Genes & development 17, 2539-2551, (2003).

167. Tang, J. Y., Hwang, B. J., Ford, J. M., Hanawalt, P. C. and Chu, G. Xeroderma pigmentosum p48 gene enhances global genomic repair and suppresses UV-induced mutagenesis. Molecular cell 5, 737-744, (2000).

168. Wakasugi, M., Shimizu, M., Morioka, H. et al. Damaged DNA-binding protein DDB stimulates the excision of cyclobutane pyrimidine dimers in vitro in concert with XPA and replication protein A. The Journal of biological chemistry 276, 15434-15440, (2001).

169. Groisman, R., Polanowska, J., Kuraoka, I. et al. The ubiquitin ligase activity in the DDB2 and CSA complexes is differentially regulated by the COP9 signalosome in response to DNA damage. Cell 113, 357-367, (2003).

170. Scrima, A., Fischer, E. S., Lingaraju, G. M. et al. Detecting UV-lesions in the genome: The modular CRL4 ubiquitin ligase does it best! FEBS Lett 585, 2818-2825, (2011).

171. Sugasawa, K., Okuda, Y., Saijo, M. et al. UV-induced ubiquitylation of XPC protein mediated by UV-DDB-ubiquitin ligase complex. Cell 121, 387-400, (2005).

172. Kapetanaki, M. G., Guerrero-Santoro, J., Bisi, D. C. et al. The DDB1-CUL4ADDB2 ubiquitin ligase is deficient in xeroderma pigmentosum group E and targets histone H2A at UV-damaged DNA sites. Proceedings of the National Academy of Sciences of the United States of America 103, 2588-2593, (2006).

173. Wang, H., Zhai, L., Xu, J. et al. Histone H3 and H4 ubiquitylation by the CUL4-DDB-ROC1 ubiquitin ligase facilitates cellular response to DNA damage. Molecular cell 22, 383-394, (2006).

174. Guerrero-Santoro, J., Kapetanaki, M. G., Hsieh, C. L. et al. The cullin 4B-based UV-damaged DNA-binding protein ligase binds to UV-damaged chromatin and ubiquitinates histone H2A. Cancer research 68, 5014-5022, (2008).
175. Nag, A., Bondar, T., Shiv, S. and Raychaudhuri, P. The xeroderma pigmentosum group E gene product DDB2 is a specific target of cullin 4A in mammalian cells. Molecular and cellular biology 21, 6738-6747, (2001).
176. Matsumoto, S., Fischer, E. S., Yasuda, T. et al. Functional regulation of the DNA damage-recognition factor DDB2 by ubiquitination and interaction with xeroderma pigmentosum group C protein. Nucleic acids research 43, 1700-1713, (2015).
177. Wang, Q. E., Zhu, Q., Wani, G. et al. DNA repair factor XPC is modified by SUMO-1 and ubiquitin following UV irradiation. Nucleic Acids Res 33, 4023-4034, (2005).
178. Poulsen, S. L., Hansen, R. K., Wagner, S. A. et al. RNF111/Arkadia is a SUMO-targeted ubiquitin ligase that facilitates the DNA damage response. J. Cell Biol 201, 797-807, (2013).
179. Akita, M., Tak, Y. S., Shimura, T. et al. SUMOylation of xeroderma pigmentosum group C protein regulates DNA damage recognition during nucleotide excision repair. Scientific reports 5, 10984, (2015).
180. van Cuijk, L., van Belle, G. J., Turkyilmaz, Y. et al. SUMO and ubiquitin-dependent XPC exchange drives nucleotide excision repair. Nature communications 6, 7499, (2015).
181. Evans, E., Moggs, J. G., Hwang, J. R., Egly, J. M. and Wood, R. D. Mechanism of open complex and dual incision formation by human nucleotide excision repair factors. The EMBO journal 16, 6559-6573, (1997).
182. Wakasugi, M. and Sancar, A. Assembly, subunit composition, and footprint of human DNA repair excision nuclease. Proceedings of the National Academy of Sciences of the United States of America 95, 6669-6674, (1998).
183. Missura, M., Buterin, T., Hindges, R. et al. Double-check probing of DNA bending and unwinding by XPA-RPA: an architectural function in DNA repair. The EMBO journal 20, 3554-3564, (2001).
184. Ogi, T., Limsirichaikul, S., Overmeer, R. M. et al. Three DNA polymerases, recruited by different mechanisms, carry out NER repair synthesis in human cells. Mol. Cell 37, 714-727, (2010).
185. Moser, J., Kool, H., Giakzidis, I. et al. Sealing of chromosomal DNA nicks during nucleotide excision repair requires XRCC1 and DNA ligase III alpha in a cell-cycle-specific manner. Molecular cell 27, 311-323, (2007).
186. Vermeulen, W. and Fousteri, M. Mammalian transcription-coupled excision repair. Cold Spring Harb. Perspect. Biol 5, a012625, (2013).
187. Groisman, R., Kuraoka, I., Chevallier, O. et al. CSA-dependent degradation of CSB by the ubiquitin-proteasome pathway establishes a link between complementation factors of the Cockayne syndrome. Genes Dev 20, 1429-1434, (2006).
188. Schwertman, P., Lagarou, A., Dekkers, D. H. et al. UV-sensitive syndrome protein UVSSA recruits USP7 to regulate transcription-coupled repair. Nat. Genet 44, 598-602, (2012).
189. Nakazawa, Y., Sasaki, K., Mitsutake, N. et al. Mutations in UVSSA cause UV-sensitive syndrome and impair RNA polymerase IIo processing in transcription-coupled nucleotide-excision repair. Nat. Genet 44, 586-592, (2012).
190. Zhang, X., Horibata, K., Saijo, M. et al. Mutations in UVSSA cause UV-sensitive syndrome and destabilize ERCC6 in transcription-coupled DNA repair. Nat. Genet 44, 593-597, (2012).
191. Fei, J. and Chen, J. KIAA1530 protein is recruited by Cockayne syndrome complementation group protein A (CSA) to participate in transcription-coupled repair (TCR). J. Biol. Chem 287, 35118-35126, (2012).
192. Tornaletti, S. and Hanawalt, P. C. Effect of DNA lesions on transcription elongation. Biochimie 81, 139-146, (1999).
193. Wilson, M. D., Harreman, M. and Svejstrup, J. Q. Ubiquitylation and degradation of elongating RNA polymerase II: the last resort. Biochim Biophys Acta 1829, 151-157, (2013).
194. Sigurdsson, S., Dirac-Svejstrup, A. B. and Svejstrup, J. Q. Evidence that transcript cleavage is essential for RNA polymerase II transcription and cell viability. Mol Cell 38, 202-210, (2010).
195. Woudstra, E. C., Gilbert, C., Fellows, J. et al. A Rad26-Def1 complex coordinates repair and RNA pol II proteolysis in response to DNA damage. Nature 415, 929-933, (2002).
196. Anindya, R., Aygun, O. and Svejstrup, J. Q. Damage-induced ubiquitylation of human RNA polymerase II by the ubiquitin ligase Nedd4, but not Cockayne syndrome proteins or BRCA1. Mol. Cell 28, 386-397, (2007).

197. Harreman, M., Taschner, M., Sigurdsson, S. et al. Distinct ubiquitin ligases act sequentially for RNA polymerase II polyubiquitylation. Proceedings of the National Academy of Sciences of the United States of America 106, 20705-20710, (2009).

198. Kuznetsova, A. V., Meller, J., Schnell, P. O. et al. von Hippel-Lindau protein binds hyperphosphorylated large subunit of RNA polymerase II through a proline hydroxylation motif and targets it for ubiquitination. Proceedings of the National Academy of Sciences of the United States of America 100, 2706-2711, (2003).

199. Bregman, D. B., Halaban, R., van Gool, A. J. et al. UV-induced ubiquitination of RNA polymerase II: a novel modification deficient in Cockayne syndrome cells. Proc. Natl. Acad. Sci. U. S. A 93, 11586-11590, (1996).

200. Ratner, N., Bloom, G. S. and Brady, S. T. A role for cyclin-dependent kinase(s) in the modulation of fast anterograde axonal transport: effects defined by olomoucine and the APC tumor suppressor protein. J. Neurosci 18, 7717-7726, (1998).

201. Starita, L. M., Horwitz, A. A., Keogh, M. C. et al. BRCA1/BARD1 ubiquitinate phosphorylated RNA polymerase II. J Biol Chem 280, 24498-24505, (2005).

202. Kleiman, F. E., Wu-Baer, F., Fonseca, D. et al. BRCA1/BARD1 inhibition of mRNA 3' processing involves targeted degradation of RNA polymerase II. Genes Dev 19, 1227-1237, (2005).

203. Becker, J., Barysch, S. V., Karaca, S. et al. Detecting endogenous SUMO targets in mammalian cells and tissues. Nat. Struct. Mol. Biol 20, 525-531, (2013).

204. Bruderer, R., Tatham, M. H., Plechanovova, A. et al. Purification and identification of endogenous polySUMO conjugates. EMBO Rep 12, 142-148, (2011).

205. Hendriks, I. A. and Vertegaal, A. C. Label-Free Identification and Quantification of SUMO Target Proteins. Methods Mol. Biol 1475, 171-193, (2016).

206. Knuesel, M., Cheung, H. T., Hamady, M., Barthel, K. K. and Liu, X. A method of mapping protein sumoylation sites by mass spectrometry using a modified small ubiquitin-like modifier 1 (SUMO-1) and a computational program. Mol. Cell Proteomics 4, 1626-1636, (2005).

207. Wohlschlegel, J. A., Johnson, E. S., Reed, S. I. and Yates, J. R., III. Improved identification of SUMO attachment sites using C-terminal SUMO mutants and tailored protease digestion strategies. J. Proteome. Res 5, 761-770, (2006).

CHAPTER 2

Ubiquitin-dependent and Independent Roles of SUMO in Proteostasis

Frauke Liebelt[1] and Alfred C.O. Vertegaal[1]

[1]Department of Cell and Chemical biology, Leiden University Medical Center, 2300 RC Leiden, The Netherlands.

Published in *Am J Physiol Cell Physiol* in 2016

ABSTRACT

Cellular proteomes are continuously undergoing alterations as a result of new production of proteins, protein folding, and degradation of proteins. The proper equilibrium of these processes is known as proteostasis, implying that proteomes are in homeostasis. Stress conditions can affect proteostasis due to the accumulation of misfolded proteins as a result of overloading the degradation machinery. Proteostasis is affected in neurodegenerative diseases like Alzheimer's disease, Parkinson's disease, and multiple polyglutamine disorders including Huntington's disease. Owing to a lack of proteostasis, neuronal cells build up toxic protein aggregates in these diseases. Here, we review the role of the ubiquitin-like posttranslational modification SUMO in proteostasis. SUMO alone contributes to protein homeostasis by influencing protein signaling or solubility. However, the main contribution of SUMO is the ability to cooperate, complement, and balance the ubiquitin-proteasome system at multiple levels. We discuss the identification of enzymes involved in the interplay between SUMO and ubiquitin, exploring the complexity of this crosstalk which regulates proteostasis. These enzymes include SUMO-targeted ubiquitin ligases and ubiquitin proteases counteracting these ligases. Additionally, we review the role of SUMO in brain-related diseases, where SUMO is primarily investigated because of its role during formation of aggregates, either independently or in cooperation with ubiquitin. Detailed understanding of the role of SUMO in these diseases could lead to novel treatment options.

Proteostasis refers to the ability of the cell to adapt to stresses and protect the normal function of individual proteins in the proteome. Proteins are the key workforce of the cell; therefore, keeping them in a balanced equilibrium by maintaining their folding and regulating their expression and degradation is critical for proper functioning of the cell[1,2]. Multiple pathways are involved in the control of this pivotal task. Molecular chaperones assist in protein folding of newly synthesized or misfolded proteins, and their expression can be increased upon proteotoxic stresses, where they contribute to process the overload of unfolded or misfolded proteins[3]. Misfolded proteins are degraded by the ubiquitin proteasome system (UPS) via the attachment of the posttranslational modifier ubiquitin, which targets proteins to the proteasome for destruction. The proteasome is a multisubunit protein complex, which is highly conserved in eukaryotes, archaea, and even present in some eubacteria, indicating its importance[4]. The proteasome is able to degrade misfolded proteins and recycle amino acids which can be reused for protein synthesis[5]. Controlled degradation of proteins is important to prevent toxic protein aggregates and in the context of signaling[1]. Chaperones and the UPS are part of a complex proteostasis network (PN)[2]. Here we review how small ubiquitin-like modifiers (SUMOs) contribute to proteostasis. SUMOs are members of the family of ubiquitin-like proteins (UbLs)[6,7]. Common hallmarks of UbLs are the presence of an ubiquitin fold, a COOH-terminal Gly-Gly motif, and an enzymatic cascade which is needed for the conjugation to their substrates (Figure 1). Although different UbLs employ distinct sets of enzymes, the mature form of SUMO is first activated by the heterodimeric SUMO activating enzyme (E1) composed of SAE1 and SAE2 (also known as UbA2), which, in an ATP dependent two-step reaction, forms a thioester-bond with SUMO. After activation, SUMO is transferred to the single SUMO E2 conjugation enzyme Ubc9 (also known as UbE2I). Ubc9 is not only able to provide the activated SUMO, but is additionally involved in substrate binding and specificity. Ubc9 has binding affinity to the SUMOylation consensus motif within the substrate, which is defined by the amino acids composition ψKXE, where ψ stands for a large hydrophobic residue and X stands for any amino acid. Some SUMOylation targets harboring a consensus motif can be SUMOylated efficiently in vitro by the addition of the E1 and E2 only. In vivo the activity of SUMO E3 ligases is necessary for efficient conjugation of SUMO to its substrates. In yeast, four E3 ligases are identified so far, Siz1, Siz2, MMS21, and Zip3[8-11]. In mammals, an ability to catalyze the conjugation of SUMO to its target proteins is demonstrated for proteins belonging to the Siz/protein inhibitor of activated STAT (PIAS) family, the nucleoporin RANBP2 and ZNF451. Several other proteins are proposed as SUMO E3 ligases, including the human polycomb protein Pc2/CBX4[12], the topoisomerase I-binding protein TOPORS[13], the tumor suppressor P14 ARF[14,15], the RWD-containing SUMOylation enhancer RSUME[16], the small G protein which is specifically expressed in the striatum RHES[17], and the Fanconi anemia protein Slx4[18,19]. SUMO E3 ligases can strengthen the interaction between Ubc9 and the target substrate, or position Ubc9 in a way that is beneficial for the transfer of SUMO to the substrate, thereby stimulating SUMOylation.

The conjugation of SUMO is a tightly regulated and dynamic process, which can be reversed by SUMO-specific proteases. Ubiquitin-like specific proteases ULP1 and ULP2 are responsible for deSUMOylation of proteins and Saccharomyces cerevisiae. ULP1 also processes the SUMO precursor protein at its COOH terminus, which is needed for the conjugation of SUMO to a target protein. Two protein families act as SUMO proteases in mammals. Members of the Ulp/sentrin-specific protease (SENP) family process SUMO precursors and deSUMOylate conjugated targets. Members of the second family of SUMO proteases are desumoylating isopeptidase (DeSI) 1 and 2, which are primarily used for deconjugation of

SUMO (reviewed in refs. 20-22). Additionally, ubiquitin-specific protease-like 1 (USPL1) has been identified as a SUMO protease[23]. In S. cerevisiae, only a single SUMO isoform has been identified, SMT3. In mammals, the SUMO family consists of three members, SUMO1, 2, and 3, encoded by three different genes. Mature SUMO2 and 3 share 97% amino acid sequence identity and are so far not distinguishable through specific antibodies and therefore often referred to as SUMO2/3. The mammalian SUMO2 and SUMO3 as well as the yeast SMT3 can form polySUMO chains owing to their intrinsic ψKXE-type SUMO conjugation consensus motifs. Mammalian SUMO1 shares only 47% amino acid sequence with SUMO2 and 3. Because of the absence of the intrinsic ψKXE-type SUMO consensus motif, SUMO1 is not efficiently incorporated in SUMO chains but can be used to terminate a SUMO2/3 chain or can be conjugated to a target substrate as single moiety[24]. However, more recently, it was found that SUMO1 contains an inverted SUMOylation motif, enabling SUMO polymerization to some extent[25]. SUMO1 and SUMO2/3 share substrates but also target distinct sets of proteins[26]. Interestingly, SUMO1-deficient mice are viable because of the ability of SUMO2 and 3 to compensate for SUMO1 loss[27]. Knockout of SUMO2 is embryonically lethal, while mice lacking SUMO3 are viable. This observation can be explained by the fact that SUMO2 is the predominantly expressed isoform[28]. SUMOylation is a modification with numerous different functions, as it can activate or repress its target proteins, it can alter protein-protein interactions or result in changes in subcellular localization[6]. Interestingly, SUMOylation levels are dynamically regulated by various stresses, linking SUMO to regulation of cellular homeostasis. In this review, we will focus on the SUMO literature concentrating on the importance of SUMOylation in the homeostasis of proteins either directly or in cooperation with ubiquitin.

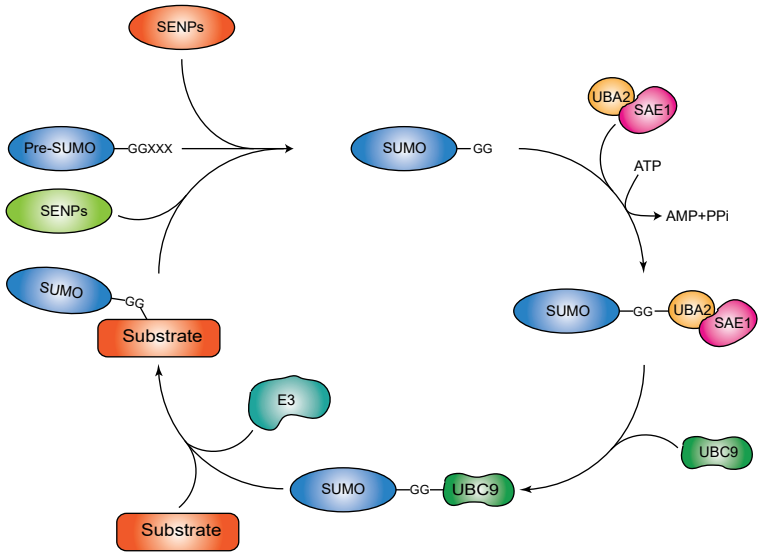

Figure 1. The SUMO cycle. The SUMO precursor protein is processed by SUMO proteases (SENPs) to expose the COOH-terminal GG motif. In an ATP-dependent step, the heterodimeric SUMO E1-activating enzyme, consisting of SAE1 and UbA2, forms a thioester bond with SUMO. SUMO is then transferred to Ubc9, the SUMO E2 conjugation enzyme, which is responsible for the isopeptide bond formation between the COOH terminal GG motif and the target lysine residue of the substrate. This step is enhanced by SUMO E3 ligases. The modification is reversible as SENPs can remove the SUMO moiety from the substrate.

SUMO IS INVOLVED IN PROTEOSTASIS VIA CROSSTALK WITH UbIQUITIN

The ubiquitin-proteasome system is the central mechanism of proteostasis and responsible for the regulated degradation of proteins and recycling of amino acids. SUMO is highly connected to this process as detailed below.

SUMO and ubiquitin can modify the same lysine residue in a protein

Recent advances in high-resolution mass spectrometry (MS) have enabled large-scale identification of SUMO acceptor lysines and ubiquitin acceptor lysines. The obtained results indicate that almost a quarter of SUMO-acceptor lysines are also used for ubiquitin conjugation, pointing towards extensive crosstalk between these modifications[29,30]. This kind of competition was first found in 1998 when Hay and coworkers showed that the inhibitor of NF-κB, IκB-α, could be SUMOylated at the same lysine residue that is also used for ubiquitination[31]. The modification of SUMO and ubiquitin of the same acceptor lysine can also act sequentially. This is illustrated by the serine hydroxymethyltransferase SHMT1, and the regulatory subunit of the IκB kinase, NEMO. For both proteins it was shown that SUMOylation stimulated their translocation to, and retention within, the nucleus. After cleavage of the SUMO moiety in the nucleus, the same lysine residue could be modified by ubiquitin, which stimulated subsequent export to the cytoplasm[32,33]. These examples illustrate that there is a tightly regulated balance, in time and space, between ubiquitin and SUMO targeting the same lysine within a protein, which determines function, localization, or stability.

The proliferating cell nuclear antigen (PCNA) is an intriguing example of the cooperative effect of SUMO and ubiquitin on the same acceptor lysine. PCNA encircles the DNA as a sliding clamp and accompanies processing DNA polymerases, additionally providing an important interaction stage for proteins involved in DNA repair (reviewed by ref. 34). In yeast, encountering a DNA lesion during replication leads to either mono- or polyubiquitination of PCNA at the lysine residue K164. While monoubiquitination stimulates the recruitment of translesion polymerases η and ζ to facilitate the error-prone DNA damage tolerance pathway, polyubiquitination of K164 promotes the error-free damage avoidance pathway[35,36]. SUMOylation of PCNA also targets K164. In contrast to the ubiquitination of PCNA, its modification by SUMO appears to be DNA damage independent but reliant on S-phase. In addition to the major SUMOylation site at K164, K127 is a minor SUMOylation site, increasingly used for modification after K164R mutagenesis[35]. SUMOylated PCNA recruits the helicase SRS2, which was shown to promote the DNA damage tolerance pathway and inhibits unscheduled homologous recombination in multiple studies[37-39]. SUMOylation of PCNA therefore promotes the ubiquitin-dependent tolerance pathway during S-phase, in case the replication fork encounters a lesion. Even though both modifications target the same lysine, the crosstalk is successive rather than competitive, comparable to the above mentioned regulation of NEMO and SHMT1.

The idea that SUMO and ubiquitin can modify the same acceptor lysine does not necessarily result in the need for successive modifications or competition. Ubiquitin and especially SUMO are only conjugated to a small subset of a given protein, making it possible for both modifiers to be present on the same lysine at the same time but in different subpopulations of the target proteins.

SUMO-targeted ubiquitin ligases

In addition to the model of exclusive occupation by either ubiquitin or SUMO at one acceptor site of a protein, there are indications that both modifications can form a hybrid chain. Site-specific mass spectrometry approaches have identified SUMOylation sites on endogenous ubiquitin at multiple positions[29]. Endogenous SUMO can also be modified by ubiquitin, preferably at the K11 position, which lies within a SUMOylation consensus site[40]. The establishment of SUMO-ubiquitin chains is catalyzed by a specific group of ubiquitin ligases, specifically targeting SUMOylated protein.

SUMOylation of a protein can directly serve as recognition signal for SUMO-targeted ubiquitin ligases (STUbLs)[41-43]. The ability of STUbLs to recognize SUMOylated proteins is mediated by their SUMO-interaction motifs (SIMs) and a RING domain, which enables them to bind to SUMOylated proteins and an E2 ubiquitin-conjugation enzyme, respectively. The presence of multiple SIMs, within the identified STUbLs, determines their preference for substrates with SUMO chains[42,43]. In S. cerevisiae, three potential STUbLs have been identified, ULS1, Slx5/Slx8, and RAD18. The ubiquitin ligase for SUMOylated proteins (ULS) 1 and the heterodimeric STUbL Slx5/Slx8 are responsible for the proteolytic control of SUMOylated proteins in yeast[43,44]. Notably, Slx5/Slx8 does not necessarily require SUMOylation of its targets, but its activity is stimulated by SUMOylation. This stimulation is likely explained by an enhancement of target-enzyme interaction via SIMs on the NH2 terminus of Slx5[45,46]. The ubiquitin ligase Rad18, which is responsible for the ubiquitination of the sliding clamp PCNA, is stimulated by the SUMOylation of PCNA in yeast. Human Rad18, however, does not show STUbL activity due to the lack of SIM motifs[47].

In humans, the E3 ubiquitin ligase RNF4 targets SUMO conjugates. RNF4 contains four putative SIMs, which show binding affinity not only to SUMO2 but also to SUMO1. However, RNF4 prefers to target proteins that are modified by SUMO chains of at least three SUMO moieties[48]. RNF4 regulates substrates involved in a multitude of pathways, including kinetochore assembly[49], cell survival upon hypoxic stress[50], mitogen-activated protein (MAP) kinase signaling[51], transcriptional responses to heat shock[52], ion transport[53], and the DNA damage response[54]. The most extensively studied substrate of RNF4 is the promyelocytic leukemia protein (PML). SUMOylation of PML is stimulated after treatment with arsenic trioxide (ATO), and SUMOylated PML is targeted by RNF4 for ubiquitination and subsequent proteasomal degradation[42,55,56]. Interestingly, it was shown that PML ubiquitination by RNF4 took place on PML itself but also on the SUMO moiety attached to PML, indicating the formation of a hybrid SUMO-ubiquitin chain[42]. PML was not only found to be SUMOylated and targeted by RNF4, but was additionally indicated to cooperate with RNF4 in the degradation of misfolded proteins in the nucleus. The polyQ pathogenic protein ataxin 1 (ATXN182Q), which is the causative, aggregation prone protein for a type of spinocerebellar ataxia (SCA), was shown to be SUMOylated. This SUMOylation was enhanced by PML and subsequently ATXN182Q could be targeted by RNF4 for ubiquitination and proteasomal degradation. RNF4 was further shown to reduce other misfolded proteins in the nucleus, including the polyQ huntingtin[57]. A general role of RNF4 in the degradation of misfolded proteins in the nucleus was proposed on the basis of this finding, highlighting the possibility of a therapeutic effect by manipulating SUMOylation in neurodegenerative diseases, which will be discussed in more detail later. Recently, the transcription factor and oncogene c-Myc was shown to be targeted by SUMO and ubiquitin modifications, regulated by RNF4. These modifications led to the rapid degradation of c-Myc in a proteasome-dependent manner. The authors showed that mutagenesis of all SUMOylation sites which were identified by mass spectrometry did

not lead to a reduced SUMOylation of c-Myc, suggesting that the attachment of SUMO to a lysine residue might be promiscuous within the protein[58]. These results are compatible with the idea that SUMO and ubiquitin modifications might be arbitrary in proteins that are targeted for degradation and the exact location of the modification plays a subordinate role here. A second human STUbL is the ubiquitin ligase RNF111, also called Arkadia. RNF111 with its three putative SIMs was identified in a bioinformatic screen for SIM-containing proteins[59]. RNF111 has previously been implicated in the TGF-β signaling pathway, where it is responsible for the ubiquitination and degradation of the negative regulators SMAD7, c-SKI, and SNON. As multiple factors involved in the TGF-β pathway are SUMOylated, including TGF-β receptor[60], SMAD3[61], SMAD4[62], and AXIN[63], the STUbL activity of RNF111 might be involved in the regulation of this pathway, but this remains largely speculative. One study showed that the SIMs of RNF111 are not needed for the degradation of c-Ski and SnoN. Intriguingly, like RNF4, RNF111 was shown to regulate the proteasomal degradation of SUMOylated PML upon ATO treatment, suggesting that both STUbLs are involved and important in the regulation of the PML nuclear bodies[64].

Hybrid SUMO-ubiquitin chains

The activity of STUbLs and the establishment of SUMO-ubiquitin chains on a protein can either act as a recruitment signal or can target proteins to the proteasome. Both processes seem to be especially important for the regulation of the chromatin environment[65-67]. The first identified hybrid SUMO-ubiquitin chain receptor involved in mediating recruitment of proteins to the chromatin is RAP80, a component of the BRCA1-A complex. RAP80 carries a tandem ubiquitin interaction motif (UIM) and a SIM, and it consistently shows preferential affinity for hybrid chains. The establishment of hybrid chains at DNA damage sites, through the activity of the SUMO-targeted ubiquitin ligase RNF4, recruits RAP80 and the BRCA1-A complex to DNA lesions[68]. In addition, the proteasomal subunit S5A/RPN10, which has protease activity, bears UIM and SIM motifs and it is intriguing to think that this protein could be responsible for the docking of hybrid SUMO-ubiquitin chains at the proteasome[69]. Furthermore, the targeting of a substrate to the proteasome via STUbL catalyzed SUMO-ubiquitin chains might possibly involve the recruitment of proteins mediating this process. A likely candidate is the AAA-ATPase P97. P97, or its yeast homologue CDC48, is able to extract ubiquitinated protein from the chromatin (reviewed by refs. 70,71). Interestingly, CDC48 and its cofactors UFD1 and NPL4 cooperate with SUMO at the chromatin. Yeast UFD1 exhibits a COOH-terminal SIM motif, which enables a noncovalent interaction between SUMO and the CDC48 UFD1-NPL4 complex[72]. Yeast UFD1 mutants displayed subnuclear foci of accumulated SUMO conjugates, indicating a role of UFD1 in the degradation of SUMOylated proteins[72,73]. Furthermore, the CDC48- UFD1-NPL4 complex was shown to physically interact with STUbLs[73]. These observations strengthened the idea that STUbL-induced proteasomal targeting of SUMO-conjugates could be facilitated by the segregase activity of CDC48, especially within the chromatin context where proteins might be “stuck” to the DNA and specific forces are needed to extract them. A site-specific mass spectrometry approach making use of genetic mutants of either the yeast STUbL subunit Slx8 or the CDC48 cofactor UFD1 identified a subset of proteins which were coordinately regulated by both. These proteins were associated with centrosomes and telomeres, showing the importance of CDC48 segregase activity on proteins bound to DNA[74]. In mammalian cells, the Fanconi anemia complex FANCI/FANCD2 (ID complex) is a target of RNF4-triggered extraction by p97. SUMOylation of the ID complex upon treatment with agents causing replication

fork stalling induced its RNF4-dependent ubiquitination. P97 together with its cofactor DVC1 was subsequently responsible for the removal of the ubiquitinated ID complex and therefore regulates the amount of activated FANCI and FANCD2 on the chromatin. Direct targeting of SUMOylated proteins by yeast CDC48 without the contribution of ubiquitin was demonstrated by Jentsch and coworkers[75]. They showed that the SUMOylated DNA repair factor RAD52 physically interacted with CDC48, leading to displacement from the chromatin of RAD52 together with its binding partner RAD51. This CDC48 effect was dependent on RAD52 SUMOylation as well as the SIM motif of Ufd1 and independent of ubiquitin, showing that CDC48 is able to directly target SUMOylated proteins[75].

SUMO deubiquitinases act on SUMO-ubiquitin chains

Signal transduction by hybrid SUMO-ubiquitin chains can be counteracted by a ubiquitin-protease with the ability to reverse the action of STUbLs. The deubiquitinating enzyme USP11 was identified as a binding partner of RNF4 through mass spectrometry analysis. In vitro experiments showed that USP11 was able to deubiquitinate hybrid SUMO2-ubiquitin chains produced by RNF4. USP11 could counteract RNF4 under normal growth conditions and within the DNA damage response[76,77]. Multiple studies showed the involvement of RNF4 and USP11 in the DNA damage response and reflect the importance of reversible ubiquitination of SUMOylated proteins[65-67,78,79]. The concept of a deubiquitinase that specifically targets hybrid SUMO-ubiquitin chains was further demonstrated by the identification of USP7 as SUMO deubiquitinase (SDUb) involved in DNA replication. USP7 was shown to establish the earlier observed SUMO-rich, ubiquitin-poor surroundings of replisomes by limiting ubiquitination of SUMOylated proteins, consistently hindering their clearance from the replication site. The authors also demonstrated that the clearance of the ubiquitinated SUMO conjugates was dependent on the action of the AAA-ATPase P97[80]. Taken together, the ability of cells to form hybrid chains between ubiquitin and SUMO, possibly branched or including different SUMO family member, opens up numerous possibilities of cooperative SUMO and ubiquitin signaling. Specific proteins are needed for the catalysis, recognition, and destabilization of hybrid chains, and only a few have been identified so far.

Ubiquitin-stimulated SUMOylation could be involved in stress responses

Multiple studies showed that, upon inhibition of the proteasome, ubiquitinated proteins as well as SUMO2/3-conjugated proteins accumulated[81,82]. The inability to degrade a SUMOylated protein via the ubiquitin-proteasome pathway after proteasome inhibition could be explanatory for the increase of SUMO conjugates. This explanation, however, implies a simultaneous increase of SUMO and ubiquitin conjugates, whereas it was shown that the increase of SUMO2/3 targets is delayed compared with ubiquitin accumulation[81,82]. A possible explanation for this observation is the direct stimulation of SUMOylation after proteasome inhibition. This possibility is supported by the finding that the accumulation of SUMO2/3-modified proteins after proteasome inhibition was likely triggered by newly synthesized misfolded proteins which failed to be degraded[82]. Interestingly, the authors of this paper showed that ubiquitin associated with the SUMO2/3 conjugates first decreased after proteasomal inhibition and then increased again with an enrichment of K63-linked ubiquitin chains, which were previously shown to be involved in the regulation of misfolded proteins. Therefore the accumulation of SUMO substrates in the cell upon proteasome inhibition is possibly only partly a result of the stabilization of SUMO substrates and might be explained by an active SUMOylation response upon misfolded protein stress. This

hypothesis is also supported by the finding that a significant amount of proteins that are SUMOylated upon heat shock, a stress-inducing unfolding of proteins, overlap with proteins that were SUMO modified after proteasome inhibition[29,82]. These data suggest a possible ubiquitination-stimulated SUMOylation of a subset of proteins.

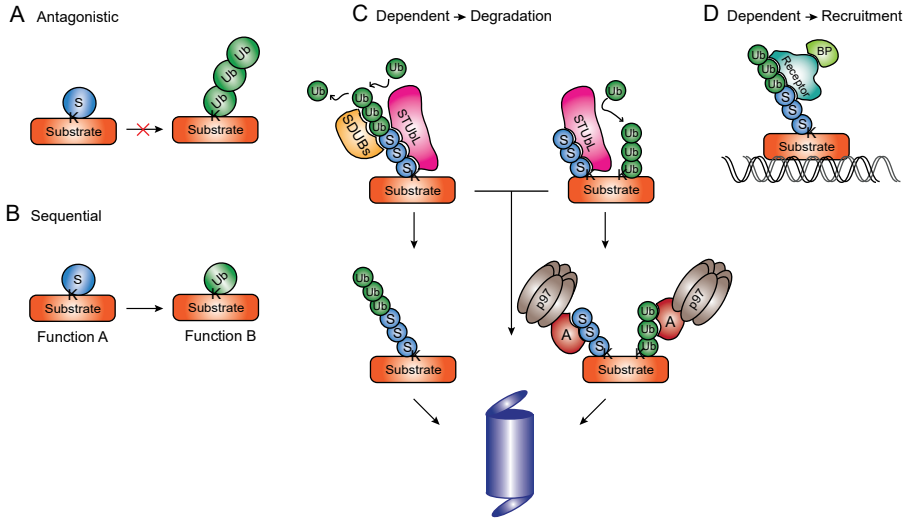

Figure 2. Crosstalk between ubiquitin and SUMO. SUMO and ubiquitin can influence one another in multiple ways as detailed below. (**A**) antagonistic. SUMO (S) and ubiquitin (Ub) can compete for the modification of acceptor lysines (K). SUMOylation could thereby antagonize the ubiquitination and subsequent degradation of a target protein (T). (**B**) sequential. SUMO and ubiquitin can modify the same lysine, thereby cooperatively controlling different functions of the target protein in space and time. (**C**) dependent-degradation. SUMO modification of a target protein can recruit a SUMO-targeted ubiquitin ligase (STUbL), which is able to ubiquitinate the protein either on the existing SUMO chain or on a different acceptor lysine. The ubiquitin chains can either direct the protein to the proteasome for degradation or recruit the CDC48/p97 chaperone via its adaptor proteins (A), which removes the ubiquitinated protein from the chromatin and delivers it to the proteasome. SUMO deubiquitinases (SDUBs) can reverse the action of STUbLs and remove ubiquitin from SUMOylated targets, thereby stabilizing the protein. (**D**) dependent recruitment. Hybrid chains of SUMO and ubiquitin generated by STUbLs can serve as recruitment platforms for receptors and binding partners (BP) at the chromatin.

SUMOYLATION REGULATES PROTEOSTASIS AT THE CHROMATIN LEVEL

Transcription factors and chromatin bound proteins are common targets of SUMOylation, and the modification of these factors results in either a repressive effect on gene expression or a transcriptional activation[83]. Investigating the positioning and functional consequences of SUMOylated chromatin bound proteins, revealed that SUMO conjugates were enriched on active chromatin and at promoters of histones and genes encoding protein biogenesis components as well as tRNA and rRNA genes. SUMOylation was shown to have a repressive function in all cases, because knockdown of Ubc9 resulted in an increased transcription of those genes[84]. Additionally, SUMO plays a role in global transcriptional downregulation in response to DNA damage[85]. These findings do not only indicate an overall repressive effect of SUMOylation on transcription factors and chromatin bound proteins, but also suggests that SUMOylation regulates protein homeostasis already at the transcriptional level. The

important role of SUMO in global transcriptional regulation is also reflected by the finding that the SUMO landscape at the chromatin is drastically changed upon heat shock (HS). HS increased the overall occurrence of SUMO at active chromatin, and SUMO was specifically enriched at promoters and lost from intergenic regions. Target genes of HS-induced chromatin-associated SUMO conjugates encode proteins involved in gene expression and posttranslational modification of RNA[86,87]. Data on the transcriptional consequences of the HS-induced SUMO recruitment to promoter regions indicate target-gene specific effects of SUMOylation. Palvimo and coworkers found that impaired SUMOylation resulted in higher transcriptional activation of genes responsive to HS, whereas HS induced repression was lost. They specifically showed that SUMO was enriched at the promoters of the heat shock protein (HSP) gene cluster upon HS and limited hyperactivation of the gene cluster, thus adapting a repressive role at those promoters[86]. In contrast, another study proposed that SUMOylation of chromatin-bound proteins upon HS is required for the maximal transcription of genes involved in cell death and survival while SUMO has a repressive effect on genes involved in gene expression and cell cycle progression. They propose a model in which SUMOylation might either act as a molecular glue to facilitate stability of protein complexes at the promoter of genes important for the stress response, or that SUMOylation might increase solubility of proteins at the chromatin and block aggregation, thereby facilitating a correct folding and functioning of chromatin-bound proteins[87]. The differences between the studies can possibly be explained by the usage of different cell lines and differences in analytical tools. Although these findings contributed to the overall understanding of SUMOylation activity at the chromatin level, the identity of the SUMO-targeted proteins at the different target genes remains to be established at large. Interestingly, Gardner and coworkers recently showed that the conserved transcriptional corepressor CYC8 is SUMOylated upon hyperosmotic stress in yeast. Loss of CYC8 SUMOylation leads to cytoplasmic inclusion formation of this protein. Thus, SUMO acts to maintain the proper function of CYC8 during hyperosmotic stress[88]. This provides an interesting example of the role of SUMO during stress to maintain the solubility and thereby the function of these proteins. SUMO could regulate other target proteins during stress in a similar manner to block their aggregation, thereby maintaining their functionality.

SUMOYLATION REGULATES PROTEIN AGGREGATION IN NEURODEGENERATIVE DISEASE

The direct and indirect roles of SUMO in proteostasis are increasingly of interest in diseases characterized by a deregulation of proteostasis, such as neurodegenerative diseases. A hallmark of neurodegenerative diseases is the progressive loss of neurons. While neurodegenerative diseases are clinically diverse, depending on the group of neurons affected, these diseases share some underlying impairments. Common compromised processes are mitochondrial function upon oxidative stress, RNA function and metabolism, the UPS system, and the altered solubility of specific disease-associated proteins[89-91]. The UPS system is being extensively investigated in this context, and failure of proper protein degradation plays an important part in the pathogenesis of neurodegenerative diseases[92]. SUMOylation is involved in multiple neurodegenerative diseases, where key proteins were found to be SUMO modified. Together with the ubiquitin system, or independently, SUMO affects protein-protein interaction, protein activity, and most importantly, stability and solubility of several disease-associated proteins (Table 1)[93]. Unraveling the influence of SUMO in these diseases can potentially lead to the development of novel drugs and

treatment strategies.

Alzheimer's disease

The molecular characteristics of Alzheimer's disease (AD) are extracellular senile plaques and intracellular neurofibrillary tangles, composed of aggregated amyloid-β (Aβ) peptides and aggregates of the microtubule-associated protein TAU, respectively[94,95]. The particular molecular causes of AD are still under investigation, but it is clear that AD is a complex, multifactorial disease. SUMOylation of the amyloid precursor protein (APP) was reported at two lysine residues, which were close to the cleavage site important for the production of Aβ. Interestingly, in the Swedish early-onset familiar form of AD, one of the identified SUMOylation sites is mutated, which indicates a potential role of SUMOylation in AD. Additionally, multiple studies reported changes in Aβ processing or production, because of manipulation of the SUMO pathway. However, the observed results are conflicting. While the RNAi knockdown of SUMO1 and SUMO2 does not affect Aβ production in HEK293 cells, it was shown that the SUMOylation of APP in HeLa cells negatively influenced the aggregation of Aβ[96,97]. Also, the effect of overexpressing SUMO3 was shown to either reduce[98] or increase[99] the production of Aβ. Dissimilarities can be explained by different experimental methods, partial redundancy of SUMO isoforms, indirect effects of manipulating the SUMO pathway, or overexpression effects. Nevertheless, involvement of SUMOylation in Aβ regulation is worth investigating in further detail. Neurofibrillary tangles, the second hallmark of AD, are aggregates of the hyperphosphorylated form of the microtubule associated, natively unfolded protein TAU, which in its nonhyperphosphorylated form is promoting tubulin stability[100,101]. The SUMOylation of TAU at lysine residue K340 promoted its hyperphosphorylation, resulting in a reduced ubiquitination, therefore potentially stabilizing TAU and promoting aggregation. In line with these findings, inhibiting the proteasome led to an increase in ubiquitination of TAU and a decrease in SUMOylation, suggesting that crosstalk between SUMOylation, ubiquitination, and phosphorylation plays a pivotal role during TAU aggregation[96,102]. The SUMOylation pathway seems to be involved in AD, although the precise molecular mechanism must be further elucidated. The establishment of a mouse model for AD which expresses tagged versions of SUMO isoforms would enable unbiased proteomic studies in a physiological context and would help to understand the global role of SUMO in the disease pathogenesis.

Parkinson's disease

Like TAU, α-SYNUCLEIN is a natively unfolded protein that is subject to protein modification by SUMO and is an important constituent of Lewy bodies. Lewy bodies are inclusions of proteins, including α-synuclein, which are hallmarks of Parkinson's disease (PD) and other so-called synucleinopathies, like dementia with Lewy bodies (DLB) and multiple system atrophy (MSA)[96,103]. In contrast to TAU, where SUMOylation was shown to promote aggregation, SUMOylation of α-SYNUCLEIN seems to increase solubility and protects against the cytotoxic effect of α-SYNUCLEIN inclusions[103,104].

Other proteins proposed to contribute to the pathogenesis of PD were reported to be SUMOylated. DJ-1, a multifunctional protein with a role in cytoprotection upon UV and oxidative stress, is strongly expressed in reactive astrocytes of patients with a sporadic form of PD and notably also in astrocytes adjacent to brain infarct regions[105,106]. SUMO1 can modify DJ-1 at K130 and consequently stimulate cell transformation and growth[107]. Mutagenesis of the K130 abolished DJ-1 function. Additionally, it was shown that a mutant

form of DJ-1, found in a small subset of PD patients, was improperly SUMOylated, which led to insolubility of DJ-1[108]. This shows that SUMOylation cannot only lead to an increased solubility of its targets, but SUMOylation at different sites can have opposite effects.

Parkin, an E3 ubiquitin ligase mutated in many cases of early-onset PD and immune-reactive with Lewy bodies in other forms of PD, was shown to selectively bind to SUMO1[109,110]. This interaction stimulated Parkin's translocation to the nucleus and its proteasomal degradation through an enhanced autoubiquitination[111]. Whether the interaction of SUMO and Parkin promotes or impedes cell survival is not yet completely understood as Parkin targets misfolded proteins and is involved in multiple processes dependent on its localization. Parkin as well as SUMOylation seem to be involved in mitochondrial fusion and fission, processes with particular importance in brain cells and neurodegeneration. Here, it was shown that the dynamine-related protein 1 (DRP1) is a target for conjugation by SUMO1, SUMO2, and SUMO3[112]. The modification of DRP1 by SUMO1 led to an increased mitochondrial fission, and SENP5 was shown to be the responsible SUMO protease in this process[113]. DRP1 is also a reported target of Parkin, which is responsible for DRP1 ubiquitination and subsequent degradation[114]. SUMOylation is thus involved in multiple processes of PD pathogenesis, and complex interplay between SUMO targets complicates the prediction of overall contribution of SUMOylation (reviewed by ref. 115).

Polyglutamine disorders

Protein aggregation and disruption of protein homeostasis is a common feature of polyglutamine disorders, characterized by the CAG repeat extension of genes which influences the gain of toxicity of their protein counterparts and their loss of normal function[116]. These diseases include Huntington's disease (HD), spinobulbar muscular atrophy (SBMA), dentatorubral-pallidoluysian atrophy (DRPLA), and spinocerebellar ataxias (SCA). SUMOylation of the toxic proteins appears to reduce their aggregation potential (Table 1)[117-120].

In Huntington's disease (HD), however, it is debated if the formation of inclusions of the causative mutant huntingtin protein (mHTT) is neurotoxic, with strong indications that this is a neuroprotective event[121-123]. Even though mHTT is found to be expressed in different cell types throughout the body, degeneration is restricted to the brain's corpus striatum. A proposed explanation for this observation is the presence of the E3 SUMO ligase Rhes in the corpus striatum. Rhes was able to stimulate the SUMOylation of mHTT, but not the wild type, and mHTT SUMOylation led to a decrease in aggregate formation and an increase of cytotoxicity in vitro and in vivo[119,124]. Rhes is an unusual SUMO E3 ligase, which shows no structural similarity with other SUMO E3s, but was shown to enhance cross-SUMOylation between the SUMO E1 and Ubc9 as well as thioester transfer from E1 to Ubc9[17]. The observation that mHTT is subject to modification by SUMO and that even though SUMOylation reduces aggregates, it has a cytotoxic rather than a cytoprotective role, illustrates that SUMOylation has diverse consequences on different disease-associated proteins in distinct neurodegenerative diseases.

Taken together, these neurodegenerative diseases, discussed above, all show the accumulation of proteins into aggregates and the involvement of SUMO in the regulation of this processes. It is, however, debatable whether those aggregates are causal or consequential, neurotoxic, or even neuroprotective. In addition, the contribution of SUMO seems to have diverse effects on different aggregates and various cellular outcomes which precludes attributing a general consequence to SUMOylation (Table 1). The range

Table 1. Involvement of SUMO in the formation of disease-associated protein aggregates

Disease	Effected protein	Consequence of aggregation	Influence of SUMO	Proposed net effect of SUMO on Cell viability	Reference
Alzheimer's Disease	AMYLOID β	Unknown if causal or consequential	Increases Aβ secretion	Negative	Dorval et al., 2007[99]
			Reduces aggregation	Positive	Zhang et al., 2008[97]
			Reduces Aβ secretion	Positive	Li et al., 2003[98]
			Increases Aβ secretion	Negative	Yun SM et al., 2013[127]
	TAU	Cytotoxic	Reduces solubility and Inhibits degradation	positive	Luo et al., 2014[102]
Parkinsons Disease	α-SYNUCLEIN	Cytotoxic	Increases solubility	positive	Krumova et al., 2011[103]
			Increases solubility	positive	Abeywardana et al., 2015[104]
	DJ-1	Associated with inclusions	Incorrect SUMOylation decreases solubility	positive and negative	Shinbo, 2006[108]
Huntington Disease	mHTT	Cytoprotective	Associates with aggregates	negative	O'Rourke et al., 2013[128]
			Stabilizes pathogenic fragment of HTT and reduces aggregation	negative	Steffan et al., 2004[119]
Spinobulbar muscular atrophy (SBMA)	ANDROGEN RECEPTOR	Cytotoxic	Increases solubility	positive	Mukherjee et al., 2009[118]
Spinocerebellar ataxin type7 (SCA7)	ATAXIN-7	Cytotoxic	Increases solubility	positive	Janer et al., 2010[117]
Dentatorubral-pallidoluysian atrophy (DRPLA)	ATROPHIN 1	Cytotoxic	Reduces aggregation	positive	Terashima, 2002[120]
Familiar amytrophic lateral sclerosis (FALS)	SOD1	Cytotoxic	Increases aggregation	negative	Fei 2006[129]

of mechanisms employed by SUMO to regulate the homeostasis of proteins is broad. The examples reviewed above show that SUMO can negatively affect protein aggregation, which is consistent with the findings that the fusion of SUMO to a protein enhances their solubility and is therefore often used as a method to produce recombinant proteins in Escherichia coli[125]. On the other hand, SUMOylation can stimulate the formation of protein complexes. Because of the existence of SIMs on proteins, which have a binding affinity to SUMO moieties attached to another protein, SUMO can stimulate complex formation. These SUMO-SIM interactions within a complex are proposed to be redundant, indicating that the overall SUMOylation status of protein complexes might be more important than SUMOylation of a single group member (reviewed by ref.126)

SUMO PLAYS A PROTECTIVE ROLE IN BRAIN ISCHEMIA

In addition to SUMO's upcoming role in neurodegenerative diseases, the role of SUMO is explored in other brain-related diseases that are connected to the distortion of proteostasis. Brain ischemia is characterized by a restriction of blood supply to a region of the brain, leading to oxygen and nutrient deprivation of cells. This shortage of supplies results in the damaging of macromolecules and a general imbalance of proteostasis including reduced production of new proteins, which can ultimately lead to cell death of neurons and severe brain damage[127]. Natural resistance against ischemia can be observed in hibernating animals. Interestingly, it was detected that SUMO2/3 conjugation is massively increased in brains of hibernating thirteen-lined ground squirrels (Ictidomys tridecemlineatus) during torpor[128]. Consistently, multiple studies showed a high increase of SUMO conjugation after transient ischemia in vitro and in vivo[128-133]. This raises the intriguing question about the functional contribution of SUMOylation to protect cells from damage during ischemia. Below, we review multiple studies aiming to answer this question.

In vitro the consequences of SUMOylation during ischemia were studied using the oxygen-glucose deprivation (OGD) model in combination with a neuroblastoma cell line or in primary neurons isolated from mice or rats[134,135]. By using these models, it was shown that stimulating SUMOylation by overexpression of Ubc9, SUMO1, and SUMO2 increased the resistance of cells towards OGD[128,136]. Consistently, decreasing global SUMOylation by expressing a dominant negative mutant of Ubc9, silencing of each of the endogenous SUMO isoforms, or the overexpression of the sentrin-specific peptidase 1 (SENP1) caused sensitization of the cells towards OGD[128,134,136,137]. These findings all argue for a cytoprotective role of SUMOylation during OGD in vitro. In vivo it was shown that the overexpression of Ubc9 in mice subjected to focal cerebral ischemia contributed to the protection against brain damage, as infarct size inversely correlated with the level of Ubc9 overexpression[138]. Further investigation of SUMOs potential neuroprotective role against ischemic damage in vivo is hampered by the challenges of establishing conditional knockout mice of the SUMO-conjugating machinery, since the SUMO E1 and E2 enzymes are essential for embryonic development. Also the differential roles of the SUMO isoforms are difficult to establish in vivo because of the redundancy of the SUMO isoforms SUMO1 and SUMO3.

In vivo proteomics reveals SUMOylation targets on ischemia

A different strategy to obtain insight in the role of SUMOylation in ischemia is the identification of SUMOylated proteins. Recent advances in proteomics and the generation of mice expressing tagged versions of the SUMO isoforms enabled the identification of

the SUMO3 proteome in mice subjected to ischemia[139]. The proteomic data suggest a global upregulation of crosstalk between SUMO and ubiquitin during ischemia, as many proteins are shown to be targets for both modifications on different lysines. Upon silencing of SUMO2 and 3, a decrease in ubiquitin conjugation in response to ischemia is detected. This observation implies a pivotal role for SUMO-dependent ubiquitination, which is regulated by SUMO-targeted ubiquitin ligases (STUbL) and reflects the involvement of SUMO in protein homeostasis[139]. Additionally, SUMO targets were enriched for proteins involved in posttranscriptional modification of RNA. Notably, after heat shock, a distinct kind of proteotoxic stress, a large group of targets increased for SUMOylation play a role in RNA posttranscriptional modification. Moreover, SUMOylated proteins were shown to be recruited to promoters of genes involved in RNA processing[86,87,140]. Taken together, those results indicate that SUMOylation might be involved, on multiple levels, in global regulation of RNA processes after different proteotoxic stresses. Although the effect of SUMOylation for a single target protein is sometimes challenging to identify, SUMOylation of several important SUMO targets could contribute to the survival of neurons after deprivation of oxygen and nutrients. One of the major SUMOylation targets after ischemic stress, identified in the proteomic study by Paschen and coworkers, is the glucocorticoid receptor (GR)[139]. The increased activity of GR, during chronic stress, was shown to increase the size of brain lesions after transient ischemia[141]. GR SUMOylation leads to repression of its transcriptional activity and could therefore be involved in promoting cell survival[142]. However, whether SUMOylation of GR directly contributes to the observed protective effect of global SUMOylation after ischemia is still unclear.

Other ubiquitin-like proteins are highly expressed on ischemia

SUMO is not the only UbL that is upregulated during torpor in hibernating squirrels. Protein modification by Isg15, Nedd8, Ufm1, and Fub1, but interestingly not ubiquitin, was increased, suggesting that posttranslational modifications are an important regulatory mechanism when energy is scarce. Possibly, this regulation facilitates the intriguing natural tolerance against ischemic conditions observed in hibernating animals[143]. The global upregulation of UbL conjugation involves two families of microRNAs, miR-200 and mi-R182, which were downregulated during hibernation torpor. Inhibiting these miRNAs led to an increase in UbL conjugation while overexpression led to a decrease in conjugates, suggesting an important role of miRNAs in regulation of UbL conjugation[143]. In conclusion, SUMOylation is suggested as a global protective mechanism against the damaging effects of oxygen and nutrient deprivation. Because of the vast bio-complexity that underlies brain injuries due to ischemia, SUMOylation with its broad variety of target proteins could be an attractive drug target. Stimulating SUMOylation could potentially have a positive effect on neuronal cell survival. Conversely, inhibition of SUMOylation was indicated to potentially promote cell death of cancer cells. The role of the SUMOylation machinery and SUMOylation targets in cancer cells was recently reviewed by Eifler and Vertegaal[144].

CONCLUSION AND FUTURE PERSPECTIVES

SUMO can either alone or in cooperation with ubiquitin regulate proteostasis in the cell. Independently and directly, SUMO is involved in the regulation of protein aggregation or solubility in neurodegenerative diseases (Table 1). The consequences of SUMOylation regarding solubility of proteins are diverse and requires additional investigation. Possibly,

SUMO regulates multiple processes in those diseases and the overall cellular outcome of SUMOylation might be difficult to predict.

For example, the SUMOylation of the polyQ androgen receptor (AR) was shown to decrease aggregation, but on the other hand, inhibiting SUMO increased AR transcriptional activity and ameliorated harmful properties of polyQ AR[118,145]. Combining the existing in vivo mouse models expressing tagged versions of SUMO[139,146] with neurodegenerative disease mouse models would allow a global identification of SUMO conjugates. This would improve the understanding of SUMO's contribution to the diseases with SUMO cycle enzymes as potential drug targets. In addition to the direct effect of SUMOylation on proteostasis, SUMO can also influence proteostasis indirectly. One example is the regulation of transcription factors by SUMOylation, which can alter expression levels of proteins involved in maintaining proteostasis[84,86,87]. The main contribution of SUMO in protein homeostasis is, however, its complex interplay with ubiquitin (Figure 2). The ubiquitin-proteasome system (UPS) is involved in multiple signaling pathways and plays a major role in quality control of proteins[147]. After synthesis, around 30% of proteins are misfolded and need to be degraded to prevent a constitutive unfolded protein response and subsequent apoptosis[148]. It is critical that the protein quality control is tightly regulated. SUMOylation was shown to either inhibit or promote ubiquitination of targets and their subsequent degradation and therefore is a component of the tightly controlled UPS. The process of SUMO-dependent ubiquitination is being extensively explored, leading to the identification of enzymes involved in this crosstalk, like STUbLs and SUMO-targeted deubiquitinases. In mammals, two enzymes of each class have been identified[42,59,76,80]. Proteins that are misfolded or unfolded during stress are ubiquitinated and targeted to the proteasome. It was found that those stresses also strongly induce SUMOylation of targets[29,81,82]. Yet, it is unclear why and how this increase in SUMOylation upon heat stress or inhibition of the proteasome takes place, but it cannot only be explained by the accumulation of SUMO-conjugates. The possibility that SUMO is actively conjugated to ubiquitin targets opens a whole new area to be explored. Do ubiquitin-targeted SUMO ligases exist? Which consequence has the SUMOylation of ubiquitinated proteins? Does this involve the ability of SUMO to alter solubility and therefore stimulates cell survival by giving the UPS time to catch up with the load of misfolded proteins? These questions need to be answered in the future and could potentially lead to the exploration of SUMO enzymes as potential drug targets in diseases that are characterized by an unbalanced proteostasis, including neurodegenerative diseases.

References

1. Balch, W. E., Morimoto, R. I., Dillin, A. and Kelly, J. W. Adapting proteostasis for disease intervention. *Science* **319**, 916-919, (2008).
2. Hipp, M. S., Park, S. H. and Hartl, F. U. Proteostasis impairment in protein-misfolding and -aggregation diseases. *Trends Cell Biol* **24**, 506-514, (2014).
3. Jeng, W., Lee, S., Sung, N., Lee, J. and Tsai, F. T. Molecular chaperones: guardians of the proteome in normal and disease states. *F1000Res* **4**, (2015).
4. Gu, Z. C. and Enenkel, C. Proteasome assembly. *Cell Mol. Life Sci* **71**, 4729-4745, (2014).
5. Hershko, A. and Ciechanover, A. The ubiquitin system. *Annu. Rev. Biochem* **67**, 425-479, (1998).
6. Flotho, A. and Melchior, F. Sumoylation: a regulatory protein modification in health and disease. *Annu. Rev. Biochem* **82**, 357-385, (2013).
7. Gareau, J. R. and Lima, C. D. The SUMO pathway: emerging mechanisms that shape specificity, conjugation and recognition. *Nat. Rev. Mol. Cell Biol* **11**, 861-871, (2010).
8. Cheng, C. H., Lo, Y. H., Liang, S. S. *et al.* SUMO modifications control assembly of synaptonemal complex and polycomplex in meiosis of Saccharomyces cerevisiae. *Genes Dev* **20**, 2067-2081, (2006).
9. Johnson, E. S. and Gupta, A. A. An E3-like factor that promotes SUMO conjugation to the yeast septins. *Cell* **106**, 735-744, (2001).
10. Takahashi, Y., Yong-Gonzalez, V., Kikuchi, Y. and Strunnikov, A. SIZ1/SIZ2 control of chromosome transmission fidelity is mediated by the sumoylation of topoisomerase II. *Genetics* **172**, 783-794, (2006).
11. Zhao, X. and Blobel, G. A SUMO ligase is part of a nuclear multiprotein complex that affects DNA repair and chromosomal organization. *Proc. Natl. Acad. Sci. U. S. A* **102**, 4777-4782, (2005).
12. Kagey, M. H., Melhuish, T. A. and Wotton, D. The polycomb protein Pc2 is a SUMO E3. *Cell* **113**, 127-137, (2003).
13. Weger, S., Hammer, E. and Heilbronn, R. Topors acts as a SUMO-1 E3 ligase for p53 in vitro and in vivo. *FEBS Lett* **579**, 5007-5012, (2005).
14. Tago, K., Chiocca, S. and Sherr, C. J. Sumoylation induced by the Arf tumor suppressor: a p53-independent function. *Proc. Natl. Acad. Sci. U. S. A* **102**, 7689-7694, (2005).
15. Woods, Y. L., Xirodimas, D. P., Prescott, A. R. *et al.* p14 Arf promotes small ubiquitin-like modifier conjugation of Werners helicase. *J. Biol. Chem* **279**, 50157-50166, (2004).
16. Carbia-Nagashima, A., Gerez, J., Perez-Castro, C. *et al.* RSUME, a small RWD-containing protein, enhances SUMO conjugation and stabilizes HIF-1alpha during hypoxia. *Cell* **131**, 309-323, (2007).
17. Subramaniam, S., Mealer, R. G., Sixt, K. M. *et al.* Rhes, a physiologic regulator of sumoylation, enhances cross-sumoylation between the basic sumoylation enzymes E1 and Ubc9. *J. Biol. Chem* **285**, 20428-20432, (2010).
18. Guervilly, J. H., Takedachi, A., Naim, V. *et al.* The SLX4 Complex Is a SUMO E3 Ligase that Impacts on Replication Stress Outcome and Genome Stability. *Mol. Cell* **57**, 123-137, (2015).
19. Ouyang, J., Garner, E., Hallet, A. *et al.* Noncovalent Interactions with SUMO and Ubiquitin Orchestrate Distinct Functions of the SLX4 Complex in Genome Maintenance. *Mol. Cell* **57**, 108-122, (2015).
20. Drag, M. and Salvesen, G. S. DeSUMOylating enzymes--SENPs. *IUbMB. Life* **60**, 734-742, (2008).
21. Hay, R. T. SUMO-specific proteases: a twist in the tail. *Trends Cell Biol* **17**, 370-376, (2007).
22. Hickey, C. M., Wilson, N. R. and Hochstrasser, M. Function and regulation of SUMO proteases. *Nat. Rev. Mol. Cell Biol* **13**, 755-766, (2012).
23. Schulz, S., Chachami, G., Kozaczkiewicz, L. *et al.* Ubiquitin-specific protease-like 1 (USPL1) is a SUMO isopeptidase with essential, non-catalytic functions. *EMBO Rep* **13**, 930-938, (2012).
24. Matic, I., van Hagen, M., Schimmel, J. *et al.* In vivo identification of human small ubiquitin-like modifier polymerization sites by high accuracy mass spectrometry and an in vitro to in vivo strategy. *Mol. Cell Proteomics* **7**, 132-144, (2008).
25. Matic, I., Schimmel, J., Hendriks, I. A. *et al.* Site-specific identification of SUMO-2 targets in cells reveals an inverted SUMOylation motif and a hydrophobic cluster SUMOylation motif. *Mol. Cell* **39**, 641-652, (2010).
26. Becker, J., Barysch, S. V., Karaca, S. *et al.* Detecting endogenous SUMO targets in mammalian cells and tissues. *Nat. Struct. Mol. Biol* **20**, 525-531, (2013).

27. Zhang, F. P., Mikkonen, L., Toppari, J. *et al.* Sumo-1 function is dispensable in normal mouse development. *Mol. Cell Biol* **28**, 5381-5390, (2008).
28. Wang, L., Wansleeben, C., Zhao, S. *et al.* SUMO2 is essential while SUMO3 is dispensable for mouse embryonic development. *EMBO Rep* **15**, 878-885, (2014).
29. Hendriks, I. A., D'Souza, R. C., Yang, B. *et al.* Uncovering global SUMOylation signaling networks in a site-specific manner. *Nat. Struct. Mol. Biol* **21**, 927-936, (2014).
30. Tammsalu, T., Matic, I., Jaffray, E. G. *et al.* Proteome-Wide Identification of SUMO2 Modification Sites. *Sci. Signal* **7**, rs2, (2014).
31. Desterro, J. M., Rodriguez, M. S. and Hay, R. T. SUMO-1 modification of IkappaBalpha inhibits NF-kappaB activation. *Mol. Cell* **2**, 233-239, (1998).
32. Anderson, D. D., Eom, J. Y. and Stover, P. J. Competition between sumoylation and ubiquitination of serine hydroxymethyltransferase 1 determines its nuclear localization and its accumulation in the nucleus. *J. Biol. Chem* **287**, 4790-4799, (2012).
33. Huang, T. T., Wuerzberger-Davis, S. M., Wu, Z. H. and Miyamoto, S. Sequential modification of NEMO/IKKgamma by SUMO-1 and ubiquitin mediates NF-kappaB activation by genotoxic stress. *Cell* **115**, 565-576, (2003).
34. Jonsson, Z. O. and Hubscher, U. Proliferating cell nuclear antigen: more than a clamp for DNA polymerases. *Bioessays* **19**, 967-975, (1997).
35. Hoege, C., Pfander, B., Moldovan, G. L., Pyrowolakis, G. and Jentsch, S. RAD6-dependent DNA repair is linked to modification of PCNA by ubiquitin and SUMO. *Nature* **419**, 135-141, (2002).
36. Stelter, P. and Ulrich, H. D. Control of spontaneous and damage-induced mutagenesis by SUMO and ubiquitin conjugation. *Nature* **425**, 188-191, (2003).
37. Burkovics, P., Sebesta, M., Sisakova, A. *et al.* Srs2 mediates PCNA-SUMO-dependent inhibition of DNA repair synthesis. *EMBO J* **32**, 742-755, (2013).
38. Papouli, E., Chen, S., Davies, A. A. *et al.* Crosstalk between SUMO and ubiquitin on PCNA is mediated by recruitment of the helicase Srs2p. *Mol. Cell* **19**, 123-133, (2005).
39. Veaute, X., Jeusset, J., Soustelle, C. *et al.* The Srs2 helicase prevents recombination by disrupting Rad51 nucleoprotein filaments. *Nature* **423**, 309-312, (2003).
40. Danielsen, J. M., Sylvestersen, K. B., Bekker-Jensen, S. *et al.* Mass spectrometric analysis of lysine ubiquitylation reveals promiscuity at site level. *Mol. Cell Proteomics* **10**, M110, (2011).
41. Perry, J. J., Tainer, J. A. and Boddy, M. N. A SIM-ultaneous role for SUMO and ubiquitin. *Trends Biochem. Sci* **33**, 201-208, (2008).
42. Tatham, M. H., Geoffroy, M. C., Shen, L. *et al.* RNF4 is a poly-SUMO-specific E3 ubiquitin ligase required for arsenic-induced PML degradation. *Nat. Cell Biol* **10**, 538-546, (2008).
43. Uzunova, K., Gottsche, K., Miteva, M. *et al.* Ubiquitin-dependent proteolytic control of SUMO conjugates. *J. Biol. Chem* **282**, 34167-34175, (2007).
44. Xie, Y., Kerscher, O., Kroetz, M. B. *et al.* The yeast Hex3.Slx8 heterodimer is a ubiquitin ligase stimulated by substrate sumoylation. *J. Biol. Chem* **282**, 34176-34184, (2007).
45. Westerbeck, J. W., Pasupala, N., Guillotte, M. *et al.* A SUMO-targeted ubiquitin ligase is involved in the degradation of the nuclear pool of the SUMO E3 ligase Siz1. *Mol. Biol. Cell* **25**, 1-16, (2014).
46. Xie, Y., Rubenstein, E. M., Matt, T. and Hochstrasser, M. SUMO-independent in vivo activity of a SUMO-targeted ubiquitin ligase toward a short-lived transcription factor. *Genes Dev* **24**, 893-903, (2010).
47. Parker, J. L. and Ulrich, H. D. A SUMO-interacting motif activates budding yeast ubiquitin ligase Rad18 towards SUMO-modified PCNA. *Nucleic Acids Res* **40**, 11380-11388, (2012).
48. Bruderer, R., Tatham, M. H., Plechanovova, A. *et al.* Purification and identification of endogenous polySUMO conjugates. *EMBO Rep* **12**, 142-148, (2011).
49. Mukhopadhyay, D. and Dasso, M. The fate of metaphase kinetochores is weighed in the balance of SUMOylation during S phase. *Cell Cycle* **9**, 3194-3201, (2010).
50. van Hagen, M., Overmeer, R. M., Abolvardi, S. S. and Vertegaal, A. C. RNF4 and VHL regulate the proteasomal degradation of SUMO-conjugated Hypoxia-Inducible Factor-2alpha. *Nucleic Acids Res* **38**, 1922-1931, (2010).

51. Guo, B. and Sharrocks, A. D. Extracellular signal-regulated kinase mitogen-activated protein kinase signaling initiates a dynamic interplay between sumoylation and ubiquitination to regulate the activity of the transcriptional activator PEA3. *Mol. Cell Biol* **29**, 3204-3218, (2009).
52. Martin, N., Schwamborn, K., Schreiber, V. *et al.* PARP-1 transcriptional activity is regulated by sumoylation upon heat shock. *EMBO J* **28**, 3534-3548, (2009).
53. Ahner, A., Gong, X. and Frizzell, R. A. Cystic fibrosis transmembrane conductance regulator degradation: cross-talk between the ubiquitylation and SUMOylation pathways. *FEBS J* **280**, 4430-4438, (2013).
54. Nie, M. and Boddy, M. N. Cooperativity of the SUMO and Ubiquitin Pathways in Genome Stability. *Biomolecules* **6**, (2016).
55. Lallemand-Breitenbach, V., Jeanne, M., Benhenda, S. *et al.* Arsenic degrades PML or PML-RARalpha through a SUMO-triggered RNF4/ubiquitin-mediated pathway. *Nat. Cell Biol* **10**, 547-555, (2008).
56. Weisshaar, S. R., Keusekotten, K., Krause, A. *et al.* Arsenic trioxide stimulates SUMO-2/3 modification leading to RNF4-dependent proteolytic targeting of PML. *FEBS Lett* **582**, 3174-3178, (2008).
57. Guo, L., Giasson, B. I., Glavis-Bloom, A. *et al.* A cellular system that degrades misfolded proteins and protects against neurodegeneration. *Mol. Cell* **55**, 15-30, (2014).
58. Gonzalez-Prieto, R., Cuijpers, S. A., Kumar, R., Hendriks, I. A. and Vertegaal, A. C. c-Myc is targeted to the proteasome for degradation in a SUMOylation-dependent manner, regulated by PIAS1, SENP7 and RNF4. *Cell Cycle* **14**, 1859-1872, (2015).
59. Sun, H. and Hunter, T. Poly-small ubiquitin-like modifier (PolySUMO)-binding proteins identified through a string search. *J. Biol. Chem* **287**, 42071-42083, (2012).
60. Kang, J. S., Saunier, E. F., Akhurst, R. J. and Derynck, R. The type I TGF-beta receptor is covalently modified and regulated by sumoylation. *Nat. Cell Biol* **10**, 654-664, (2008).
61. Imoto, S., Ohbayashi, N., Ikeda, O. *et al.* Sumoylation of Smad3 stimulates its nuclear export during PIASy-mediated suppression of TGF-beta signaling. *Biochem. Biophys. Res. Commun* **370**, 359-365, (2008).
62. Lee, P. S., Chang, C., Liu, D. and Derynck, R. Sumoylation of Smad4, the common Smad mediator of transforming growth factor-beta family signaling. *J. Biol. Chem* **278**, 27853-27863, (2003).
63. Kim, M. J., Chia, I. V. and Costantini, F. SUMOylation target sites at the C terminus protect Axin from ubiquitination and confer protein stability. *FASEB J* **22**, 3785-3794, (2008).
64. Erker, Y., Neyret-Kahn, H., Seeler, J. S. *et al.* Arkadia, a novel SUMO-targeted ubiquitin ligase involved in PML degradation. *Mol. Cell Biol* **33**, 2163-2177, (2013).
65. Galanty, Y., Belotserkovskaya, R., Coates, J. and Jackson, S. P. RNF4, a SUMO-targeted ubiquitin E3 ligase, promotes DNA double-strand break repair. *Genes Dev* **26**, 1179-1195, (2012).
66. Vyas, R., Kumar, R., Clermont, F. *et al.* RNF4 is required for DNA double-strand break repair in vivo. *Cell Death Differ* **20**, 490-502, (2013).
67. Yin, Y., Seifert, A., Chua, J. S. *et al.* SUMO-targeted ubiquitin E3 ligase RNF4 is required for the response of human cells to DNA damage. *Genes Dev* **26**, 1196-1208, (2012).
68. Guzzo, C. M., Berndsen, C. E., Zhu, J. *et al.* RNF4-dependent hybrid SUMO-ubiquitin chains are signals for RAP80 and thereby mediate the recruitment of BRCA1 to sites of DNA damage. *Sci. Signal* **5**, ra88, (2012).
69. Guzzo, C. M. and Matunis, M. J. Expanding SUMO and ubiquitin-mediated signaling through hybrid SUMO-ubiquitin chains and their receptors. *Cell Cycle* **12**, 1015-1017, (2013).
70. Baek, G. H., Cheng, H., Choe, V. *et al.* Cdc48: a swiss army knife of cell biology. *J. Amino. Acids* **2013**, 183421, (2013).
71. Meyer, H. and Weihl, C. C. The VCP/p97 system at a glance: connecting cellular function to disease pathogenesis. *J. Cell Sci* **127**, 3877-3883, (2014).
72. Nie, M., Aslanian, A., Prudden, J. *et al.* Dual recruitment of Cdc48 (p97)-Ufd1-Npl4 ubiquitin-selective segregase by small ubiquitin-like modifier protein (SUMO) and ubiquitin in SUMO-targeted ubiquitin ligase-mediated genome stability functions. *J. Biol. Chem* **287**, 29610-29619, (2012).
73. Kohler, J. B., Jorgensen, M. L., Beinoraite, G., Thorsen, M. and Thon, G. Concerted action of the ubiquitin-fusion degradation protein 1 (Ufd1) and Sumo-targeted ubiquitin ligases (STUbLs) in the DNA-damage response. *PLoS. One* **8**, e80442, (2013).
74. Kohler, J. B., Tammsalu, T., Jorgensen, M. M. *et al.* Targeting of SUMO substrates to a Cdc48-Ufd1-Npl4 segregase and STUbL pathway in fission yeast. *Nat. Commun* **6**, 8827, (2015).

75. Bergink, S., Ammon, T., Kern, M. *et al.* Role of Cdc48/p97 as a SUMO-targeted segregase curbing Rad51-Rad52 interaction. *Nat. Cell Biol* **15**, 526-532, (2013).

76. Hendriks, I. A., Schimmel, J., Eifler, K., Olsen, J. V. and Vertegaal, A. C. Ubiquitin-specific Protease 11 (USP11) Deubiquitinates Hybrid Small Ubiquitin-like Modifier (SUMO)-Ubiquitin Chains to Counteract RING Finger Protein 4 (RNF4). *J. Biol. Chem* **290**, 15526-15537, (2015).

77. Wu, H. C., Lin, Y. C., Liu, C. H. *et al.* USP11 regulates PML stability to control Notch-induced malignancy in brain tumours. *Nat. Commun* **5**, 3214, (2014).

78. Schoenfeld, A. R., Apgar, S., Dolios, G., Wang, R. and Aaronson, S. A. BRCA2 is ubiquitinated in vivo and interacts with USP11, a deubiquitinating enzyme that exhibits prosurvival function in the cellular response to DNA damage. *Mol. Cell Biol* **24**, 7444-7455, (2004).

79. Wiltshire, T. D., Lovejoy, C. A., Wang, T. *et al.* Sensitivity to poly(ADP-ribose) polymerase (PARP) inhibition identifies ubiquitin-specific peptidase 11 (USP11) as a regulator of DNA double-strand break repair. *J. Biol. Chem* **285**, 14565-14571, (2010).

80. Lecona, E., Rodriguez-Acebes, S., Specks, J. *et al.* USP7 is a SUMO deubiquitinase essential for DNA replication. *Nat. Struct. Mol. Biol*, (2016).

81. Schimmel, J., Larsen, K. M., Matic, I. *et al.* The ubiquitin-proteasome system is a key component of the SUMO-2/3 cycle. *Mol. Cell Proteomics* **7**, 2107-2122, (2008).

82. Tatham, M. H., Matic, I., Mann, M. and Hay, R. T. Comparative proteomic analysis identifies a role for SUMO in protein quality control. *Sci. Signal* **4**, rs4, (2011).

83. Ouyang, J., Valin, A. and Gill, G. Regulation of transcription factor activity by SUMO modification. *Methods Mol. Biol* **497**, 141-152, (2009).

84. Neyret-Kahn, H., Benhamed, M., Ye, T. *et al.* Sumoylation at chromatin governs coordinated repression of a transcriptional program essential for cell growth and proliferation. *Genome Res* **23**, 1563-1579, (2013).

85. Hendriks, I. A., Treffers, L. W., Verlaan-de Vries, M., Olsen, J. V. and Vertegaal, A. C. SUMO-2 Orchestrates Chromatin Modifiers in Response to DNA Damage. *Cell Rep* **10**, 1778-1791, (2015).

86. Niskanen, E. A., Malinen, M., Sutinen, P. *et al.* Global SUMOylation on active chromatin is an acute heat stress response restricting transcription. *Genome Biol* **16**, 153, (2015).

87. Seifert, A., Schofield, P., Barton, G. J. and Hay, R. T. Proteotoxic stress reprograms the chromatin landscape of SUMO modification. *Sci. Signal* **8**, rs7, (2015).

88. Oeser, M. L., Amen, T., Nadel, C. M. *et al.* Dynamic Sumoylation of a Conserved Transcription Corepressor Prevents Persistent Inclusion Formation during Hyperosmotic Stress. *PLoS Genet* **12**, e1005809, (2016).

89. Carvalho, C., Correia, S. C., Cardoso, S. *et al.* The role of mitochondrial disturbances in Alzheimer, Parkinson and Huntington diseases. *Expert Rev. Neurother* **15**, 867-884, (2015).

90. Schulz, J. B. and Dichgans, J. Molecular pathogenesis of movement disorders: are protein aggregates a common link in neuronal degeneration? *Curr. Opin. Neurol* **12**, 433-439, (1999).

91. Vance, C., Rogelj, B., Hortobagyi, T. *et al.* Mutations in FUS, an RNA processing protein, cause familial amyotrophic lateral sclerosis type 6. *Science* **323**, 1208-1211, (2009).

92. Zheng, C., Geetha, T. and Babu, J. R. Failure of ubiquitin proteasome system: risk for neurodegenerative diseases. *Neurodegener. Dis* **14**, 161-175, (2014).

93. Krumova, P. and Weishaupt, J. H. Sumoylation in neurodegenerative diseases. *Cell Mol. Life Sci* **70**, 2123-2138, (2013).

94. LaFerla, F. M., Green, K. N. and Oddo, S. Intracellular amyloid-beta in Alzheimer's disease. *Nat. Rev. Neurosci* **8**, 499-509, (2007).

95. Tiraboschi, P., Hansen, L. A., Thal, L. J. and Corey-Bloom, J. The importance of neuritic plaques and tangles to the development and evolution of AD. *Neurology* **62**, 1984-1989, (2004).

96. Dorval, V. and Fraser, P. E. Small ubiquitin-like modifier (SUMO) modification of natively unfolded proteins tau and alpha-synuclein. *J. Biol. Chem* **281**, 9919-9924, (2006).

97. Zhang, Y. Q. and Sarge, K. D. Sumoylation of amyloid precursor protein negatively regulates Abeta aggregate levels. *Biochem. Biophys. Res. Commun* **374**, 673-678, (2008).

98. Li, Y., Wang, H., Wang, S. *et al.* Positive and negative regulation of APP amyloidogenesis by sumoylation. *Proc. Natl. Acad. Sci. U. S. A* **100**, 259-264, (2003).

99. Dorval, V., Mazzella, M. J., Mathews, P. M., Hay, R. T. and Fraser, P. E. Modulation of Abeta generation by small ubiquitin-like modifiers does not require conjugation to target proteins. *Biochem. J* **404**, 309-316, (2007).

100. Alonso, A. C., Li, B., Grundke-Iqbal, I. and Iqbal, K. Mechanism of tau-induced neurodegeneration in Alzheimer disease and related tauopathies. *Curr. Alzheimer Res* **5**, 375-384, (2008).

101. Iqbal, K. and Grundke-Iqbal, I. Alzheimer neurofibrillary degeneration: significance, etiopathogenesis, therapeutics and prevention. *J. Cell Mol. Med* **12**, 38-55, (2008).

102. Luo, H. B., Xia, Y. Y., Shu, X. J. *et al.* SUMOylation at K340 inhibits tau degradation through deregulating its phosphorylation and ubiquitination. *Proc. Natl. Acad. Sci. U. S. A* **111**, 16586-16591, (2014).

103. Krumova, P., Meulmeester, E., Garrido, M. *et al.* Sumoylation inhibits alpha-synuclein aggregation and toxicity. *J. Cell Biol* **194**, 49-60, (2011).

104. Abeywardana, T. and Pratt, M. R. Extent of Inhibition of alpha-Synuclein Aggregation in Vitro by SUMOylation Is Conjugation Site- and SUMO Isoform-Selective. *Biochemistry* **54**, 959-961, (2015).

105. Bandopadhyay, R., Kingsbury, A. E., Cookson, M. R. *et al.* The expression of DJ-1 (PARK7) in normal human CNS and idiopathic Parkinson's disease. *Brain* **127**, 420-430, (2004).

106. Neumann, M., Muller, V., Gorner, K. *et al.* Pathological properties of the Parkinson's disease-associated protein DJ-1 in alpha-synucleinopathies and tauopathies: relevance for multiple system atrophy and Pick's disease. *Acta Neuropathol* **107**, 489-496, (2004).

107. Takahashi, K., Taira, T., Niki, T. *et al.* DJ-1 positively regulates the androgen receptor by impairing the binding of PIASx alpha to the receptor. *J. Biol. Chem* **276**, 37556-37563, (2001).

108. Shinbo, Y., Niki, T., Taira, T. *et al.* Proper SUMO-1 conjugation is essential to DJ-1 to exert its full activities. *Cell Death Differ* **13**, 96-108, (2006).

109. Kitada, T., Asakawa, S., Hattori, N. *et al.* Mutations in the parkin gene cause autosomal recessive juvenile parkinsonism. *Nature* **392**, 605-608, (1998).

110. Schlossmacher, M. G., Frosch, M. P., Gai, W. P. *et al.* Parkin localizes to the Lewy bodies of Parkinson disease and dementia with Lewy bodies. *Am. J. Pathol* **160**, 1655-1667, (2002).

111. Um, J. W. and Chung, K. C. Functional modulation of parkin through physical interaction with SUMO-1. *J. Neurosci. Res* **84**, 1543-1554, (2006).

112. Figueroa-Romero, C., Iniguez-Lluhi, J. A., Stadler, J. *et al.* SUMOylation of the mitochondrial fission protein Drp1 occurs at multiple nonconsensus sites within the B domain and is linked to its activity cycle. *FASEB J* **23**, 3917-3927, (2009).

113. Zunino, R., Schauss, A., Rippstein, P., Andrade-Navarro, M. and McBride, H. M. The SUMO protease SENP5 is required to maintain mitochondrial morphology and function. *J. Cell Sci* **120**, 1178-1188, (2007).

114. Wang, H., Song, P., Du, L. *et al.* Parkin ubiquitinates Drp1 for proteasome-dependent degradation: implication of dysregulated mitochondrial dynamics in Parkinson disease. *J. Biol. Chem* **286**, 11649-11658, (2011).

115. Eckermann, K. SUMO and Parkinson's disease. *Neuromolecular. Med* **15**, 737-759, (2013).

116. La Spada, A. R., Paulson, H. L. and Fischbeck, K. H. Trinucleotide repeat expansion in neurological disease. *Ann. Neurol* **36**, 814-822, (1994).

117. Janer, A., Werner, A., Takahashi-Fujigasaki, J. *et al.* SUMOylation attenuates the aggregation propensity and cellular toxicity of the polyglutamine expanded ataxin-7. *Hum. Mol. Genet* **19**, 181-195, (2010).

118. Mukherjee, S., Thomas, M., Dadgar, N., Lieberman, A. P. and Iniguez-Lluhi, J. A. Small ubiquitin-like modifier (SUMO) modification of the androgen receptor attenuates polyglutamine-mediated aggregation. *J. Biol. Chem* **284**, 21296-21306, (2009).

119. Steffan, J. S., Agrawal, N., Pallos, J. *et al.* SUMO modification of Huntingtin and Huntington's disease pathology. *Science* **304**, 100-104, (2004).

120. Terashima, T., Kawai, H., Fujitani, M., Maeda, K. and Yasuda, H. SUMO-1 co-localized with mutant atrophin-1 with expanded polyglutamines accelerates intranuclear aggregation and cell death. *Neuroreport* **13**, 2359-2364, (2002).

121. Arrasate, M., Mitra, S., Schweitzer, E. S., Segal, M. R. and Finkbeiner, S. Inclusion body formation reduces levels of mutant huntingtin and the risk of neuronal death. *Nature* **431**, 805-810, (2004).

122. Kuemmerle, S., Gutekunst, C. A., Klein, A. M. *et al.* Huntington aggregates may not predict neuronal death in Huntington's disease. *Ann. Neurol* **46**, 842-849, (1999).

123. Saudou, F., Finkbeiner, S., Devys, D. and Greenberg, M. E. Huntingtin acts in the nucleus to induce apoptosis but death does not correlate with the formation of intranuclear inclusions. *Cell* **95**, 55-66, (1998).

124. Subramaniam, S., Sixt, K. M., Barrow, R. and Snyder, S. H. Rhes, a striatal specific protein, mediates mutant-huntingtin cytotoxicity. *Science* **324**, 1327-1330, (2009).

125. Malakhov, M. P., Mattern, M. R., Malakhova, O. A. *et al.* SUMO fusions and SUMO-specific protease for efficient expression and purification of proteins. *J. Struct. Funct. Genomics* **5**, 75-86, (2004).

126. Jentsch, S. and Psakhye, I. Control of nuclear activities by substrate-selective and protein-group SUMOylation. *Annu. Rev. Genet* **47**, 167-186, (2013).

127. Yun, S. M., Cho, S. J., Song, J. C. *et al.* SUMO1 modulates Abeta generation via BACE1 accumulation. *Neurobiol. Aging* **34**, 650-662, (2013).

128. O'Rourke, J. G., Gareau, J. R., Ochaba, J. *et al.* SUMO-2 and PIAS1 Modulate Insoluble Mutant Huntingtin Protein Accumulation. *Cell Rep* **4**, 362-375, (2013).

129. Fei, E., Jia, N., Yan, M. *et al.* SUMO-1 modification increases human SOD1 stability and aggregation. *Biochem. Biophys. Res. Commun* **347**, 406-412, (2006).

130. White, B. C., Sullivan, J. M., DeGracia, D. J. *et al.* Brain ischemia and reperfusion: molecular mechanisms of neuronal injury. *J. Neurol. Sci* **179**, 1-33, (2000).

131. Lee, Y. J., Miyake, S., Wakita, H. *et al.* Protein SUMOylation is massively increased in hibernation torpor and is critical for the cytoprotection provided by ischemic preconditioning and hypothermia in SHSY5Y cells. *J. Cereb. Blood Flow Metab* **27**, 950-962, (2007).

132. Cimarosti, H., Lindberg, C., Bomholt, S. F., Ronn, L. C. and Henley, J. M. Increased protein SUMOylation following focal cerebral ischemia. *Neuropharmacology* **54**, 280-289, (2008).

133. Loftus, L. T., Gala, R., Yang, T. *et al.* Sumo-2/3-ylation following in vitro modeled ischemia is reduced in delayed ischemic tolerance. *Brain Res* **1272**, 71-80, (2009).

134. Wang, Z., Wang, R., Sheng, H. *et al.* Transient ischemia induces massive nuclear accumulation of SUMO2/3-conjugated proteins in spinal cord neurons. *Spinal Cord* **51**, 139-143, (2013).

135. Yang, W., Sheng, H., Warner, D. S. and Paschen, W. Transient focal cerebral ischemia induces a dramatic activation of small ubiquitin-like modifier conjugation. *J. Cereb. Blood Flow Metab* **28**, 892-896, (2008).

136. Yang, W., Sheng, H., Warner, D. S. and Paschen, W. Transient global cerebral ischemia induces a massive increase in protein sumoylation. *J. Cereb. Blood Flow Metab* **28**, 269-279, (2008).

137. Cimarosti, H., Ashikaga, E., Jaafari, N. *et al.* Enhanced SUMOylation and SENP-1 protein levels following oxygen and glucose deprivation in neurones. *J. Cereb. Blood Flow Metab* **32**, 17-22, (2012).

138. Hillion, J. A., Takahashi, K., Maric, D. *et al.* Development of an ischemic tolerance model in a PC12 cell line. *J. Cereb. Blood Flow Metab* **25**, 154-162, (2005).

139. Lee, Y. J., Castri, P., Bembry, J. *et al.* SUMOylation participates in induction of ischemic tolerance. *J. Neurochem* **109**, 257-267, (2009).

140. Datwyler, A. L., Lattig-Tunnemann, G., Yang, W. *et al.* SUMO2/3 conjugation is an endogenous neuroprotective mechanism. *J. Cereb. Blood Flow Metab* **31**, 2152-2159, (2011).

141. Lee, Y. J., Mou, Y., Maric, D. *et al.* Elevated global SUMOylation in Ubc9 transgenic mice protects their brains against focal cerebral ischemic damage. *PLoS One* **6**, e25852, (2011).

142. Yang, W., Sheng, H., Thompson, J. W. *et al.* Small ubiquitin-like modifier 3-modified proteome regulated by brain ischemia in novel small ubiquitin-like modifier transgenic mice: putative protective proteins/pathways. *Stroke* **45**, 1115-1122, (2014).

143. Golebiowski, F., Matic, I., Tatham, M. H. *et al.* System-wide changes to SUMO modifications in response to heat shock. *Sci. Signal* **2**, ra24, (2009).

144. Balkaya, M., Prinz, V., Custodis, F. *et al.* Stress worsens endothelial function and ischemic stroke via glucocorticoids. *Stroke* **42**, 3258-3264, (2011).

145. Davies, L., Karthikeyan, N., Lynch, J. T. *et al.* Cross talk of signaling pathways in the regulation of the glucocorticoid receptor function. *Mol. Endocrinol* **22**, 1331-1344, (2008).

146. Lee, Y. J., Johnson, K. R. and Hallenbeck, J. M. Global protein conjugation by ubiquitin-like-modifiers during ischemic stress is regulated by microRNAs and confers robust tolerance to ischemia. *PLoS One* **7**, e47787, (2012).

147. Eifler, K. and Vertegaal, A. C. SUMOylation-Mediated Regulation of Cell Cycle Progression and Cancer. *Trends Biochem. Sci* **40**, 779-793, (2015).

148. Chua, J. P., Reddy, S. L., Yu, Z. *et al.* Disrupting SUMOylation enhances transcriptional function and ameliorates polyglutamine androgen receptor-mediated disease. *J. Clin. Invest* **125**, 831-845, (2015).

149. Tirard, M., Hsiao, H. H., Nikolov, M. *et al.* In vivo localization and identification of SUMOylated proteins in the brain of His6-HA-SUMO1 knock-in mice. *Proc. Natl. Acad. Sci. U. S. A* **109**, 21122-21127, (2012).

150. Goldberg, A. L. Protein degradation and protection against misfolded or damaged proteins. *Nature* **426**, 895-899, (2003).

151. Schubert, U., Anton, L. C., Gibbs, J. *et al.* Rapid degradation of a large fraction of newly synthesized proteins by proteasomes. *Nature* **404**, 770-774, (2000).

CHAPTER 3

SUMOylation and the HSF1-regulated Chaperone Network Converge to Promote Proteostasis in Response to Heat Shock

Frauke Liebelt[1,3], Rebecca M. Sebastian[2,3], Christopher L. Moore[2], Monique P.C.Mulders[1], Huib Ovaa[1], Matthew D. Shoulders[2,4], Alfred C.O. Vertegaal[1,4]

[1]Department of Cell and Chemical Biology, Leiden University Medical Center, Leiden, RA 2300, The Netherlands,

[2]Department of Chemistry, Massachusetts Institute of Technology, Cambridge, MA 02139, United States

[3]These authors contributed equally; [4]These authors contributed equally

Published in *Cell Reports* in 2019

ABSTRACT

The role of stress-induced increases in SUMO2/3 conjugation during the heat shock response (HSR) has remained enigmatic. We investigated SUMO signal transduction at the proteomic and functional level during the HSR in cells depleted of proteostasis network com-ponents via chronic heat shock factor 1 inhibition. In the recovery phase post-heat shock, high SUMO2/3 conjugation was prolonged in cells lacking sufficient chaperones. Similar re-sults were obtained upon inhibiting HSP90, indicating that increased chaperone activity during the HSR is critical for recovery to normal SUMO2/3 levels post-HS. Proteasome inhibition likewise prolonged SUMO2/3 conjugation, indicating that stress-induced SUMO2/3 targets are subsequently degraded by the ubiquitin-proteasome system. Functionally, we suggest that SUMOylation can enhance solubility of target proteins upon HS, a phenomenon that we experimentally observe in vitro. Collectively, our results implicate SUMO2/3 as a rapid re-sponse factor that coordinates proteome degradation and assists the maintenance of proteo-stasis upon proteotoxic stress.

INTRODUCTION

The composition of the cellular proteome is dynamically matched to functional re-quirements via transcription, splicing, new protein synthesis, and protein turnover. Throughout this process, protein misfolding and aggregation are minimized by an extensive proteostasis network comprising chaperones, quality control mechanisms, and degradation pathways. The proteostasis network both facilitates productive folding and removes terminally misfolded or aggregated proteins[1,2].

Upon proteotoxic stress, the proteostasis network can become overloaded by excess misfolded proteins. Cellular responses like the heat shock response (HSR) are induced to resolve the misfolding and prevent the formation of toxic and/or insoluble protein aggregates. The HSR is coordinated by heat shock factors (HSFs) that induce the transcription of chaperones and quality control factors to resolve excessive protein misfolding[3]. HSF1 is the master regulator of the HSR. HSF1 is continuously expressed, and displays low basal activity sufficient only to maintain normal levels of cytosolic and nuclear proteostasis network components in the absence of proteotoxic stress. The majority of HSF1 under these conditions is maintained inactive in the cytoplasm in a monomeric form, apparently via binding to chaperones[4,5]. Increasing levels of misfolded proteins owing to either chronic proteotoxic stress (e.g., constitutive expression of a mutant, misfolding protein) or acute proteotoxic stress (e.g., HS or heavy metal oxidants) leads to chaperones being titrated off of HSF1 by interaction with the accumulating misfolding proteins, inducing HSF1 homotrimerization and translocation to the nucleus to initiate the extensive HSR transcriptional program[6]. Once the proteotoxic stress has been resolved, HSF1 is inactivated again via post-translational modifications or via binding to excess chaperones[7].

In addition to transcriptional remodeling, proteotoxic stress is known to rapidly but transiently induce high levels of specific protein post-translational modifications, including substantial increases in conjugation to ubiquitin (Ub), O-linked glycans, and small-ubiquitin related modifiers (SUMO)[8-13]. It is well-appreciated that Ub modification can enhance proteostasis in response to proteotoxic stress via promoting proteasomal degradation of misfolded proteins, and that O-glycosylation can inhibit the aggregation of at least certain intrinsically disordered proteins[14,15]. However, the role of dramatic increases in SUMO2/3 modification levels upon proteotoxic stress has remained enigmatic.

The SUMO family is a group of highly conserved proteins with a similar three-dimensional fold to Ub[16-18]. Like Ub, SUMO dynamically modifies lysine side chains on sub-strate proteins[19,20]. Three major isoforms (SUMO1, 2, and 3) are ubiquitously expressed in mammalian cells[16,21]. SUMO1 only shares 48% sequence identity with SUMO2 and SUMO3. SUMO2 and SUMO3 share the vast majority of their amino acid sequences (95% se-quence identity), cannot be distinguished by extant antibodies, and as such are often referred to collectively as SUMO2/3.

Shortly after the discovery of the SUMO2/3 family members, it was observed that these SUMO modifications rapidly accumulate upon HS, in contrast to SUMO1[10,21]. Proteomic analysis revealed increases in SUMO2/3 conjugation for a wide range of substrates[8,9,22]. Notably, SUMO2 is recruited to open chromatin during HS[23] and appears to be indispensable for full activation of the inducible HSPA1A (HSP70) gene[24]. Modification of HSF1 by both SUMO1 and SUMO2/3 is also induced during stress, and may modulate the transcription of heat shock proteins (HSPs) during later stages of stress[25,26]. Although stress-induced SUMOylation is widespread, the potential proteostatic functions and regulation of this

modification, which typically recovers to normal levels in a matter of 2–4 hrs after HS, are poorly understood.

We present evidence that the composition and activities of the cellular proteostasis network regulate SUMO2/3 dynamics during HS, and are critical determinants in the degra-dation of SUMOylated substrates by the ubiquitin-proteasome system. We further identify a unique subset of SUMOylated proteins that preferentially maintain SUMOylation for prolonged time periods during chronic proteostasis impairment. Finally, we present evidence that SUMOylation reduces the aggregation of substrate proteins *in vitro*. Our results implicate SUMOylation as a rapid response mechanism that is integrated within the chaperone and quality control networks, is essential for coordinating substrate degradation in response to proteotoxic stress, and may prevent substrate aggregation at least in certain cases. Considering the number of SUMOylated substrates associated with neurodegeneration and cancer[27,28], these findings lay the foundation for investigating the intersection of SUMO2/3 modifications with protein quality control systems in disease progression and severity.

RESULTS

Depletion of Proteostasis Factors via Chronic HSF1 Inhibition Delays Recovery of SUMO2/3 Conjugation Levels after Heat Shock

As SUMO2/3 conjugation is stimulated by a variety of stressors associated with protein misfolding, including heat and oxidative stress, we were first interested in determining whether an impaired protein folding environment sensitizing cells to proteotoxic stress would modulate stress-induced SUMOylation. To create an impaired proteostasis network, we globally depleted cytosolic and nuclear proteostasis factors by using chemical biology tools to regulate the activity of the master cytosolic proteostasis transcription factor HSF1. We previously showed that a doxycycline (Dox)-inducible, constitutively active dominant-negative variant of HSF1, termed dn-cHSF1 29, can inhibit the activity of endogenous HSF1 with high selectivity and potency (Figure 1A). Chronic expression of dn-cHSF1 results in reduced steady-state levels of key proteostasis network components, especially HSP40, HSP70, and HSP90 (Figure 1B; see also 29).

We examined the effects of this chaperone depletion on the dynamics of SUMO2/3 conjugation both during and after HS in HEK293T-REx cells. As expected, immediately post-HS a strong increase in SUMO2/3 conjugation was observed (Figure 1C). When HSF1 was not inhibited prior to HS, the rate of return to normal SUMO2/3 conjugation levels was rapid, with complete return to basal SUMOylation achieved within 2 hrs of recovery at 37 °C. In sharp contrast, chronic inhibition of HSF1 prior to HS delayed recovery of SUMO2/3 conjugation levels beyond 4 hrs during recovery at 37 °C (Figures 1C and S1A). Importantly, control experiments in HEK293T-REx cells expressing a Dox-inducible GFP construct did not show any Dox-mediated changes in SUMOylation dynamics (Figure S1B), confirming that the delayed recovery was due to the induction of dn-cHSF1. Metabolic activity after HS was not significantly reduced following chronic HSF1 inhibition (Figure S1C), indicating that cell growth was not influenced and that sustained SUMOylation could not be attributed to an overall impairment in cell health during HS recovery.

The difference in the recovery rates could not be attributed to either increases in basal SUMO2/3 conjugation, or to an increase in initial SUMOylation levels immediately following HS (Figures 1C and S1A). Instead, it was specifically the recovery to normal SUMO2/3 levels that was delayed by chronic HSF1 inhibition. Notably, these observations were not limited

to HEK293T-REx cells, as we observed a similar delay in recovery when HSF1 was chronically inhibited prior to HS in LX2 hepatic stellate cells (Figure S1D).

Chronic inhibition of HSF1 via Dox-induced expression of dn-cHSF1 not only basally depletes chaperones, but also prevents HSR induction upon HS. To distinguish between SUMO2/3 retention resulting from inhibition of the HS-induced HSR versus reduced basal proteostasis capacity prior to HS, we next sought to uncouple HSR inhibition from basal depletion of chaperones owing to chronic HSF1 inhibition by transiently inhibiting the HSR without significantly reducing basal expression of chaperones. Briefly, we expressed a genetic fusion of dn-cHSF1 conjugated to a destabilized variant of Escherichia coli dihydrofolate reductase (DHFR), which is rapidly degraded by the proteasome unless a stabilizing ligand (trimethoprim; TMP) is added to the cell culture media[29]. Using this system, we found that acute TMP treatment (4 hr) did not substantially impact basal chaperone expression (Figure 1D). However, HS-induced transcription of HSF1-mediated genes was substantially impaired (Figure S1E).

Using cells expressing the DHFR.dn-cHSF1 construct, we examined the dynamics of stress-responsive SUMO2/3 conjugation following acute (4 hr TMP) HS inhibition versus chronic (48 hr TMP) chaperone depletion prior to HS. Acute TMP treatment did not substantially alter either the accumulation of SUMO2/3 conjugates during HS or the rate of recovery (Figures 1D and 1E). In contrast, chronic inhibition of HSF1 using this TMP-regulated HSF1 construct fully recapitulated the consequences of Dox-inducible dn-cHSF1 expression (Figures 1D and 1E). Thus, alterations in stress-responsive SUMOylation dynamics are attributable to chronic HSF1 inhibition that engenders depletion of critical components within the proteostasis network and sensitizes the system to proteotoxic stress.

Proteomic Identification of SUMOylated Proteins Whose Recovery to Normal SUMO-Conjugation Levels post- Heat Shock is Delayed by Chronic HSF1 Inhibition

We next sought to identify the specific SUMOylation targets that preferentially retain SUMO2/3 when proteostasis capacity is reduced. To address this question, we used nickel-nitrilotriacetic acid (Ni-NTA) beads to purify SUMOylated proteins from HEK293T-REx cells co-expressing a His10-tagged SUMO2 along with Dox-inducible dn-cHSF1. Cells co-expressing a Dox-inducible GFP and His10-SUMO2 were used as a control for any effects of Dox treatment. Cells lacking the His10-SUMO2 construct were used as a control for non-specific binding to Ni-NTA beads.

We then used quantitative proteomics to study SUMO2 target protein dynamics be-fore, during, and after HS in basal and chronic HSF1 inhibition conditions (Figure 2A). Immunoblot analysis of the input samples prior to mass spectrometry analysis fully recapitulated our findings from Figure 1 (Figure 2B). In the proteomics, with a low stringency requiring only an average fold change ≥ 2, we identified 450 proteins that consistently showed increased SUMOylation immediately following HS. The extent of SUMO2 conjugation on 89% (n = 399) of these proteins returned to normal levels during the 4 hr recovery period in untreated cells. In contrast, recovery to normal SUMO2 levels was delayed for 77% (306) of the identified proteins when HSF1 was chronically inhibited (Table S1). We also observed striking enrichment of SUMOylated HSF1 immediately after HS and during recovery following Dox treatment, which can be attributed to a large extent to overexpression of dn-cHSF1 (Figure 2C). These observations demonstrate the vast influence of the proteostasis network on SUMOylated protein dynamics during HS recovery. Notably, we did not observe a global effect on the extent of SUMOylation immediately post-HS owing to chronic HSF1 inhibition.

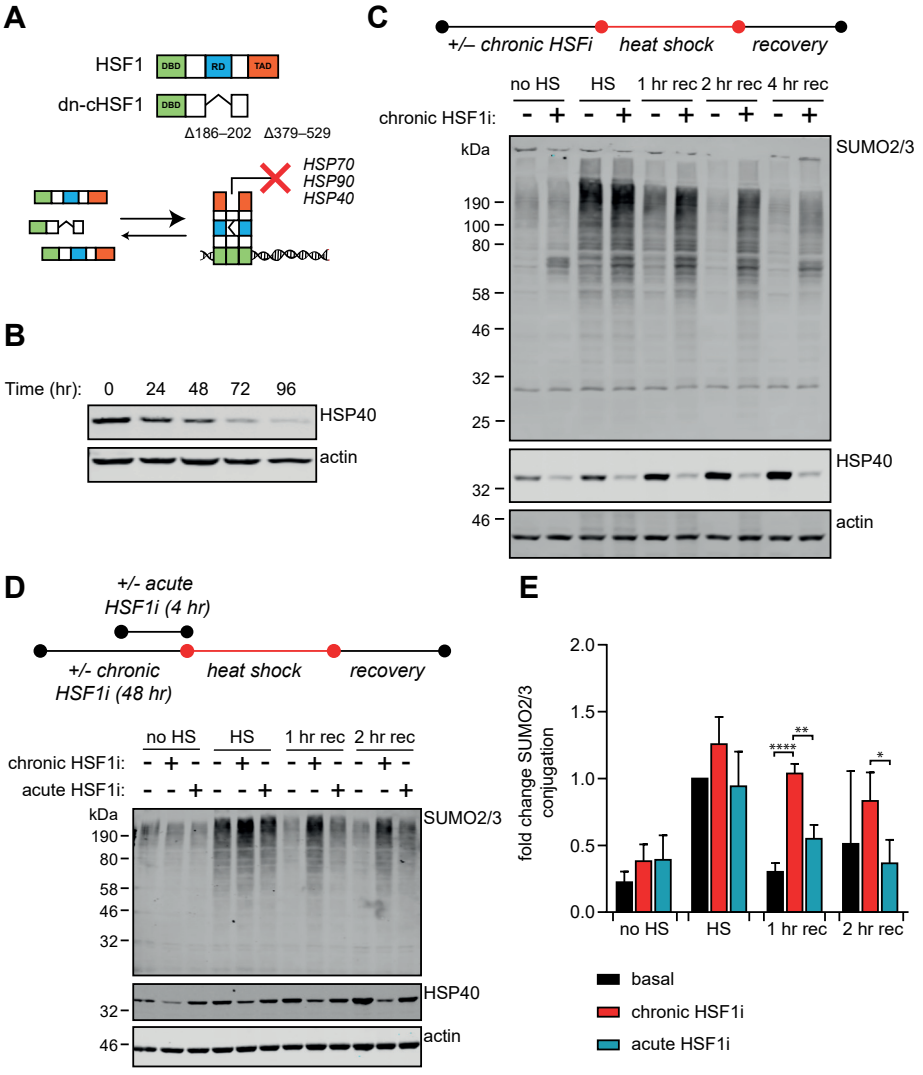

Figure 1. Depletion of Proteostasis Factors via Chronic HSF1 Inhibition Delays Recovery to Normal SUMO2/3 Conjugation Levels after Heat Shock. (**A**) Use of a dominant-negative, constitutively active HSF1 construct (dn-cHSF1), created via disruption of the regulatory domain (RD) by removing amino acids 186–202 combined with deletion of the transcription activation domain (TAD), for inhibition of endogenous HSF1. (**B**) Western blot analysis of HSP40 protein levels in response to different time periods of Dox-induced dn-cHSF1 induction in HEK293T-REx cells. (**C**) HEK293T-REx cells expressing Dox-inducible dn-cHSF1 were treated with Dox for 48 hrs (chronic HSF1i) prior to heat shock (HS). Cells were exposed to a HS at 43 °C for 75 min before returning to 37 °C for a recovery period (rec) and lysed as indicated. Total amounts of SUMOylated proteins were analyzed by immunoblotting. HSP40 levels were used to confirm induction of the heat shock response and functional HSF1 inhibition. (**D**) HEK293T-REx cells constitutively expressing DHFR.dn-cHSF1 were treated with trimethoprim (TMP) for 48 hrs (chronic HSF1 inhibition) or 4 hrs (acute HSF1 inhibition) prior to HS. Cells were subsequently exposed to HS and recovery as described in (A). Total amounts of SUMOylated proteins were determined by immunoblotting. (**E**) Quantification of total SUMO2/3 conjugation from (D) as compared to SUMOylation post-HS in basal proteostasis conditions. n = 3, error bars indicate standard deviation. Significance was determined using ANOVA analysis followed by post-hoc Tukey analysis, * = $p < 0.05$; ** = $p < 0.005$, **** = $p < 0.0001$.
See also Figure S1.

We also did not observe global changes in SUMOylation or SUMOylation dynamics as a result of Dox treatment in the Dox-inducible GFP control cells (Figures 2C and S2A, Table S1). We next set out to identify high-confidence proteins for validation and follow-up studies. We therefore adjusted our selection criteria to proteins having a ≥ 2-fold change as well as a p-value < 0.05 and identified 344 high-confidence SUMO2 target proteins that were significantly enriched immediately following HS, regardless of treatment condition (Tables S1 and S2). The extent of SUMO2 conjugation on 49% (n = 170) of these proteins returned to normal levels during the 4-hr recovery period in untreated cells (Table S3). Of this subset, recovery to normal SUMOylation levels was delayed for 42% (n = 72) of the identified proteins when HSF1 was chronically inhibited (Figure 2C and Table S4), as compared to vehicle treatment.

High-confidence SUMO2 conjugates whose recovery to basal SUMOylation levels was delayed by chronic HSF1 inhibition were enriched for DNA-associated factors, including proteins involved in transcription, recombination, and DNA repair (Figures 2D and S2B), consistent with the predominantly nuclear localization of SUMO. We further validated delayed SUMO2/3 recovery under conditions of chronic HSF1 inhibition for a number of the proteins identified in our mass spectrometry screen, engendering high confidence in our mass spectrometry results (Figure S3). Interestingly, we could also confirm a HSF1 inhibition-dependent effect on the SUMOylation dynamics of FoxM1 post-HS. FoxM1 is a protein that did not quite meet our strict filtering conditions for Figure 2C, indicating that such a stringent selection criteria can lead to false negatives. In combination with our low-stringency data analysis, these results further support the thesis that the proteostasis network is required to resolve a significant fraction of HS-induced SUMO2 targets.

Chronic HSF1 Inhibition Interferes with Degradation of SUMOylated and Ubiquitinated Proteins during Heat Shock Recovery

The clearance of SUMOylated proteins observed during HS recovery may occur ei-ther by removal of SUMO2/3 by the action of SUMO-specific proteases (SENPs) or by degradation of the SUMO2/3-conjugated proteins 30. Using a recently developed set of activity-based probes[31], we performed activity profiling of a set of endogenously expressed SENPs. The results indicated that proteostasis modulation by chronic HSF1 inhibition did not affect the activity of SENPs during HS or recovery (Figure S4).

We next sought to define if SUMOylated proteins were subjected to degradation during HS recovery. We first examined the effects of proteasome inhibition on SUMO2/3 conjugation during HS and recovery using two commercially available proteasome inhibitors, MG-132 and bortezomib. We observed that bortezomib did not induce basal SUMOylation at concentrations with comparable proteasome inhibitory activity as MG-132 (Figure S5A; note that bortezomib does not inhibit the β2 catalytic subunit of the proteasome, whereas MG-132 does inhibit this subunit[32]). We therefore chose to proceed with bortezomib to isolate HS and proteostasis-dependent impacts on degradation of SUMOylated proteins.

We found that proteasome inhibition using bortezomib delayed the recovery of global SUMO2/3 conjugates post-HS in a manner similar to the consequences of chronic HSF1 inhibition prior to HS. Indeed, either proteasome inhibition or chronic HSF1 inhibition resulted in SUMOylation remaining at > 80% of the levels of the maximal SUMOylation in vehicle-treated samples following a 2-hr recovery period. Notably, the effects of proteasome inhibition and chronic HSF1 inhibition on delaying SUMO2/3 recovery were partially additive, with SUMO2/3 conjugation remaining near 100% throughout the recovery period

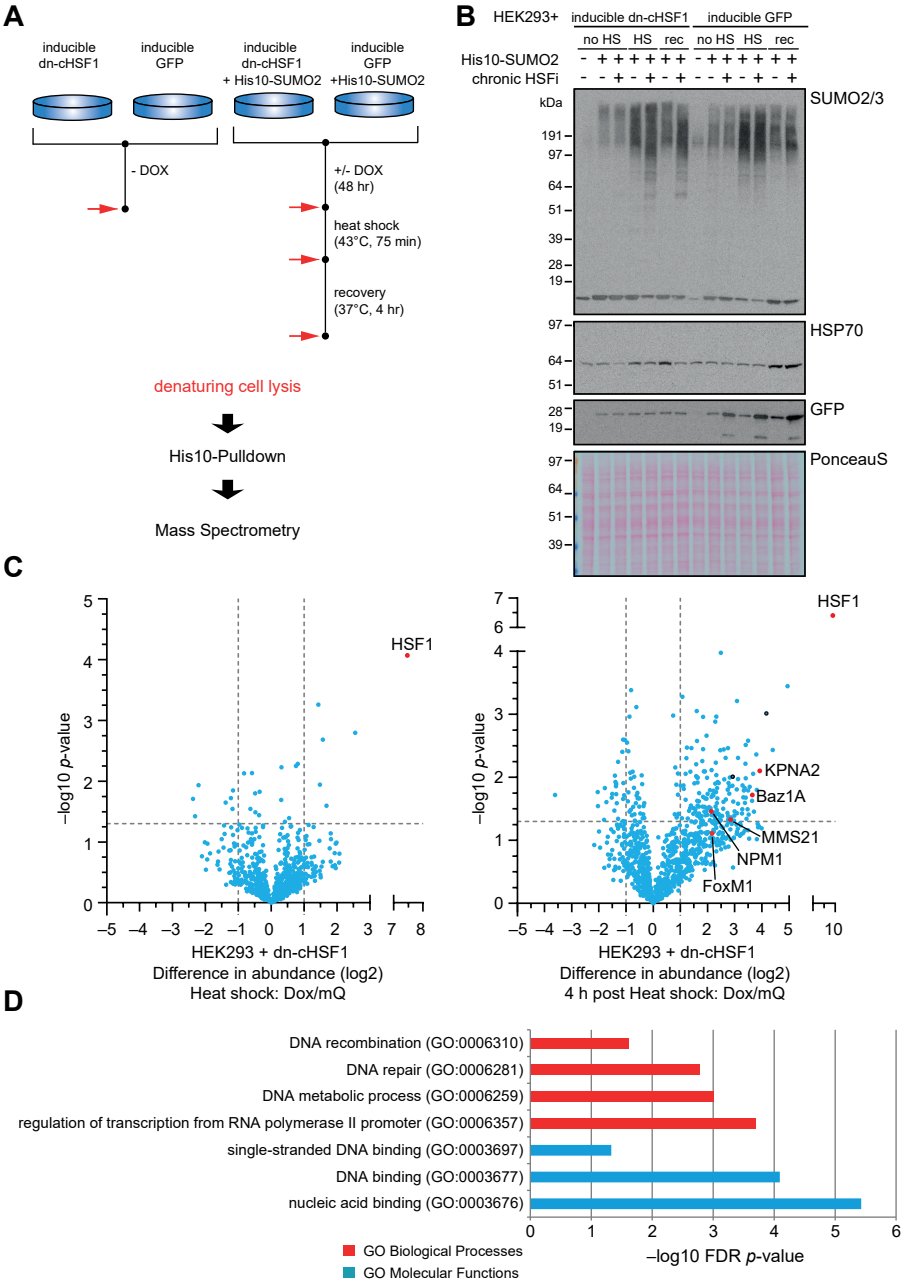

Figure 2. Proteomic Identification of SUMOylated Proteins Whose Recovery to Normal SUMO-conjugation Levels Post- Heat Shock is Delayed by Chronic HSF1 Inhibition. (**A**) Workflow for Figure 2. HEK293T-REx cells stably co-expressing His10-SUMO2 and either Dox-inducible dn-cHSF1 or Dox-inducible GFP were treated with Dox for 48 hrs (chron-ic HSF1 inhibition) prior to heat shock (HS). Cells were exposed to HS at 43 °C for 75 min before returning to 37 °C for a recovery period (rec). Red arrows indicate time points at which cells were lysed. SUMOylated proteins were purified by means of His10-pulldown, proteins were trypsinized, and peptides were analyzed by mass spectrometry. (**B**) Immunoblotting of cell lysates from (A) using antibodies against SUMO2/3, HSP70, and

when the treatments were applied in combination (Figures 3A, S5B, and S5C). Collectively, these observations suggest that a large fraction of SUMO2/3 conjugates are degraded by the proteasome in the recovery phase post-HS, indicating impaired degradation and, therefore, a stabilization of SUMO2/3 conjugates as a consequence of chronic HSF1 inhibition.

Because proteasomal degradation of proteins is regulated by ubiquitination, we next investigated Ub dynamics during HS recovery. Similar to SUMOylation dynamics, we observed an increase in Ub conjugates during HS that was rapidly reduced to pre-HS levels during the recovery period (Figure 3B). Chronic HSF1 inhibition prior to HS delayed recovery of Ub conjugation post-HS, although to a substantially lesser extent than for proteasome inhibition (Figures 3B and S5D). These results suggest that proteostasis factors, transcribed by HSF1, facilitate proteasomal degradation of ubiquitinated as well as SUMOylated substrates during HS recovery. As simultaneous inhibition of the proteasome and HSF1 resulted in a slight additive stabilization of SUMOylated proteins, but not of ubiquitinated proteins, we would not exclude an additional proteasome-independent pathway by which chaperones and other proteostasis factors stimulate a decrease in SUMOylation during recovery post-HS.

We next investigated if the identities of the ubiquitinated and SUMOylated substrates affected by chronic HSF1 inhibition coincided. Here, we examined Ub- and SUMO2- purified fractions for the presence and dynamics of specific proteins that we previously identified as showing delayed recovery to normal SUMO2 levels in Figure 2. The SUMOylation of the cell cycle regulator Forkhead box transcription factor FoxM1 was induced upon HS and decreased to pre-HS levels during recovery, but was stabilized by either proteasome inhibition or chronic HSF1 inhibition (Figure 3C). FoxM1 ubiquitination was also induced by HS and recovered post-HS in a proteasome and HSF1-dependent manner (Figure 3D). Additional SUMO2 substrates, identified by proteomics, showed similar SUMOylation and ubiquitination dynamics, indicating that both modifications were affected by chronic HSF1 inhibition on the same substrate proteins (Figures S5E and S5F).

Collectively, these data suggest that proteasomal degradation is a major, but not the exclusive, fate of SUMO2/3 and Ub conjugates during HS recovery. Chronic HSF1 inhibition interferes with this proteasomal degradation and therefore stabilizes ubiquitinated as well as SUMOylated subsets of the same target protein.

Chronic HSF1 Inhibition Selectively Impairs Degradation of SUMO2/3 and Ub co-modified Proteins during Heat Shock Recovery

SUMO and Ub both covalently attach to lysine residues in target proteins. The modifications are mutually exclusive at a specific modification site. However, SUMOylation and ubiquitination frequently co-exist at different sites on the same protein[33,34]. We observed in Figures 3C and 3D that FoxM1 was modified by both SUMO2/3 and Ub, and that the

< GFP. Total amounts of proteins in each lane were visualized by Ponceau S staining. (**C**) Volcano plots depicting statistical differences in abundance between proteins identified by mass spectrometry. Dashed lines indicate a cut-off at a *p* value ≤ 0.05 (–log10 *p* value ≤ 1.3) and a fold change of 2 (log2 = 1). Left panel shows SUMOylated proteins identified immediately post-HS in the Dox-inducible dn-cHSF1 cell line, specifically in the Dox-treated sample compared to the untreated sample. Right panel shows SUMOylated proteins identified 4 hrs post–HS in the Dox-inducible dn-cHSF1 cell line compared to the untreated sample. Proteins marked in red are either HSF1 or proteins that were further validated. (**D**) Selection of enriched gene ontology terms of biological processes and molecular functions for selected proteins that significantly retained SUMOylation 4 hrs post-HS when HSF1 activity was chronically inhibited.

See also Figures S2 and S3 and Tables S1, S2, S3, and S4.

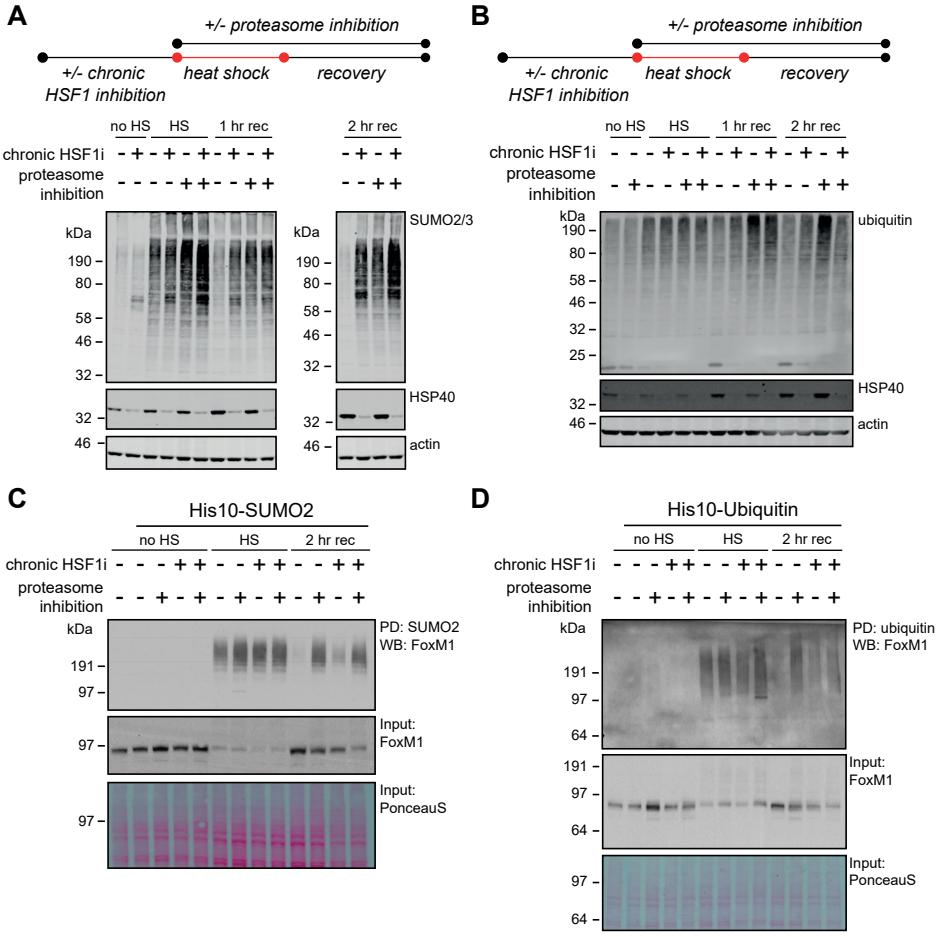

Figure 3. Chronic HSF1 Inhibition Interferes with Degradation of SUMOylated and Ubiquitinated Proteins during Heat Shock Recovery. (**A**) HEK293T-REx cells expressing Dox-inducible dn-cHSF1 were treated with Dox for 48 hr (chronic HSF1 inhibition), with 100 nM bortezomib (proteasome inhibition) immediately prior to heat shock (HS), or a combination of both. Cells were exposed to HS at 43 °C for 75 min before returning to 37 °C for a recovery period (rec) and lysed as indicated. Total amounts of SUMOylated proteins were analyzed by immunoblotting. HSP40 levels were used to confirm induction of the heat shock response and functional HSF1 inhibition. (**B**) HEK293T-REx cells expressing Dox-inducible dn-cHSF1 were treated as in (A). Total amounts of ubiquitinated proteins were analyzed by immunoblotting. (**C**) HEK293T-REx cells stably co-expressing His10-SUMO2 and Dox-inducible dn-cHSF1 were treated as in (A). SUMOylated proteins were purified by means of His10-purification. Elutions and inputs were analyzed by immunoblotting for FoxM1. Ponceau S stain was used as a loading control for inputs. (**D**) HEK293T-REx cells stably co-expressing His10-Ub and Dox-inducible dn-cHSF1 were treated as in (A). Ubiquitinated proteins were purified by means of His10-purification. Elutions and inputs were analyzed by immunoblotting for FoxM1. Ponceau S stain was used as a loading control for inputs. See also Figures S4 and S5.

dynamics of both modifications were influenced by chronic HSF1 inhibition. We therefore wondered if depletion of proteostasis network components by chronic HSF1 inhibition would preferentially impair degradation of the co-modified fraction of ubiquitinated or SUMOylated proteins.

We first examined the dynamics of ubiquitinated proteins in SUMO2 pulldowns and vice versa during either proteasome inhibition or chronic HSF1 inhibition. Within the SUMOylated

fraction, Ub was co-enriched upon HS, indicating an enrichment of co-modified proteins. The extent of Ub co-enrichment fell during HS recovery, but was enhanced by either chronic HSF1 inhibition or proteasome inhibition (Figure 4A). We observed the same dynamics for SUMO2/3 substrates within the Ub-purified proteins (Figure 4B). Collectively, these results support the conclusion that chaperone depletion interferes with the degradation of co-modified proteins during HS recovery.

We next wondered if the effect of chronic HSF1 inhibition was restricted to co-modified proteins, or if the stabilization of SUMO2/3 was merely a consequence of the stabilization of all ubiquitinated proteins. To answer this question, we investigated the ratio of SUMO2/3 in the pool of Ub-modified proteins. By inhibiting the proteasome, we expected to inhibit the degradation of all Ub-modified substrates, including co-modified proteins. If chronic HSF1 inhibition interfered mainly with the degradation of co-modified proteins, we would expect the ratio of SUMO2/3-modified to total Ub-modified proteins within the Ub-purified substrates to increase, as co-modified proteins would be stabilized whereas substrates modified by Ub alone would continue to be degraded. As shown in Figure 4C, we indeed observed a significant difference in SUMO/Ub ratio in the Ub-purified pool of proteins between proteasome inhibition and chronic HSF1 inhibition during the recovery post-HS, indicating a mechanism by which HSF1-induced factors selectively influence the degradation of co-modified proteins rather than all ubiquitinated proteins.

HSP90 Plays a Key Role in the Recovery to Normal SUMO2/3 Modification Levels following Heat Shock

As chronic HSF1 inhibition results in a reduction in proteostasis network capacity (Figure 1B), our data suggest that maintaining sufficient proteostasis capacity is critical for regulating the dynamics of SUMO2/3 and Ub substrates during HS recovery. We therefore sought to identify whether inhibition of specific proteostasis components would be sufficient to recapitulate the delayed recovery of SUMO2/3- and Ub-modified targets we initially observed with chronic HSF1 inhibition.

Using STA-9090 to inhibit HSP90, we examined the dynamics of SUMO2/3 and Ub conjugates following HS. We found that HSP90 inhibition, like chronic HSF1 inhibition, resulted in delayed recovery of > 50% of SUMO2/3 conjugates following a 2-hr recovery period (Figures 5A, 5B, and S6A). Similarly, we observed a delayed recovery post-HS of total ubiquitination upon HSP90 inhibition (Figures S6B and S6C). To investigate if HSP90 inhibition affects the same SUMOylated substrates we previously identified using proteomics (Figure 2), we purified SUMO2 conjugates and Ub conjugates and examined the dynamics of target proteins upon HS following either chaperone depletion or HSP90 inhibition. Indeed, we observed a HSF1- and HSP90-dependent decrease of FoxM1 SUMOylation and ubiquitination during the recovery period (Figures 5C and 5E). Similar effects were observed for other proteins (Figures S6D and S6E). HSP90 inhibition also prolonged retention of co-modified proteins, as observed for SUMO2/3 co-modified proteins in the Ub pulldowns and vice versa (Figures 5D, 5F, and S6F), and led to an increase in SUMO2/3 relative to Ub within Ub-purified proteins (Figure S6F).

Collectively, these data indicate that HSP90 inhibition alone can at least partially recapitulate the effects of chronic HSF1 inhibition, delaying the recovery of SUMOylated and Ub co-modified substrates post-HS. These observations suggest that HSP90 is a key chaperone effector that promotes the degradation of co-modified proteins.

SUMOylation of Substrate Proteins Enhances Solubility

A key role of Ub on the co-modified proteins appears to be efficient proteasome delivery and processing of the target protein. In contrast, the role of SUMO is less clear. We noted that SUMO has been used extensively as a solubility tag to prevent inclusion body formation during protein expression in *Escherichia coli*[35,36] and is also proposed to modulate aggregation of proteins associated with neurodegenerative disorders[28,37]. Therefore, we next used an *in vitro* assay to explore the possibility that rapid SUMO2/3 conjugation could act as a solubility tag on target proteins identified from our proteomic studies. Solubility enhancement mediated by SUMOylation could prevent aggregation of terminally misfolded proteins prior to their clearance by proteasomal degradation, a process that could be facilitated by chaperones during HS recovery.

To address this possibility, we investigated the aggregation behavior of selected SUMO-tagged proteins identified from our proteomics screen in Figure 2, using *in vitro* thermal shift assays. MMS21 was expressed in *E. coli* with or without an N-terminal SUMO3 tag, and the isolated protein was analyzed by a thermal shift assay to determine the aggregation temperature (T_{agg})[38]. We observed that the Tagg of N-SUMO3-MMS21 was ~7 °C higher than that of untagged MMS21 (Figure 6A).

This intriguing result, obtained using a non-natural N-terminal fusion of a single SUMO3 moiety to MMS21, prompted us to then further investigate a more biologically realistic situation. Given that proteins from the proteomics screen were often conjugated to multiple SUMO2/3 moieties, we explored the impact of multiple SUMO2/3 modifications on FoxM1 using *in vitro* SUMOylation. Similar to MMS21, conjugation of SUMO2/3 protected FoxM1 against heat-induced aggregation (Figure 6B). Furthermore, increasing SUMOylation appeared to stabilize FoxM1 additively, with higher order SUMO2/3 conjugates showing almost no aggregation at temperatures up to 70 °C. The presence of unmodified FoxM1 was also prolonged in the soluble fraction when SUMOylated proteins were present, indicating that the presence of SUMOylated proteins could even have a beneficial effect on the solubility of non-SUMOylated proteins in the vicinity (Figure 6B). We further investigated the impact of SUMOylation on FoxM1 during extended HS at moderate temperatures identical to the temperatures used in cellular studies. While unmodified FoxM1 demonstrated progressive aggregation at 43 °C, highly SUMOylated FoxM1 remained soluble throughout the duration of HS (Figure 6C). These results suggest that SUMO alters biophysical properties of the target protein and thereby decreases aggregation propensity. In cells, a likely consequence would be the promotion of proteasomal clearance during HS recovery by preventing the formation of otherwise insoluble and potentially irreversible aggregates.

DISCUSSION

The dynamic nature of protein post-translational modifications makes them particularly well-suited to regulate cellular processes during stress responses, as they can act rapidly in response to stimuli and their reversible nature makes them suitable to act in a transient manner. Here, we have explored the enigmatic role of SUMO signaling in the HSR and identified a unique subset of HS induced SUMO2/3 targets preferentially regulated by the proteostasis network.

The precise mechanism for enhanced SUMOylation upon heat stress remains to be investigated in detail. Pinto and co-workers have shown that heat stress inactivates SUMO proteases[39]. Our data recapitulate this observation, as we observe the inactivation of SENP1

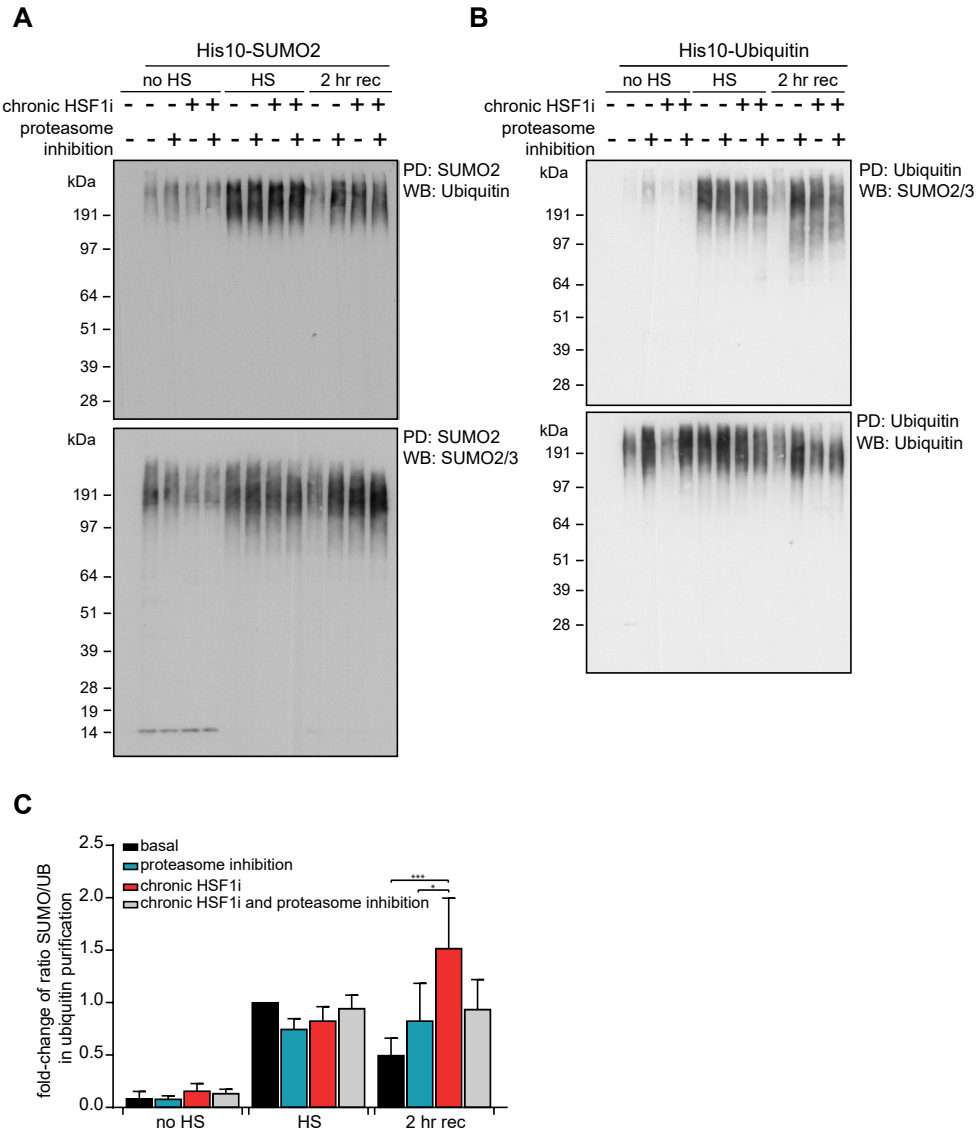

Figure 4. Chronic HSF1 inhibition selectively impairs degradation of SUMO2/3 and Ub co-modified proteins during heat shock recovery. (**A**) HEK293T-REx cells stably co-expressing His10-SUMO2 and Dox-inducible dn-cHSF1 were treated with Dox for 48 hrs (chronic HSF1i) prior to heat shock (HS), with 100 nM bortezomib (proteasome inhibition) immediately prior to HS, or a combination of both. Cells were exposed to a HS at 43 °C for 75 min before returning to 37 °C for a recovery period (rec) and lysing as indicated. Elutions were analyzed by immunoblotting for Ub and SU-MO2/3. (**B**) HEK293T-REx cells stably co-expressing His10-Ub and Dox-inducible dn-cHSF1 were treated as in (A). Elutions were analyzed by immunoblotting for SUMO2/3 and Ub. (**C**) Quantification of (B). Graph shows fold change of the ratio of SUMOylated proteins over ubiquitinated proteins in His10-Ub purified elutions as compared to the ratio after HS under basal proteostasis conditions. n = 3, error bars represent SD. Significance was determined using ANOVA followed by post-hoc Tukey's multiple comparison test, * = $p < 0.05$; *** = $p < 0.001$.

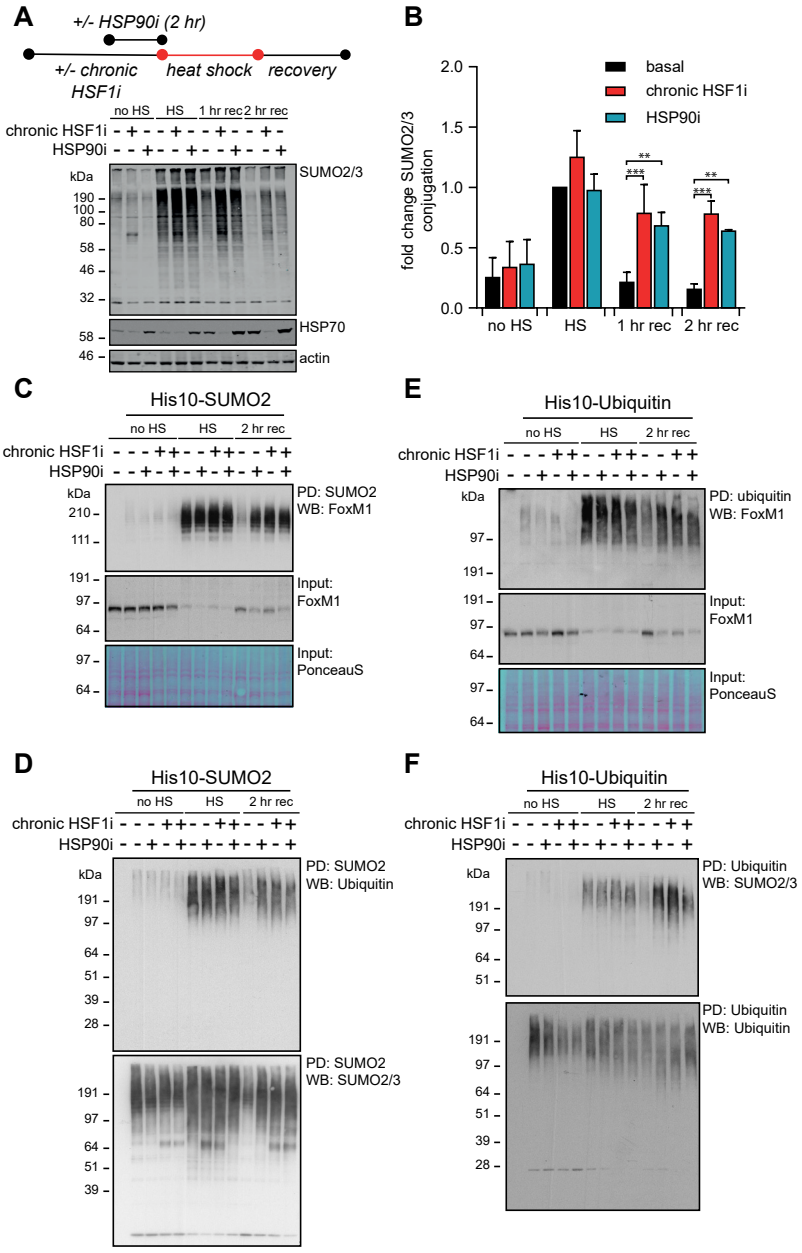

Figure 5. HSP90 Plays a Key Role in the Recovery of SUMO2/3 Modification Following Heat Shock. (**A**) HEK293T-REx cells expressing Dox-inducible dn-cHSF1 were either treated with Dox for 48 hrs (chronic HSF1 inhibition) prior to heat shock (HS), with 500 nM STA-9090 (HSP90i) 2 hrs prior to HS, or with a combination of both. Cells were exposed to a HS at 43 °C for 75 min before returning to 37 °C for a recovery period (rec) and lysed as indicated. Total amounts of SUMOylated proteins were analyzed by immunoblotting. HSP70 levels were used to confirm induction of the heat shock response and functional HSF1 inhibition. (**B**) Quantification of fold-change of SUMOylation from (A) as compared to SUMOylation after HS under the basal proteostasis conditions. n = 3, error bars indicate standard deviation. Significance was determined using ANOVA analysis followed by post-hoc Tukey analysis, * = $p < 0.05$; *** = < 0.0005. (**C**) HEK293T-REx cells stably co-expressing His10-SUMO2 and Dox-inducible dn-cHSF1 were

and SENP3 in response to heat stress (Figure S4B). Whether prolonged inactivation of SUMO proteases is responsible for prolonged increases of SUMOylation upon heat stress combined with chronic HSF1 inhibition is less clear, as our data did not convincingly show an HSF1-dependent inactivation of SENPs (Figure S4B). Alternatively, prolonged increases in activity of the SUMO conjugation machinery could explain prolonged increases of SUMOylation upon heat stress combined with chronic HSF1 inhibition. If this is the case, then we would expect higher auto-SUMOylation activity of SUMO E3 ligases[40]. SUMOylation of PIAS family members PIAS4 and MMS21 did increase in response to chronic HSF1 inhibition, as shown by mass spectrometry. We confirmed this result for MMS21 by immunoblotting (Figure S3A). We therefore expect that PIAS4 and MMS21 could mechanistically contribute to enhanced SUMOylation upon chronic HSF1 inhibition.

Conjugation of SUMO2/3 May Act as an Early Responder to Misfolded Proteins during Heat Shock

The key function of the transcription factor HSF1 is to activate genes encoding chap-erones and other proteostasis factors required to address protein misfolding induced by increased temperature or other stressors[41]. The transcriptional nature of this response results in a time gap between the rapid onset of proteotoxic stress and the availability of sufficient amounts of new chaperones to address the misfolded proteins[42]. Given that SUMOylation accumulates rapidly after onset of HS, and the extensive use of SUMO as a linear fusion to recombinant proteins to enhance solubility[43,44], we hypothesized that SUMOylation could potentially be functioning to deter aggregation during early stages of HS.

We explored the effect of SUMOylation on the solubility of target proteins upon HS *in vitro* and established that SUMOylation can have a profoundly solubilizing effect on its target proteins. Given the low substrate occupancy of SUMO2/3 on target proteins, it is unlikely that SUMOylation *in vivo* globally shifts the aggregation propensity of the total pool for its targets. Rather, these data suggest that SUMOylation may function to survey and tag unfolded proteins at particular risk for aggregation and facilitate their degradation through subsequent ubiquitination and proteasomal degradation. N-Linked glycosylation in the endoplasmic reticulum is also known to enhance solubility and facilitate interactions with protein folding machinery[45], suggesting that cells commonly utilize post-translational modifications to support proteostasis during stress conditions. These results therefore provide a possible method for cells to address the time-gap between stress onset and increased chaperone levels by acting as an early-response factor that can act rapidly to keep unfolded proteins soluble and prevent their accumulation into insoluble aggregates.

Mechanistically, it has been shown previously that the SUMO conjugation machinery recognizes disordered regions in target proteins[46]. As proteins that are unfolded will display increased levels of disordered regions, direct recognition of these regions by the SUMO conjugation machinery may provide a mechanism for this machinery to focus on unfolded target proteins. Under normal proteostasis conditions, SUMO mostly targets lysines which are located in a SUMOylation consensus motif (ψKxE, where ψ is a large hydrophobic amino

<treated as in (A) with a 2 hr recovery at 37 °C. SUMOylated proteins were purified by means of His10-purification. Elutions and inputs were analyzed by immunoblotting for FoxM1. Ponceau S stain was used as a loading control for inputs. (**D**) As for (C). Elutions were analyzed by immunoblotting for Ub and SUMO2/3. (E) HEK293T-REx cells stably co-expressing His10-Ub and Dox-inducible dn-cHSF1 were treated as in (A) with a 2 hrs recovery at 37 °C. Ubiquitinated proteins were purified by means of His10-purification. Elutions and inputs were analyzed by immunoblotting for FoxM1. Ponceau S stain was used as a loading control for inputs. (**F**) As for (E). Elutions were analyzed by immunoblotting for SUMO2/3 and Ub. See also Figure S6.

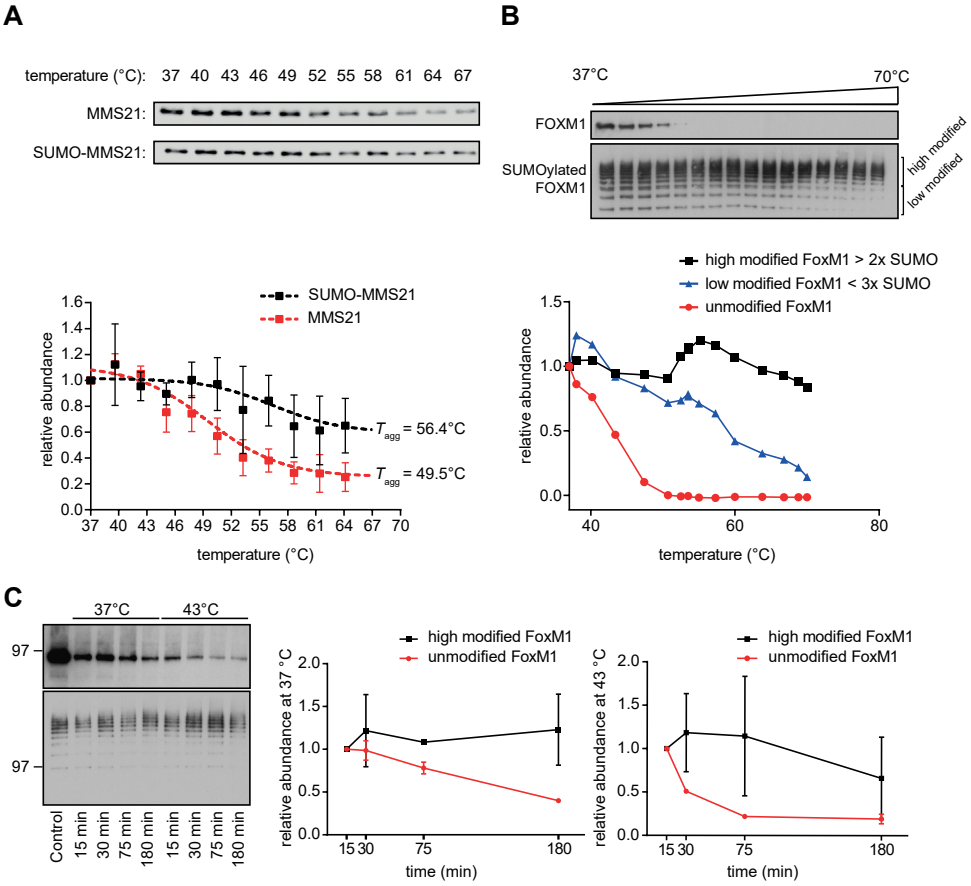

Figure 6. SUMOylation of Substrate Proteins Enhances Solubility. (**A**) Recombinant MMS21 fused to SUMO3 was exposed to increasing temperatures (37–67 °C). Soluble fractions were isolated from temperature-induced aggregates by centrifugation and analyzed by immunoblotting with a specific antibody against MMS21. The plot shows relative fold change of soluble MMS21 normalized to the soluble MMS21 at 37 °C, n = 3, error bars represent standard deviation. Data were fit to a sigmoidal curve in Prism to determine aggregation temperature (T_{agg}). (**B**) Recombinant FoxM1 was expressed and in vitro SUMOylated in E. coli, and in-vitro thermal shift performed as in (A). The soluble fraction of non-modified and SUMOylated FoxM1 was then analyzed by immunoblotting for FoxM1. The plots show relative fold-change of FoxM1 in the soluble fraction, comparing the highly SUMOylated FoxM1 species (>FoxM1-3x SUMO), modestly SUMOylated FoxM1 species (<FoxM1-3x SUMO) and un-modified FoxM1. (**C**) Recombinant FoxM1 was expressed and in vitro SUMOylated in E. coli, subsequently purified and incubated at either 37 °C or 43 °C for 15, 30, 75 min or 180 min. The soluble fraction of non-modified and SUMOylated FoxM1 was then analyzed by immunoblotting for FoxM1. The plots show relative fold change of FoxM1 in the soluble fraction comparing the highly SUMOylated FoxM1 species (>FoxM1-3x SUMO) to unmodified FoxM1 in two biological replicates.

acid). SUMOylation was reported to become more promiscuous during HS, targeting lysines that are not located in the consensus motif and demonstrating the possibility of a more general protective purpose for SUMOylation during HS[22].

Our results indicate that both SUMO2/3 and Ub are involved in the HSR. Whereas Ub has been named after its 'ubiquitous' cellular levels[47], SUMO has previously been consid-ered to be a low abundance protein[48]. Our data thus pose the challenge as to why a low abundance protein modifier would be used to deal with extensive protein misfolding. Proteomics

methods have been developed that can determine the copy numbers of proteins in cells[49]. The authors have shown that Ub is indeed one of the most abundant cellular proteins, with over 14 million copies per cell, ranking as the 10th most abundant cellular protein. Intriguingly, they found nearly 9 million copies of SUMO2 per cell, ranking SUMO2 as the 20st most abundant cellular protein. Thus, the difference in overall copy number per cell between Ub and SUMO2 is small. Additionally, given that Ub is present throughout the cell whereas SUMO2 is predominantly located in the nucleus, nuclear SUMO2 and Ub levels are expected to be rather similar. Therefore, SUMO2 should also be considered to be an abundant protein, making it a suitable early-response factor.

Despite the high abundance of SUMO and global SUMO conjugation within the nucleus, especially after HS, only a small fraction of a specific protein pool is targeted for SUMOylation. Whereas the SUMO- and ubiquitin-modified versions of target proteins are degraded by the proteasome, we did not observe that proteasomal inhibition affected the total pool of these targets, due to the substoichiometric nature of the modifications. We did, however, observe a clear stabilization of the SUMOylated and ubiquitinated version of selected targets in our bortezomib experiments (Figure 3 and S5). This finding is in line with earlier observations in the ubiquitin field indicating that the ubiquitiated portion of many proteins increased in response to proteasomal inhibition without noticeable changes in total levels of these proteins[50].

Because SUMO modifications are not known to directly target proteins to the proteasome for degradation, we consider it likely that subsequent ubiquitination is required for target protein degradation. Therefore, early conjugation of SUMO2/3 and subsequent ubiquitination works in concert to likely minimize aggregation of misfolded proteins by ensuring solubility and also by promoting degradation, respectively (Figure 7).

Proteostasis Factors facilitate Proteasomal Degradation of Co-modified Proteins

In the absence of HSF1, prolonged retention of SUMO2/3 during HS recovery indicates that proteostasis factors are required to resolve irreversible folding problems. Although SUMO2/3 might be able to act as an early-response factor to prevent aggregation of misfolded proteins, this action is apparently insufficient for refolding of the majority of proteins involved. Dissolution of misfolded proteins can either be carried out via refolding of the misfolded proteins, or via degradation by the ubiquitin-proteasome system. The pronounced effects of proteasome inhibition on overall SUMO2/3 conjugate levels during HS recovery indicates that a majority of SUMO2/3 targets are degraded. Refolding of SUMOylated misfolded proteins by the chaperones thus appears to not be very successful. Nevertheless, chaperones, especially HSP90, appear to be needed to facilitate the proteasomal degradation of misfolded proteins. Whether this degradation is mediated by HSP90 directly via either shuttling co-modified proteins to the proteasome or an effect of HSP90 on the activity of the proteasome itself remains to be resolved. Both scenarios seem possible, as chaperones have been identified as proteasome-interacting factors[51]. Of note, chaperones are predominantly located in the cytoplasm, indicating limited availability of chaperones for the regulation of nuclear proteins. In contrast, SUMO2/3 are predominantly located in the nucleus and could therefore potentially compensate for the limited availability of chaperones in the nucleus at the early phase of the HSR.

Chaperone-dependent degradation or refolding both prevent the formation of protein aggregates that are linked to many diseases, including aging-related neurodegeneration[52,53]. Once aggregates have formed, they appear to be resistant to protein degradation and pos-

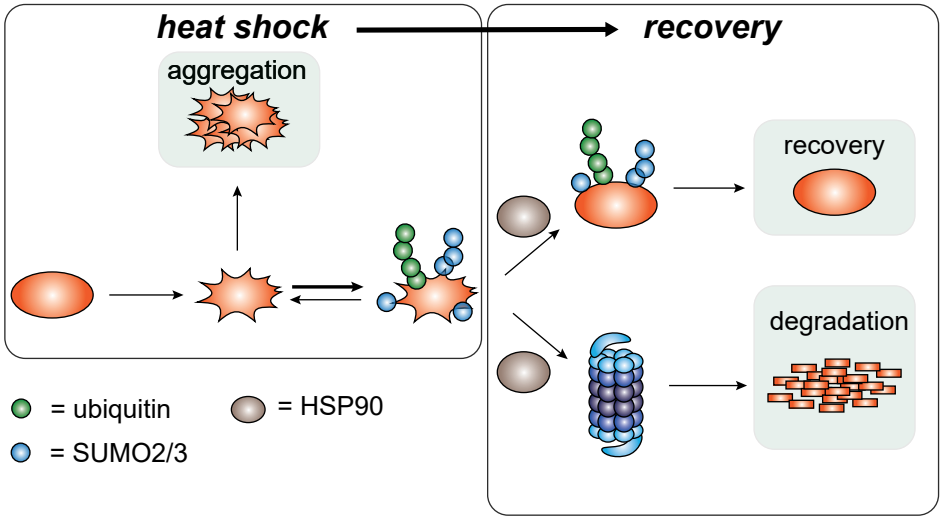

Figure 7. SUMO2/3 plays a Key Role as an Integrated Component of the Proteotoxic Stress Response.
Upon HS, a transient increase in SUMO2/3 conjugation to target proteins is observed, which may function in part to prevent irreversible aggregation of target proteins (reduced aggregation was demonstrated in vitro). SUMO2/3 modified proteins are frequently co-modified by Ub, and a large fraction of these co-modified proteins are subsequently degraded by the proteasome during HS recovery in a chaperone-dependent manner.

sess a high propensity to self-propagate and accrue in inclusion bodies [54]. Interestingly, SUMO has been found in disease-associated protein aggregates[55], suggesting a possible role in responding to or modifying aggregation-prone proteins. Our findings demonstrate clear con-nections between a functional proteostasis network and the post-translational modifications of Ub and SUMO2/3. Further improving our understanding of these connections might aid the development of treatment strategies for diseases characterized by the accumulation of toxic protein aggregates.

ACKNOWLEDGEMENTS
We thank Dr. R. González-Prieto for assistance with mass spectrometry. The laboratory of A.C.O.V. is supported by the European Research Council (ERC) and the Netherlands Organisation for Scientific Research (NWO). This work was also supported by the National Institute on Aging of the NIH Grant 5R21AG054961 to M.D.S and by the National Institute of Environmental Health Sciences of the NIH under award P30-ES002109. C.L.M. was supported by an NSF Graduate Research Fellowship. The mass spectrometry proteomics data have been deposited to the ProteomeXchange Consortium via the PRIDE partner repository with the dataset identifier PXD010231.

AUTHOR CONTRIBUTIONS
A.C.O.V. and M.D.S. conceived the project. F.L., R.M.S., C.L.M., A.C.O.V. and M.D.S. designed experiments. F.L., R.M.S., and C.L.M. conducted experiments. M.P.C.M. and H.O. provided key reagents. F.L., R.M.S., A.C.O.V., and M.D.S. drafted the manuscript. All authors analyzed data and edited the manuscript.

DECLARATION OF INTERESTS

H.O. is founder and a shareholder of UbiqBio B.V., a company that markets research reagents. All other authors declare no competing interests.

SUPPLEMENTARY DATA

Supplementary data tables can be found online

Key Recource Table

REAGENT or RESOURCE	SOURCE	IDENTIFIER
Antibodies		
SUMO2/3 mouse monoclonal	Abcam	Cat# ab81371; RRID:AB_1658424
SUMO2/3 mouse monoclonal	University of Iowa	8A2
HSP40 rabbit polyclonal	Enzo	Cat# ADI-SPA-400; RRID:AB_10631418
HSP70 rabbit polyclonal	Enzo	Cat# ADI-SPA-811D; RRID:AB_2621431
β-Actin mouse monoclonal	Sigma	Cat# A1978; RRID:AB_476692
ACF1/Baz1A rabbit polyclonal	Bethyl Laboratories	Cat# A301-318A-T; RRID:AB_937730
RCH1/KPNA2 rabbit polyclonal	Bethyl Laboratories	Cat# A300-483A-T; RRID:AB_451018
MMS21 rabbit polyclonal	Bethyl Laboratories	Cat# A300-129A; RRID:AB_2142840
NPM 1 rabbit polyclonal	Bethyl Laboratories	Cat# A302-402A; RRID:AB_1907285
SENP1 rabbit monoclonal	Abcam	Cat# ab108981; RRID:AB_10862449
SENP3 rabbit monoclonal	Cell Signaling Techol-ogy	Cat# 5591P; RRID:AB_10695540
SETDB1 rabbit monoclonal	Cell Signaling Techol-ogy	Cat# 2196S; RRID:AB_823637
SENP6 mouse monoclonal	Sigma	Cat # WHP0026054M1; RRID:AB_1843525
FoxM1	Santa Cruz	Cat# sc-502; RRID:AB_631523
Ubiquitin Mouse monoclonal	Millipore	Cat# 04-263; RRID:AB_612093
Ubiquitin	Santa Cruz	Cat# sc-8017; RRID:AB_628423
Bacterial and Virus Strains		
BL21(DE3)	New England BioLabs	Cat# C2527I
Chemicals, Peptides, and Recombinant Proteins		
STA-9090	MedChem Express	Cat# HY-15205
Doxycyline	Alfa Aesar	Cat# J63805
Trimethoprim	Matrix	Cat# 058373
Bortezomib	ChemGood	Cat# C-1279
MG-132	Fischer Scientific	Cat# NC9326288
Resazurin Sodium Salt	Sigma	Cat# R7017-5G
Rho-SUMO2-PA	31	NA
K11 di-SUMO VA ABP	31	NA
Critical Commercial Assays		
4–12% BoltTM Bis–Tris	ThermoFisher	NW04125BOX
NuPageTM 3–8% Tris-acetate	ThermoFisher	EA03755BOX
EZNA Total RNA Kit I	Omega	Cat# R6834-02
High-Capacity cDNA Reverse Transcription Kit	Applied Biosystems	Cat# 4368814
Fast Start Universal SYBR Green Master Mix	Roche	Cat# 4913850001
Deposited Data		

ProteomeXchange (via PRIDE database)	This paper	PXD010231
Experimental Models: Cell Lines		
Human: HEK293T-REx	Life Technologies	Cat# R71007
Human: LX2	EMD Millipore	Cat# SCC064; RRID:CVCL_5792
Recombinant DNA		
pET-15b	Novagen	Cat# 69661
pET11a-SUMO3	56	Addgene Plasmid #53143
pDEST17	Invitrogen	Cat# 11803012
pT-E1E2S2	57	NA
Lentiviral His10-SUMO2 IRES GFP	58	NA
Lentiviral His10-Ubiquitin IRES Puro	34	NA
pLenti CMV/TO Zeo dn-cHSF1	29	NA
pLenti CMV/TO Zeo GFP	29	NA
pLenti CMV Puro DHFR.dn-cHSF1	29	NA
Software and Algorithms		
MaxQuant ver 1.5.6.0	Max Planck Institute	http://www.biochem.mpg.de/5111795/maxquant
Perseus ver 1.5.6	Max Planck Institute	http://www.biochem.mpg.de/5111810/perseus
PANTHER	Gene Ontology Consortium	http://pantherdb.org/
Image Studio Lite ver 5.2	Li-COR	https://www.licor.com/bio/products/software/
GraphPad Prism 7	GraphPad	https://www.graphpad.com
ImageJ	Fiji	https://imagej.net/Welcome
Other		
Triple-disc C18 reverse phase stage-tips	59	NA

Contact For Reagent And Resource Sharing
Further information and requests for resources and reagents should be directed to and will be fulfilled by the Lead Contact, Matthew D. Shoulders (mshoulde@mit.edu).

Experimental Model And Subject Details
Human cell lines HEK293T-REx cells (human embryonic kidney, female) and LX2 cells (human hepatic stellate, male) were cultured at 37 °C in DMEM supplemented with 10% FBS and 1% penicillin/streptomycin/glutamine in a 5% CO2 atmosphere.
Environmental Stress Conditions: All heat shock experiments were performed at 43 °C and 5% CO2 for 75 min. For the recovery post-heat shock, cells were kept at 37 °C and 5% CO2 for the indicated time periods.

METHOD DETAILS

Lentivirus
Stable HEK293T-REx cells containing the Dox-inducible dn-cHSF1 and constitutively expressing FKBP.cHSF1 were prepared as previously described[29]. Lentiviruses encoding His10-SUMO2-WT-IRES-GFP[58] or His10-ubiquitin-WT-IRES-puro were transduced with an MOI (multiplicity of infection) of 3 using the third-generation lentiviral system into the previously generated HEK293T-REx cells containing both FKBP.cHSF1 and Dox-inducible dn-cHSF1 29. His10-SUMO2-WT-IRES-GFP expressing cells were sorted by fluorescence-aided cell sorting (FACS) on the BD FACSAriaIIITM cell sorter for low GFP expression to limit His10-SUMO2 expression. His10-ubiquitin-WT-IRES-PURO expressing cells were selected by supplementing the cell medium with 1μg/ml puromycin.

Immunoblotting Analysis
Cells were lysed in SNTBS buffer consisting of 2% SDS, 1% N-P40, 50 mM TRIS at pH 7.5, and 150 mM NaCl for whole lysate analysis of HEK293T-REx and LX2 cells. Proteins were separated by a 4–10% SDS-PAGE gel then transferred to a nitrocellulose membrane. Pulldown elutions and inputs were separated on either 4–12% BoltTM Bis-Tris or NuPageTM 3–8% Tris-acetate (anti-Baz1A) gradient gels. Following a 30 min blocking step in 5% milk, blots were incubated overnight with the appropriate primary antibodies and for 1 hr with the appropriate 680 or 800 nm fluorophore labeled secondary antibodies from Li-COR Biosciences or HRP-conjugated goat anti-mouse IgG, HRP-conjugated donkey anti-rabbit IgG from Pierce. Detection was performed on a Li-COR Biosciences Odyssey Imager for fluorophore-coupled secondary antibodies and with PierceTM ECL Plus Western Blotting substrate for HRP-coupled secondary antibodies. Band quantification was performed in Image Studio Lite or ImageJ (Fiji).

Quantitative RT-PCR.
The relative mRNA expression levels of selected heat shock re-sponse genes were measured using quantitative RT-PCR. HEK293T-REx cells expressing DHFR.dn-cHSF1 were treated with 10 μM TMP for 0, 2, 4, or 8 hr prior to challenge with a heat shock at 43 °C for 75 min. RNA was extracted using the EZNA Total RNA Kit I (Omega). qRT-PCR reactions were performed on cDNA prepared from 1000 ng of total cellular RNA using the High-Capacity cDNA Reverse Transcription Kit (Applied Biosystems). The Fast Start Universal SYBR Green Master Mix (Roche) and appropriate primers purchased

Sigma were used for amplifications (6 min at 95 °C then 45 cycles of 10 s at 95 °C, 30 s at 60 °C) in a Light Cycler 480 II Real-Time PCR machine. The primers used for DNAJB1 were 5′-TGTGTGGCTGCACAGTGAAC-3′ (forward) and 5′-ACGTTTCTCGGGTGTTTTGG-3′ (reverse), primers for HSPA1A were 5′-GGAGGCGGAGAAGTACA-3′ (forward) and 5′-GCTGATGATGGGGTTACA-3′(reverse), primers for HSP90AA1 were 5′-GATAAACCCTGACCATTCC-3′ (forward) and 5′-AAGACAGGAGCGCAGTTTCATAAA-3′ (reverse) and primers for RPLP2 5′-CCATTCAGCTCACTGATAACCTTG-3′ (forward) and 5′-CGTCGCCTCCTACCTGCT-3′ (reverse). Transcripts were normalized to the housekeep-ing genes RPLP2 and all measurements were performed at least in triplicate. Data were analyzed using the LightCycler® 480 Software, Version 1.5 (Roche) and data are reported as the mean ±95% confidence intervals.

Resazurin Assay.

HEK293T-REx cells expressing dn-cHSF1 were plated at 5,000 cells/well in a 96-well black bottom plate. Cells were subsequently treated with either Dox or DMSO for 48 hr prior to HS. Cells were exposed to HS at 43 °C for 75 min before returning to 37 °C for recovery. At the indicated time points post recovery, 15.00 µl of a 0.10 mg/mL solution of resazurin (sodium salt) was added to wells. Reduction of resazurin was monitored by fluorescence on a Gen5 plate reader (λ_{ex}: 530, λ_{em}: 590) following a 2 hr incubation at 37 °C. Fold change in metabolic activity was determined from the non-heat shocked controls within each treatment condition.

Isolation of His10-SUMO2 and His10-Ub substrates.

Purification of SUMOylated and ubiquitinated proteins was performed as described previously[58]. In short, cells expressing His10-SUMO2 or His10-Ub were washed three time in ice-cold PBS, and then a small fraction was used as an input control lysed in SNTBS lysis buffer (2% SDS, 1% NP-40, 50 mM Tris pH 7.5, 150 mM NaCl) while the remaining cells were lysed in denaturing lysis buffer containing 6 M guanidine-HCl, 100 mM Na2HPO4/NaH2PO4 and 10 mM TRIS, buffered at pH 8. Lysates were normalized for protein content, supplemented with 10 mM imidazole pH 8 and 5 mM β-mercaptoethanol and subsequently incubated with 20 µl dry volume Ni-NTA agarose beads/ml lysate overnight at 4 °C. Beads were subsequently washed with wash buffers 1 to 4. Wash buffer 1 contained 6M guanidine-HCL, 100 mM Na2HPO4/NaH2PO4, 10 mM Tris pH 8, 10 mM imidazole pH 8, 0.2% Triton X-100 and 5 mM β-mercaptoethanol. Wash buffer 2 contained 8 M urea, 100 mM Na2HPO4/NaH2PO4, 10 mM Tris pH 8, 10 mM imidazole pH 8, 0.2% Triton X-100 and 5 mM β-mercaptoethanol. Wash buffer 3 contained 8 M urea, 100 mM Na2HPO4/NaH2PO4, 10 mM Tris pH 6.3, 10 mM imidazole pH 7, 0.2% Tri-ton X-100 and 5 mM β-mercaptoethanol. Wash buffer 4 contained 8 M urea, 100 mM Na2HPO4/NaH2PO4, 10 mM Tris pH 6.3, 0.1% Triton X-100 and 5 mM β-mercaptoethanol. For purifications which were subsequently analyzed by mass spectrometry, wash buffer 2 contained only 0.1% Triton X-100 and Triton X-100 was left out of wash buffers 3 and 4. Washes were performed for 15 min at room temperature and wash 4 was performed twice. His10-tagged proteins were eluted twice with 7 M urea, 100 mM Na2HPO4/NaH2PO4, 10 mM Tris pH 7 and 500 mM imidazole. For mass spectrometry, elutions were concentrated by using a 100k cut-off filter and diluted with ammonium bicarbonate (ABC) to a concentration of 50 mM. Samples were reduced with dithiothreitol (DTT) and alkylated with cloroacetamide (CAA). Eluted fractions were further diluted with 50 mM ABC to attain a final urea concentra-tion of 2 M.Proteins were digested with sequencing grade trypsin in a 1:50 enzyme-to-protein ratio overnight at 25

°C. Peptides were acidified with 2% trifluoroacedic acid (TFA). The peptide samples were subsequently desalted and concentrated using homemade reversed phase StageTips. For the StageTips, three layers of C18 matrix was gently pushed into filter-less 200µl pipet tips. The matrix was activated by HPLC-grade methanol, subsequently washed twice with 80% acetonitrile (ACN) in 0.1% formic acid (FA) and equilibrated with 0.1% FA. Sample was passed through the StageTip and was subsequently washed twice with 0.1% FA and centrifuged to complete dryness[59]. Peptides were eluted twice from StageTips using 40% acetonitrile (ACN) in 1% formic acid (FA) and 60% ACN in 1% FA, respectively.

Mass Spectrometry Data Collection and Analysis.

Four biological replicates were measured in technical duplicates by nanoflow liquid chromatography-tandem mass spectrometry (nanoLC-MS/MS) on a Q-Exactive Orbitrap (ThermoFisher). Raw data were processed using MaxQuant (1.5.6.0) software. MaxQuant analysis was carried out as previously described[58]. Default settings of MaxQuant software were employed with the following changes, "Label-free quantification (LFQ)" and "Match between runs" were enabled. All settings of MaxQuant parameters can be found via the PRIDE repository and dataset identifier PXD010231. Identified proteins were statistically analyzed using Perseus Software (version 1.5.6). The same experimental conditions of four biological replicates were grouped and LFQ intensities were log2-transformed. Protein groups that were identified in at least three biological replicates in at least one group were selected for further analysis. Missing values were imputed by the software using normally distributed values with a 1.8 (log2) downshift and a 0.3 (log2) width based on total matrix values. Differences in LFQ intensities between groups were analyzed by a two-sample t-test. Proteins were selected based on their fold change and p-value. Protein groups identified in the His10-SUMO2 dn-cHSF1 or GFP cell lines, which did not show a significant change in LFQ intensities (p-value ≤ 0.05) in at least one of the experimental conditions compared to the appropriate parental cell lines, were excluded. Heat shock-responsive SUMOylation of proteins was defined by a ≥ 2-fold increase in abundance post-heat shock compared to no heat shock controls with a p-value ≤ 0.05, in both vehicle and Dox-treated conditions. Proteins that recovered to normal SUMOylation levels post-heat shock were selected based on a ≥ 2-fold decrease 4 hr post-heat shock compared to immediately post-heat shock with a p-value ≤ 0.05. Proteins that retained SUMOylation during heat shock recovery owing to chronic HSF1 inhibition were selected if they showed ≥ 2-fold en-richment in the Dox-treated condition 4 hr post-heat shock condition compared to the vehicle-treated control condition 4 hr post-heat shock with a p-value ≤ 0.05 in addition to no significant difference under the same condition in the inducible GFP cell line. Gene Ontology enrichment analysis was performed on 125 proteins retained during heat shock recovery after chronic HSF1 inhibition using the Gene Ontology Consortium PANTHER Overrepresentation test (release date 2017-12-05) with the annotation version that was released on 2017-11-12.

Cloning, expression and purification of SUMO-MMS21.

PCR amplifications of the cDNA coding region of human MMS21 (Dharmacon OHS1770-202324443) and SUMO3 (Addgene #53143) were cloned into pET-15b vectors containing a 6×-His tag for purification. BL21(DE3) E.coli were transformed with these plasmids, and expression was induced over-night at 16 °C by the addition of isopropyl β-D-1-thiogalactopyranoside (IPTG). Bacteria were lysed by sonication in lysis buffer containing 50 mM Tris, 300 mM NaCl, 10 mM imidazole, 5 mM DTT, 1 mM PMSF, 1 mg/mL lysozyme, 10%

glycerol, at pH 7.8. Recombinant His6-SUMO3-MMS21 and His6-MMS21 were purified by Ni-NTA beads and eluted using 250 mM Imidazole (pH 7.8).

SUMOylation and purification of recombinant FOXM1.
Plasmids containing His6-FoxM1 (pDEST17) and SUMO2+SUMOylation machinery (pT-E1E2S2)[57] were transfected or co-transfected into BL21 E.coli. Expression of proteins was induced overnight at 25 °C by the addition of isopropyl β-D-1-thiogalactopyranoside (IPTG). Bacteria were lysed in 50mM HEPES (pH 7.6), 0.5 M NaCl. 25 mM MgCl2, 50% glycerol, 10% NP-40, 20 mM Imidazole (pH 8), 1 mM PMSF, 1/10ml protease inhibitor cocktail tablets, EDTA-free (SIGMA). Recombinant His6-FoxM1 was purified using TALON metal affinity resin and eluted from beads with 400 mM imidazole (pH 8).

Thermal Shift Analyses.
Recombinant MMS21 or FoxM1 was aliquoted into 11 or 16 samples of 50 µl each and incubated at increasing temperatures from 30–70 °C for 5 min using gradient settings on a Bio-Rad C1000TM Thermal Cycler or a Veriti TM 96-Well Thermal Cycler. For the experiments described in Figure 6C, FoxM1 was aliquoted into samples of 50 µl and incubated for the indicated time periods at the indicated temperatures using a thermo-mixer (Eppendorf). Samples were left to cool down at RT for 3 min then 4 °C for 3 min. 40 µl aliquots were transferred to a micro-centrifuge tube and centrifuged at 20000 x g for 20 min. 25 µl of the soluble fractions were used for immunoblotting analysis.

SENP labelling with activity-based probes (ABPs).
HEK293T-REx cells stably expressing Dox-inducible dn-cHSF1 were treated with Dox for 48 hr prior to heat shock. Cell were exposed to heat shock at 43 °C for 75 min before returning to 37 °C for a 2 hr recovery period. Cells were lysed prior to heat shock, immediately after heat shock, or after 2 hr of recovery. After washing with PBS, cell pellet was split into two. Cell lysates were prepared by resuspending cell pellets in two pellet volumes of lysis buffer (containing 0.25 M sucrose, 20 mM Mops-KOH (pH = 7.4), 1 mM EDTA-NaOH, 1 tablet/10 ml complete mini protease inhibitor cocktail (Sigma), 1 mM DTT) or lysis buffer containing 20 mM N-ethylmaleimide (NEM) and lysed by sonication. After centrifugation (20,000 × g, 4 °C, 5 min), total protein concentration in the supernatant was determined by Bradford. 100 µl of supernatant (~200 µg total protein) was labelled with either 8 µg of Rho-SUMO2-PA or K11 di-SUMO VA ABP for 30 min at 37 °C. The reaction was terminated by the addition of NuPage LDS sample buffer (Invitrogen)[31].

Quantification and statistical analysis
Unless otherwise indicated, experiments were performed in biological triplicate. Results are presented as mean ± standard deviation. Significance for immunobloting quantification was determined using ANOVA analysis followed by post-hoc Tukey analysis (* = $p < 0.05$; *** = $p < 0.0005$). For analysis of data from the mass spectrometry experiments, differences in LFQ intensities between treatment groups were analyzed by a two-sample t-test. Information on biological replicates and statistical significance is included in the figure legends.

Data and software availability
The mass spectrometry proteomics data have been deposited to the ProteomeXchange Consortium via the PRIDE partner repository with the dataset identifier PXD010231.

Supplemental Information

Table S1. Complete list of identified protein groups including statistics, Related to Figure 2
Table S2. List of SUMOylated proteins in response to heat shock, Related to Figure 2
Table S3. List of SUMOylated proteins that recover post-heat shock, Related to Figure 2
Table S4. List of SUMOylated proteins that recover dependent on HSF1 activity, Related to Figure 2

References

1. Kim, Y. E., Hipp, M. S., Bracher, A., Hayer-Hartl, M. and Hartl, F. U. Molecular chaperone functions in protein folding and proteostasis. Annu Rev Biochem 82, 323-355, (2013).
2. Labbadia, J. and Morimoto, R. I. The biology of proteostasis in aging and disease. Annu Rev Biochem 84, 435-464, (2015).
3. Akerfelt, M., Morimoto, R. I. and Sistonen, L. Heat shock factors: integrators of cell stress, development and lifespan. Nat Rev Mol Cell Biol 11, 545-555, (2010).
4. Zou, J., Guo, Y., Guettouche, T., Smith, D. F. and Voellmy, R. Repression of heat shock transcription factor HSF1 activation by HSP90 (HSP90 complex) that forms a stress-sensitive complex with HSF1. Cell 94, 471-480, (1998).
5. Shi, Y., Mosser, D. D. and Morimoto, R. I. Molecular chaperones as HSF1-specific transcriptional repressors. Genes Dev 12, 654-666, (1998).
6. Zhong, M., Orosz, A. and Wu, C. Direct sensing of heat and oxidation by Drosophila heat shock transcription factor. Mol Cell 2, 101-108, (1998).
7. Westerheide, S. D., Anckar, J., Stevens, S. M., Jr., Sistonen, L. and Morimoto, R. I. Stress-inducible regulation of heat shock factor 1 by the deacetylase SIRT1. Science 323, 1063-1066, (2009).
8. Golebiowski, F., Matic, I., Tatham, M. H. et al. System-wide changes to SUMO modifications in response to heat shock. Sci.Signal. 2, ra24, (2009).
9. Tatham, M. H., Matic, I., Mann, M. and Hay, R. T. Comparative proteomic analysis identifies a role for SUMO in protein quality control. Sci.Signal. 4, rs4, (2011).
10. Tempe, D., Piechaczyk, M. and Bossis, G. SUMO under stress. Biochem.Soc.Trans. 36, 874-878, (2008).
11. Guo, C. and Henley, J. M. Wrestling with stress: roles of protein SUMOylation and deSUMOylation in cell stress response. IUbMB Life 66, 71-77, (2014).
12. Sohn, K. C., Lee, K. Y., Park, J. E. and Do, S. I. OGT functions as a catalytic chaperone under heat stress response: a unique defense role of OGT in hyperthermia. Biochem Biophys Res Commun 322, 1045-1051, (2004).
13. Martinez, M. R., Dias, T. B., Natov, P. S. and Zachara, N. E. Stress-induced O-GlcNAcylation: an adaptive process of injured cells. Biochem Soc Trans 45, 237-249, (2017).
14. Marotta, N. P., Lin, Y. H., Lewis, Y. E. et al. O-GlcNAc modification blocks the aggregation and toxicity of the protein alpha-synuclein associated with Parkinson's disease. Nat Chem 7, 913-920, (2015).
15. Hastings, N. B., Wang, X., Song, L. et al. Inhibition of O-GlcNAcase leads to elevation of O-GlcNAc tau and reduction of tauopathy and cerebrospinal fluid tau in rTg4510 mice. Mol Neurodegener 12, 39, (2017).
16. Geiss-Friedlander, R. and Melchior, F. Concepts in sumoylation: a decade on. Nat.Rev.Mol.Cell Biol. 8, 947-956, (2007).
17. Huang, W. C., Ko, T. P., Li, S. S. and Wang, A. H. Crystal structures of the human SUMO-2 protein at 1.6 A and 1.2 A resolution: implication on the functional differences of SUMO proteins. Eur.J.Biochem. 271, 4114-4122, (2004).
18. Flotho, A. and Melchior, F. Sumoylation: a regulatory protein modification in health and disease. Annu.Rev. Biochem. 82, 357-385, (2013).
19. Van der Veen, A. G. and Ploegh, H. L. Ubiquitin-like proteins. Annu.Rev.Biochem. 81, 323-357, (2012).
20. Streich, F. C., Jr. and Lima, C. D. Structural and functional insights to ubiquitin-like protein conjugation. Annu Rev Biophys 43, 357-379, (2014).
21. Saitoh, H. and Hinchey, J. Functional heterogeneity of small ubiquitin-related protein modifiers SUMO-1 versus SUMO-2/3. J.Biol.Chem. 275, 6252-6258, (2000).
22. Hendriks, I. A., D'Souza, R. C., Yang, B. et al. Uncovering global SUMOylation signaling networks in a site-specific manner. Nat Struct Mol Biol 21, 927-936, (2014).
23. Seifert, A., Schofield, P., Barton, G. J. and Hay, R. T. Proteotoxic stress reprograms the chromatin landscape of SUMO modification. Sci Signal 8, rs7, (2015).
24. Martin, N., Schwamborn, K., Schreiber, V. et al. PARP-1 transcriptional activity is regulated by sumoylation upon heat shock. EMBO J. 28, 3534-3548, (2009).
25. Hietakangas, V., Ahlskog, J. K., Jakobsson, A. M. et al. Phosphorylation of serine 303 is a prerequisite for the stress-inducible SUMO modification of heat shock factor 1. Mol. Cell Biol 23, 2953-2968, (2003).

26. Brunet, S. M., De, T. A., Hammann, A. et al. Heat shock protein 27 is involved in SUMO-2/3 modification of heat shock factor 1 and thereby modulates the transcription factor activity. Oncogene 28, 3332-3344, (2009).
27. Seeler, J. S. and Dejean, A. SUMO and the robustness of cancer. Nat Rev Cancer 17, 184-197, (2017).
28. Krumova, P. and Weishaupt, J. H. Sumoylation in neurodegenerative diseases. Cell Mol.Life Sci. 70, 2123-2138, (2013).
29. Moore, C. L., Dewal, M. B., Nekongo, E. E. et al. Transportable, Chemical Genetic Methodology for the Small Molecule-Mediated Inhibition of Heat Shock Factor 1. ACS Chem Biol 11, 200-210, (2016).
30. Schimmel, J., Larsen, K. M., Matic, I. et al. The ubiquitin-proteasome system is a key component of the SUMO-2/3 cycle. Mol.Cell Proteomics 7, 2107-2122, (2008).
31. Mulder, M. P. C., Merkx, R., Witting, K. F. et al. Total Chemical Synthesis of SUMO and SUMO-Based Probes for Profiling the Activity of SUMO-Specific Proteases. Angew Chem Int Ed Engl, (2018).
32. Berkers, C. R., Verdoes, M., Lichtman, E. et al. Activity probe for in vivo profiling of the specificity of proteasome inhibitor bortezomib. Nat Methods 2, 357-362, (2005).
33. Lamoliatte, F., McManus, F. P., Maarifi, G., Chelbi-Alix, M. K. and Thibault, P. Uncovering the SUMOylation and ubiquitylation crosstalk in human cells using sequential peptide immunopurification. Nat Commun 8, 14109, (2017).
34. Cuijpers, S. A. G., Willemstein, E. and Vertegaal, A. C. O. Converging Small Ubiquitin-like Modifier (SUMO) and Ubiquitin Signaling: Improved Methodology Identifies Co-modified Target Proteins. Mol Cell Proteomics 16, 2281-2295, (2017).
35. Malakhov, M. P., Mattern, M. R., Malakhova, O. A. et al. SUMO fusions and SUMO-specific protease for efficient expression and purification of proteins. J.Struct.Funct.Genomics 5, 75-86, (2004).
36. Butt, T. R., Edavettal, S. C., Hall, J. P. and Mattern, M. R. SUMO fusion technology for difficult-to-express proteins. Protein Expr. Purif 43, 1-9, (2005).
37. Henley, J. M., Craig, T. J. and Wilkinson, K. A. Neuronal SUMOylation: mechanisms, physiology, and roles in neuronal dysfunction. Physiol Rev 94, 1249-1285, (2014).
38. Vedadi, M., Niesen, F. H., Allali-Hassani, A. et al. Chemical screening methods to identify ligands that promote protein stability, protein crystallization, and structure determination. Proceedings of the National Academy of Sciences of the United States of America 103, 15835-15840, (2006).
39. Pinton, G. F., Dahl, J., Rosenzweig, S. and Trahey, G. E. A heterogeneous nonlinear attenuating full-wave model of ultrasound. IEEE Trans. Ultrason. Ferroelectr. Freq. Control 56, 474-488, (2009).
40. Zhou, W., Ryan, J. J. and Zhou, H. Global analyses of sumoylated proteins in Saccharomyces cerevisiae. Induction of protein sumoylation by cellular stresses. J. Biol. Chem 279, 32262-32268, (2004).
41. Anckar, J. and Sistonen, L. Regulation of HSF1 function in the heat stress response: implications in aging and disease. Annu Rev Biochem 80, 1089-1115, (2011).
42. Khalil, S., Luciano, J., Chen, W. and Liu, A. Y. Dynamic regulation and involvement of the heat shock transcriptional response in arsenic carcinogenesis. Journal of cellular physiology 207, 562-569, (2006).
43. Marblestone, J. G., Edavettal, S. C., Lim, Y. et al. Comparison of SUMO fusion technology with traditional gene fusion systems: enhanced expression and solubility with SUMO. Protein Sci. 15, 182-189, (2006).
44. Butt, T. R., Edavettal, S. C., Hall, J. P. and Mattern, M. R. SUMO fusion technology for difficult-to-express proteins. Protein Expr.Purif. 43, 1-9, (2005).
45. Helenius, A. and Aebi, M. Roles of N-linked glycans in the endoplasmic reticulum. Annu Rev Biochem 73, 1019-1049, (2004).
46. Hendriks, I. A., Lyon, D., Young, C. et al. Site-specific mapping of the human SUMO proteome reveals co-modification with phosphorylation. Nat Struct Mol Biol 24, 325-336, (2017).
47. Cook, J. and Chock, P. B. Ubiquitin: a review on a ubiquitous biofactor in eukaryotic cells. Biofactors 1, 133-146, (1988).
48. Wilson, V. G. and Heaton, P. R. Ubiquitin proteolytic system: focus on SUMO. Expert.Rev.Proteomics 5, 121-135, (2008).
49. Nagaraj, N. and Mann, M. Quantitative analysis of the intra- and inter-individual variability of the normal urinary proteome. J. Proteome. Res 10, 637-645, (2011).
50. Kim, W., Bennett, E. J., Huttlin, E. L. et al. Systematic and quantitative assessment of the ubiquitin-modified proteome. Mol. Cell 44, 325-340, (2011).

51. Guerrero, C., Tagwerker, C., Kaiser, P. and Huang, L. An integrated mass spectrometry-based proteomic approach: quantitative analysis of tandem affinity-purified in vivo cross-linked protein complexes (QTAX) to decipher the 26 S proteasome-interacting network. Mol.Cell Proteomics. 5, 366-378, (2006).
52. Kopito, R. R. Aggresomes, inclusion bodies and protein aggregation. Trends Cell Biol 10, 524-530, (2000).
53. Balchin, D., Hayer-Hartl, M. and Hartl, F. U. In vivo aspects of protein folding and quality control. Science 353, aac4354, (2016).
54. Jucker, M. and Walker, L. C. Self-propagation of pathogenic protein aggregates in neurodegenerative diseases. Nature 501, 45-51, (2013).
55. Liebelt, F. and Vertegaal, A. C. Ubiquitin-dependent and independent roles of SUMO in proteostasis. Am J Physiol Cell Physiol 311, C284-296, (2016).
56. Flotho, A., Werner, A., Winter, T. et al. Recombinant reconstitution of sumoylation reactions in vitro. Methods Mol.Biol. 832, 93-110, (2012).
57. Uchimura, Y., Nakamura, M., Sugasawa, K., Nakao, M. and Saitoh, H. Overproduction of eukaryotic SUMO-1- and SUMO-2-conjugated proteins in Escherichia coli. Anal.Biochem. 331, 204-206, (2004).
58. Hendriks, I. A. and Vertegaal, A. C. Label-Free Identification and Quantification of SUMO Target Proteins. Methods Mol Biol 1475, 171-193, (2016).
59. Rappsilber, J., Mann, M. and Ishihama, Y. Protocol for micro-purification, enrichment, pre-fractionation and storage of peptides for proteomics using StageTips. Nat.Protoc. 2, 1896-1906, (2007).

Figure S1

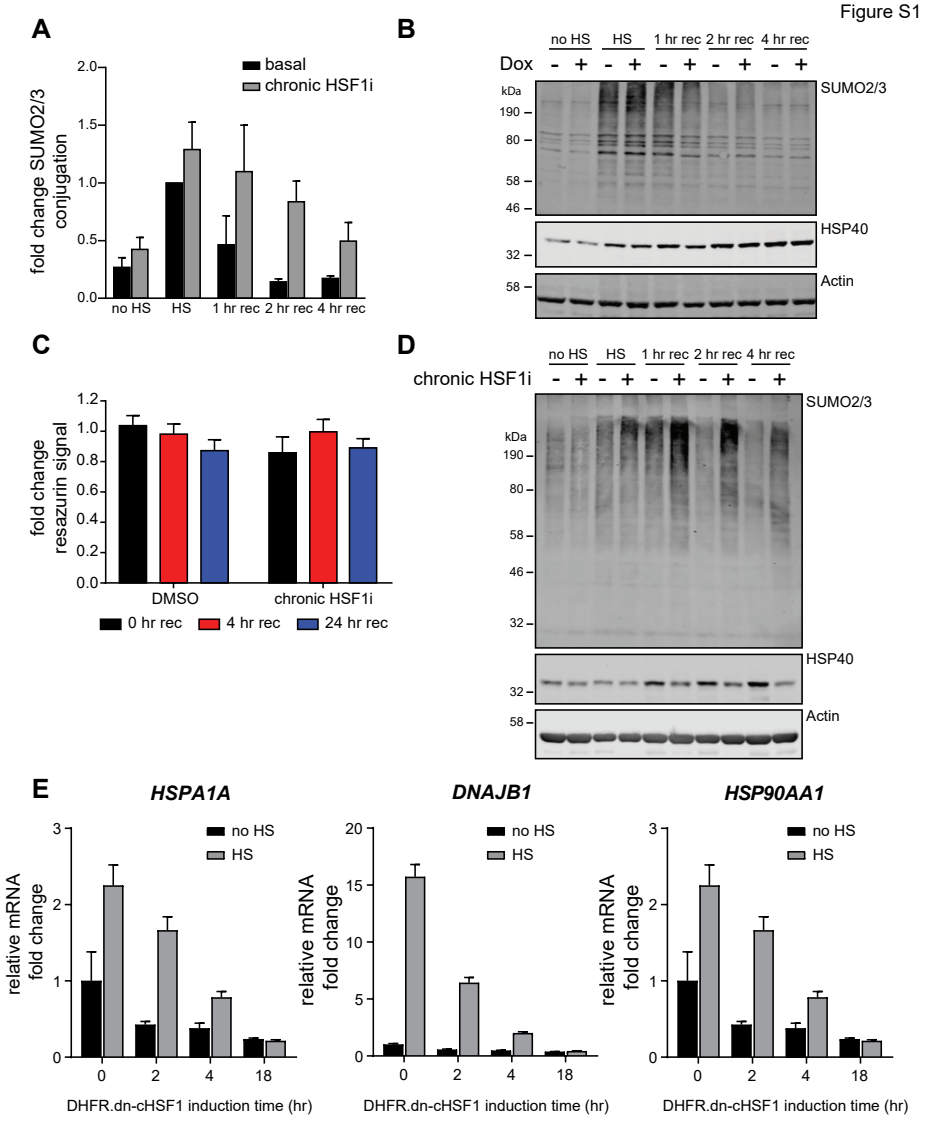

Figure S1. Depletion of proteostasis factors via chronic HSF1 inhibition delays recovery of SUMO2/3 conjugation levels after heat shock. Related to Figure 1. (**A**) Quantification of conjugated SUMO2/3 substrates from Figure 1C. Bar graphs show the fold change in SUMO2/3 conjugation at the specified time points as compared to the vehicle-treated HS sample. Error bars indicate the standard deviation, n = 3. HS, heat shock; rec, heat shock recovery. (**B**) HEK293T-REx cells expressing Dox-inducible GFP were treated with Dox for 48 hr prior to HS. Cells were exposed to HS at 43 °C for 75 min before returning to 37 °C for recovery (rec) and lysed as indicated. Total amounts of SUMOylated proteins were analyzed by immunoblotting. HSP40 levels were used to confirm induction of the heat shock response. β-Actin was used as a loading control. (**C**) HEK293T-REx cells expressing Dox-inducible dn-cHSF1 were treated with Dox for 48 hr prior to HS. Cells were exposed to HS at 43 °C for 75 min before returning to 37 °C for recovery. Analysis of cell viability was performed using the resazurin assay before HS, or at the indicated recovery time points. (**D**) LX2 cells expressing DHFR.dn-cHSF1 were treated with TMP for 48 hr (chronic HSF1i) prior to heat shock (HS). Cells were exposed to HS and lysed at indicated time points. Total amounts of SUMOylated proteins were analyzed by immunoblotting. HSP40 levels were used to confirm induction of the heat shock response and to confirm functional HSF1 inhibition. β-Actin was used as a loading control. (**E**) HEK293T-REx cells expressing DHFR.dn-cHSF1 were treated with either TMP or vehicle for the indicated time points before exposing to a 1-hr HS at 43 °C. Bar graphs show relative fold change of HSPA1A (HSP70.1) and DNAJB1 (HSP40) and HSP90AA1 (HSP90) mRNA analyzed by qRT-PCR.

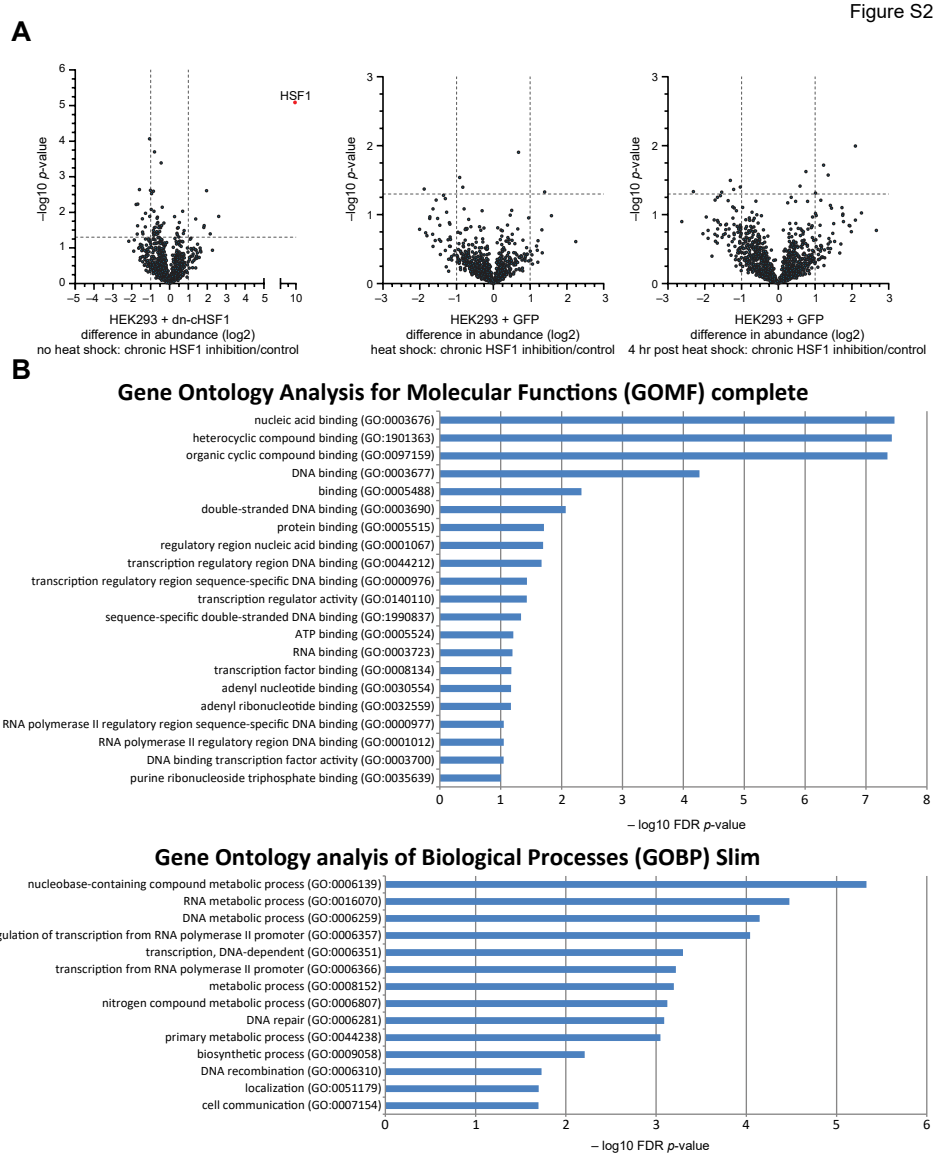

Figure S2. SUMOylation response of control conditions and complete GO analysis of SUMOylated proteins whose recovery after heat shock was delayed by chronic HSF1 inhibition. Related to Figure 2.

(**A**) Volcano plots depicting the statistical differences in abundance between proteins identified by mass spectrometry. Dashed lines indicate a cut-off at a p-value ≤ 0.05 (–log10 p-value = 1.3) and a fold change ≥ 2 (log2 = 1). The left panel shows SUMOylated proteins identified prior to heat shock (HS) in the Dox-inducible dn-cHSF1 cell line specifically in the Dox-treated (chronic HSF1i) sample as compared to the untreated sample. The middle panel shows SUMOylated proteins identified immediately after HS in the Dox-inducible GFP cell line, specifically in the Dox-treated sample as compared to the untreated sample. The right panel shows SUMOylated proteins identified 4 hr post HS in the Dox-inducible GFP cell line, specifically in the Dox-treated sample as compared to the untreated sample. (**B**) Complete gene ontology analysis for molecular functions (GOMF) of proteins whose recovery post-HS was delayed by chronic HSF1 inhibition. Terms with a –log10 False Discovery Rate (FDR) > 2 are shown (upper panel). SLIM biological processes (GOBP) of proteins whose recovery after HS was delayed by chronic HSF1 inhibition. Terms with a –log10FDR of > 1.3 are shown.

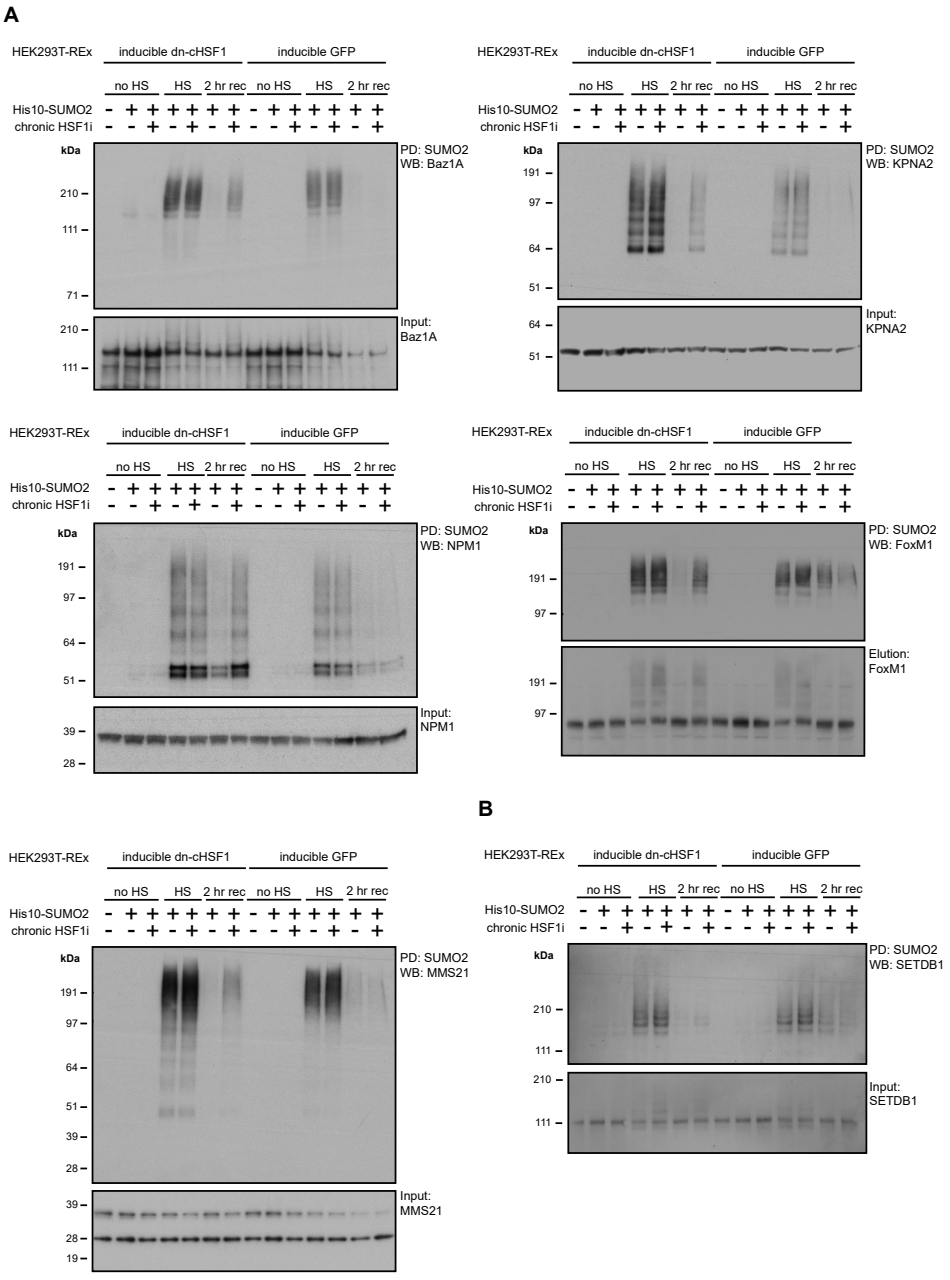

Figure S3. Validation of SUMOylation targets that were identified by proteomics. Related to Figure 2.
(**A**) SUMOylation targets whose recovery after heat shock (HS) was delayed by chronic HSF1 inhibition. HEK293T-REx cells stably co-expressing His10-SUMO2 and Dox-inducible dn-cHSF1 or GFP were treated with Dox for 48 hr (chronic HSF1i) prior to HS. Cells were exposed to HS at 43 °C for 75 min before returning to 37 °C for a 2-hr recovery period (rec) and lysed as indicated. SUMOylated proteins were purified by means of His10-purification. Elutions and inputs were analyzed by immunoblotting for Baz1A (upper left panel), KPNA2 (upper middle panel), MMS21 (upper right panel), NPM1 (lower left panel) and FoxM1 (lower right panel). (**B**) SUMOylation targets whose recovery after HS was not delayed by chronic HSF1 inhibition. HEK293T-REx cells stably co-expressing His10-SUMO2 and Dox-inducible dn-cHSF1 were treated as in (A). Elutions and inputs were analyzed by immunoblotting for SETDB1.

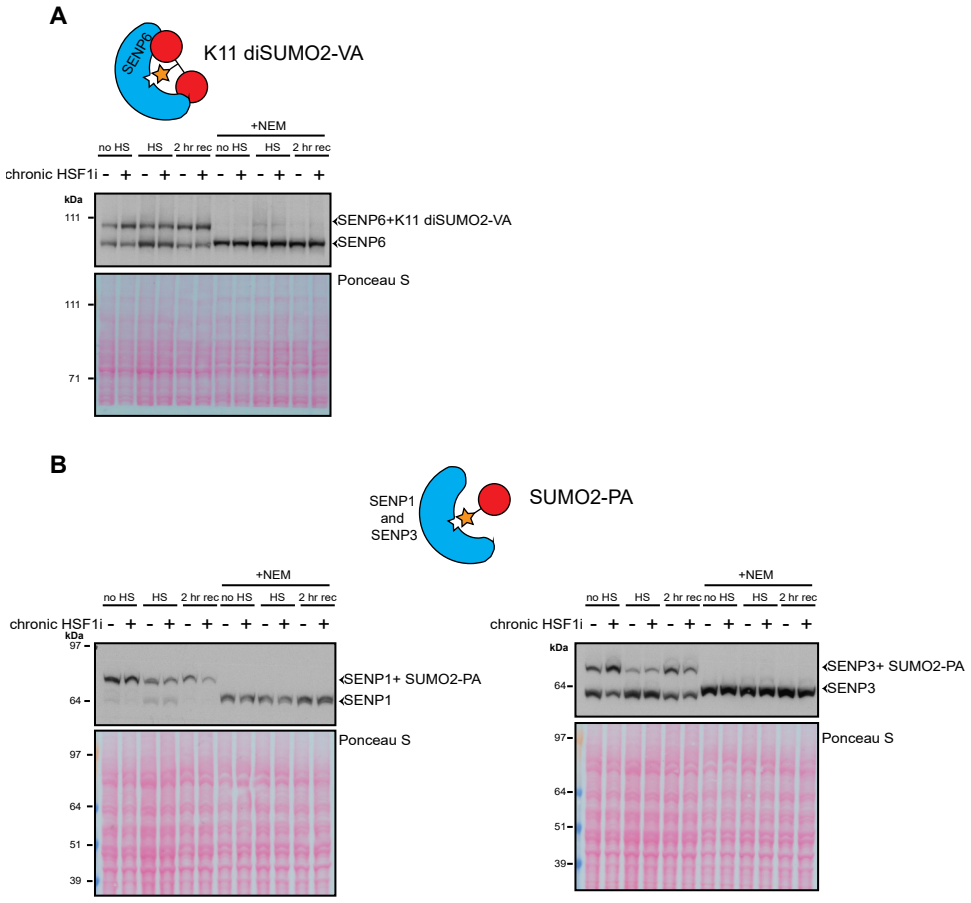

Figure S4. Modulation of the proteostasis network does not alter activity of SENPs. Related to Figure 3. (**A**) Where indicated, HEK293T-REx cells expressing Dox-inducible dn-cHSF1 were treated with Dox for 48 hr (chronic HSF1i) prior to heat shock (HS). Cells were exposed to HS at 43 °C for 75 min before returning to 37 °C for a 2-hr recovery period (rec). Cells were lysed in native lysis buffer with or without N-ethylmaleimide (NEM), a cysteine protease inhibitor which should inhibit activity and therefore labelling of the SENPs. Lysates were incubated with K11 diSUMO2-vinylamide (VA) activity-based probe (ABP) for 30 min at 37 °C. Immunoblot analysis was performed using a specific antibody against SENP6. Active SENPs are covalently labelled with the ABP, which leads to a size shift on the SDS gel. (**B**) HEK293T-REx cells were treated as in (A), labelling of active SENPs was carried out with SUMO2-propargyl (PA) ABP. Immunoblot analysis was performed using specific antibodies against SENP1 (left panel) and SENP3 (right panel).

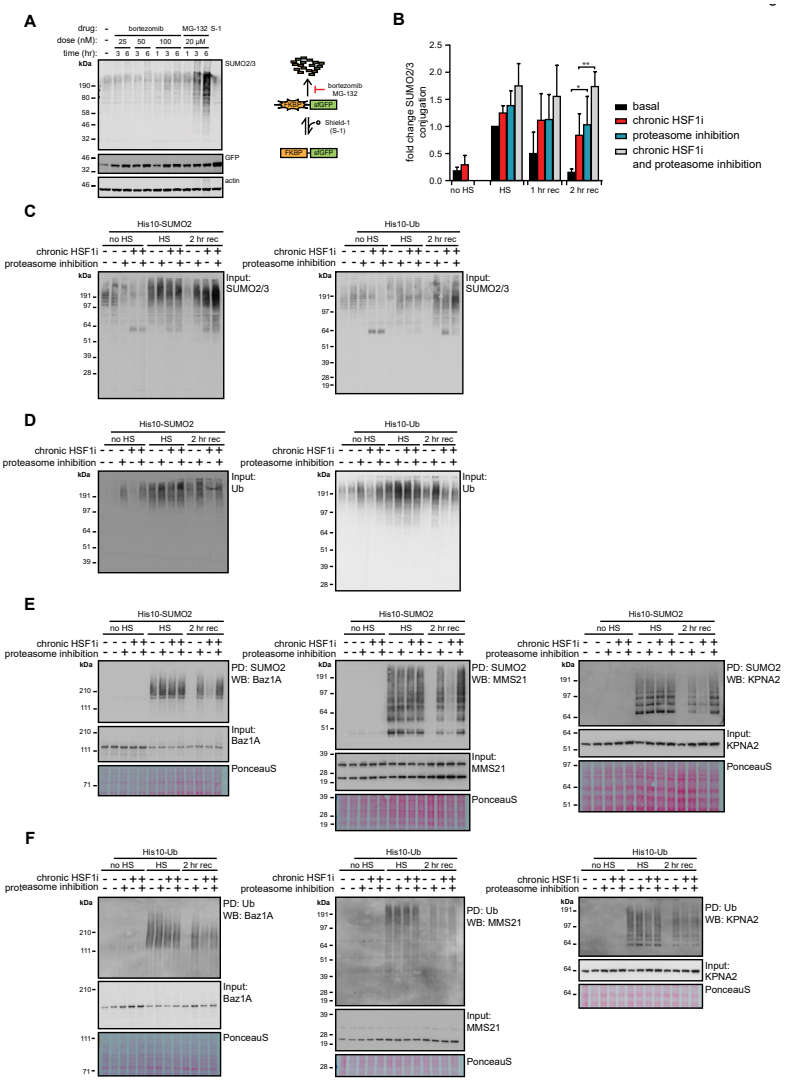

Figure S5. An intact proteostasis network is needed for degradation of SUMO and Ub substrates during heat shock recovery. Related to Figure 3. (**A**) HEK293T-REx cells stably expressing FKBP.sfGFP were treated with up to 100 nM bortezomib or 20 μM MG-132 for up to 6 hr of treatment. Total amounts of SUMOylated proteins were analyzed by immunoblotting. Proteasome inhibition was analyzed by immunoblotting for GFP to confirm stabilization of FKBP-sfGFP. The ligand for FKBP, Shield-1 (S-1), was used as a positive control for FKBP-sfGFP stabilization. (**B**) Quantification of fold change of SUMOylation before, during, and after HS as shown in Figure 3A. n = 3, error bars indicate standard deviations. Significance was determined using ANOVA analysis followed by post-hoc Tukey analysis, * = $p < 0.05$; ** = $p < 0.005$. (**C**) HEK293T-REx cells stably co-expressing His10-SUMO2 or His10-Ub and Dox-inducible dn-cHSF1 were treated with Dox for 48 hr (chronic HSF1i) prior to heat shock (HS), with 100 nM bortezomib (proteasome inhibition) immediately prior to HS, or with a combination of both. Cells were exposed to HS at 43 °C for 75 min before returning to 37 °C for a 2-hr recovery period (rec) and lysed as indicated. Input samples were analyzed by immunoblotting for SUMO2/3. (D) HEK293T-REx cells stably co-expressing His10-SUMO2 or His10-Ub and DOX-inducible dn-cHSF1 were treated as in (C). Input samples were analyzed by immunoblotting for Ub. (**E**) HEK293T-REx cells stably co-expressing His10-SUMO2 and Dox-inducible dn-cHSF1 were treated with Dox for 48 hr (chronic HSF1i) prior to heat shock (HS), with 100 nM bortezomib (proteasome inhibition) immediately prior to HS, or with a combination of both. Cells were treated as in (C). SUMOylated proteins were purified by means of His10-purification. Elutions and inputs were analyzed by immunoblotting for Baz1A (left panel), MMS21 (middle panel) and KPNA2 (right panel). Ponceau S stain was used as a loading control for inputs. (**F**) HEK293T-REx cells stably co-expressing His10-Ub and DOX-inducible dn-cHSF1 were treated as in (C). Ubiquitinated proteins were purified by means of His10-purification. Elutions and inputs were analyzed by immunoblotting for Baz1A (left panel), MMS21 (middle panel) and KPNA2 (right panel). Ponceau S stain was used as a loading control for inputs.

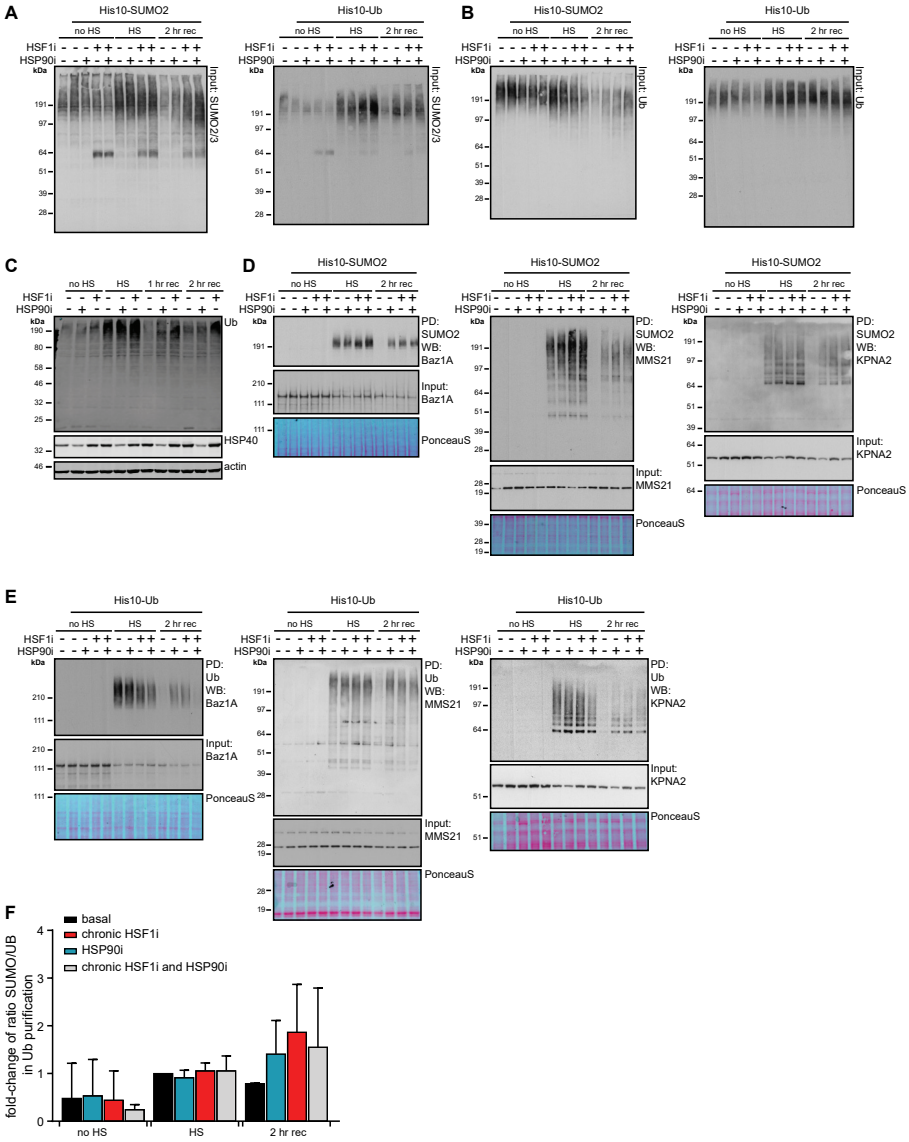

Figure S6. HSP90 plays a key role in the recovery of SUMO2/3 modification to normal levels following heat shock. Related to Figure 5. (**A**) HEK293T-REx cells stably co-expressing His10-SUMO2 or His10-Ub and Dox-inducible dn-cHSF1 were treated with Dox for 48 hr (chronic HSF1i) prior to heat shock (HS), with 500 nM STA-9090 2 hr (HSP90i) prior to HS, or a combination of both. Cells were exposed to HS at 43 °C for 75 min before returning to 37 °C for a 2-hr recovery period (rec) and lysed as indicated. Inputs were analyzed by immunoblotting for SUMO2/3. (**B**) HEK293T-REx cells stably co-expressing His10-SUMO2 or His10-Ub and Dox-inducible dn-cHSF1 were treated as in (A). Inputs were analyzed by immunoblotting for Ub. (**C**) HEK293T-REx cells stably expressing Dox-inducible dn-cHSF1 were treated as in (A). Cells were exposed to HS at 43 °C for 75 min before returning to 37 °C for a recovery period (rec) and lysed as indicated. Total amounts of ubiquitinated proteins were analyzed by immunoblotting. HSP40 levels were used to confirm induction of the heat shock response and to confirm functional HSF1 inhibition. β-Actin was used as a loading control. (**D**) HEK293T-REx cells stably co-expressing His10-SUMO2 and Dox-inducible dn-cHSF1 were treated as in (A). SUMOylated proteins were purified by means of His10-purification. Elutions and inputs were analyzed by immunoblotting for Baz1A (left panel), MMS21 (middle panel) and KPNA2 (right panel). Ponceau S stain was used as a loading control for inputs. (**E**) HEK293T-REx cells stably co-expressing His10-Ub and Dox-inducible dn-cHSF1 were treated as in (A). Ubiquitinated proteins were purified by means of His10-purification. Elutions and inputs were analyzed by immunoblotting for Baz1A (left panel), MMS21 (middle panel) and KPNA2 (right panel). Ponceau S stain was used as a loading control for inputs. (**F**) Bar graph showing the fold-change of the ratio SUMO/Ub within the Ub purified fraction. Error bars represent standard deviation, n = 3.

CHAPTER 4

The Poly-SUMO2/3 Protease SENP6 Enables Assembly of the Constitutive Centromere-Associated Network By Group-deSUMOylation

Frauke Liebelt[1], Nicolette S. Jansen[1], Sumit Kumar[1], Ekaterina Gracheva[1], Laura A. Claessens[1], Matty Verlaan-de Vries[1], Edwin Willemstein[1], Alfred C.O. Vertegaal[1]

[1]Cell and Chemical Biology, Leiden University Medical Center, Leiden, The Netherlands

Published in *Nature Communications* in 2019

ABSTRACT

In contrast to our extensive knowledge on ubiquitin polymer signaling, we are severely limited in our understanding of poly-SUMO signaling. We set out to identify substrates conjugated to SUMO polymers, using knockdown of the poly-SUMO2/3 protease SENP6. We identify over 180 SENP6 regulated proteins that represent highly interconnected functional groups of proteins including the constitutive centromere-associated network (CCAN), the CENP-A loading factors Mis18BP1 and Mis18A and DNA damage response factors. Our results indicate a striking protein group de-modification by SENP6. SENP6 deficient cells are severely compromised for proliferation, accumulate in G2/M and frequently form micronuclei. Accumulation of CENP-T, CENP-W and CENP-A to centromeres is impaired in the absence of SENP6. Surprisingly, the increase of SUMO chains does not lead to ubiquitin-dependent proteasomal degradation of the CCAN subunits. Our results indicate that SUMO polymers can act in a proteolysis-independent manner and consequently, have a more diverse signaling function than previously expected.

INTRODUCTION

Protein post-translational modifications (PTMs) play key roles in virtually all cellular processes. PTMs include small chemical modifications like phosphorylation and modifications by small proteins belonging to the ubiquitin family[1-4]. Ubiquitin signal transduction includes extensive polymer formation via all of its seven internal lysines[5] and via head-to-tail linear polymers[6]. Ubiquitin polymers are well known for their classical role in targeting proteins to the proteasome for degradation[7]. All ubiquitin chains formed via internal lysines accumulate upon proteasome inhibition, with the exception of K63 linked chains[8]. Ubiquitin chains are disassembled by proteases in a chain-type dependent manner[9].

Small Ubiquitin-like Modifiers (SUMOs) regulate proteins via mono-SUMOylation, multi-SUMOylation and poly-SUMOylation[3]. SUMOylation can collectively target groups of proteins that are functionally or physically connected, making single SUMO modification events redundant and potentially explaining the simplicity of the SUMOylation machinery, which comprises a modest set of enzymes in contrast to hundreds of enzymes participating in ubiquitin signaling[10]. SUMOs predominantly signal via monomers under regular cell culture conditions involving dynamic deSUMOylation by SUMO specific proteases[11].

Two of the three conjugated mammalian SUMO family members, SUMO2 and -3, are able to efficiently form SUMO polymers via internal SUMOylation sites in their flexible N-terminal domains in vitro[12] and in cells[13,14]. These chains are stabilized or increased by cellular stress, such as heat shock[15]. SUMO E3 ligases have the ability to catalyze auto-modification by SUMO polymers[16] and are consequently key substrates for the SUMO-chain targeted ubiquitin ligase (STUbL) RNF4[17]. In Sacharomyces cerevisiae SUMO chain formation is regulated by the covalent SUMO attachment to the single SUMO E2 conjugating enzyme, Ubc9. This activity is counterbalanced by the SUMO specific protease Ulp2 that is able to disassemble the accumulated SUMO chains[18,19]. SUMO chains contribute to synaptonemal complex formation during meiosis in yeast[18,20] and are required to prevent aneuploidy[21].

In mammalian cells two members of the SUMO specific protease (SENP) family, SENP6 and SENP7, are responsible for the depolymerization of SUMO chains[22, 23]. These proteases predominantly localize throughout the nucleoplasm and possess conserved sequence insertions within their catalytic domain, which are absent from the catalytic domains of the other SENP family members. These insertions are proposed to be responsible for their poly-SUMO2/3 specificity[24-28]. The importance of a balanced regulation of SUMO chains was demonstrated by studies in mammalian cells where SENP6 depletion, and subsequent accumulation of SUMO2/3 conjugates led to severe mitotic problems and reduction in cell survival[29,30]. The identity of the regulated substrates remains largely unknown.

SUMO chains were identified as substrates for STUbLs[31]. These STUbLs were identified in yeast[32-34] and contain multiple SUMO Interaction Motifs (SIMs), explaining their preference for poly- and multi-SUMOylated proteins[35]. The initially identified substrate for the mammalian STUbL RNF4 was the promyelocytic leukemia protein PML[35,36]. PML and the PML-RARα oncogene product are targeted for degradation by the proteasome upon ubiquitination by RNF4 in response to arsenic trioxide treatment-induced poly-SUMOylation[35,37]. The centromere protein CENP-I was proposed to be regulated in a similar fashion. SENP6 is necessary to trim down the SUMO chain which would otherwise lead to the RNF4-mediated ubiquitination and proteasomal degradation of CENP-I[30].

In contrast to our extensive knowledge on ubiquitin polymer formation, we are limited in our understanding of SUMO polymers, particularly due to limited knowledge of the

identity of the substrates modified by these polymers. We set out to identify these target proteins, capitalizing on our developed SUMO purification technology[38] combined with knockdown of the poly-SUMO2/3 processing protease SENP6. We identify several highly interconnected groups of proteins that are regulated by SENP6, indicating a striking group de-modification and involvement of SENP6 in multiple crucial cellular processes. One of the identified interconnected groups regulated by SENP6 represents most of the subunits of the constitutive centromere-associated network (CCAN), including the previously identified subunit CENP-I. Accumulation of poly-SUMO2/3 on CCAN subunits leads to a reduced abundance of these proteins at the chromatin and the centromere. Surprisingly, we fail to observe an accumulation of SUMOylated or ubiquitinated CCAN proteins upon inhibition of the proteasome and RNF4 knockdown, which contradicts the classical consequence of poly-SUMO2/3 accumulation. We conclude that SUMO polymers can also act in a proteolysis-independent manner and therefore have diverse signaling functions.

RESULTS

SENP6 is vital for proliferation and cell cycle progression

SENP6 and SENP7 are the mammalian SUMO proteases with a preference for poly-SUMO2/3 (Figure 1a). SENP6 is able to rapidly depolymerize SUMO2 chains in vitro, while cleaving di-SUMO moieties much less efficiently (Figure 1b). Knockdown of SENP6 caused an increase in high-molecular weight SUMO2/3 conjugates, but knockdown of SENP7 did not, whereas combined knockdown of both SENP6 and SENP7 caused a stronger increase in SUMO2/3 conjugates (Figure 1c and Supplementary Figure 1d). Since SENP6 was previously proposed to be essential for mitotic progression and cell survival[29,30,39] we aimed to further investigate its function. Knockdown of SENP6 by two independent shRNAs reduced colony formation to a large extent, demonstrating an important contribution of SENP6 to cell proliferation (Figure 1d). We investigated cell cycle profiles of SENP6 depleted cells and observed an increase of cells in G2/M phase (Figure 1e, Supplementary Figure 2). Furthermore, we observed clear signs of mitotic problems. Knocking down SENP6 strongly induced the formation of micronuclei, which are a hallmark for lagging acentric chromosomes during anaphase due to faulty mitotic processes (Figure 1f)[40]. In conclusion, our results confirm that SENP6 is essential for cell proliferation and cell cycle progression with a prominent role during mitosis.

>Figure 1. SENP6 is important for cell proliferation and cell cycle progression. a SENP6 cleaves poly-SUMO2/3 from target substrates. **b** Recombinant poly-SUMO2/3 was treated in vitro with recombinant SENP6 for the indicated time and immunoblotting was performed using a SUMO2/3 specific antibody. **c** U-2 OS cells were left untreated or transfected with either a pool of four siRNAs against SENP6 (siSENP6), SENP7 (siSENP7), a combination of both or a pool of four non-targeting siRNAs (NTP). Cell lysates were analysed two days post transfection by immunoblotting using antibodies against SENP6, SENP7 and SUMO2/3. **d** U-2 OS cells were infected with lentiviruses encoding shRNAs against SENP6 or a non-targeting control (ctrl) shRNA. Colony formation was determined by crystal violet staining. Line graphs represent the absorbance of solubilized crystal violet of two independent biological replicates (n = 2 independent experiments). **e** Scatter plot showing the percentages of HeLa cells in each cell-cycle phase (G1, S and G2/M) of four biological replicates (n = 4 independent experiments). HeLa cells were treated with lentiviruses as in panel (**d**). Cells were fixed and prepared for flow cytometry analysis four days post infection. Gray circles represent non-treated cells, blue squares represent control (ctrl) shRNA, purple triangles represent SENP6 shRNA1, red triangles = SENP6 shRNA2. Error bars represent standard deviation and p-values are derived from two-sided two-samples t-tests and FDR corrected. $**p < 0.01$, $***p < 0.0001$. **f** U-2 OS cells were treated

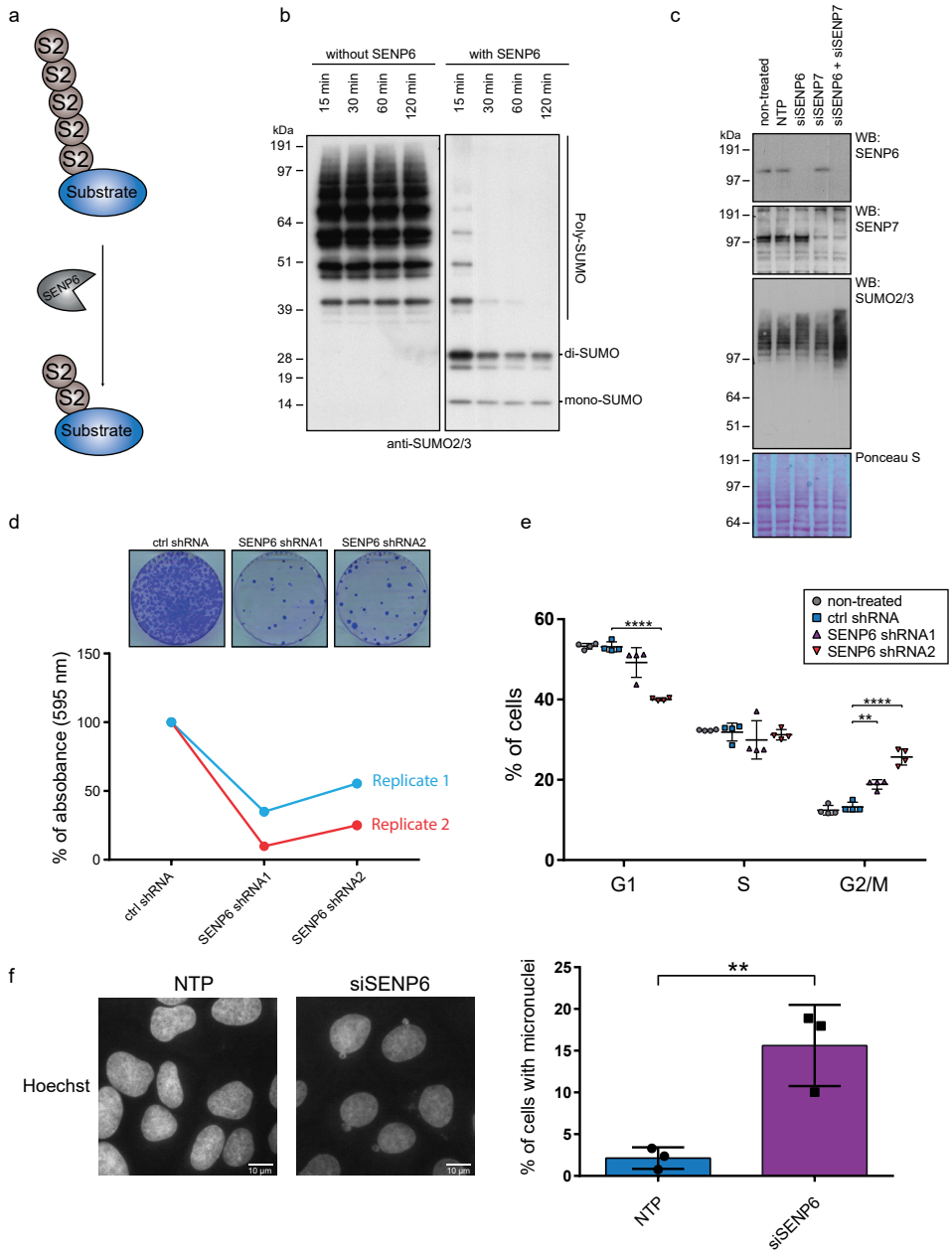

either with a pool of four siRNAs against SENP6 (siSENP6, blue bar) or NTP control (purple bar). Cells were fixed for microscopy two days post transfection and nuclei were stained with Hoechst. Ten pictures per condition of three biological replicates were taken. Total amounts of interphase nuclei and amounts of nuclei associated with one or more micronuclei were counted. Representative micrographs are shown. Scale bars = 10 µm. The bar graph shows the average percentage of cells that were associated with micronuclei over three biological replicates. Error bars represent standard deviations and the *p*-value is derived from a two-sided two-sample t-test with n = 3 independent experiments. ***p* <0.01. Source data are provided as a Source Data file.

Identifying target proteins regulated by SUMO polymers

To obtain global insight into the signaling by poly-SUMO2/3 and the cellular pathways involved, we set out to identify poly-SUMOylated proteins regulated by SENP6. For this purpose, we combined our SUMO2 purification methodology[38] with knockdown of SENP6 by two independent shRNAs in a label-free quantitative proteomics approach (Figure 2a). U-2 OS cells stably expressing His10-tagged SUMO2 were treated with lentivirus encoding either a non-targeting control shRNA or one of the two SENP6 targeting shRNAs. Both shRNAs efficiently depleted SENP6 and caused a major increase in high-molecular weight SUMO2 conjugates as well as free SUMO chains (Figure 2b). SUMO2 conjugates were purified by means of a His10-pulldown and identified by mass spectrometry and quantified using MaxQuant and Perseus software (Supplementary Data 1)[41,42]. Overall, we identified 180 SUMO target proteins enriched at least two-fold upon knockdown of SENP6 by each shRNA separately (Supplementary Data 2). Intriguingly, the identified SUMOylation targets regulated by SENP6 included ten out of the sixteen subunits of the constitutive centromere-associated network (CCAN), indicating a remarkable group deSUMOylation (Figure 2c). Other highly regulated SUMO targets included proteins that are associated with the DNA damage response (Figure 2c).

SENP6 demonstrates group deSUMOylation activity

Subsequently, we analyzed the set of SENP6 regulated proteins using bio-informatics. STRING interaction network analysis[43] revealed a large interconnected set of nuclear proteins (Figure 3a). Highly interconnected subclusters were revealed by the Cytoscape plug-in MCODE[44]. The most interconnected clusters consisted of proteins that are involved in the DNA damage response (Figure 3b), regulation and assembly of the kinetochore (Figure 3c), ribosomal RNA metabolism (Figure 3d) and DNA recombination (Figure 3e). Previously identified proteins regulated by SUMO chains such as SUMO E3 ligases, the nuclear body component PML, DNA damage response factors BRCA1 and BARD1 and centromeric protein CENP-I were identified in our screen, serving as positive controls[17,29,30].

To identify enriched Gene Ontology (GO) terms within the SENP6-regulated protein population, we made use of the online gene ontology tool (Geneontology.org), focusing on the categories of cellular compartments, molecular functions and biological processes. The analysis confirmed that the identified proteins were strongly enriched for nuclear proteins functioning in DNA-associated processes like DNA repair, chromosome segregation and regulation of the cell cycle (Figure 3f). The highly interconnected networks of proteins that are regulated by SENP6 demonstrate striking group deSUMOylation.

poly-SUMO accumulates on CCAN subunits upon SENP6 knockdown

The overall dynamics of SUMO2/3 modification in the absence of SENP6 were striking, including SUMOylation changes of up to ~900-fold (Supplementary Data 1 and 2). We verified dynamics of SENP6-mediated deSUMOylation using immunoblotting. In agreement with the mass spectrometry data, we confirmed massive build-up of SUMO chains on CENP-B, -C, -H, -I, -K, and -T with SUMO conjugates extending all the way to the top of the protein gels in a manner reminiscent to ubiquitin polymers. Continuous processing of the poly-SUMO2/3 by SENP6 under regular cell culture conditions has prevented the identification of the CCAN subunits as SUMOylation targets up to this moment. Likewise, we confirmed extensive SUMOylation of other mitotic regulators such as KIF18A, which is involved in chromosome congression, Mis18BP1, which is involved in the positioning of the

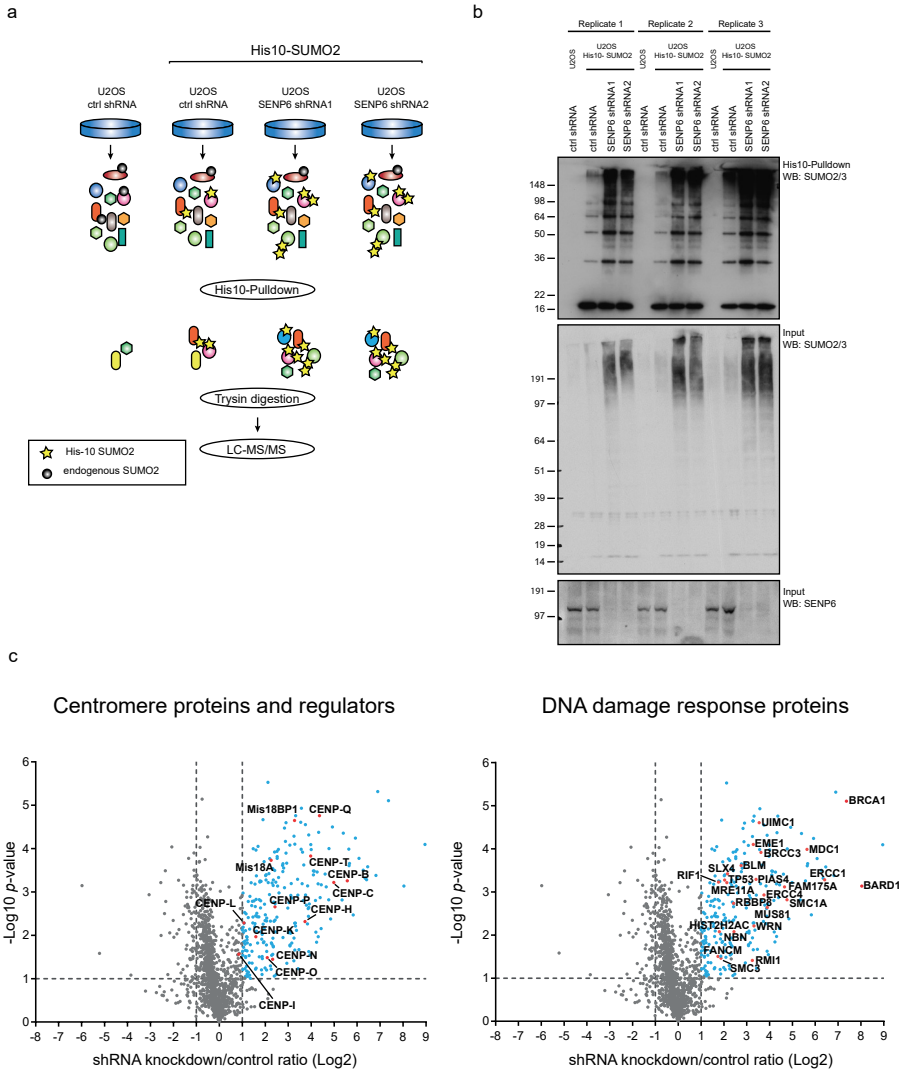

Figure 2. Identification of target proteins regulated by SUMO polymers. a Experimental set up for the identification of SENP6 regulated proteins. U-2 OS cells stably expressing His10-SUMO2 were infected with lentiviruses encoding shRNAs targeting SENP6 or a non-targeting control (ctrl) shRNA. Cells were lysed 3 days post infection and SUMOylated proteins were enriched by means of Ni-NTA pulldown. Enriched SUMOylated proteins were trypsin digested and prepared for label-free quantitative mass spectrometry. Peptides were identified by LC-MS/MS. The four experimental conditions of three biological replicates were analysed in two technical repeats per sample, resulting in a total of 24 MS runs. Black circles represent endogenous SUMO, yellow stars represent exogeneous His10-SUMO2. **b** Immunoblot analysis of the three biological replicates analyzed by mass spectrometry. An antibody against SUMO2/3 was used to confirm efficient enrichment of SUMO conjugates and an increase of SUMO conjugates upon SENP6 knock down. An antibody against SENP6 was used to confirm efficient knockdown. **c** Volcano plot showing all identified proteins within the SENP6 knockdown samples compared to the non-targeted control shRNA. Dashed lines indicate a cut-off at 2-fold change (log2=1) and a *p*-value of 0.05 (-log10=1.3), *n* = 3 independent experiments. SUMOylated proteins represented as blue circles were more abundant after SENP6 knockdown. The left panel shows identified centromere proteins and proteins involved in centromere regulation represented by red circles, whereas the right panel shows DNA damage response proteins represented by red circles. Source data are provided as a Source Data file.

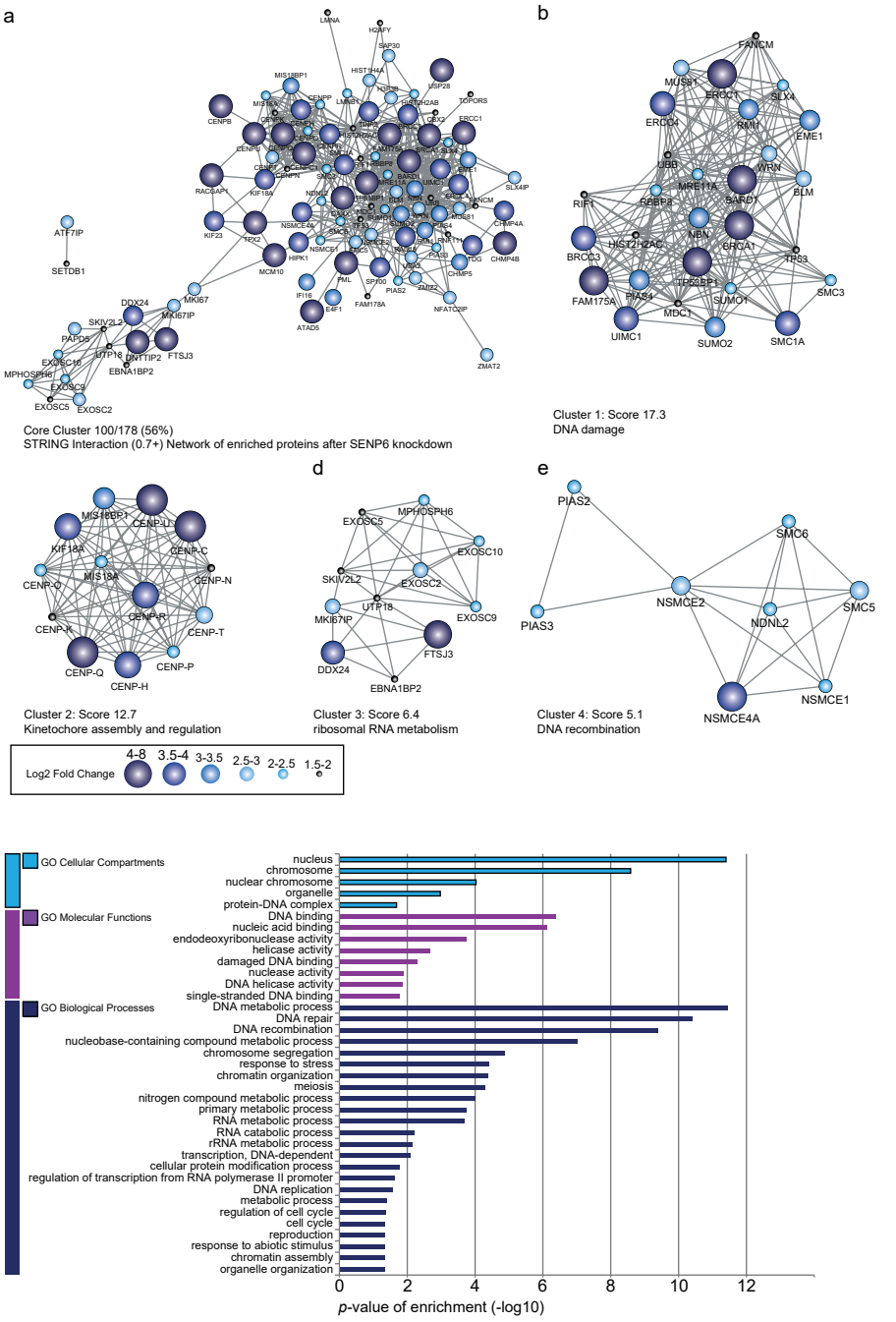

Figure 3. SENP6 demonstrates group deSUMOylation activity. a STRING network analysis of enriched proteins after SENP6 knockdown, with a STRING interaction confidence of 0.7 or higher. Cytoscape software was used to visualize the interaction network. Colour and node size indicate the fold-change differences in abundance after SENP6 knockdown compared to the non-targeting control. **b** MCODE was used to extract the most highly interconnected clusters form the network shown in (**a**). Cluster 1 contains multiple proteins involved in DNA

histone H3 variant CENP-A, and KIF23, which plays a role in cytokinesis (Figure 4a). SUMO chains did not generally build up on all SUMO targets, as shown for DNA topoisomerases IIα and IIβ (Figure 4b). Consistent with the mass spectrometry results, SUMOylation of CENP-A could not be detected by immunoblotting (Figure 4c). In vitro SUMOylation of CENP-T with SUMO2 either WT or lysine-less SUMO2 (K0), which is unable to form SUMO polymers, showed that the high molecular weight signal of SUMOylated CENP-T could be attributed to poly-SUMOylation (Supplementary Figure 1a). Mass spectrometry analysis of in vitro SUMOylated CENP-T revealed the presence of poly-SUMO2/3 on CENP-T (Supplementary Figure 1b). Furthermore, we demonstrated that SENP6 is able to directly target poly-SUMOylated CENP-T and depolymerize the accumulated high molecular weight poly-SUMO2 chain in vitro (Supplementary Figure 1c).

Proteasomal degradation-independent function of poly-SUMO

SUMO chains were previously found to accumulate on CENP-I, PML and PML-RARα and were proposed to mediate the recruitment of the STUbL RNF4. Ubiquitination by RNF4 caused their degradation by the proteasome[30,35,37]. We investigated the fate of SUMOylated CCAN family members upon inhibition of the proteasome by immunoblotting. Surprisingly, we noted a reduction in SUMOylation of CENP-K, -T, -I, -C and -H upon proteasome inhibition instead of an increase as would be expected. However, total SUMO conjugates showed a substantial increase after SENP6 knockdown and proteasome inhibition compared to SENP6 knockdown only (Figure 5a). Additionally, SENP6 knockdown led to a global increase of ubiquitinated proteins within the SUMOylated fraction and SUMOylated proteins within the ubiquitinated fraction that further increased by proteasome inhibition (Supplementary Figure 3a, b). These observations indicate that a substantial fraction of SENP6 regulated SUMO conjugates are destabilized by ubiquitination and proteasomal degradation, while modified CCAN subunits have a different fate.

To verify that accumulation of SUMO chains on the CCAN subunits may not target them to the proteasome, we investigated the ubiquitinated fractions of some of the CCAN proteins. A small fraction of CENP-K was ubiquitinated under control condition, but neither proteasome inhibition, nor SENP6 knockdown or a combination of both led to a substantial accumulation of ubiquitinated CENP-K (Figure 5b). The ubiquitination of CENP-T was barely visible by immunoblot analysis after ubiquitin purification, but CENP-T ubiquitination did not seem to be stabilized by SENP6 knockdown while a slight increase was visible upon proteasome inhibition, notably also under control conditions (Figure 5b).

Our results indicate that there is a small fraction of ubiquitinated CCAN subunits and while we clearly observe an increase in SUMOylation after SENP6 knockdown we fail to observe an increase in ubiquitination of these proteins even after proteasome inhibition. Also, shRNA mediated knockdown of RNF4 did not obviously stabilize SUMOylated CENP-T, -K and -H (Supplementary Figure 4a). Taken together, our findings indicate that SUMO chains on the CCAN family members do not act as a degradation signal, pointing towards a non-classical role of poly-SUMO2/3 signaling. However, shRNA mediated knockdown of RNF4 did

<damage response. **c** Cluster 2 includes multiple kinetochore and kinetochore associated proteins. **d** Cluster 3 includes proteins that are involved in ribosomal RNA metabolism. Cluster 4 contains proteins associated with DNA recombination and the SUMOylation pathway. **f** Gene Ontology (GO) enrichment analysis of SENP6 regulated proteins. The bar graph shows the most significantly overrepresented GO terms for biological processes (BP) in light blue, molecular functions (MF) in purple and cellular compartments (CC) in dark blue compared against the annotated human proteome. Source data are provided as a Source Data file.

stabilize SUMOylated Mis18BP1 (Supplementary Figure 4a). Moreover, we verified that the knockdown efficiency of RNF4 in our experiments was sufficient to reduce ubiquitination of PML in response to As2O3 treatment (Supplementary Figure 4b).

SENP6 knockdown reduces CENP-T and CENP-W at centromeres

To address the functional consequences of highly increased SUMOylation of the CCAN proteins in the absence of SENP6, we studied their subcellular localization by immunofluorescence (Figure 6). We focused on CENP-T and CENP-W, which are direct binding partners and together with CENP-S and CENP-X form one of the five subcomplexes of the CCAN[45]. CENP-T is critical for the assembly of other CCAN components except for CENP-C. CENP-T and -C act in two parallel pathways to recruit the KNL1/Mis12 complex/ Ndc80 complex (KMN) network, which is the microtubule-binding platform of the kinetochore[46,47]. CENP-T, -W, -S and -X possess a histone fold and together form a nucleosome-like structure which enables DNA binding. Therefore, this complex is an important link between DNA and microtubules[45]. We found that after treatment with a non-targeted siRNA pool (NTP), CENP-T accumulated into bright distinct foci in mitotic and interphase cells as expected, marking the centromere. However, in the absence of SENP6, we noted that centromeric accumulation of CENP-T was reduced in mitotic cells as well as in interphase cells, indicating that deSUMOylation by SENP6 is required for its centromeric localization throughout the cell cycle (Figure 6a and Supplementary Figure 5a, b). CENP-W, the direct binding partner of CENP-T, also showed reduced accumulation at centromere foci (Figure 6b and Supplementary Figure 5c, d). In conclusion, deSUMOylation of the CCAN subunits CENP-T and CENP-W by SENP6 is important for efficient localization to mitotic and interphase centromeres.

Furthermore, we tested whether poly-SUMOylation of Mis18BP1 and Mis18A upon SENP6 knockdown affects the activity of the MIS18 complex to incorporate CENP-A in centromeres. We found that knockdown of SENP6 reduces the accumulation of CENP-A in centromeres (Figure 6c and Supplementary Figure 5e-g). This effect could be rescued by expressing exogenous knockdown-resistant wild-type SENP6, but not by exogenous knockdown-resistant catalytic dead SENP6 (Figure 7 and Supplementary Figure 6a, b). In our rescue experiments of the second shRNA directed against SENP6, we noticed a slight increase and a slight decrease of average CENP-A foci intensities in the two replicates that cancelled out each other.

Subcellular localization of SENP6

To address whether deSUMOylation of Mis18BP1 and CCAN subunits occurs at centromeres or in the nucleoplasm prior to accumulation of Mis18BP1 and CCAN subunits at centromeres, we investigated the subcellular localization of SENP6 by fluorescence microscopy. We found that SENP6 does not accumulate at centromeres in mitotic cells or in interphase cells (Figure 8). Instead SENP6 is located in the nucleoplasm in interphase cells and in a pattern excluded from condensed chromosomes in mitotic cells. It is therefore likely that deSUMOylation of Mis18BP1 and CCAN subunits occurs prior to their accumulation at centromeres.

Chromatin-depletion of CCAN proteins upon SENP6 knockdown

Since we have shown that SENP6 is responsible for the group deSUMOylation of the CCAN proteins, we wondered if the decreased accumulation at the centromere of CENP-T and -W does also apply to the other CCAN components. Therefore, we isolated chromatin fractions from cells either treated with a non-targeted siRNA pool or a pool of four siRNAs

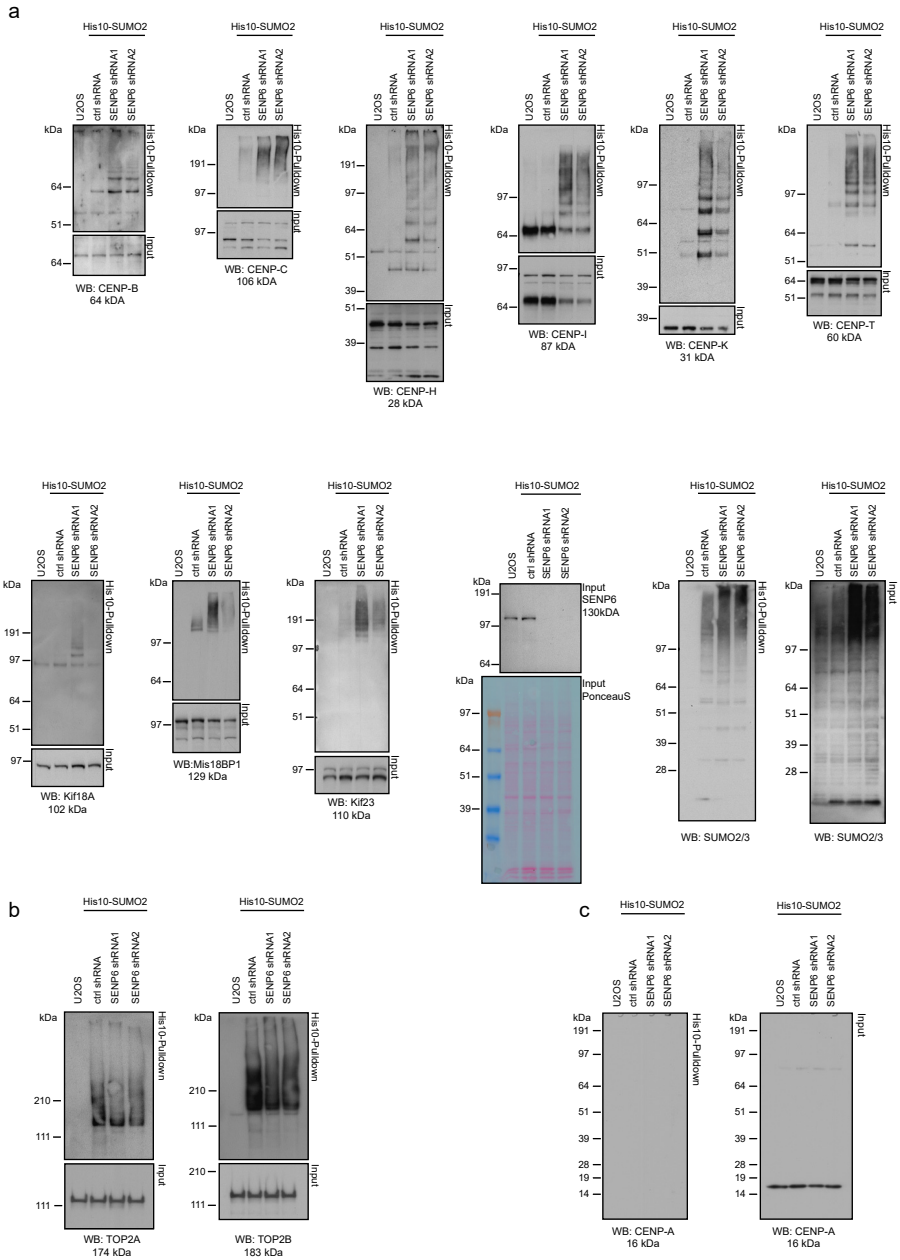

Figure 4. Immunoblot validation of proteins identified by mass spectrometry. a U-2 OS cells stably expressing His10-SUMO2 were infected with lentiviruses encoding shRNAs against SENP6 or a non-targeting control shRNA (ctrl shRNA). Cells were lysed three days post infection and SUMOylated proteins were enriched by means of Ni-NTA pulldown. Inputs and His10-pulldown elutions were analysed by immunoblotting with the indicated antibodies. SENP6 and SUMO antibodies were used as control for efficient knockdown of SENP6 and increase of SUMO conjugates. **b** Aliquots of the same samples as in (**a**) were analysed by immunoblotting against Topoisomerases 2α and 2β that did not show increased SUMOylation in the mass spectrometry screening.
c The same samples as in (**a**) and (**b**) were analysed by immunoblotting against CENP-A.
Source data are provided as a Source Data file.

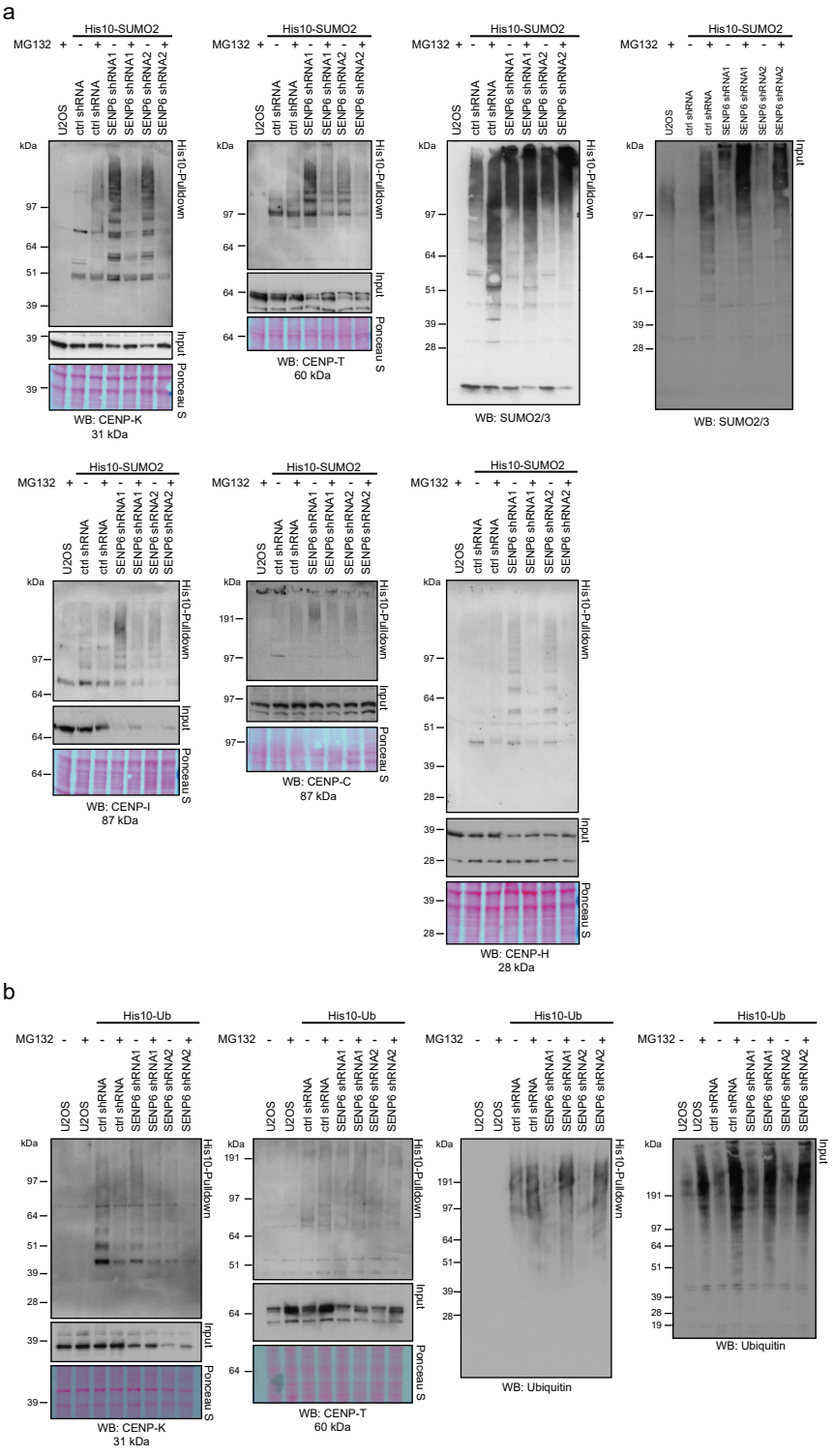
a
His10-SUMO2
MG132
U2OS
ctrl shRNA
SENP6 shRNA1
SENP6 shRNA2
kDa
His10-Pulldown
Input
Ponceau S
WB: CENP-K
31 kDa
WB: CENP-T
60 kDa
WB: SUMO2/3
WB: SUMO2/3
WB: CENP-I
87 kDa
WB: CENP-C
87 kDa
WB: CENP-H
28 kDa
b
His10-Ub
WB: CENP-K
31 kDa
WB: CENP-T
60 kDa
WB: Ubiquitin
WB: Ubiquitin

<Figure 5. Poly-SUMOylation does not lead to destabilization of CCAN proteins. a U-2 OS cells stably expressing His10-SUMO2 were infected with lentiviruses encoding shRNAs against SENP6 or a non-targeting control shRNA (ctrl shRNA) three days prior to lysis. Where indicated, cells were treated with 10μM MG132 for 4 hours prior to lysis. Cells were lysed and SUMOylated proteins were enriched by means of Ni-NTA pulldown. Inputs and His10-pulldown elutions were analysed by immunoblotting with the indicated antibodies. Equal loading was verified by Ponceau S staining. **b** U-2 OS cells stably expressing His10-ubiquitin were infected with lentiviruses encoding shRNAs against SENP6 or a non-targeting control shRNA (ctrl shRNA) three days prior to lysis. Where indicated cells were treated with 10μM MG132 for 4 hours prior to lysis. Cells were lysed and ubiquitinated proteins were enriched by means of Ni-NTA pulldown. Inputs and His10-pulldown elutions were analysed by immunoblotting with the indicated antibodies. Equal loading was verified by Ponceau S staining. Source data are provided as a Source Data file.

directed against SENP6. Additional to CENP-T, we could identify CENP-C, -K, -Q, -P, -N, -O, and -I to be substantially depleted from the chromatin fraction after SENP6 knockdown. CENP-H, -A and -U were depleted to a lesser degree (Figure 9a and Supplementary Data 3). Immunoblot validation of CENP-K, -P/O, -T and -C confirmed that SENP6 knockdown induced chromatin depletion of these proteins. The depletion of CENP-H and CENP-A from the chromatin was less pronounced, in agreement with the mass spectrometry data (Figure 9b and Supplementary Data 3).

A lack of functional SIMs in CCAN subunits

SUMOylation is involved in the build-up of protein complexes via phase separation[48]. Surprisingly, SUMOylation of CCAN subunits prevents efficient assembly of the complex. Phase separation of PML bodies requires the presence of functional SUMO Interaction Motifs[48]. We searched for SIMs in CCAN subunits and noticed only a few potential SIMs in CENP-C,-K,-I and -P (Supplementary Figure 7a)[49]. We could show that CENP-C, -H, -K and -T were unable to bind to a recombinant SUMO trimer despite the presence of potential SIMs in CENP-C and -K in contrast to the well-known SUMO polymer binder RNF4 and SENP6 itself (Supplementary Figure 7b). This is consistent with our finding that SUMOylation does not stimulate CCAN complex formation. Collectively, our data indicate that subunits of all five CCAN subcomplexes are dependent on deSUMOylation by SENP6 to accumulate at the chromatin, which is a prerequisite to form a functional CCAN network and the basis for the KMN network to assemble during mitosis and promote faithful chromosome congression and segregation (Figure 9c).

DISCUSSION

In contrast to widespread knowledge on signal transduction by polymeric ubiquitin, signal transduction by polymeric SUMO has remained virtually unexplored. Uncovering around 180 target proteins linked to poly-SUMO2/3 is a major step forward in our understanding of SUMO polymer signaling, since this provides key insight into the cellular processes regulated by SUMO polymers. Here, we focused on the large group of CCAN proteins, which are regulated by SUMO2/3. Immunoblotting experiments revealed extensive SUMO chains assembled on these targets that appear similar in size to ubiquitin chains. The absence of these chains in the presence of SENP6 indicated their dynamic nature and rapid processing under regular cell culture conditions, leaving only mono- or di-SUMO molecules attached[11,25]. In agreement with the preference of SENP6 for SUMO chains, mono-SUMO2 attached to CENP-T and free di-SUMO2 are processed less efficiently by SENP6 (Figure 1b and Supplementary Figure 1c).

We have uncovered an extensive set of target proteins regulated by poly-SUMO2/3,

employing knockdown of SENP6, the major protease that removes SUMO chains from target proteins. In the absence of SENP6, SUMO chains accumulated to high levels on at least 180 targets, including multiple highly interconnected protein networks, such as the constitutive centromere-associated network (CCAN), a large group of DNA damage response factors, proteins involved in ribosomal RNA metabolisms or factors which regulate DNA replication. These different functional groups of target proteins are each regulated in a strikingly group-like manner, suggesting localized activity of SENP6 under regular cell culture conditions. The observed co-regulation of the CCAN proteins by SUMO chains is an exciting example of co-regulation of a group of functionally related proteins as initially proposed by Erica Johnson for the yeast septins[50] and further developed by Stefan Jentsch for yeast proteins involved in DNA repair[10]. A related key question is how these chains are assembled. According to the model proposed by Stefan Jentsch, the SIMs in the SUMO E3 ligases play a major role to recruit and stabilize these E3 ligases at the site of an initial SUMOylation event, enabling a wave of SUMOylation in a highly localized manner[10]. Likewise, the SIMs which are located in the N-terminus of SENP6 could potentially tether the protease to a SUMOylation hub, leading to the deSUMOylation of all proteins in the vicinity (Figure 9c). The principle of group regulation explains the relatively small number of identified SUMO E3 ligases and SUMO proteases and also provides an explanation for the redundancy of single SUMOylation and deSUMOylation events.

Our data indicate that SENP6 and SENP7 have largely non-overlapping roles, since SENP7 was unable to functionally compensate for the absence of SENP6. This would indicate that the substrates for SENP7 differ from the substrates for SENP6, or that SENP7 is active in different cell types or at different times compared to SENP6. Most interestingly, SENP7 was found to regulate the enrichment of the histone mark H3K9Me3 reader HP1 specifically at the pericentric heterochromatin that is critical for centromere function[51,52]. SENP7 depletion leads to a delocalization of HP1 but can be rescued completely by catalytically dead SENP7, thus the regulatory control of SENP7 of the pericentric heterochromatin is independent of its protease activity[53,54]. However, SENP7 protease activity was shown to counter chromatin condensation upon DNA damage via the deSUMOylation of KAP1/TRIM28 thereby preventing recruitment of chromatin condensation-stimulating remodelers and indirectly leading to chromatin relaxation and proficient DNA damage repair[55].

Recently, SENP6 was also shown to target KAP1/TRIM28 in mouse rib chondrocytes. The failure of deSUMOylation of KAP1/TRIM28 was shown to be responsible for increased p53 activity which led to enhanced senescence and apoptosis of chondrocytes and osteochondroprogenitor cells responsible for the observed premature aging phenotype of mice deficient for SENP6[56]. These findings together with our observations demonstrate that SENP6 and SENP7 are involved in similar cellular pathways, such as centromere integrity and the DNA damage response, but how SENP6 and SENP7 are orchestrated together in these processes needs to be further investigated. Of note, the observed premature aging phenotype in induced SENP6 knock-out mice resembles phenotypes of mice deficient in DNA repair and surveillance proteins[57]. In line with this observation, our project uncovered an extensive set of DNA damage response factors regulated by SUMO chains. This argues for a key regulatory role of SENP6 and poly-SUMO2/3 in the DNA damage response that is much broader than the initially identified RPA70 protein[58].

Poly-SUMO2/3, which accumulated in response to SENP6 knockdown, on CCAN subunits inhibited their accumulation at the centromeres. SENP6 depletion was earlier demonstrated to result in failure of chromosome congression due to RNF4-dependent degradation of

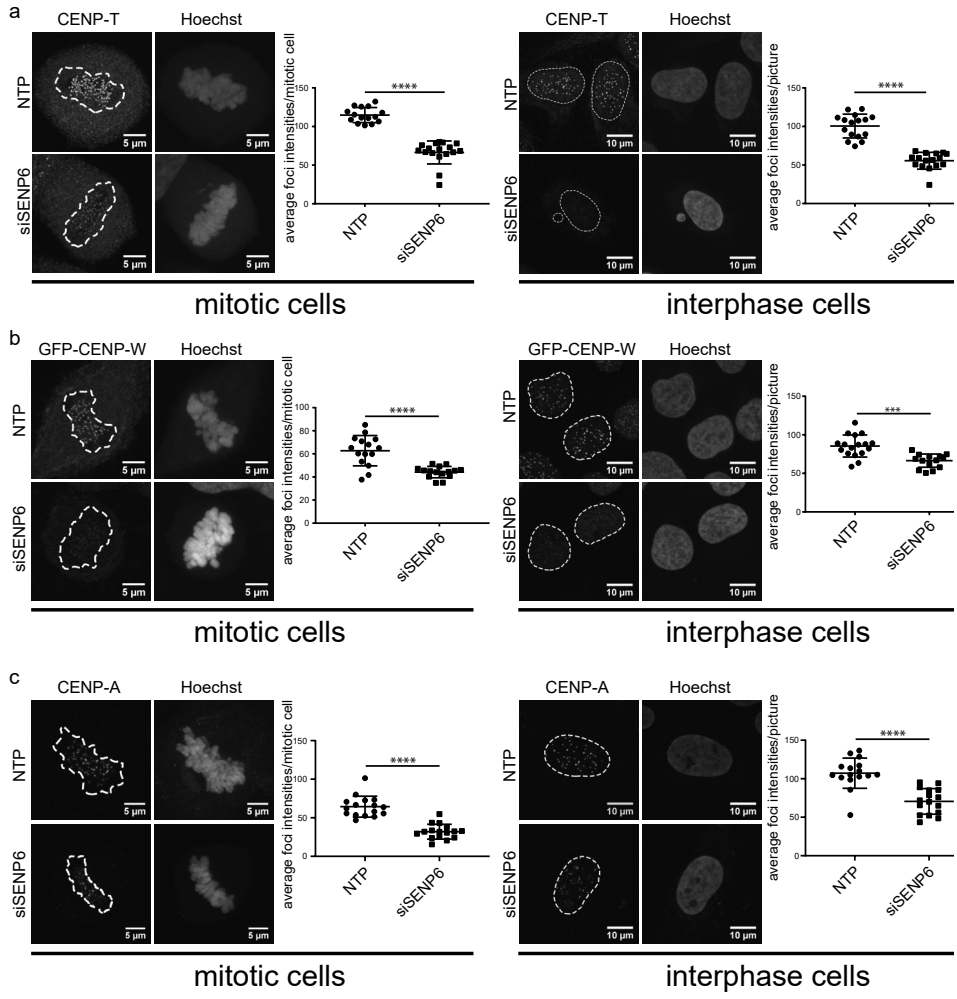

Figure 6. Poly-SUMO2/3 prevent accumulation of CCAN proteins at centromeres. a U-2 OS cells were transfected either with a pool of four siRNAs against SENP6 (siSENP6) or a pool of four non-targeting siRNAs (NTP). Cells were fixed and stained with Hoechst to visualize DNA and CENP-T antibody two days post-transfection. Panels show representative pictures of mitotic (left panel) and interphase cells (right panel). Scatter plots show quantifications of the average CENP-T foci intensities per cell (for mitotic cells) or per picture (for interphase cells). A two-sided t-test was performed. ****p <0.0001. n (NTP mitotic cells) = 15; n (siSENP6 mitotic cells) = 16; n (NTP interphase cells) = 16; n (siSENP6 interphase cells) = 16. Dashed lines indicate areas of DNA. **b** U-2 OS cells stably expressing GFP-CENP-W were treated as in panel (**a**). Cells were fixed and stained with Hoechst to visualize DNA and GFP antibody to enhance GFP signal. Left panels show representative pictures of mitotic (left panels) and interphase cells (right panels). Scatter plots show quantifications of the average CENP-W foci intensities per cell (for mitotic cells) or per picture (for interphase cells). A two-sided t-test was performed. ****p <0.0001; ***p <0.001. n (NTP mitotic cells) = 15; n (siSENP6 mitotic cells) = 15; n (NTP interphase cells) = 16; n (siSENP6 interphase cells) = 16. **c** U-2 OS cells were treated as in panel (**a**), fixed and stained with Hoechst to visualize DNA and CENP-A antibody two days post transfection. Panels show representative pictures of mitotic (left panel) and interphase cells (right panel). Scatter plots show quantifications of the average intensities of CENP-A foci per cell (for mitotic cells) or per picture (for interphase cells). A two-sided t-test was performed. ****p <0.0001. n (NTP mitotic cells) = 16, n (siSENP6 mitotic cells) = 16; n (NTP interphase cells) = 16, n (siSENP6 interphase cells) = 16. Dashed lines indicate areas of DNA. Scale bars = 5 µm (mitotic cells), 10 µm (interphase cells). All error bars shown represent standard deviation (SD). Source data are provided as a Source Data file.

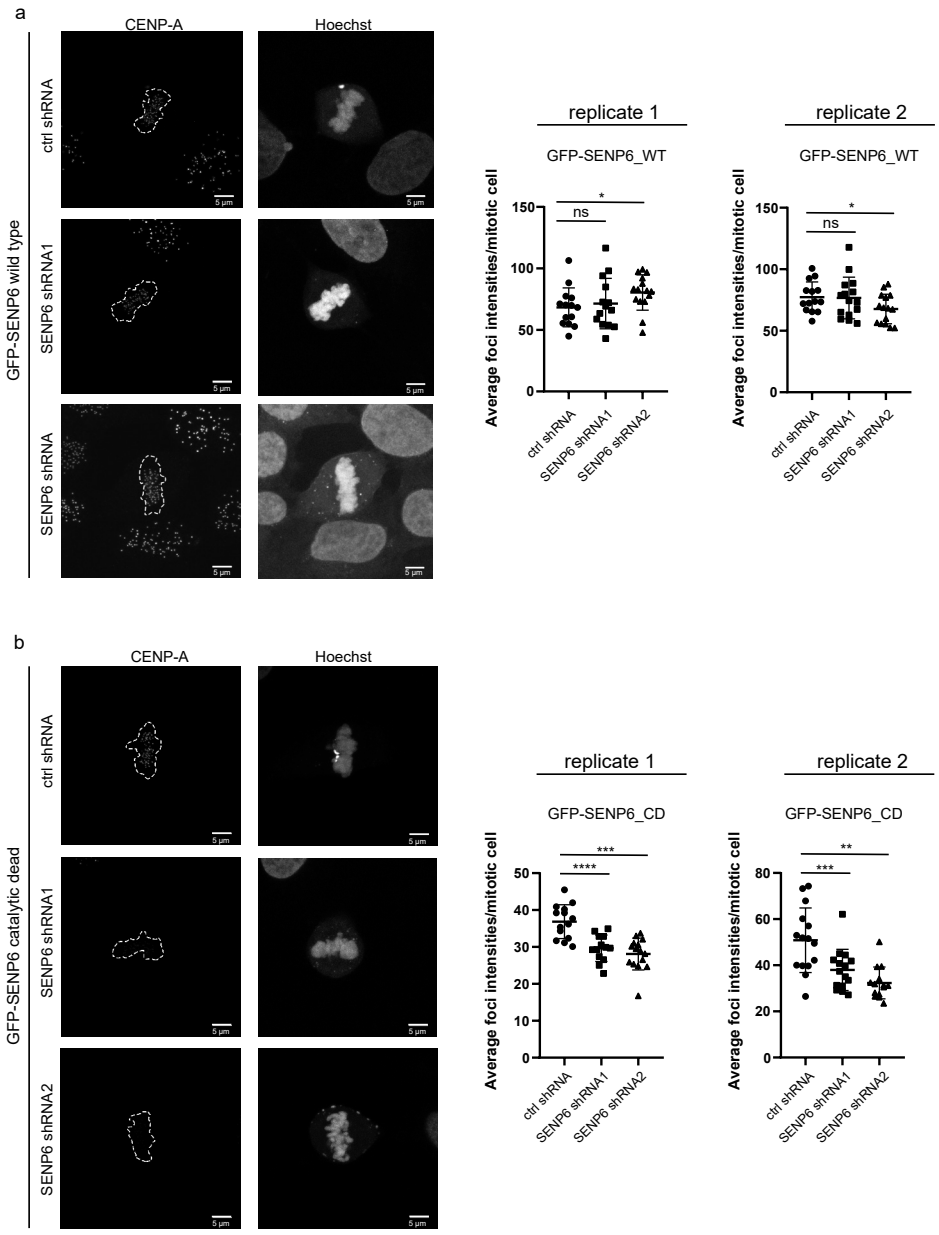

CENP-I and subsequently reduced recruitment of the KMN network components Ndc80 and Mis12[30]. Here we show that most CCAN subunit are regulated by SENP6. We hypothesize that the downstream effects on Ndc80 and Mis12 upon SENP6 knockdown are mediated by the global induction of poly-SUMO2/3 on multiple CCAN subunits. We demonstrate a significant SENP6 knockdown-induced reduction of CENP-T and W foci. These members of the CCAN network make direct contact with Ndc80 and therefore qualify, as much as CENP-I, as initial points of misregulation[46]. The accumulation of CENP-A at centromeres is

<Figure 7. CCAN protein localization at the centromere depends on catalytic activity of SENP6. Knockdown of SENP6 can be rescued by reintroduction of wild-type SENP6, but not by reintroduction of catalytic dead SENP6. **a**,**b** U-2 OS cells stably expressing inducible shRNA-resistant GFP-tagged wild-type (WT) (**a**) or catalytic dead (CD) SENP6 (**b**) were established. Expression of these constructs was induced by doxycycline for 24 h prior to transduction with lentiviruses encoding SENP6 shRNAs. Medium was replaced 1 day post infection. The next day, cells were seeded on coverslips and grown overnight. Subsequently, cells were fixed and stained with Hoechst to visualize DNA and CENP-A antibody. Panels show representative pictures of mitotic cells. Scatter plots show quantifications of the average CENP-A foci intensities per cell for two independent replicates. The data were statically analysed by two-sided t-test. *$p \leq 0.05$; **$p \leq 0.01$; ***$p \leq 0.001$, ****$p \leq 0.0001$. For **a** replicate 1: *n* (ctrl shRNA) = 14 cells, *n* (SENP6 shRNA2) = 14 cells; *n* (SENP6 shRNA2) = 15 cells; replicate 2: *n* (ctrl shRNA) = 14 cells, *n* (SENP6 shRNA2) = 15 cells; *n* (SENP6 shRNA2) = 15 cells. For **b** replicate 1: *n* (ctrl shRNA) = 14 cells, *n* (SENP6 shRNA2) = 13 cells; *n* (SENP6 shRNA2) = 15 cells; replicate 2: *n* (ctrl shRNA) = 15 cells, *n* (SENP6 shRNA2) = 15 cells; *n* (SENP6 shRNA2) = 14 cells. Dashed lines indicate areas of DNA. Scale bars = 5 µm. Error bars represent standard deviation. Source data are provided as a Source Data file.

also reduced, most likely as a result of poly-SUMOylation of Mis18BP1 and Mis18A in the absence of SENP6. It should be noted that stabilization of CENP-A at centromeres requires the presence of CCAN subunits[59,60].

Recently, it has been shown that SUMOylation can lead to phase-separation of proteins, exemplified by the PML-body[48]. In case of the CCAN, we found that extensive SUMOylation does reduce instead of enhance protein complex formation. The main difference between the PML-body and the CCAN appears to be the presence of functional SIMs in PML-body components and the very limited set of potential SIMs in CCAN subunits. Our data thus indicate that SUMO polymers on centromeric proteins have an opposite role to counteract centromere assembly. One possible explanation could be that the bulky accumulated poly-SUMO2/3 chains interfere with the formation of the CCAN at the centromeres by steric hindrance due to interfering with direct binding to other CCAN proteins or to centromeric DNA.

The known function of SUMO chains is their role in protein degradation. SUMO chains provide an efficient binding site for SUMO-Targeted Ubiquitin Ligases including RNF4. Tandem arrays of SIMs in RNF4 enable preferential binding to SUMO chains[35]. Ubiquitination of SUMOylated proteins targets them to the proteasome for degradation. The initially identified substrates for this combinatorial PTM pathway are PML and the protein product of the causative fusion gene for Acute Promyelocytic Leukemia, PML-RARα[35,37]. In agreement with this model, we have recently shown that the large majority of proteins that are co-modified by SUMO and ubiquitin accumulated upon proteasome inhibition61. No CCAN subunits were identified in this screen with the only exception of CENP-C.

Additionally, we tested this model for centromeric proteins conjugated to poly-SUMO2/3, which accumulated in absence of SENP6, and surprisingly found that proteasome inhibition did not enhance the presence of SUMO chains on these proteins. In contrast, we mainly noted a reduction in SUMO chain levels attached to centromeric proteins upon proteasome inhibition, most likely due to a reduced pool of free SUMO. We also failed to observe an increase in ubiquitination of the individual CCAN proteins following SENP6 depletion and proteasome inhibition whereas we noticed a global increase of co-modified proteins as expected. We therefore hypothesize that SUMO chains attached to centromeric proteins are not functioning as a degradation signal. SUMO2/3 chain formation is thought to occur predominantly via lysine 11, which is embedded in a SUMOylation consensus motif, defined by ψKxE motif (where ψ represents hydrophobic amino acids and x represents any amino acid). Site-specific mass spectrometry has however identified different SUMO lysines which mediate polymerization, indicating potential for differential SUMO chain architecture[62]. Whether different SUMO chains mediate different biological fates of target proteins

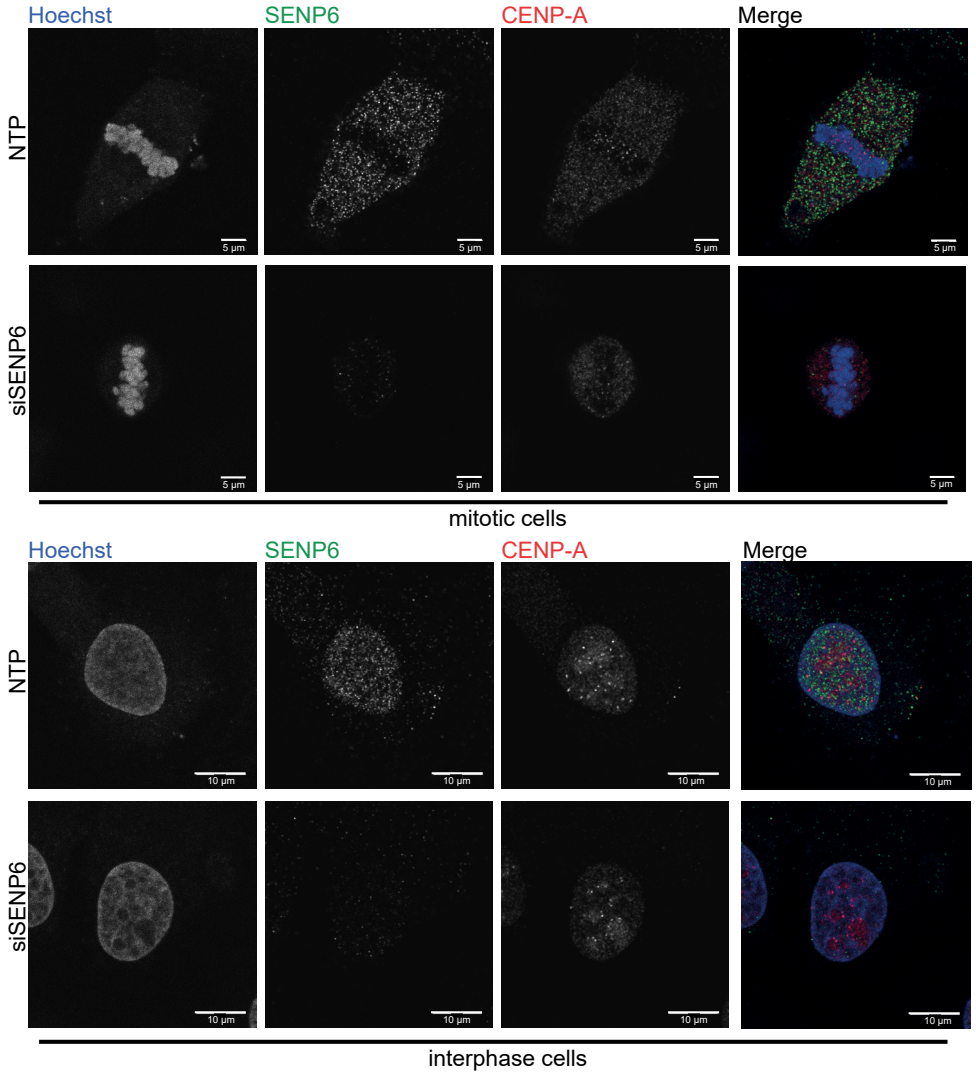

Figure 8. SENP6 localizes to the nucleoplasm. U-2 OS cells were grown on coverslips overnight, transfected either with a pool of four siRNAs against SENP6 (siSENP6) or a pool of four non-targeting siRNAs (NTP). Cells were fixed two days post transfection and co-stained with Hoechst to visualize DNA and antibodies directed against SENP6 and CENP-A. Panels show representative pictures of mitotic (upper panel) and interphase cells (lower panel). Scale bar = 5 µm (mitotic cells), 10 µm (interphase cells). Source data are provided as a Source Data file.

analogous to the ubiquitin system and recruit SENPs, STUbLs or other effector proteins with varying affinities remains to be investigated.

In summary, we provide a resource of target proteins regulated by poly-SUMO2/3 that encompasses multiple protein clusters, including a cluster of centromere-associated proteins and a cluster of DNA damage response factors. Detailed functional analysis of this large set of SUMO polymer targets might widen our understanding on the diverse roles of SUMO polymers in biology. This is analogous to the ever increasing roles uncovered

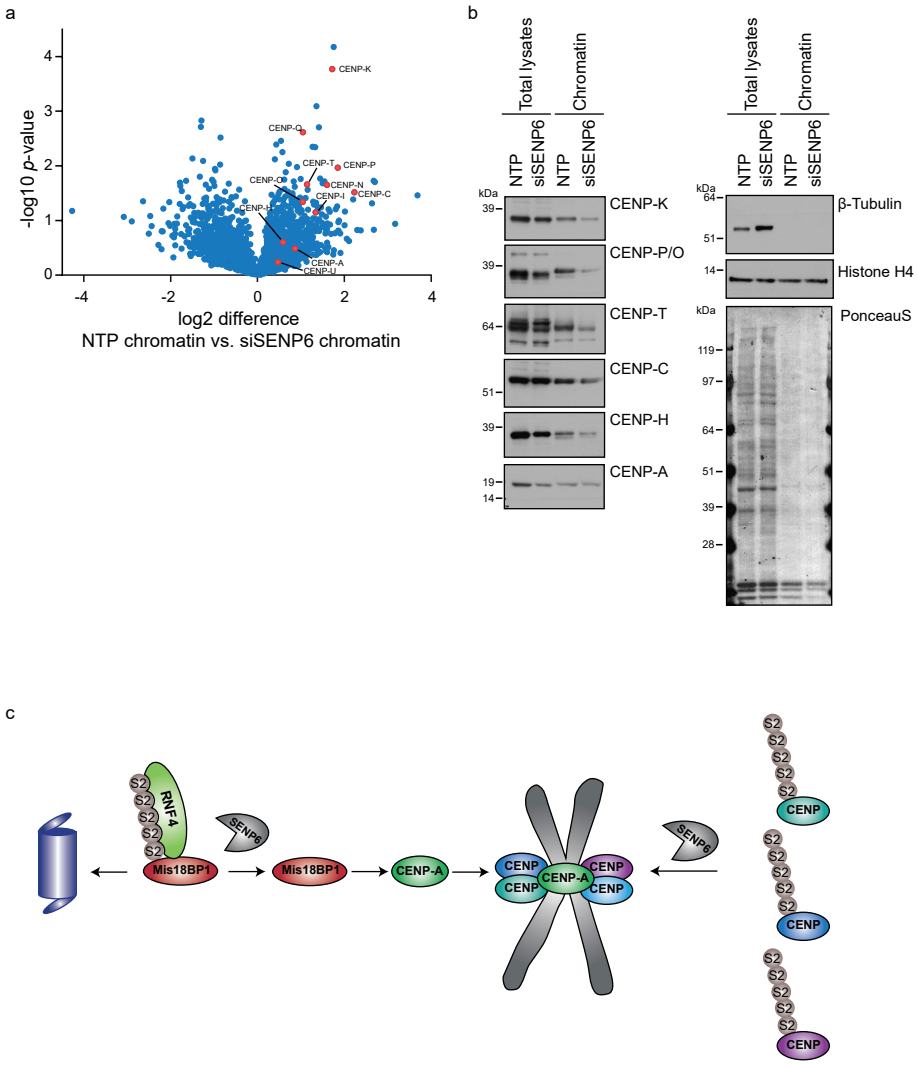

Figure 9. SENP6 knockdown leads to the depletion of multiple CCAN proteins from chromatin. a U-2 OS cells were transfected either with a pool of four siRNAs against SENP6 (siSENP6) or a pool of four non-targeting siRNAs (NTP). Chromatin fractions were isolated and proteins were analyzed by mass spectrometry. Volcano plot showing all identified proteins within the NTP treated sample compared to the siSENP6 treated sample. All identified inner kinetochore proteins are represented by red circles. *n* = 4 independent experiments **b** Samples from (**a**) were analyzed by immunoblotting using antibodies against several inner kinetochore proteins, as well as β-tubulin and histone H4 as control for efficient fractionation. Source data are provided as a Source Data file. **c** Model of SENP6 regulation of CCAN protein. SENP6 deSUMOylated CCAN proteins as well as Mis18BP1. SENP6 depletions leads to RNF4-mediated degradation of Mis18BP1 and consequently the failure of CENP-A to accumulate at the centromere. Reduced CENP-A levels as well as accumulated SUMO chains on other CCAN family members hinder efficient CCAN protein complex formation at the centromere.

for ubiquitin polymers[63]. We also demonstrate that SENP6 depletion leads to a reduction in cell proliferation and mitotic problems that ultimately lead to cell death, implicating a clinical potential for a SENP6 inhibitor against highly proliferative cancer cells. The recently

published SUMO E1 inhibitor also caused mitotic problems, especially the accumulation of anaphase bridges[64,65]. Combined this indicates that precise timing of SUMO conjugation and SUMO deconjugation are both essential for proper mitotic progression. Targeting the SUMO conjugation machinery and deconjugation machinery might therefore both be beneficial as anti-cancer strategies. Unravelling signal transduction by poly-SUMO2/3 might enhance our insight into the regulatory consequences of SUMO polymers and could potentially be employed to reduce cancer cell proliferation.

METHODS

Cell culture and generation of cell lines

U-2 OS cells (ATCC® HTB-96™) (gender: female), HeLa cells (EMBL) (gender: female), HEK293T66 and HEK293GP67 cells were cultured in Dulbecco's modified Eagle's medium (DMEM) (high glucose, pyruvate, Gibco™) supplemented with 10 % FCS and 100U/ml penicillin and 100µg/ml streptomycin (Gibco™) For induction of PML ubiquitination by RNF4, cells were treated with As2O3 (Sigma Aldrich, 17971) at 1 µM for 4 hours.

In-vitro SUMOylation and deSUMOylation assay

Recombinant human CENP-T-FLAG or human CENP-T-HA were expressed in U-2 OS cells and purified using Anti-FLAG M2 agarose affinity gel (Sigma Aldrich, A2220) or EZview Red Anti-HA Affinity Gel (Sigma Aldrich, E6779), respectively. The purified recombinant proteins were eluted with 150 ng/µl FLAG (custom made) or HA (Sigma Aldrich, I2149) peptide in 50 Mm HEPES pH 7.4, 150 mM KCl, 10 % Glycerol. In vitro SUMOylation was carried out by incubating 150 ng recombinant CENPT-FLAG or CENPT-HA with 500 ng SAE1/2, 2.0 µg Ubc9, 2.0 µg SUMO-2, 50 mM Tris pH 7.5, 5 mM MgCl2, 2 mM ATP, 3.5 U/µl Creatine kinase, 10 mM Creatine phosphate, 0.6 U/µl inorganic pyrophosphate in 20 µl reaction at 37 °C for 3 h. Additionally CENP-T-HA was also SUMOylated with SUMO-2 lysine-deficient mutant (K0). As a negative control, recombinant CENP-T-FLAG and CENP-T-HA were treated similarly but leaving out SAE1/2 and SUMO-2 respectively from the reaction. For SENP6 deconjugation assay 10 µl of SUMOylated CENP-T-FLAG was incubated with 150 nM recombinant human SENP6 catalytic domain in buffer containing 25 mM Tris pH8.0, 150 mM NaCl. 0.1 % Tween-20, 2 mM DTT at 37 °C for 2 h and the reaction was stopped by adding NuPage LDS (4x) sample buffer. Plasmids used for the production of recombinant CENPT-FLAG, CENPT-HA, SAE1/2, Ubc9, SUMO2 WT, SUMO2 K0 and SENP6 catalytic domain are listed in Supplementary Table 2.

Lentivirus production and transduction

For lentiviral production of shRNAs, HEK 293T cells were transfected with lentiviral packaging plasmids and plasmids containing SENP6 or RNF4 targeting shRNA or non-targeting control shRNA. Lentivirus was harvested in DMEM medium. For shRNA mediated knockdown experiments, cells were infected with a multiplicity of infection (MOI) of 3 with third generation lentiviruses encoding shRNAs targeting SENP6 or RNF4. Transductions were performed in DMEM containing 8 µg/ml polybrene. 24 h post-infection medium was replaced. Cells were lysed 3 days post infection. Plasmids for lentivirus production and targeted shRNAs as well as the non-targeting control shRNA SHC002 are derived from Mission shRNA library (Sigma) and are listed in Supplementary Table 2.

Retrovirus production and transduction

For stable expression of human GFP-CENP-W, HEK 293GP cells were transfected with pBabe-puro-GFP-CENPW together with a plasmid encoding the viral envelop VSV-G protein. Retrovirus was harvested and transduction of U-2 OS and HeLa cells was performed in DMEM containing 8 µg/ml polybrene. Cells expressing GFP-CENPW were selected with 1 µg/ml puromycin supplemented DMEM medium. Plasmids for retroviral production are listed in Supplementary Table 2.

siRNA-mediated knockdown

For siRNA mediated knockdown of SENP6, 10 nM SMARTpool ON-TARGETplus SENP6 siRNA or SMARTpool ON-TARGETplus non-targeting siRNA (Dharmacon) was mixed with Opti-MEM (Gibco) and Lipofectamine RNAiMAX (Thermo Fischer Scientific, 13778075) before transfection of U-2 OS cells. Cells were processed 48 hours after transfection. siRNA mediated knockdown of CENP-A was performed using the same transfection protocol with 10 nM and 50 nM of SMARTpool ON-TARGETplus CENPA siRNA (Dharmacon). Cells were processed 48 hours after the final transfection. siRNAs used for SENP6 and CENPA knockdown are listed in Supplementary Table 2.

Colony formation assay

For colony formation assays, batches of 1 million U-2 OS cells were each infected with a MOI of 3 with lentiviruses encoding shRNA against SENP6. One day post-infection 2500 cells were seeded for each condition onto 10 cm diameter dishes in triplo. Cell were fixed on day 14 post infection with 100 % methanol for 30 min at -20. Colonies were stained with 0.05 % crystal violet solution for 20 min. before rinsing of the plates with water. Subsequently, crystal violet was solubilized with 1.5 ml MetOH for 10 min and absorbance was measured at 595 nM.

Rescue experiments

U-2 OS cells stably expressing inducible wild-type or catalytically dead GFP-SENP6 fusion constructs were established. These constructs carried silent mutations to make them resistant against shRNA-mediated knockdown. Oligos used to introduce the mutations in SENP6 are listed in Supplementary Table 2. Cells were seeded in 10 cm plates at a density of 0.8x106 cells. The next day, expression of the GFP-SENP6 fusion constructs was induced with doxycycline at 1 µg/ml. The following day, cells were infected with third generation lentiviruses encoding shRNAs targeting SENP6 or control at MOI of 3. Medium was refreshed the following day. The next day, cells were seeded on coverslips for microscopy and in 12-well plates for lysis. After overnight incubation, cells were fixed and processed for microscopy or lysed and processed for immunoblotting.

Fluorescent-Activated Cell Sorting

Assessment of cell cycle progression was essentially performed as previously described68 with minor modifications. In brief, cells were harvested by trypsinization washed once in PBS and resuspended in 1 ml of PBS. 4 ml of 100 % ethanol was added and the cells were fixed at 4ºC overnight. On the day of flow cytometry analysis, the cells were first centrifuged at 500 xg for 2 minutes, the supernatant was removed and the cells were washed with PBS and 2 % calf serum. Then, the cells were pelleted again and resuspended in 500 µl of PBS complemented with 2 % calf serum, 25 µg/ml propidium iodide (Sigma-Aldrich, P4170) and 100 µg/ml RNAse A (Sigma-Aldrich, R6513). Cellular DNA content was determined by flow cytometry with the BD LSRII system and BD FACS DIVA Software (BD Biosciences Clontech). Cell cycle analysis was performed with FlowJo version 10 software using the Watson univariate model. Samples were included in analysis when the values of coefficient of variance (CV) of G1 and G2/M peaks were below 5.

His10-SUMO2 and His10-ubiquitin purification

His10-SUMO2 conjugates were purified as previously described38. In brief, U-2 OS cells

stably expressing His10-SUMO2 were lysed in 25 pellet volumes of 6 M Guanidine-HCL, 100 mM sodium phosphate, 10 mM Tris, buffered at a pH of 8.0. Lysates were subsequently snap-frozen and stored at -80 until further processing. Lysates were thawn at RT, sonicated 2x for 5 sec at 30 W and subsequently supplemented with 5 mM β-mercaptoethanol and 50 mM Imidazole pH 8.0. Prewashed Ni-NTA beads (Qiagen, 30210) were added to the lysates and incubated for 3-5 hours at RT or overnight at 4 ˚C. Ni-NTA beads were washed with wash buffer 1-4, respectively; Wash buffer 1: 6 M Guanidine-HCL, 100 mM sodium phosphate, 10 mM TRIS, 10 mM Imidazole, 5 mM β-mercaptoethanol, 0,2 % Triton X-100. Wash buffer 2: 8 M Urea, 100 mM sodium phosphate, 10 mM TRIS, 10 mM imidazole, 5mM β-mercaptoethanol, 0,2 % Triton X-100. Wash buffer 3: 8 M urea, 100 mM sodium phosphate, 10 mM TRIS, 10 mM imidazole, 5 mM β-mercaptoethanol, 0.2 % Triton X-100. Wash buffer 4: 8 M urea, 100 mM sodium phosphate, 10 mM TRIS, 5 mM β-mercaptoethanol, 0.1 % Triton X-100. For samples used for subsequent mass spectrometry analysis, 0.2 % Triton X-100 was included in Wash 1 and 0,1 % Triton X-100 was included in Wash 2, Wash 3 and Wash 4 did not contain Triton X-100. Purified proteins were twice eluted in one bead volume of 7 M urea, 100 mM sodium phosphate, 10 mM TRIS and 500 mM imidazole pH 7.0.

Chromatin fractionation

Cell were harvested washed twice in ice-cold PBS. A small fraction of cell suspension was lysed in SNTBS (2 % SDS, 1 % NP-40, 50 mM Tris pH 7.5, 150 mM NaCl) buffer as input control. The residual cells were lysed in buffer A (10 mM HEPES, 10 mM KCL, 1.5 mM MgCl2, 10 % glycerol, 340 mM sacharose, 1 mM DTT, 1 protease inhibitor tablet without EDTA (Complete Mini protease inhibitor cocktail, Sigma-Aldrich, 11836170001)/ 10 ml. The lysate was subsequently supplemented with Triton X-100 to a final concentration of 0.1 %. The lysate was incubated on ice for 8 min and subsequently centrifuged at 1300 xg for 5 min at 4 °C. Supernatant was collected as cytoplasmic fraction. Pellet was washed twice with buffer A and subsequently lysed in buffer B (3 mM EDTA, 0.2 mM EGTA, 1 mM DTT, 1 protease inhibitor tablet without EDTA/ 10 ml) for 30 min at 4 °C. After centrifugation at 1700 xg for 5 min at 4 °C supernatant (nucleoplasmic fraction) was separated from pellets (chromatin fraction). The chromatin fraction was further diluted in 100 µl SNTBS buffer and heated to 99 °C for 10 min.

SUMO Q87R in vitro SUMOylation of CENPT

Recombinant CENP-T-HA was SUMOylated in vitro by adding 50 mM Tris pH 7.5, 5 mM MgCl2, 2 mM ATP, 3.5 U/ml Creatine kinase, 10 mM Creatine phosphate, 0.6 U/ml inorganic pyrophosphate, 5 µg SAE1/2, 20 µg Ubc9, and 20 µg FLAG-SUMO-2-Q87R to 2 µg samples of CENPT-HA in a volume of 200 µl and incubating for 3 h at 37 °C. As a negative control, recombinant CENPT-HA was treated similarly but leaving out FLAG-SUMO-2-Q87R from the reaction. For the mass spec analysis SUMOylated CENP-T-HA was incubated with 50 µl prewashed EZview Red Anti-HA Affinity Gel (Sigma Aldrich, E6779) for 2 h at 4 °C in 50 mM Tris pH 7.5 and 150 mM NaCl. HA beads were washed with 50 mM Tris pH 7.5, 150 mM NaCl, and 20 mM NEM to eliminate the SUMO machinery. Subsequently, beads were washed three times with 50 mM ammonium bicarbonate and subsequently incubated with 2 µg of trypsin (Promega, V5111) overnight at 37 °C. The samples were passed through a pre-washed 0.45 µm filter (Millipore) to remove the HA- beads and acidified with 2 % trifluoroacetic acid (Sigma). Peptides were desalted and concentrated on triple-disc C18 reverse phase Stage Tips. Peptides were eluted with acetonitrile, vacuum dried and dissolved in 0.1 % folic acid.

Plasmids used for the production of recombinant CENPT-HA, FLAG-SUMO-2-Q87R, SAE1/2 and Ubc9 are listed in Supplementary Table 2.

In solution digestion and stage tipping

His10-SUMO2 purified elutions were concentrated using a 100 kD cut-off filter and diluted with ammonium bicarbonate (ABC) to an end-concentration of 50 mM. Samples were reduced with DTT in two steps, first to 1 mM DTT and subsequently to 6 mM DTT. In between the reduction steps, sample was alkylated using 5 mM cloroacetamide. Proteins were first digested with Lys-C (Promega, VA1170) in a 1:100 enzyme-to-protein ratio for 5 hours. Peptides were diluted with 50 mM ABC before trypsin (Promega, V5111) digestion. Trypsin digestion was carried out in a 1:100 enzyme-to-protein ratio, overnight and in the dark at RT. After digestion peptides were acidified with 2 % trifluoroacetic acid and then desalted and concentrated on triple-disc C18 reverse phase StageTips 69. Peptides were eluted with acetonitrile, vacuum dried and dissolved in 0.1 % folic acid.

In gel digestion

Chromatin fractions in SNTBS buffer were loaded onto a precast 4-12 % Bis-Tris gel (Bold, Thermo Fischer Scientific). Proteins were excised from the gel, divided into two fractions (high and low molecular weight bands) and cut into small 1x1 mm cubes. Gel pieces were destained with 25 mM ammonium bi-carbonate (ABC) in 50 % acetonitrile (ACN) twice for 20 min at 15 °C. Gel pieces were dehydrated with 100 % ACN for 10 min at 25 °C and subsequently vacuum dried. Gel pieces were rehydrated and proteins were reduced with 10 mM dithiothreitol (DTT) in 50 mM ABC and incubated for 60 min at 56 °C. Gel pieces were subsequently alkylated with 55 mM iodoacetamide in 50 mM ABC for 45 min at 25 °C. Gel pieces were subsequently washed twice with 50 mM ABC followed by dehydration with 100 % ACN. Gel pieces were vacuum dried and rehydrated with 12.5 ng/µl trypsin (Promega, V5111) in ABC overnight. After acidifying the gel pieces with 100 % trifluoroacetic acid (TFA), peptides were extracted twice from gel pieces with 3 % trifluoroacetic acid (TFA) in 30 % ACN followed by dehydration with 100 % ACN. Peptides were vacuum dried to remove ACN, acidified with 2 % TFA and subsequently desalted and concentrated on triple-disc C18 reverse phase Stage Tips. Peptides were eluted with ACN, vacuum dried and dissolved in 0.1 % folic acid.

Electrophoresis and immunoblotting

Proteins were separated on either precast 4-12 % Bis-Tris gradient gels (Bold, Thermo Fischer Scientific) or precast 3-8 % Tris-Acetate gels (NuPage, Thermo Fischer Scientifc). Separated proteins were subsequently transferred to Amersham Protran Premium 0.45 µm nitrocellulose membranes (Sigma-Aldrich) using a submarine system. Membranes were stained with Ponceau S solution for visualization of total protein content and blocked with PBS containing 8 % milk powder and 0.05 % Tween-20 before incubating with the primary antibodies. Primary antibodies were diluted in 8 % milk, 0.05 % Tween-20, 1 x PBS and incubated with membranes overnight at 4 °C. Primary antibodies and dilutions used are listed in Supplementary Table 1. Donkey anti-rabbit IgG-HRP and goat anti-mouse IgG-HRP were used as secondary antibodies 1:5000 dilution in 8% milk. Signal was detected and captured by using Pierce ECL2 (Life technologies) and RX medical film (Fuji).

LC-MS/MS analysis

Vacuum-dried peptides were resuspended in 0.1 % formic acid (FA) prior to liquid chromatography-tandem mass spectrometry. All analyses were performed on an EASY-nLC 1000 system (Proxeon, Odense, Denmark) connected to a Q-Exactive Orbitrap (Thermo Fisher Scientific, Germany) through a nano-electrospray ion source. Separation of peptides was achieved using a 15 cm analytic column with an inner diameter of 75 µm, packed in-house with 1.9 C18-AQ beads. For the identification of SENP6-regulated proteins, peptides were analyzed over a 120 min gradient from 2% to 95% acetonitrile (ACN) in 0.1% FA. The mass spectrometer was operated in data-dependent acquisition mode using a top 10 method. Full-scan MS spectra acquired at a target value of 3E6 and a resolution of 70,000. The Higher-Collisional Dissociation (HCD) tandem MS/MS were acquired using a target value of 1E5, a resolution of 17,500 and a normalized collision energy (NCE) of 25%. The maximum injection times for MS1 and MS2 were 20 ms and 60 ms, respectively. For the identification of chromatin-associated proteins upon SENP6 depletion, peptides were analyzed over a 4-hour gradient from 2% to 95% CAN in 0.1% FA. The mass spectrometer was operated in data-dependent acquisition mode using a top 7 method. Full-scan MS spectra acquired at a target value of 3E6 and a resolution of 70,000. The Higher-Collisional Dissociation (HCD) tandem MS/MS were acquired using a target value of 1E5, a resolution of 35,000 and a normalized collision energy (NCE) of 25%. The maximum injection times for MS1 and MS2 were 50 ms and 120 ms, respectively.

MaxQuant data analysis

For the analysis of SENP6-regulated SUMO proteins, four experimental conditions were performed in biological triplicate and each sample was measured with two technical repeats, which resulted in a total of 24 MS runs. All RAW data were analyzed using MaxQuant software version 1.5.3.30[41] and its integrated search engine Andromeda. The search was performed against an in silico digested reference proteome for Homo Sapiens obtained from Uniprot.org (June 24th 2016). Database searches were performed with Trypsin and Lys-C allowing 2 missed cleavages. Carbamidomethyl was set as fixed modification and the variable modifications of oxidation (M) and acetyl (protein N-term) were allowed with a max number of 5 modifications per peptide. Fast Label-free quantification (LFQ) was enabled with a LFQ minimal ratio count of 2, a LFQ minimal number of neighbors of 3 and 6 LFQ average number of neighbors. Match-between runs was enabled with a match time window of 0.7 min and an alignment time window of 20 min. A maximum peptide mass of 4600 Da was permitted. A first search with a peptide tolerance of 20 ppm was performed to determine a mass and time recalibration. A second search with a peptide tolerance of 4.5 ppm was performed as main search and the results were used for further analysis. Desired false discovery rates (FDRs) for peptide spectrum match (PSM) and protein level was set to 1%. A minimal score for modified peptides of 40 was applied, together with a minimal delta score for modified peptides of 6. For protein identification the minimum number of razor + unique peptide was set to 1, as was the minimum number of peptides.

For the identification of chromatin-associated proteins upon SENP6 depletions, 4 experimental condition (1: non-targeting siRNA LOW molecular weight bands, 2: non-targeting siRNA HIGH molecular weight bands, 3: SENP6-targeting siRNA LOW molecular weight bands, 4: SENP6-targeting siRNA HIGH molecular weight bands), were collected in four biological replicates and measured with one technical repeat, resulting in a total of 16 MS runs. All RAW data were analyzed using MaxQuant software version 1.5.3.30[41] and its integrated search engine

Andromeda. The search was performed against an in silico digested reference proteome for Homo Sapiens obtained from Uniprot.org (June 24th 2016) . Database searches were performed with Trypsin/P allowing 2 missed cleavages. Carbamidomethyl was set as fixed modification and the variable modifications of oxidation (M) and acetyl (protein N-term) were allowed with a max number of 5 modifications per peptide. Label-free quantification (LFQ) was enabled with a LFQ minimal ratio count of 2. Match-between runs was enabled with a match time window of 0.7 min and an alignment time window of 20 min. A maximum peptide mass of 4600 Da was permitted. A first search with a peptide tolerance of 20 ppm was performed to determine a mass and time recalibration. A second search with a peptide tolerance of 4.5 ppm was performed as main search and the results were used for further analysis. Desired false discovery rates (FDRs) for peptide spectrum match (PSM) and protein level was set to 1%. A minimal score for modified peptides of 40 was applied, together with a minimal delta score for modified peptides of 6. For protein identification the minimum number of razor + unique peptide was set to 1, as was the minimum number of peptides.
For the SUMO chain detection on in-vitro SUMOylated CENP-T, the search was performed against an in silico digested Uniprot reference proteome for Homo Sapiens obtained from Uniprot.org (March 24th 2016). Database searches were performed with Trypsin/P allowing 3 missed cleavages. Maximum number of modifications per peptide was set to 3, with the following variable modifications: Carbamidomethyl (default), protein N-terminal acetylation (default) methionine oxidation (default), QQTGG modification on lysine and to facilitate the detection of pyroQQTGG (PyroQ) remnants on lysines, pyroQQTGG settings were imported into the Andromeda search engine[70]. Fast Label-free quantification (LFQ) was enabled with a LFQ minimal ratio count of 2, a LFQ minimal number of neighbors of 3 and 6 LFQ average number of neighbors. Match-between runs was enabled with a match time window of 0.7 min and an alignment time window of 20 min. A maximum peptide mass of 6000 Da was permitted. A first search with a peptide tolerance of 20 ppm was performed to determine a mass and time recalibration. A second search with a peptide tolerance of 4.5 ppm was performed as main search and the results were used for further analysis. Desired false discovery rates (FDRs) for peptide spectrum match (PSM) and protein level was set to 1%. A minimal score for modified peptides of 40 was applied, together with a minimal delta score for modified peptides of 6. For protein identification the minimum number of razor + unique peptide was set to 1, as was the minimum number of peptides.

Perseus data analysis

For identification of SENP6 regulated SUMOylated proteins, MaxQuant 'protein groups' output tables were subsequently filtered and statistically analyzed using the software package Perseus, version 1.5.0.31[42]. Proteins with potential incorrect identifications ('only identified by site' or 'reverse') were removed before the LFQ intensities were log2 transformed. Replicates of the same condition were grouped together. The data were filtered for protein groups which had at least three valid values in at least one group. Missing values were replaced by imputation using normally distributed values based on the total data matrix with a randomized 0.3 (log2) width and a 1.8 (log2) down shift. To obtain p values and log2 differences of the protein LFQ intensities in different conditions, a series of two-sided two samples t-tests were performed. Within the Supplementary Data 1 and 2, the header of each column for p values and log2 differences of LFQ intensities indicate the compared conditions. Putative SENP6 regulated SUMO targets were selected based on following criteria: 1) The protein LFQ intensity has a log2 difference of at least 1 (2-fold change) with

a -log10 p value of at least 1.3 ($p < 0.05$) in any of the His10-SUMO2 expressing conditions tested (two-sided t-test) against the parental condition (no His10-SUMO2 expression). 2) The protein LFQ intensity has a log2 difference of at least 1 with a -log10 p-value of at least 1.3 in both SENP6 knockdown conditions when tested (two-sided t-test) against the His10-SUMO expressing nontargeting control condition.
For the analysis of chromatin-associated proteins upon SENP6 knockdown, MaxQuant 'protein groups' output tables were subsequently filtered and statistically analyzed using the software package Perseus, version 1.5.2.4[42]. Proteins with potential incorrect identifications ('only identified by site' or 'reverse') were removed before the LFQ intensities were log2 transformed. Replicates of the same condition were grouped together. [the data were filtered for protein groups which had at least three valid values in at least one group.] Missing values were replaced by imputation using normally distributed values based on the total data matrix with a randomized 0.3 (log2) width and a 1.8 (log2) down shift. To obtain p values and log2 differences of the protein LFQ intensities in different conditions, a series of two-sided two samples t-tests were performed. In Supplementary Data 3, the header of each column for p values and log2 differences of LFQ intensities indicate the compared conditions. Putative SENP6 regulated chromatin components were selected based on the following criterium: The protein LFQ intensity has a log2 difference of at least 1 (2-fold change) with a -log10 p value of at least 1.3 ($p < 0.05$) in the SENP6 knockdown conditions tested (two-sided t-test) against the non-targeting control knockdown condition.

Gene ontology and STRING network analysis
Gene ontology analysis was performed using the gene ontology consortium web tool (www.geneontology.org). For the evaluation of enriched GO terms of the identified SENP6-regulated proteins the PATHER overrepresentation test (released 20171205) was used. The proteins were analysed for overrepresentation of PANTHER GO- Slim biological process, PANTHER GO- Slim cellular component and PANTHER GO-Slim molecular function terms using the Fischer exact test.
Network analysis of SENP6 regulated SUMO targets (Supplementary Data 2) was performed using the online STRING data base v10.5 (www.String-db.org) [71]. The following setting were applied: Output settings: high confidence interaction score (0.7), edges show protein connections based on textmining, experiments, databases, co-expression, neighborhood, co-occurrence and gene fusion. The network was subsequently exported as TVS (tab separated values) file and imported into Cytoscape version 3.6.1 for further visualization and network analysis. The cytoscape plugin MCODE (molecular complex detection) version 1.5.1 was used to identify highly connected sub-clusters of proteins using a degree cut off of 2, Cluster finding: haircut, a node score cut-off of 0.2, a K-core of 2 and a max depth of 100.

Immunostaining for microscopy
For immunostainings with CENP-T, GFP, CENP-A and SENP6 antibody, cells were grown on coverslips and fixed for 15 min with 4 % paraformaldehyde in PBS, briefly rinsed with PBS and permeabilized for 15 min at RT with 1x PBS containing 0.05 % Triton X-100. Cells were blocked for 15 min at RT in 0.1 M Tris-HCL pH 7.5, 0.15 M NaCl, 5 mg/ml Boehringer Blocking Reagent (TNB) and incubated with primary antibodies diluted in TNB for 1 hour. Cells were washed 4 times with PBS containing 0.05 % Tween-20. Secondary antibodies were diluted 1:500 in TNB and incubated for 30 min. Coverslips were washed 4x with 0.05 % Tween, 1x PBS and DNA was visualized using 10 mg/ml Hoechst diluted in 0.05 % Tween, 1x PBS.

Coverslips were subsequently mounted onto microscopy slides using CitiFluor mounting medium (Science Services, E17970-25). Antibodies and dilutions are listed in Supplementary Table 1.

Imaging and Image analysis

Images were acquired using a Leica SP8 confocal microscope. For foci quantification of mitotic cells, approximately 15-2 z-stacks were acquired at 0.2 µm steps and a final pixel size of 45 nm using a 63x objective, 1.4 Numerical aperture (NA). For foci quantification of interphase cells approximately 6-12 z-stacks were acquired at 0.2 µm steps and a final pixel size of 90 nm using a 63x, 1.4 Numerical aperture (NA) objective. Data were analyzed using Image J (Fiji) software. For the analysis of centromere foci, the area of the DNA was selected based on the Hoechst staining. Subsequently, centromere foci were identified by localization of local maxima using the find maxima function within the preselected area. The intensity of each foci was measured for 15 pictures per condition and biological replicate. Statistical significance was determined by two-sided t-tests. *$p \leq 0.05$; **$p \leq 0.01$; ***$p \leq 0.001$, ****$p \leq 0.0001$.

Purification of His10-SUMO-trimer binding proteins

Purification of His10-SUMO-trimer binding proteins was essentially performed as described before[64]. In brief, BL21 competent E. coli cells (New England Biolabs, Cat#C2527I) were transformed with pHIS-TEV30a:His10-ΔN11-SUMO2-trimer. When the bacterial culture reached an OD600 of 0.6, recombinant protein expression was induced overnight at 25 °C with 0.5 mM IPTG. Subsequently, cells were lysed in 50 mM HEPES pH7.6, 25 mM MgCl2, 0.5 M NaCl, 20 % glycerol, 0.1 % N-P40, 50 mM imidazole, 1 mM phenylmethanesulfonylfluoride (PMSF), and protease inhibitor cocktail without EDTA (Complete Mini protease inhibitor cocktail, Sigma-Aldrich, 11836170001). The His10-SUMO2-trimer was purified from lysate by incubation with Ni-NTA beads for 3 h at 4 °C. Beads were washed twice in lysis buffer including PMSF and protease inhibitor cocktail and twice in lysis buffer without PMSF and protease inhibitor cocktail. The His10-SUMO2-trimer was eluted with lysis buffer plus 500 mM imidazole for 10 min at 4 °C. The elution step was repeated three times. For the binding assay, His10-SUMO2-trimer was rebound to Ni-NTA beads. Five 15-cm dishes of U-2 OS cells per sample were lysed in 1 ml of 50 mM Tris pH 7.5, 150 mM NaCl, 0.5 % NP-40, 50 mM imidazole, sonicated and centrifuged at 20,000 × g for 1 h at 4 °C. The supernatant was incubated with recombinant His10-SUMO2-trimer bound to Ni-NTA beads for 2 h at 4 °C. As a control, U-2 OS lysates were incubated with Ni-NTA beads without His10-SUMO2-trimer. Samples were washed three times with 50 mM Tris pH 7.5, 150 mM NaCl, 0.5 % NP-40, 50 mM imidazole and three times with 50 mM Tris pH 7.5, 150 mM NaCl including tube changes. Binding partners of His10-SUMO2-trimer were eluted with 8 M urea in 50 mM Tris pH 7.5 for 30 min at room temperature and analysed by immunoblotting. Plasmids used are listed in Supplementary Table 2.

Statistics

Unless otherwise indicated, experiments were performed in biological triplicate. Results are presented as mean ± standard deviation. For FACS cell cycle progression analysis, p values were determined by multiple t-tests and corrected for multiple testing by applying the false discovery rate (FDR) by Benjamini, Krieger and Yekutieni. For mass spectrometry data, p values were determined using two-sided t-tests. For microscopy analysis of foci intensities p

values were determined using two-sided t-test. (* = $p < 0.05$, ** = $p < 0.01$, *** = $p < 0.001$, **** = $p < 0.0001$).

Data and software availability

All relevant data are available from the authors.

The mass spectrometry proteomics data have been deposited to the ProteomeXchange Consortium via the PRIDE partner repository with the dataset identifier PXD011963.

The source data underlying Figs 1b-f, 2b, c, 3a-f, 4a-c, 5a, b, 6a-c, 7a,b and 9a,b and Supplementary Figs 1a-d, 3a, b, 4a, b, 5a-g, 6a, b and 7b are provided as a Source Data file.

References

1. Hynes, N.E. *et al.* Signalling change: signal transduction through the decades. *Nat. Rev. Mol. Cell Biol.* **14**, 393-398 (2013).
2. Gareau, J.R. & Lima, C.D. The SUMO pathway: emerging mechanisms that shape specificity, conjugation and recognition. *Nat. Rev. Mol. Cell Biol.* **11**, 861-871 (2010).
3. Flotho, A. & Melchior, F. Sumoylation: a regulatory protein modification in health and disease. *Annu. Rev. Biochem.* **82**, 357-385 (2013).
4. Deribe, Y.L., Pawson, T. & Dikic, I. Post-translational modifications in signal integration. *Nat. Struct. Mol. Biol* **17**, 666-672 (2010).
5. Peng, J. *et al.* A proteomics approach to understanding protein ubiquitination. *Nat. Biotechnol.* **21**, 921-926 (2003).
6. Rieser, E., Cordier, S.M. & Walczak, H. Linear ubiquitination: a newly discovered regulator of cell signalling. *Trends Biochem. Sci.* **38**, 94-102 (2013).
7. Goldberg, A.L. Protein degradation and protection against misfolded or damaged proteins. *Nature* **426**, 895-899 (2003).
8. Xu, P. *et al.* Quantitative proteomics reveals the function of unconventional ubiquitin chains in proteasomal degradation. *Cell* **137**, 133-145 (2009).
9. Kulathu, Y. & Komander, D. Atypical ubiquitylation - the unexplored world of polyubiquitin beyond Lys48 and Lys63 linkages. *Nat. Rev. Mol. Cell Biol.* **13**, 508-523 (2012).
10. Psakhye, I. & Jentsch, S. Protein group modification and synergy in the SUMO pathway as exemplified in DNA repair. *Cell* **151**, 807-820 (2012).
11. Bekes, M. *et al.* The dynamics and mechanism of SUMO chain deconjugation by SUMO-specific proteases. *J. Biol. Chem.* **286**, 10238-10247 (2011).
12. Tatham, M.H. *et al.* Polymeric chains of SUMO-2 and SUMO-3 are conjugated to protein substrates by SAE1/SAE2 and Ubc9. *J. Biol. Chem.* **276**, 35368-35374 (2001).
13. Matic, I., Macek, B., Hilger, M., Walther, T.C. & Mann, M. Phosphorylation of SUMO-1 occurs in vivo and is conserved through evolution. *J. Proteome. Res.* **7**, 4050-4057 (2008).
14. Ulrich, H.D. The fast-growing business of SUMO chains. *Mol. Cell* **32**, 301-305 (2008).
15. Golebiowski, F. *et al.* System-wide changes to SUMO modifications in response to heat shock. *Sci. Signal* **2**, ra24 (2009).
16. Eisenhardt, N. *et al.* A new vertebrate SUMO enzyme family reveals insights into SUMO-chain assembly. *Nat. Struct. Mol. Biol.* **22**, 959-967 (2015).
17. Kumar, R., Gonzalez-Prieto, R., Xiao, Z., Verlaan-de Vries, M. & Vertegaal, A.C.O. The STUbL RNF4 regulates protein group SUMOylation by targeting the SUMO conjugation machinery. *Nat. Commun.* **8**, 1809 (2017).
18. Klug, H. *et al.* Ubc9 sumoylation controls SUMO chain formation and meiotic synapsis in Saccharomyces cerevisiae. *Mol. Cell* **50**, 625-636 (2013).
19. Li, S.J. & Hochstrasser, M. The yeast ULP2 (SMT4) gene encodes a novel protease specific for the ubiquitin-like Smt3 protein. *Mol. Cell Biol.* **20**, 2367-2377 (2000).
20. Cheng, C.H. *et al.* SUMO modifications control assembly of synaptonemal complex and polycomplex in meiosis of Saccharomyces cerevisiae. *Genes Dev.* **20**, 2067-2081 (2006).
21. Ryu, H.Y., Wilson, N.R., Mehta, S., Hwang, S.S. & Hochstrasser, M. Loss of the SUMO protease Ulp2 triggers a specific multichromosome aneuploidy. *Genes Dev.* **30**, 1881-1894 (2016).
22. Hickey, C.M., Wilson, N.R. & Hochstrasser, M. Function and regulation of SUMO proteases. *Nat. Rev. Mol. Cell Biol.* **13**, 755-766 (2012).
23. Mukhopadhyay, D. & Dasso, M. Modification in reverse: the SUMO proteases. *Trends Biochem. Sci* **32**, 286-295 (2007).
24. Choi, S.J. *et al.* Negative modulation of RXRalpha transcriptional activity by small ubiquitin-related modifier (SUMO) modification and its reversal by SUMO-specific protease SUSP1. *J. Biol. Chem.* **281**, 30669-30677 (2006).
25. Mukhopadhyay, D. *et al.* SUSP1 antagonizes formation of highly SUMO2/3-conjugated species. *J. Cell Biol.* **174**, 939-949 (2006).

26. Shen, L.N., Dong, C., Liu, H., Naismith, J.H. & Hay, R.T. The structure of SENP1-SUMO-2 complex suggests a structural basis for discrimination between SUMO paralogues during processing. *Biochem. J.* **397**, 279-288 (2006).
27. Lima, C.D. & Reverter, D. Structure of the human SENP7 catalytic domain and poly-SUMO deconjugation activities for SENP6 and SENP7. *J. Biol. Chem.* **283**, 32045-32055 (2008).
28. Alegre, K.O. & Reverter, D. Structural insights into the SENP6 Loop1 structure in complex with SUMO2. *Protein Sci* **23**, 433-441 (2014).
29. Hattersley, N., Shen, L., Jaffray, E.G. & Hay, R.T. The SUMO protease SENP6 is a direct regulator of PML nuclear bodies. *Mol. Biol. Cell* **22**, 78-90 (2011).
30. Mukhopadhyay, D. & Dasso, M. The fate of metaphase kinetochores is weighed in the balance of SUMOylation during S phase. *Cell Cycle* **9**, 3194-3201 (2010).
31. Sriramachandran, A.M. & Dohmen, R.J. SUMO-targeted ubiquitin ligases. *Biochim. Biophys. Acta* **1843**, 75-85 (2014).
32. Prudden, J. *et al.* SUMO-targeted ubiquitin ligases in genome stability. *EMBO J.* **26**, 4089-4101 (2007).
33. Sun, H., Leverson, J.D. & Hunter, T. Conserved function of RNF4 family proteins in eukaryotes: targeting a ubiquitin ligase to SUMOylated proteins. *EMBO J.* **26**, 4102-4112 (2007).
34. Uzunova, K. *et al.* Ubiquitin-dependent proteolytic control of SUMO conjugates. *J. Biol. Chem* **282**, 34167-34175 (2007).
35. Tatham, M.H. *et al.* RNF4 is a poly-SUMO-specific E3 ubiquitin ligase required for arsenic-induced PML degradation. *Nat. Cell Biol.* **10**, 538-546 (2008).
36. Weisshaar, S.R. *et al.* Arsenic trioxide stimulates SUMO-2/3 modification leading to RNF4-dependent proteolytic targeting of PML. *FEBS Lett.* **582**, 3174-3178 (2008).
37. Lallemand-Breitenbach, V. *et al.* Arsenic degrades PML or PML-RARalpha through a SUMO-triggered RNF4/ubiquitin-mediated pathway. *Nat. Cell Biol.* **10**, 547-555 (2008).
38. Hendriks, I.A. & Vertegaal, A.C. Label-Free Identification and Quantification of SUMO Target Proteins. *Methods Mol. Biol* **1475**, 171-193 (2016).
39. Hart, T. *et al.* High-Resolution CRISPR Screens Reveal Fitness Genes and Genotype-Specific Cancer Liabilities. *Cell* **163**, 1515-1526 (2015).
40. Fenech, M. *et al.* Molecular mechanisms of micronucleus, nucleoplasmic bridge and nuclear bud formation in mammalian and human cells. *Mutagenesis* **26**, 125-132 (2011).
41. Tyanova, S., Temu, T. & Cox, J. The MaxQuant computational platform for mass spectrometry-based shotgun proteomics. *Nat. Protoc.* **11**, 2301-2319 (2016).
42. Tyanova, S. *et al.* The Perseus computational platform for comprehensive analysis of (prote)omics data. *Nat. Methods* **13**, 731-740 (2016).
43. Szklarczyk, D. *et al.* The STRING database in 2017: quality-controlled protein-protein association networks, made broadly accessible. *Nucleic Acids Res.* **45**, D362-D368 (2017).
44. Bader, G.D. & Hogue, C.W. An automated method for finding molecular complexes in large protein interaction networks. *BMC. Bioinformatics* **4**, 2 (2003).
45. Nishino, T. *et al.* CENP-T-W-S-X forms a unique centromeric chromatin structure with a histone-like fold. *Cell* **148**, 487-501 (2012).
46. Rago, F., Gascoigne, K.E. & Cheeseman, I.M. Distinct organization and regulation of the outer kinetochore KMN network downstream of CENP-C and CENP-T. *Curr. Biol.* **25**, 671-677 (2015).
47. McKinley, K.L. *et al.* The CENP-L-N Complex Forms a Critical Node in an Integrated Meshwork of Interactions at the Centromere-Kinetochore Interface. *Mol. Cell* **60**, 886-898 (2015).
48. Banani, S.F. *et al.* Compositional Control of Phase-Separated Cellular Bodies. *Cell* **166**, 651-663 (2016).
49. Vogt, B. & Hofmann, K. Bioinformatical detection of recognition factors for ubiquitin and SUMO. *Methods Mol. Biol.* **832**, 249-261 (2012).
50. Johnson, E.S. & Blobel, G. Cell cycle-regulated attachment of the ubiquitin-related protein SUMO to the yeast septins. *J. Cell Biol* **147**, 981-994 (1999).
51. Peters, A.H. *et al.* Loss of the Suv39h histone methyltransferases impairs mammalian heterochromatin and genome stability. *Cell* **107**, 323-337 (2001).

52. Obuse, C. *et al.* A conserved Mis12 centromere complex is linked to heterochromatic HP1 and outer kinetochore protein Zwint-1. *Nat. Cell Biol.* **6**, 1135-1141 (2004).
53. Romeo, K. *et al.* The SENP7 SUMO-Protease Presents a Module of Two HP1 Interaction Motifs that Locks HP1 Protein at Pericentric Heterochromatin. *Cell Rep.* **10**, 771-782 (2015).
54. Maison, C. *et al.* The SUMO protease SENP7 is a critical component to ensure HP1 enrichment at pericentric heterochromatin. *Nat. Struct. Mol. Biol.* **19**, 458-460 (2012).
55. Garvin, A.J. *et al.* The deSUMOylase SENP7 promotes chromatin relaxation for homologous recombination DNA repair. *EMBO Rep.* **14**, 975-983 (2013).
56. Li, J. *et al.* Desumoylase SENP6 maintains osteochondroprogenitor homeostasis by suppressing the p53 pathway. *Nat. Commun.* **9**, 143 (2018).
57. Hoeijmakers, J.H. DNA damage, aging, and cancer. *N Engl. J. Med.* **361**, 1475-1485 (2009).
58. Dou, H., Huang, C., Singh, M., Carpenter, P.B. & Yeh, E.T. Regulation of DNA repair through deSUMOylation and SUMOylation of replication protein A complex. *Mol. Cell* **39**, 333-345 (2010).
59. Hori, T., Shang, W.H., Takeuchi, K. & Fukagawa, T. The CCAN recruits CENP-A to the centromere and forms the structural core for kinetochore assembly. *J. Cell Biol.* **200**, 45-60 (2013).
60. Falk, S.J. *et al.* Chromosomes. CENP-C reshapes and stabilizes CENP-A nucleosomes at the centromere. *Science* **348**, 699-703 (2015).
61. Cuijpers, S.A.G., Willemstein, E. & Vertegaal, A.C.O. Converging Small Ubiquitin-like Modifier (SUMO) and Ubiquitin Signaling: Improved Methodology Identifies Co-modified Target Proteins. *Mol. Cell. Proteomics* **16**, 2281-2295 (2017).
62. Hendriks, I.A. & Vertegaal, A.C. A comprehensive compilation of SUMO proteomics. *Nat. Rev. Mol. Cell Biol* **17**, 581-595 (2016).
63. Komander, D. & Rape, M. The ubiquitin code. *Annu. Rev. Biochem.* **81**, 203-229 (2012).
64. Eifler, K. *et al.* SUMO targets the APC/C to regulate transition from metaphase to anaphase. *Nat. Commun.* **9**, 1119 (2018).
65. He, X. *et al.* Probing the roles of SUMOylation in cancer cell biology by using a selective SAE inhibitor. *Nat. Chem. Biol.* **13**, 1164-1171 (2017).
66. DuBridge, R.B. *et al.* Analysis of mutation in human cells by using an Epstein-Barr virus shuttle system. *Mol. Cell Biol.* **7**, 379-387 (1987).
67. Burns, J.C., Friedmann, T., Driever, W., Burrascano, M. & Yee, J.K. Vesicular stomatitis virus G glycoprotein pseudotyped retroviral vectors: concentration to very high titer and efficient gene transfer into mammalian and nonmammalian cells. *Proc. Natl. Acad. Sci. U S A* **90**, 8033-8037 (1993).
68. Schimmel, J. *et al.* Uncovering SUMOylation Dynamics during Cell-Cycle Progression Reveals FoxM1 as a Key Mitotic SUMO Target Protein. *Mol. Cell* **53**, 1053-1066 (2014).
69. Rappsilber, J., Mann, M. & Ishihama, Y. Protocol for micro-purification, enrichment, pre-fractionation and storage of peptides for proteomics using StageTips. *Nat. Protoc.* **2**, 1896-1906 (2007).
70. Hendriks, I.A. & Vertegaal, A.C. A high-yield double-purification proteomics strategy for the identification of SUMO sites. *Nat. Protoc.* **11**, 1630-1649 (2016).
71. Szklarczyk, D. *et al.* STRING v10: protein-protein interaction networks, integrated over the tree of life. *Nucleic Acids Res.* **43**, D447-D452 (2015).

4

THE POLY-SUMO2/3 PROTEASE SENP6 ENABLES ASSEMBLY OF THE CONSTITUTIVE CENTROMERE-ASSOCIATED NETWORK BY GROUP-DESUMOYLATION

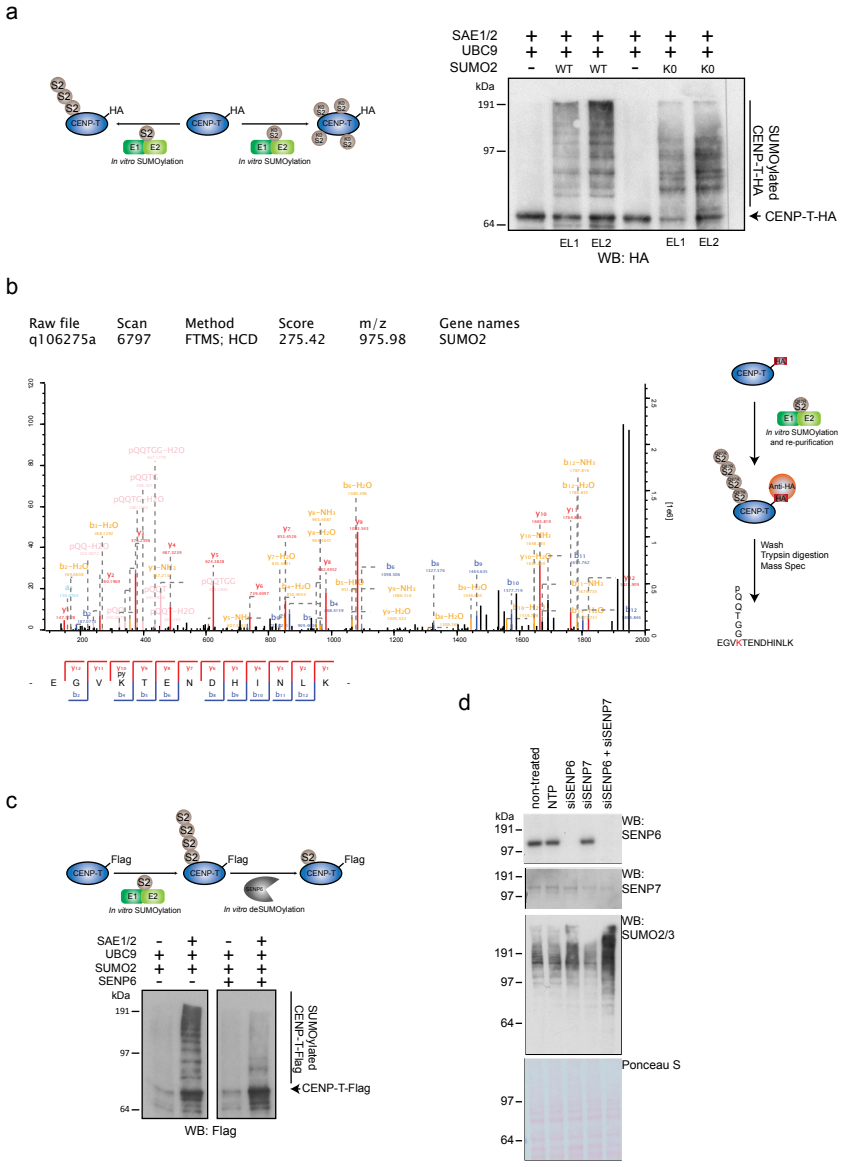

Supplementary Figure 1. SENP6 deSUMOylates poly-SUMO2/3 modified CENP-T. a CENP-T-HA was purified from cells and elutions one and two (EL1 and EL2) were *in vitro* SUMOylated with either recombinant SUMO2 WT or lysine-deficient SUMO2 (K0). CENP-T-HA was visualized by immunoblotting against the HA epitope. Unmodified CENP-T-HA is indicated by an arrow. Modification with SUMO2 WT but not with SUMO2 K0 led to high-molecular weight conjugates of CENP-T, indicating the presence of SUMO chains. **b** Purified CENP-T-HA was *in vitro* SUMOylated with recombinant Q87R SUMO2, re-purified, washed and trypsin digested. MS/MS spectrum representing pyroQQTGG modified K11-SUMO peptide identified by mass spectrometry. The presence of the branched peptide SUMO K11 - (pyro)QQTGG on the *in vitro* SUMOylated CENP-T indicates the presence of SUMO chains on CENP-T. **c** *In vitro* SUMOylated CENP-T-Flag was treated with recombinant SENP6. CENP-T-Flag was visualized by immunoblotting against the Flag epitope. Unmodified CENP-T-Flag is indicated by arrow. Recombinant SENP6 was able to efficiently deSUMOylate *in vitro* SUMOylated CENP-T. **d** U-2 OS cells were left untreated or transfected with either a pool of four siRNAs against SENP6 (siSENP6), SENP7 (siSENP7), a combination of both (siSENP6 + siSENP7) or a pool of four non-targeting siRNAs (NTP). Cell lysates were analysed two days post transfection by immunoblotting using antibodies against SENP6, SENP7 and SUMO2/3. Source data are provided as a Source Data file.

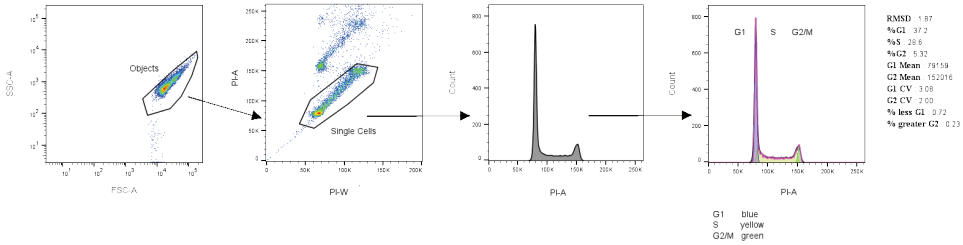

Supplementary Figure 2. Gating strategy for cell cycle analysis upon SENP6 knockdown.
Gating strategy underlying Fig. 1e. HeLa cells were treated with lentiviruses encoding shRNAs against SENP6 or a non-targeting control shRNA. Cells were fixed and prepared for flow cytometry analysis four days post infection.

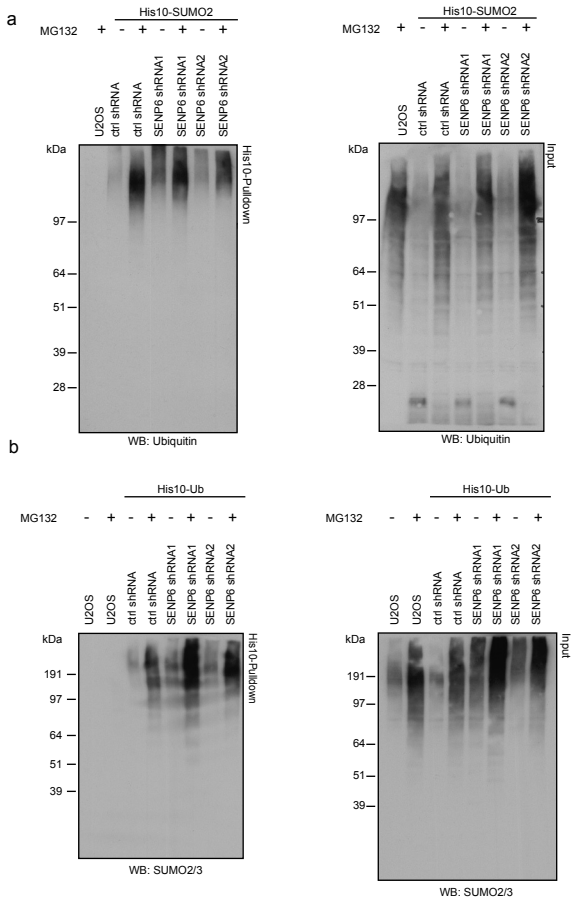

Supplementary Figure 3. SENP6 knockdown increases SUMO and ubiquitin co-modified substrates. a U-2 OS cells stably expressing His10-SUMO2 were infected with lentiviruses encoding shRNAs against SENP6 or a non-targeting control (ctrl) shRNA three days prior to lysis. Where indicated, cells were treated with 10 µM MG132 for 4 hours prior to lysis. Cells were lysed and SUMOylated proteins were enriched by means of Ni-NTA pulldown. Inputs and His10-purified samples were analysed by immunoblotting against ubiquitin. The observed increase of ubiquitin conjugates confirms efficient inhibition of the proteasome by MG132. **b** U-2 OS cells stably expressing His10-ubiquitin were treated as in (A). Input and His10-purified samples were analysed by immunoblotting against SUMO2/3. As expected, inhibition of the proteasome led to a global increase in SUMO conjugates. Source data are provided as a Source Data file.

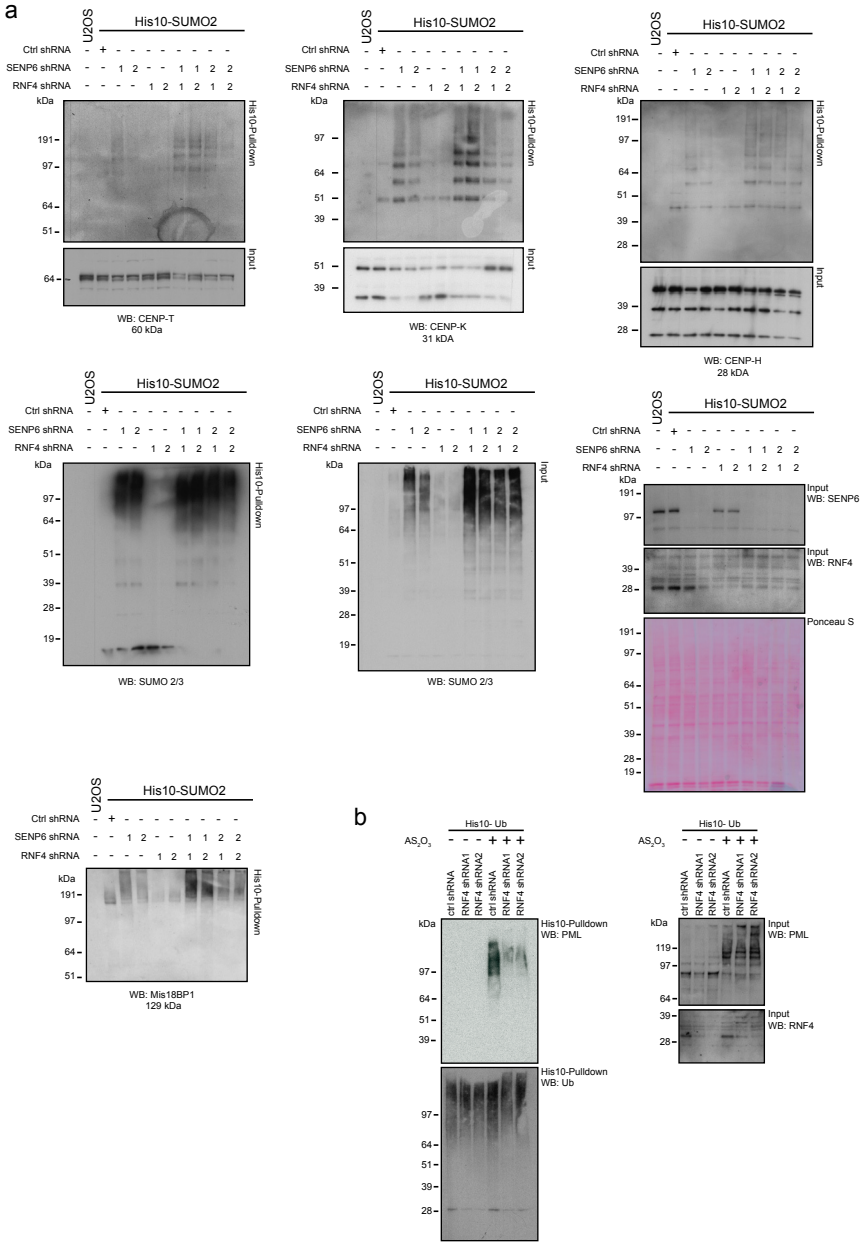

Supplementary Figure 4. SUMOylated CCAN subunits are not stabilized upon RNF4 knockdown. a U-2 OS cells stably expressing His10-SUMO2 were infected with lentiviruses encoding either one of the two shRNAs directed against SENP6 or against RNF4 or co-infected with a combination of one SENP6- and one RNF4-directed shRNA as indicated. Cells were lysed 3 days post infection and SUMOylated proteins were enriched by means of Ni-NTA pulldown. Inputs and His10-purified samples were analysed by immunoblotting against the indicated proteins. Compared to SENP6 depletion alone, co-depletion with RNF4 did not lead to a stabilization of SUMOylated CENP-T, CENP-K and CENP-H, but did lead to a stabilization of SUMOylated Mis18BP1. **b** U-2 OS cells stably expressing His10-ubiquitin were infected with lentiviruses encoding shRNAs directed against RNF4 or a control shRNA (ctrl) and lysed two days post infection. Where indicated, cells were treated with 1µM arsenic trioxide (AS_2O_3) four hours before lysis. Ubiquitinated proteins were enriched by means of Ni-NTA pulldown. Inputs and His10-purified samples were analysed by immunoblotting against the indicated proteins. PML ubiquitination is induced by AS_2O_3 in a RNF4-dependent manner, validating the shRNA-mediated RNF4 knockdown used. Source data are provided as a Source Data file.

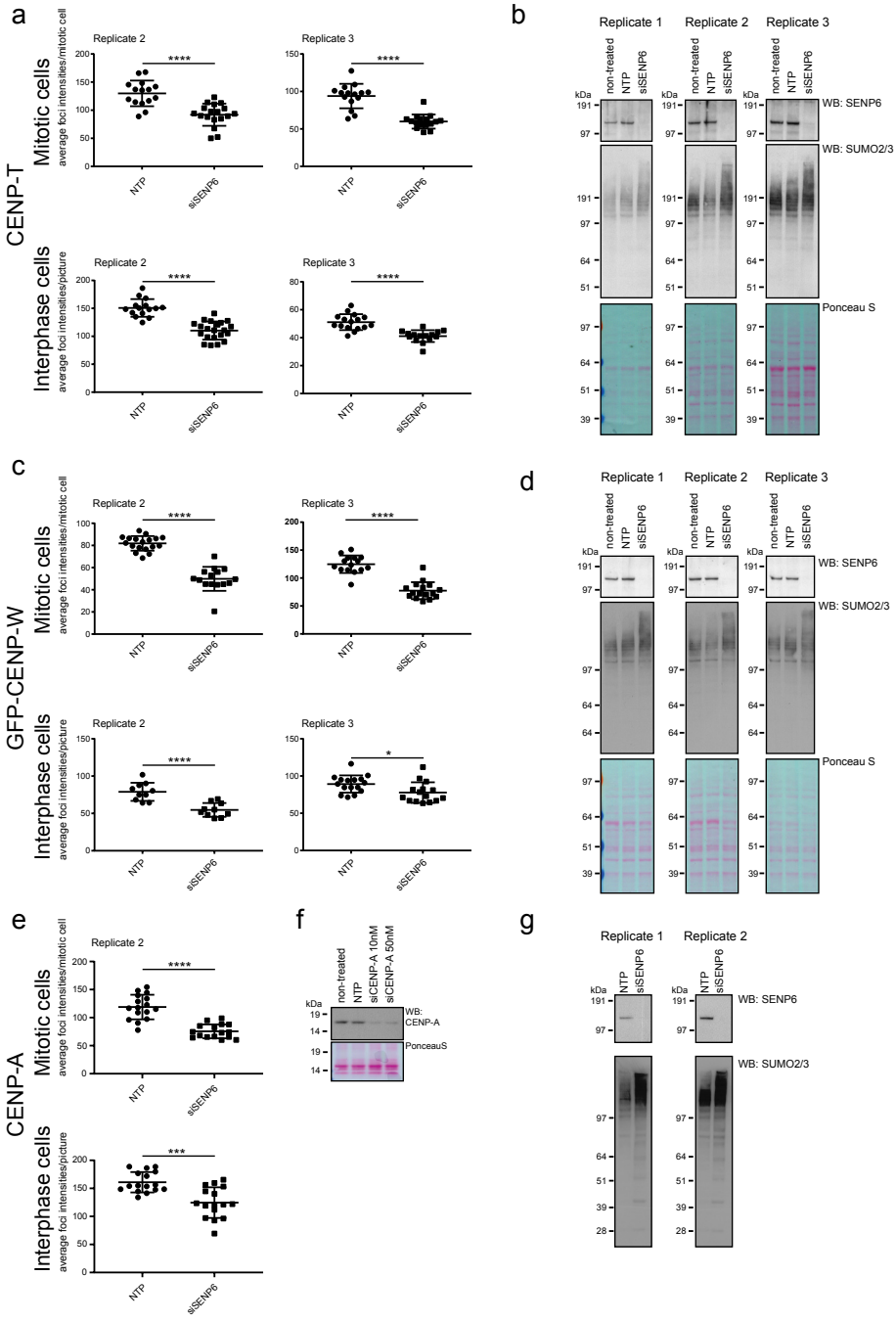
a
CENP-T
Mitotic cells
Interphase cells
average foci intensities/mitotic cell
average foci intensities/picture
Replicate 2
Replicate 3
NTP
siSENP6
b
Replicate 1
Replicate 2
Replicate 3
non-treated
NTP
siSENP6
kDa
WB: SENP6
WB: SUMO2/3
Ponceau S
c
GFP-CENP-W
d
e
CENP-A
f
siCENP-A 10nM
siCENP-A 50nM
WB: CENP-A
PonceauS
g

<Supplementary Figure 5. The Inner kinetochore proteins are less abundant at the centromere upon SENP6 knockdown. a Quantifications of replicate 2 and 3 of CENP-T foci analysis shown in Figure 6a. Scatterplots show quantification of the average CENP-T foci intensities per cell (mitotic cells) or per picture (interphase cells). A two-sided t-test was performed. ****p <0.0001. Replicate 2: n (NTP mitotic cells) = 15; n (siSENP6 mitotic cells) = 18; n (NTP interphase cells) = 15; n (siSENP6 interphase cells) = 21; Replicate 3: n (NTP mitotic cells) = 15; n (siSENP6 mitotic cells) = 16; n (NTP interphase cells) = 16; n (siSENP6 interphase cells) = 15. **b** Immunoblot analysis of non-treated cells or cells treated with a pool of four siRNAs against SENP6 (siSENP6) or a pool of four non-targeting siRNAs (NTP), confirming efficient SENP6 knockdown leading to high-molecular weight SUMOylated proteins. Cells were set up and treated in parallel to cells used in (**a**) and Figure 6a. Loading was verified by Ponceau S staining. **c** Quantifications of replicate 2 and 3 of CENP-W foci analysis shown in Figure 6b. Scatterplots show quantification of the average CENP-W foci intensities per cell (mitotic cells) or per picture (interphase cells). A two-sided t-test was performed. ****p <0.0001, *p <0.05. Replicate 2: n (NTP mitotic cells) = 18; n (siSENP6 mitotic cells) = 15; n (NTP interphase cells) = 10; n (siSENP6 interphase cells) = 10; Replicate 3: n (NTP mitotic cells) = 15; n (siSENP6 mitotic cells) = 16; n (NTP interphase cells) = 16; n (siSENP6 interphase cells) = 15. **d** Immunoblot analysis of non-treated cells or cells treated with a pool of four siRNAs against SENP6 (siSENP6) or a pool of four non-targeting siRNA (NTP), confirming efficient SENP6 knockdown leading to high-molecular weight SUMOylated proteins. Cells were set up and treated in parallel to cells used in (**c**) and Figure 6b. Loading was verified by Ponceau S staining. **e** Quantifications of replicate 2 of CENP-A foci analysis shown in Figure 6c. Scatterplots show quantification of the average CENP-T foci intensities per cell (mitotic cells) or per picture (interphase cells). A two-sided t-test was performed. ****p <0.0001. Replicate 2: n (NTP mitotic cells) = 16; n (siSENP6 mitotic cells) = 16; n (NTP interphase cells) = 16; n (siSENP6 interphase cells) = 16. **f** U-2 OS cells were either left untreated or treated with a pool of four non-targeting siRNAs (NTP) or a pool of four siRNA targeting CENP-A (siCENP-A). Cells were lysed two days post transfection and lysates were analysed by immunoblotting with antibodies against CENP-A. CENP-A antibody signal is reduced in cells treated with siCENP-A, validating the specificity antibody. **g** Immunoblot analysis cells treated with a pool of four siRNAs against SENP6 (siSENP6) or a pool of four non-targeting siRNA (NTP), confirming efficient SENP6 knockdown leading to high-molecular weight SUMOylated proteins. Cells were set up and treated in parallel to cells used in (**e**) and Figure 6c. Source data are provided as a Source Data file. All Error bars shown represent standard deviations.

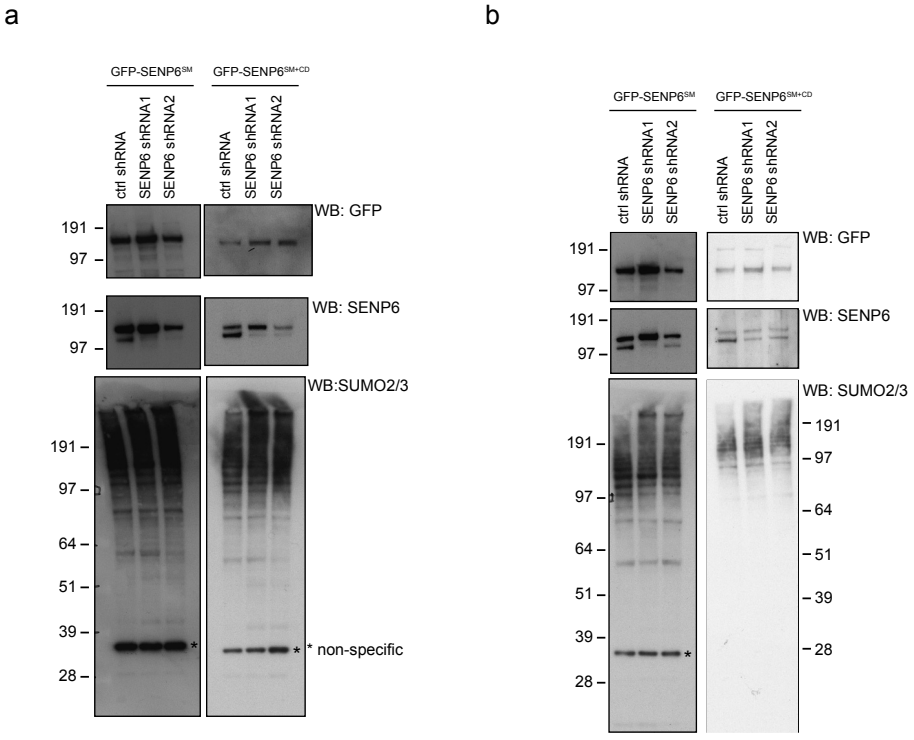

Supplementary Figure 6. Knockdown of SENP6 can be rescued by re-introduction of wild-type SENP6, but not by re-introduction of catalytic dead SENP6. a and **b** U-2 OS cells stably expressing inducible shRNA-resistant (SM) GFP-tagged wild-type or catalytic dead (CD) SENP6 were established. Expression of these constructs was induced by Doxycycline for 24 hours prior to transduction with lentiviruses encoding SENP6 shRNAs. Medium was replaced one day post infection. The next day, cells were seeded in 12-well plates and grown overnight. Subsequently, cells were lysed and immunoblotting was performed using antibodies against GFP, SENP6 and SUMO2/3 to verify knockdown and rescue. * indicates a non-specific band. Results of the first replicate are shown in **a** and results of the second replicate are shown in **b**. Source data are provided as a Source Data file.

a

SIMa : (PILVM)-(ILVM)-X-(ILVM)-(DSE)(3)
SIMb : (PILVM)-(ILVM)-D-L-T
SIMr : (DSE)(3)-(ILVM)-X-(ILVMF)(2)

Protein	SIMa	SIMb	SIMr
CENP-C	No	No	932-938 EESVLLF
CENP-K	No	No	204-210 ESSVNLI
CENP-I	No	No	106-112 SEEIDIL
CENP-P	No	No	64-70 ESELSFL

b

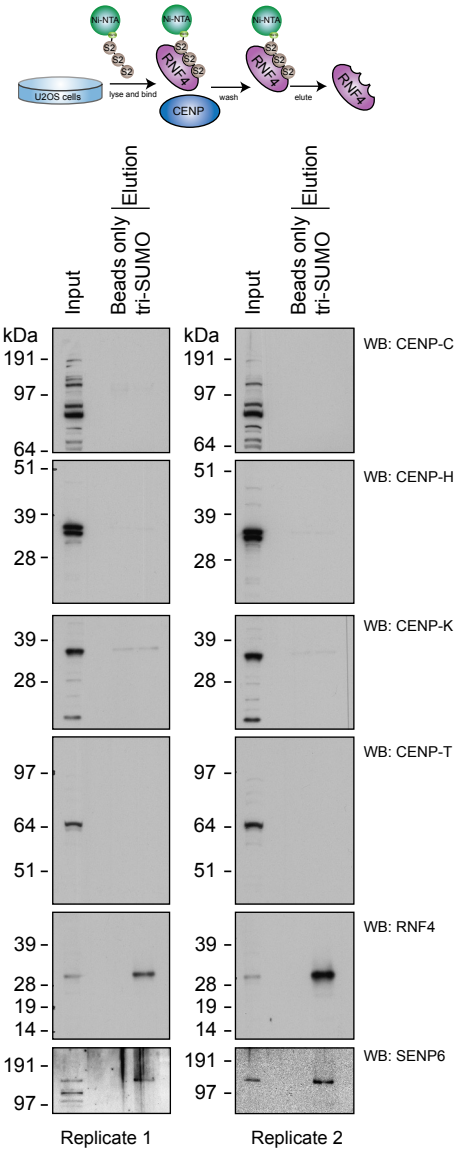

Supplementary Figure 7 CCAN proteins are unable to bind SUMO trimer. a Three predicted SUMO interaction motifs (SIMs) are defined by a stretch of hydrophobic residues (P,I,L,V or M) either followed or preceded by acidic residues (D or E) and residues which can be phosphorylated (S or T). The table shows the presence of SIMs within the 16 CCAN subunits. Only four CCAN subunits (CENP-C, -K, -I and -P) contain sequence-defined predicted SIMs. Subunits, location and sequences of predicted SIMs are listed. **b** His10-SUMO2-trimer binding proteins were purified from U-2 OS lysates and subsequently analysed by immunoblotting against the indicated proteins. Selected CENPs do not bind to recombinant SUMO-trimer. RNF4 and SENP6 were included as positive controls. Source data are provided as a Source Data file.

CHAPTER 5

Transcription-Coupled Nucleotide Excision Repair is Coordinated by Ubiquitin and SUMO in Response to Ultraviolet Irradiation

Frauke Liebelt[1], Joost Schimmel[1,2], Matty Verlaan – de Vries[1], Esra Klemann[1], Martin E. van Royen[3], Yana van der Weegen[2], Martijn S. Luijsterburg[2], Leon H. Mullenders[2,4], Alex Pines[5], Wim Vermeulen[5], Alfred C.O. Vertegaal[1]

[1]Department of Cell and Chemical Biology, Leiden University Medical Center, Einthovenweg 20, Leiden, 2333 ZC, the Netherlands.

[2]Department of Human Genetics, Leiden University Medical Center, Einthovenweg 20, Leiden, 2333 ZC, the Netherlands.

[3]Department of Pathology, Cancer Treatment Screening Facility (CTSF), Erasmus Optical Imaging Centre (OIC), Erasmus University Medical Center, Wytemaweg 80, 3015 CN, Rotterdam, The Netherlands

[4]Department of Genetics, Research Institute of Environmental Medicine (RIeM), Nagoya University, Japan

[5]Department of Molecular Genetics, Oncode Institute, Erasmus MC, University Medical Center Rotterdam, Dr Molewaterplein 40, 3015 GD, Rotterdam, The Netherlands.

Accepted for publication in *Nucleic Acid Research*

ABSTRACT

Cockayne Syndrome (CS) is a severe neurodegenerative and premature aging autosomal-recessive disease, caused by inherited defects in the *CSA* and *CSB* genes, leading to defects in transcription-coupled nucleotide excision repair (TC-NER) and consequently hypersensitivity to UV irradiation. TC-NER is initiated by lesion-stalled RNA polymerase II, which stabilizes the interaction with the SNF2/SWI2 ATPase CSB to facilitate recruitment of the CSA E3 Cullin ubiquitin ligase complex. However, the precise biochemical connections between CSA and CSB are unknown. The small ubiquitin-like modifier SUMO is important in the DNA damage response. We found that CSB, among an extensive set of other target proteins, is the most dynamically SUMOylated substrate in response to UV irradiation. Inhibiting SUMOylation reduced the accumulation of CSB at local sites of UV irradiation and reduced recovery of RNA synthesis. Interestingly, CSA is required for the efficient clearance of SUMOylated CSB. However, subsequent proteomic analysis of CSA-dependent ubiquitinated substrates revealed that CSA does not ubiquitinate CSB in a UV-dependent manner. Surprisingly, we found that CSA mediates the ubiquitination of the large subunit of RNA polymerase II, RPB1 directly or indirectly. Combined, our results indicate that the CSA, CSB, RNA polymerase II triad is coordinated by ubiquitin and SUMO in response to UV irradiation. Furthermore, our work provides a resource of SUMO targets regulated in response to UV or Ionizing Radiation.

INTRODUCTION

The integrity of DNA is continuously challenged by exogenous and endogenous DNA-damaging agents, such as genotoxic chemicals, ionizing radiation (IR), ultraviolet radiation (UV) or reactive oxygen species (ROS)[1]. A multitude of cellular mechanisms collectively called the DNA damage response (DDR), ensure efficient response to genotoxic insults including recognition and repair of DNA lesions. IR induces a set of different types of DNA damage, including oxidized bases, single and double strand breaks (DSBs). The latter are among the most cytotoxic DNA lesions and are repaired by homologous recombination (HR), non-homologous end-joining (NHEJ) and alternative end-joining (Alt-EJ)[2-4].

UV induces cyclobutane pyrimidine dimers (CPD), a photolesion with mild helix- distorting properties and 6-4 photoproducts (6-4PP), a photolesion with strong helix distorting properties, that both strongly interfere with DNA transacting processes. In human skin cells CPDs and 6-4PPs are exclusive removed by nucleotide excision repair (NER). UV-induced photolesions in the transcribed strand of actively transcribed regions are repaired by transcription-coupled NER (TC-NER), whereas CPDs and 6-4PPs localized throughout the genome are repaired by global genome NER (GG-NER)[5]. TC-NER and GG-NER differ in the molecular recognition of the DNA lesion, but share the subsequent steps, including lesion verification, excision of 22-30 nucleotides around the lesion and gap filling by DNA synthesis. Proteins that are involved in DNA repair pathways need to be tightly regulated to avoid inappropriate DNA processing. Post-translational modifications like phosphorylation, PARylation, ubiquitination and SUMOylation play pivotal roles in this regulation[6].

Small Ubiquitin-like MOdifier (SUMO) is a 11 kDa protein that can be covalently attached to lysine residues in substrate proteins via an enzymatic cascade, involving a heterodimeric SUMO activating E1 enzyme, a single SUMO conjugating E2 enzyme and a limited number of SUMO E3 ligases[7]. SUMOylation is a highly dynamic process due to the presence of SUMO specific proteases that can reverse the SUMOylation of target proteins[8]. Mammals express at least three SUMO family members, SUMO1-3, with SUMO2 being the most abundant and essential member[9]. Hundreds of target proteins are regulated by SUMO under both normal and cellular stress conditions[10]. The consequences of SUMOylation are specific for different target proteins and can include the alteration of interactions with other proteins, the alteration of enzymatic activity, or influencing substrate stability.

The first link between SUMOylation and DNA repair was revealed in studies on Base Excision Repair (BER), where SUMOylation induces a conformational change in the Thymine-DNA glycosylase protein and thereby stimulates the repair process[11,12]. Furthermore, two SUMO E3 ligases, PIAS1 and PIAS4, accumulate at DSBs. These E3 ligases SUMOylate BRCA1 to induce its activity and SUMOylation is required for the accumulation of different repair components to facilitate repair of DSBs[13].

SUMO and ubiquitin also act together in the DDR, best exemplified by the modification of the homo-trimeric, ring shaped protein Proliferating Cell Nuclear Antigen (PCNA). PCNA encircles DNA where it acts as a processing factor for DNA polymerases and as an interaction platform for proteins involved in DNA metabolism. Mono-ubiquitination of PCNA on lysine 164 upon DNA damage induces the recruitment of polymerases needed for translesion synthesis, whereas SUMOylation on the same lysine inhibits recombination during DNA synthesis by recruiting the anti-recombinogenic helicase Srs2[14,15]. The role of SUMO and ubiquitin crosstalk in DNA repair was further emphasized by the observation that the SUMO-dependent recruitment of RNF4, a well-studied SUMO-targeted ubiquitin ligase (STUbL), to

DSBs induces a ubiquitination signal that is essential for efficient repair of DSBs[16,17].
RNF111, another STUbL, was shown to regulate the ubiquitination of XPC in GG-NER. XPC is part of the GG-NER initiating XPC-RAD23-CETN2 DNA damage recognizing complex. RNF111-mediated XPC ubiquitination is required for efficient progression of the NER reaction by stimulating the handover between XPC and the structure specific endonucleases XPG and ERCC1/XPF[18-20].
Ubiquitin also plays a pivotal role in the regulation of TC-NER. Two key factors in TC-NER are Cockayne Syndrome (CS) gene products CSA and CSB. CS is an autosomal-recessive disease and patients display severe neurodegenerative and premature aging. CSA- and CSB-deficient cells are both impaired in TC-NER and consequently hypersensitive to UV irradiation. TC-NER is initiated by stalling of RNA polymerase II at lesions, stabilizing the interaction with the SNF2/SWI2 ATPase CSB to facilitate recruitment of the CSA protein. CSA is part of an E3 Cullin ubiquitin ligase complex. CSA was proposed to ubiquitinate and destabilize CSB[21]. UVSSA, a more recently identified player in TC-NER, was shown to counteract this CSA-dependent destabilization of CSB by recruiting the deubiquitinating enzyme USP7[22,23]. Additionally, the UV-induced ubiquitination of the elongating RNA polymerase II (RNAPIIo) is dependent on UVSSA[24]. Collectively, these data indicate a pivotal role for post-translational modifications during the DNA damage response.
Here we set out to investigate potential biochemical connections between CSA and CSB. In our hands, CSA did not act as a ubiquitin E3 ligase for CSB in a UV-regulated manner. In contrast, we found that the ubiquitination of RNAPIIo is regulated by the CSA complex in response to UV. Furthermore, we found that CSB is the most strongly regulated substrate for the ubiquitin-like protein SUMO2 in response to UV. Clearance of SUMOylated CSB was dependent on CSA. Our data indicate that SUMOylated CSB, CSA and ubiquitinated RNAPIIo are connected and function together to promote efficient TC-NER.

RESULTS

Identification of SUMOylated proteins in response to IR- or UV-induced DNA damage

We set out to identify dynamic SUMO2 target proteins that are involved in the DDR, employing an unbiased quantitative proteomics approach that we previously developed[25]. We have focussed on SUMO2 since this is the most abundant mammalian SUMO family member[26]. Proliferating U-2 OS cells stably expressing His10-SUMO2 were irradiated with either 20 J/m^2 UV-light or 4 Gy of IR or mock treated (untreated control). Moreover, parental U-2 OS cells were irradiated with either UV or IR as control for a-specific binding to the Ni-NTA beads. Parental U-2 OS cells were lysed after 1 h recovery upon DNA damage induction and U-2 OS His10-SUMO2 cells were lysed after 1 h or 6 h recovery upon DNA damage induction. SUMOylated proteins were subsequently purified, trypsin digested and peptides were analysed by mass spectrometry (Figure 1A). We verified the SUMO enrichment efficiency by immunoblotting (Figure 1B).

Label free quantification of proteins that were identified by mass spectrometry revealed 513 putative SUMO targets (Table S1). Strikingly, significantly more proteins were modified by SUMO in response to UV compared to IR. After 1 h recovery post-UV irradiation we identified 30 proteins that were enhanced for SUMOylation compared to the mock treated control and this number increased to 58 proteins at 6 h recovery post-UV irradiation. 21 proteins showed enhanced SUMOylation after 1 h recovery post-IR and after 6 h recovery post-IR as few as 5 proteins showed increased SUMOylation compared to the mock treated control (Figure 1C, Table S2). The DNA damage checkpoint protein MDC1 was identified as SUMO target protein in all conditions (Figure 1D and 1E), in line with earlier observations[27] and thus served as a positive control. XPC SUMOylation in response to UV (Figure S1) likewise served as a positive control[18].

We also observed that 41 out of 58 proteins that showed increased SUMOylation 6 h after UV irradiation were neither SUMOylated after 1 h recovery upon UV damage nor in response to IR induced damages (Figure 1E, Table S2), showing that they were specifically targeted for SUMOylation at a later time point after UV damage. Our data demonstrate that UV-induced DNA lesions activate a unique and more pronounced SUMOylation response compared to IR, indicating important roles of SUMOylation during cellular responses to UV lesions at early and later stages.

STRING network analysis of SUMOylation targets identified after 6 h recovery upon UV irradiation, revealed interconnected groups of proteins. We identified functional clusters of proteins involved in the DNA damage response, transcription, the SUMO pathway, ribosomal biogenesis and RNA processing. Interestingly, amongst the proteins associated with transcription we identified multiple components of the TFIID basal transcription factor complex (Figure 1F, Table S2).

UV-induced SUMOylation of CSB is dependent on transcription and located at the N-terminus

The most dynamic SUMO2 target protein that we identified was CSB, showing a massive ~1000-fold increase in SUMOylation specifically upon UV-induced damage at both recovery time points, but not in response to IR (Figure 1D). Since CSB is a crucial player in the TC-NER pathway, we chose to investigate the role of CSB SUMOylation in more detail. Since UV is known to strongly inhibit transcription elongation whereas IR hardly does, it is likely that particularly lesion-stalled transcription complexes trigger CSB SUMOylation. We explored

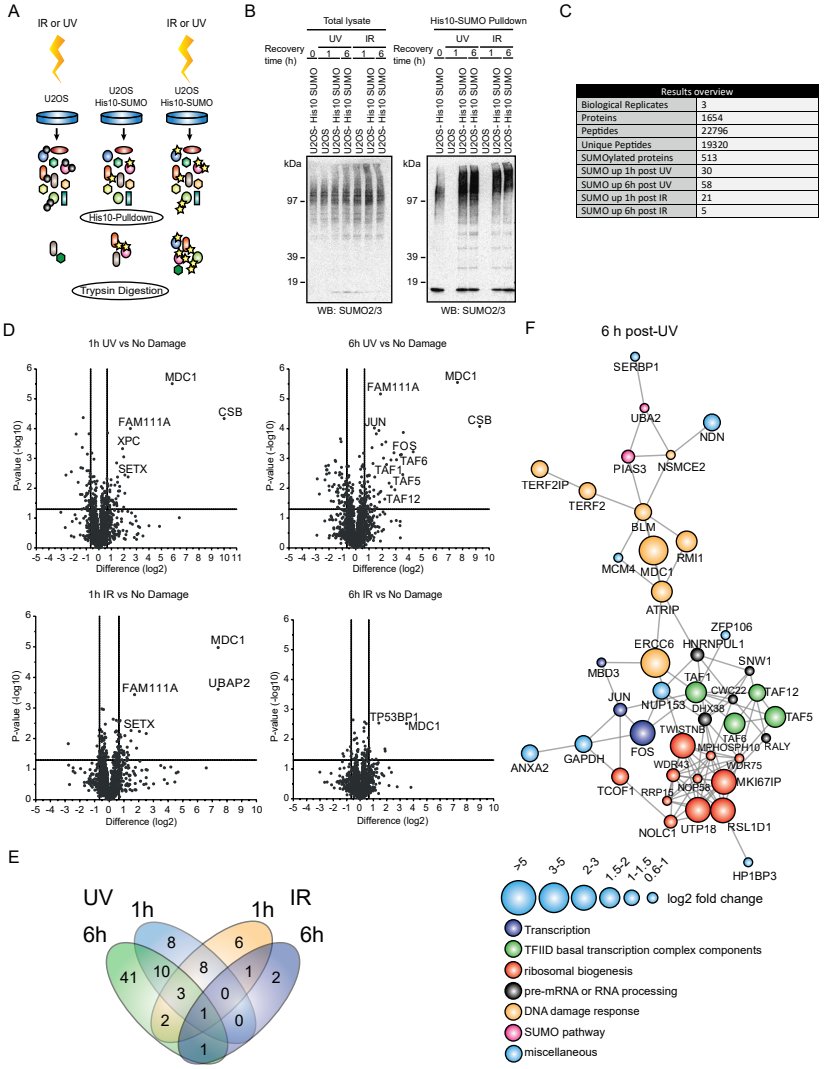

Figure 1. Identification of SUMOylated proteins in response to IR- or UV-induced DNA damage. (**A**) Experimental set-up. U-2 OS cells stably expressing His10-SUMO2 or parental cells were irradiated with ultraviolet light (UV) (20 J/m^2), Ionizing radiation (IR) (4 Gy) or were mock treated. Cells were lysed 1 h or 6 h after DNA damage induction and SUMOylated proteins were purified by means of Ni-NTA pulldown. Purified proteins were trypsin digested and peptides were analysed by mass spectrometry. (**B**) Total lysates and His10-SUMO2 purified fractions were analysed by immunoblotting using a specific antibody against SUMO2/3. (**C**) The experiment, as described in (A) was performed in triplicate and protein groups were selected. SUMOylated proteins required a minimal fold change of 1.5 with a *p*-value <0.05 in at least one of the U-2 OS His10-SUMO2 conditions compared to the parental control. SUMO targets after 1 h or 6 h IR or UV damage required a minimal fold change of 1.5 with a *p*-value lower than 0.05 compared to the His10-SUMO2 expressing mock treated control. (**D**) Volcano plots showing all identified proteins. Dashed lines indicate cut-off of 1.5-fold change (log2 of 0.66) and a *p*-value of 0.05 (–log10 of 1.3). Selected SUMO targets are marked in a red and display a label. (**E**) Venn diagram showing overlap of SUMO2 targets in different conditions. (**F**) Protein interaction network based on the STRING database showing connections between SUMO2 targets identified 6 h after UV irradiation with a medium confidence level of 0. 4. Increased node size represents increased log2 fold change in LFQ intensities relative to mock treated control. Colours of nodes indicate main functional groups.

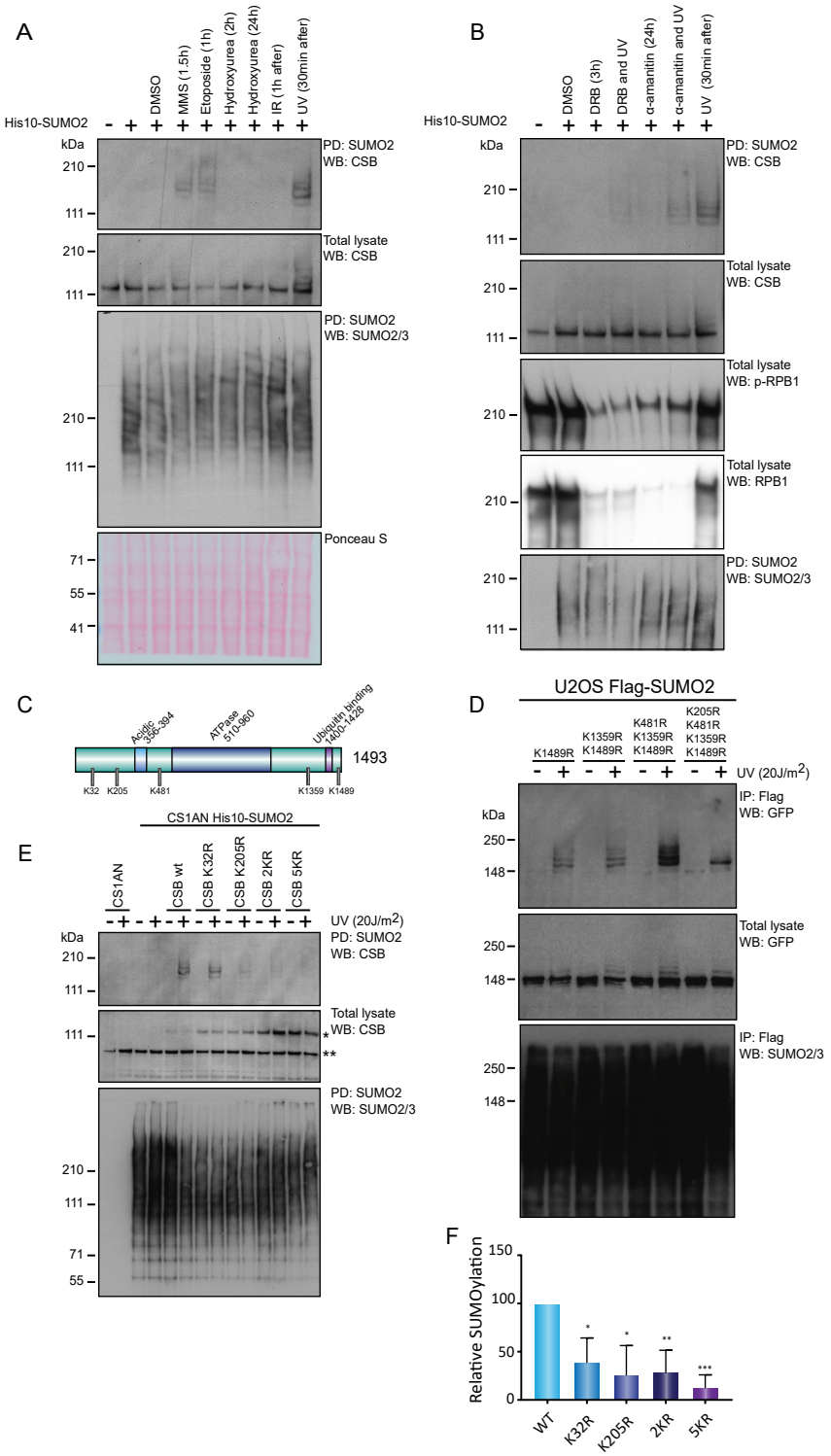
A
His10-SUMO2
DMSO
MMS (1.5h)
Etoposide (1h)
Hydroxyurea (2h)
Hydroxyurea (24h)
IR (1h after)
UV (30min after)
kDa
PD: SUMO2
WB: CSB
Total lysate
WB: CSB
PD: SUMO2
WB: SUMO2/3
Ponceau S
B
DRB (3h)
DRB and UV
α-amanitin (24h)
α-amanitin and UV
Total lysate
WB: p-RPB1
Total lysate
WB: RPB1
C
Acidic
395-394
ATPase
510-960
Ubiquitin binding
1400-1426
1493
K32
K205
K481
K1359
K1489
D
U2OS Flag-SUMO2
K1489R
K1359R
K1489R
K481R
K1359R
K1489R
K205R
K481R
K1359R
K1489R
UV (20J/m2)
IP: Flag
WB: GFP
Total lysate
WB: GFP
IP: Flag
WB: SUMO2/3
E
CS1AN His10-SUMO2
CS1AN
CSB wt
CSB K32R
CSB K205R
CSB 2KR
CSB 5KR
UV (20J/m2)
PD: SUMO2
WB: CSB
Total lysate
WB: CSB
PD: SUMO2
WB: SUMO2/3
F
Relative SUMOylation
WT
K32R
K205R
2KR
5KR

<Figure 2. UV-induced SUMOylation of CSB is dependent on transcription and located at the N-terminus. (**A**) U-2 OS cells stably expressing His10-SUMO2 were left untreated or were treated with either DMSO, or 0.02 % MMS, 50 μM etoposide, 2 mM hydroxyurea, 4 Gy IR or 20 J/m^2 UV. Times indicate treatment period of cells with the compound before lysis. For IR and UV treated cells, times represent recovery period after treatment. SUMO2 conjugates were enriched by Ni-NTA pulldown (PD). Total lysates and SUMO2-enriched fractions were analysed by immunoblotting using antibodies against CSB or SUMO2/3. MMS, methyl methanesulfonate; IR, Ionizing radiation; UV, ultraviolet light irradiation. (**B**) U-2 OS cells stably expressing His10-SUMO2 were treated with DRB or α-amanitin and/or UV irradiation (20 J/m^2). Times indicate treatment period with the compound before lysis. For irradiation, these times indicate recovery period after irradiation prior to lysis. For DRB and UV irradiated sample, cells were treated with DRB 3 h prior to UV irradiation and lysed 30 min after the UV treatment. For α-amanitin and UV irradiated samples, cells were treated 24 h prior to UV irradiation and lysed 30 min after UV treatment. SUMO2 conjugates were enriched by Ni-NTA pulldown. Total lysates and SUMO2-enriched fractions were analysed by immunoblotting using antibodies against CSB, p-RPB1 (S2/S5), RPB1, or SUMO2/3. DRB, 5,6-dichloro-1-beta-D-ribofuraosylbenzimidazole. (**C**) Schematic overview of CSB including known domains and localization of SUMOylation consensus sites (ψKXE). (**D**) U-2 OS cells stably expressing Flag-SUMO2 were infected with retroviruses encoding different SUMOylation consensus site mutants of GFP-CSB, as indicated. Cells were treated with UV irradiation (20 J/m^2) and lysed after 1 h recovery. SUMO2 conjugates were enriched by Flag IP. Total lysates and SUMO2-enriched fractions were analysed by immunoblotting using antibodies against GFP or SUMO2/3. (**E**) CS1AN cells stably expressing His10-SUMO2 were infected with lentiviruses encoding different CSB SUMOylation consensus site mutants. Cells were treated with UV irradiation (20 J/m^2) and lysed after 30 min recovery. SUMO2 conjugates were enriched by Ni-NTA pulldown. Total lysates and SUMO2-enriched fractions were analysed by immunoblotting using antibodies against CSB or SUMO2/3. * marks the exogenously expressed CSB construct. ** marks the CSB-piggyBac transposable element derived 3 fusion (CPFP)[59]. K32, 205R (2KR); K32, 205, 481, 1359, 1489R (5KR). (**F**) Quantification of (E). Relative amount of SUMOylated CSB was determined based on immunoblots. Intensities were corrected for exogenous CSB expression levels (see * in Figure 2E) and protein loading as determined by expression of CPFP (** in Figure 2E) and Ponceau S stain. Values were normalized to CSB WT SUMOylation. Error bars represent SD of the mean obtained from three independent experiments *p-value <0.05; ** p-value <0.01; *** p-value <0.001 (two-sided).

a wider range of DNA-damaging agents for their ability to induce CSB SUMOylation and found that SUMOylation of CSB is also induced by methyl methanesulfonate (MMS) and etoposide in addition to UV (Figure 2A). Etoposide is also an inhibitor of transcription elongation and consistently induced CSB SUMOylation (Figure 2A). Furthermore, MMS induced CSB SUMOylation, which could indicate that the concentration and duration of the MMS treatment likewise resulted in stalling of transcription. These agents also induce transcription-blocking DNA lesions that can be repaired by TC-NER[28,29]. Other types of DNA lesions like hydroxyurea-induced replication stress or IR-induced double strand breaks (DSBs), did not stimulate the SUMOylation of CSB (Figure 2A).

Subsequently, we tested whether CSB SUMOylation was dependent on active transcription and on the stalling of RNAPIIo at the lesion. To evaluate this, we treated U-2 OS His10-SUMO2 cells with 5,6-Dichlorobenzimidazole 1-β-D-ribofuranoside (DRB) or α-amanitin, two potent inhibitors of RNAPII[30], prior to induction of DNA lesions by UV irradiation. α-amanitin interferes with a conformational change of RPB1 underlying the transcription mechanism; therefore, it inhibits elongation. DRB inhibits CDK-Activating Kinase (CAK), which is associated with TFIIH, thereby blocks transcription initiation. DRB treatment reduced phosphorylated RPB1 (p-RPB1) and total RPB1 as expected and the reduction in p-RPB1 in response to α-amanitin is due to a striking reduction in total amount of RPB1 (Figure 2B). We observed that UV-induced SUMOylation of CSB was decreased in cells that were pre-treated with these inhibitors. Blocking either initiation or elongation of transcription did itself not result in CSB SUMOylation (Figure 2B), indicating that transcription and the stalling of RNAPII at the lesion is a prerequisite for CSB SUMOylation.

In order to investigate the role of CSB SUMOylation during the UV response we aimed

to identify the SUMO target lysines of CSB. CSB is a 1493 aa protein that includes five lysines embedded in SUMOylation consensus motifs, which are characterized by a large hydrophobic residue (ψ) upstream, and a glutamic acid two positions downstream of the lysine (ψKxE) (Figure 2C). We constructed lysine to arginine point mutants to disrupt potential SUMOylation sites in GFP-tagged CSB, starting from the most C-terminal lysine and mutating upstream SUMOylation motifs consecutively. Next, we compared SUMOylation levels of the different CSB mutants after UV irradiation by exogenous expression in U-2 OS His10-SUMO2 cells. Mutating the three most distal potential SUMOylation sites (K481,1359,1489R) did not strongly affect UV-induced CSB SUMOylation. However, adding the more N-terminal mutation K205R caused a pronounced SUMOylation decrease (Figure 2D). We expected that the residual SUMOylation of the CSB quadruple mutant (K205,481,1359,1489R) was located at position K32. Mutating both N-terminal lysine (2KR) or all five consensus sites (5KR) led to a complete loss of UV-induced SUMOylation (Figure S2).

To further investigate the SUMO acceptor sites of CSB, we generated single mutants for K205R and K32R in addition to a 2KR (K205R and K32R) and a 5KR (K32,205,481,1359,1489R) mutant. These mutants, together with a His10-SUMO2 construct, were expressed in the CSB-deficient patient cell line, CS1AN (Figure 2E). Mutating either of the N-terminal lysines (K32 or K205) resulted in a significant reduction of CSB SUMOylation when corrected for exogenous expression levels, although uncorrected SUMOylation levels were lower in the K205R mutant than in the K32R mutant. The CSB^{5KR} mutant showed a pronounced additive reduction in CSB SUMOylation levels (Figure 2E and 2F). Collectively, our results show that CSB is predominantly SUMOylated at two N-terminal lysine residues and that the SUMOylation is dependent on active transcription and the stalling of RNAPII at the lesion.

SUMOylation is necessary for efficient recruitment of CSB to UV-damaged DNA and for transcription recovery after UV damage

Next, we aimed to evaluate if SUMOylation is needed for efficient transcription recovery after UV-induced lesions, which is dependent on functional TC-NER. To address this, we made use of RPE1 cells harbouring inducible shRNAs targeting the SUMO E1 subunit UBA2, to reduce global SUMOylation levels (Figure S3). We measured the relative amount of RNA synthesis, represented by the incorporation of 5-ethynyl-uridine (EU) into nascent RNA, after UV irradiation in cells with reduced SUMOylation levels. Shortly after irradiation the RNA synthesis dropped due to stalling of elongating RNA polymerases (RNAPIIo). In wild-type human cells with fully functional TC-NER, lesions are efficiently repaired and UV inhibited RNA synthesis resumes in a time dependent manner[31], frequently via reinitiation of RNA synthesis[32]. Contrary, CS cells with defective TC-NER are incapable of restoring UV-inhibited RNA synthesis. We observed that reduction of SUMOylation, due to the induced knockdown of UbA2, had no impact on the UV-induced inhibition of transcription but merely delayed the recovery of RNA synthesis (RRS) after UV irradiation (Figure 3A), demonstrating a role of SUMOylation in the transcription recovery after UV damage, most likely facilitating the repair of UV-induced lesions or stimulating transcriptional restart.

Subsequently, we tested whether this delay in RRS after UV irradiation upon UbA2 knockdown could be attributed to lack of SUMOylation of CSB. For this purpose, we employed CS1AN cells, a CSB-deficient patient cell line. We re-introduced GFP-tagged wild-type CSB (WT) or a double mutant of CSB (K32,205R: 2KR), lacking the main SUMOylation sites (Figure S2). Cells expressing CSB 2KR showed a statistically significant reduction in RRS 24h after UV irradiation (Figure 3B and S4), indicating that CSB SUMOylation contributes to the delay in

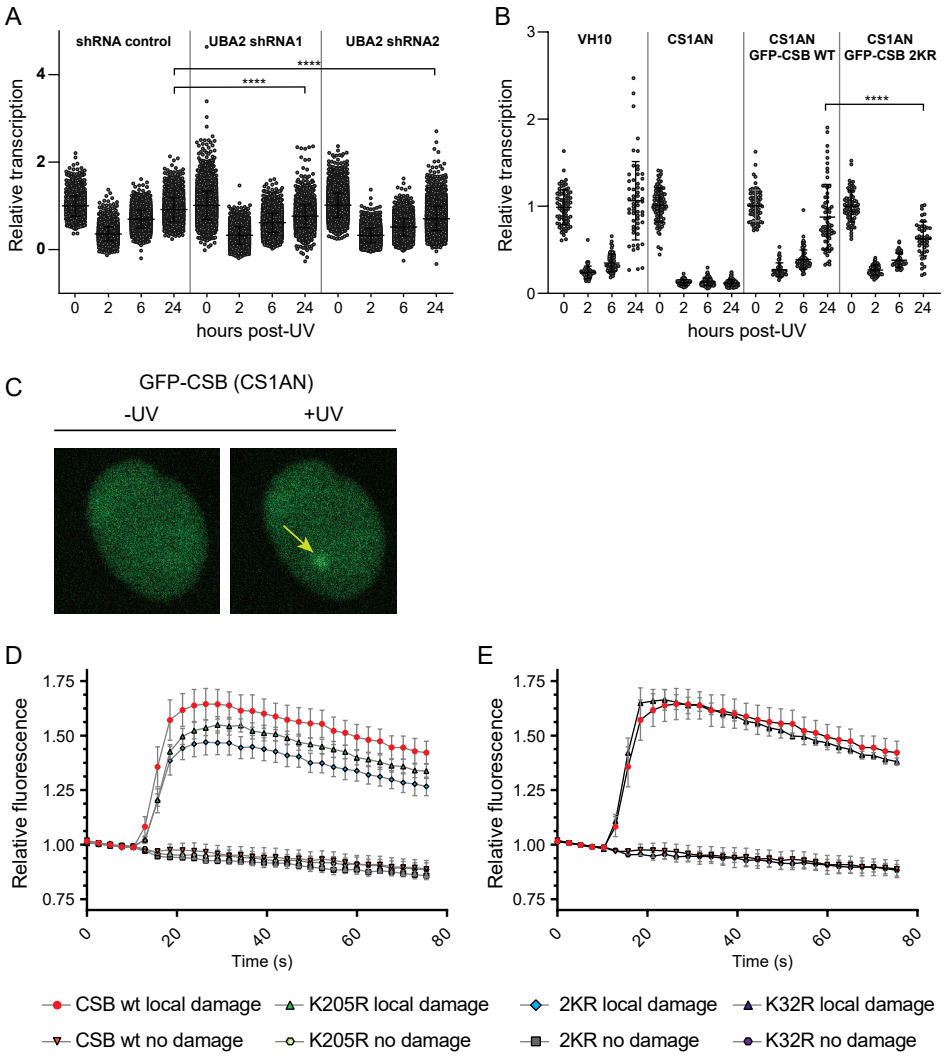

Figure 3. SUMOylation is necessary for efficient transcription recovery after UV damage and for efficient recruitment of CSB to UV-damaged DNA. (**A**) Two independent doxycycline (Dox)-inducible shRNAs against UbA2 and a non-targeted control shRNA were stably expressed in RPE1 cells. Knockdown was induced by Dox and cells were treated with 10 J/m^2 UV. Relative RNA synthesis was measured by incorporation of EdU, prior to UV, and at 2, 6 and 24 h post-UV irradiation. Error bars represent SD of the mean of three independent experiments. Data were analysed by one-way Anova followed by a Tukey's multiple comparison test. **** represents *p*-value <0.0001. (**B**) The experiment described in (A) was repeated, using CSB-deficient patient cells (CS1AN) without rescue, or expressing GFP-tagged CSB wild-type or 2KR mutant (K32R, K205R) and VH10 cells. Recovery times after UV irradiation are indicated. All datapoints, average RRS and SD for triplicate experiments are shown. Data were analysed by one-way Anova followed by a Tukey's multiple comparison test. **** represents *p*-value <0.0001. (**C-E**) Accumulation kinetics of fluorescent intensities at locally induced UV damage of GFP-CSB WT and mutants expressed in CS1AN cells. Relative fluorescence was measured in the local damage area and in a non-treated area in the cell nucleus as shown in (C). Results shown are the means of four independent experiments. Error bars represent the SD. The left panel shows kinetics of CSB WT, CSB K205R and CSB 2KR (K32R, K205R). Panel E shows kinetics of CSB WT and CSB K32R.

RRS upon UbA2 knockdown (Figure 3A).
To gain more insight into the role of CSB SUMOylation during the cellular response to UV irradiation, we next investigated the recruitment of the SUMOylation-mutants of CSB to locally induced UV lesions in living cells (Figure 3C). For this purpose, we fused CSB^{WT}, CSB^{K32R}, CSB^{K205R} and CSB^{2KR} to GFP, induced local UV damage using a UV-C laser and measured the recruitment kinetics of GFP-CSB to the damage site[22,33]. Four replicates showed a reduced recruitment of the CSB^{K205R} mutant compared to CSB^{WT} (Figure 3D). Unlike CSB^{K205R} single mutant, the CSB^{K32R} mutant doesn't seem to have any obvious defect in recruitment to the local damage sites (Figure 3E). Interestingly, the CSB^{2KR} mutant showed a more pronounced impairment of recruitment that might indicate a functional contribution of CSB^{K32} SUMOylation in the absence of CSB^{K205} SUMOylation (Figure 3D and E). Collectively, we showed that SUMOylation is needed for efficient transcription recovery after UV irradiation and that decreased CSB SUMOylation impairs the recruitment and/or stabilization of CSB at the damage site.

SUMOylation of CSB influences binding to RNA polymerase associated proteins
Our results described in the previous section could potentially be explained by a SUMOylation-dependent alteration of CSB protein interactions. SUMOylation is a low stoichiometric post-translational modification, making it difficult to study direct protein interactions *in vivo*. Therefore, we have used a strategy to study SUMOylation-dependent alterations in protein interactions of CSB using an *in vitro* approach[34]. Since the main UV-induced SUMOylation sites were located in the N-terminal part of CSB, we focussed on this part of the protein. We co-transformed *E.coli* with a plasmid encoding GST-tagged CSB truncation mutant (aa 1-341) and a plasmid encoding the SUMOylation machinery and subsequently purified the SUMOylated truncated CSB protein (SUMO-CSB). To ensure the same amounts of CSB protein in the SUMOylated and non-SUMOylated sample, we equally divided the purified SUMO-CSB sample and deSUMOylated one half by adding recombinant sentrin/SUMO specific protease 2 (SENP2). SUMOylation and deSUMOylation of CSB were confirmed by immunoblotting (Figure S5). We included a third sample with GST only as negative control (Figure 4B). GST, SUMO-CSB and CSB were subsequently incubated with a lysate of UV irradiated CS1AN cells. After incubation, beads were washed and purified proteins were trypsin-digested on the beads. Interactomes were analysed using mass spectrometry (Figure 4A and 4B).
We selected differentially binding proteins based on the fold change and *p*-value of their abundances in the SUMO-CSB sample compared to unmodified CSB. Proteins that showed no differential binding compared to the GST control were excluded. The presence of SUMO2 as the most significant and enriched protein identified, confirmed and validated the approach (Figure 4D). Of the 641 proteins identified, 46 proteins co-enriched with CSB irrespective of SUMOylation, compared with the GST control (Figure 4C and 4E, Table S3). 25 proteins showed increased binding to SUMO-CSB compared to unmodified CSB, whereas 23 proteins showed preferential binding to unmodified CSB compared to SUMO-CSB (Figure 4C and 4D, Table S3). Within the protein group that co-enriched with SUMO-CSB, we identified multiple RNA polymerase associated factors that were not previously described to bind to CSB, including polymerase I transcript release factor (PTRF). PTRF is involved in termination and re-initiation of RNA polymerase I transcription[35,36]. Consistently, CSB is a known regulator of RNA polymerase I transcription[37]. Furthermore, we identified MTA1, a member of the NURD complex to have a preference for SUMO-CSB. Other subunits of the NURD complex bound unmodified CSB equally well (Figure 4E).

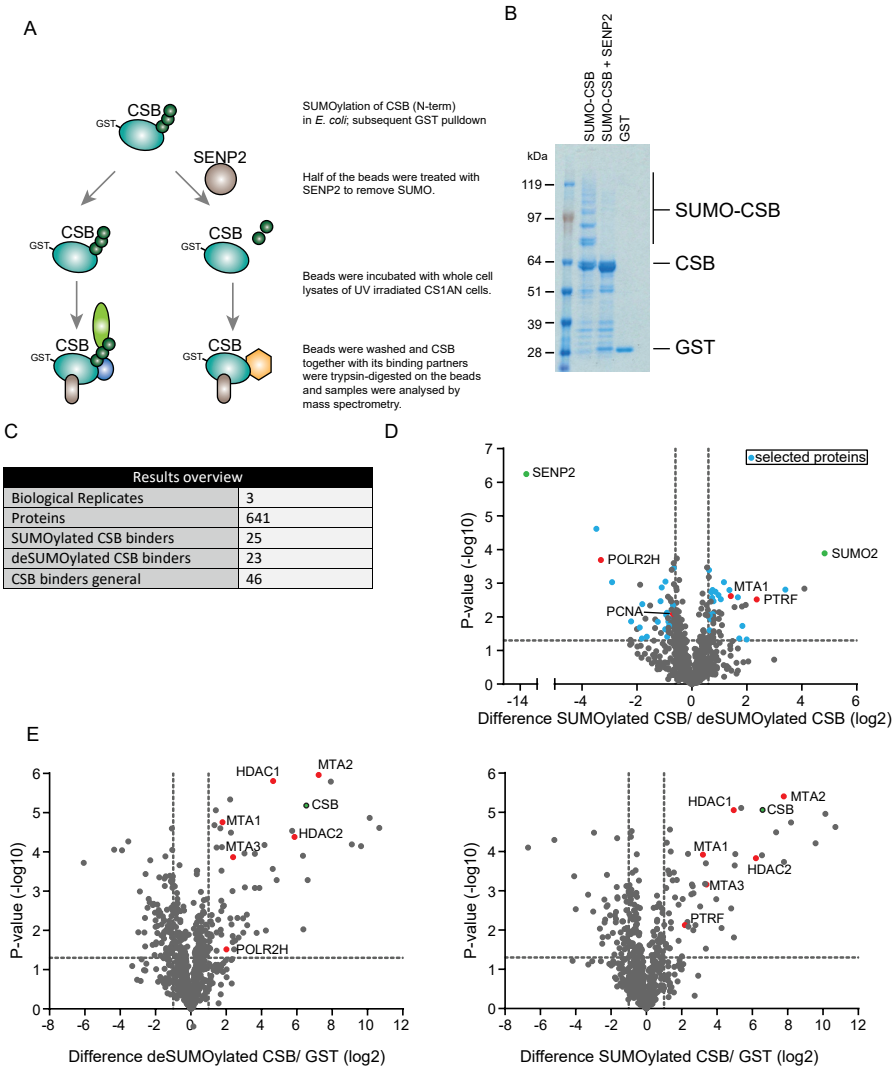

Figure 4. SUMOylation of CSB influences binding to RNA polymerase associated proteins. (**A**) Schematic overview of experimental set-up. GST tagged truncated CSB protein (aa 1-341) and SUMO machinery were co-expressed in *E.coli* and subsequently purified with glutathione resin. The resulting sample was split in two equal aliquots and one aliquot was treated with SENP2 overnight. De-SUMOylated and SUMOylated truncated CSB were incubated with lysates of UV-treated CS1AN cells. After incubation and washing, proteins were trypsinized on the resin and peptides were analysed by mass spectrometry. (**B**) Coomassie stain showing SUMOylated truncated CSB, unmodified truncated CSB and GST control. (**C**) The table shows a summary of identified proteins. Putative bindings partners are defined as proteins that are significantly different between non-SUMOylated CSB and SUMOylated CSB samples and are also significantly enriched compared to the GST control. (**D**) Volcano plot showing relative LFQ intensities of proteins in SUMOylated CSB samples compared to deSUMOylated CSB samples. Dashed lines indicate a cut-off of 1.5-fold change (log2 of 0.66) and a p-value of 0.05 (-log10 1.3). Putative differential binding partners which are also enriched compared to the GST control are marked in blue. Proteins that function as internal control are marked in green. In text discussed proteins are marked in red. (**E**) Volcano plot showing relative LFQ intensities of proteins in deSUMOylated CSB sample compared with GST control (left panel) or SUMOylated CSB samples compared with GST control (right panel). Proteins that function as internal controls are marked in green. Proteins discussed in the text are marked in red.

SUMO Interaction Motifs (SIMs) enable non-covalent interaction between SUMOylated proteins and readers. These SIMs have been defined as SIMa, [PILVM]-[ILVM]-X-[ILVM]-[DSE](3), SIMb, [PILVM]-[ILVM]-D-L-T or SIMr, [DSE](3)-[ILVM]-X-[ILVMF](2) by Vogt and Hofmann[38]. PTRF and MTA1 are missing these SIMs. Of note, this is no formal proof that they cannot bind SUMO.
Interestingly, we found that the RNA polymerase subunit PolR2H (Rbp8) and PCNA have a preference for unmodified CSB. PolR2H might represent the elongating RNAPIIo to which CSB is known to bind. PCNA is a crucial component of TC-NER, as it is responsible for the recruitment of the gap-filling DNA polymerases[39,40]. In conclusion, our data suggest that SUMOylation of CSB alters its protein interactions including to RNA polymerase associated proteins, which could contribute to efficient TC-NER.

CSA destabilizes SUMOylated CSB

Another well-described function of SUMOylation is the destabilization of target proteins by recruitment of STUbLs, leading to the subsequent ubiquitination and proteasomal degradation of the SUMO-target protein. Interestingly, the WD repeat protein CSA that is recruited to UV-induced DNA lesions in a CSB-dependent manner[41], was shown to be a substrate receptor of a Cullin/RING (CRL) ubiquitin E3 ligase complex and was previously proposed to target CSB for ubiquitination[21,42]. Therefore, we investigated the influence of the CSA-CRL complex on CSB SUMOylation. To this end, we employed U-2 OS cells stably expressing His-tagged SUMO2 to enable SUMO2 purification. CSA was knocked down using an shRNA-based approach (Figure S6). These cells were treated with UV irradiation or were left untreated as indicated. Subsequently, cells were lysed 1, 3 or 6 h after UV irradiation and SUMOylated proteins were enriched by Ni-NTA pulldown. As shown in the middle panel of Figure S6, efficient and equal SUMO enrichment was confirmed by immunoblotting. The top panel shows that one set of CSA knockdown cells showed considerably higher levels of SUMOylated CSB compared to parental U-2 OS cells and one set of CSA knockdown cells did not.
To further investigate a potential role for CSA in regulating the levels of SUMOylated CSB, we employed a CRISPR-Cas9-based knockout approach (Figure 5A). Deletion of CSA was verified by immunoblotting (Figure 5B). Efficient enrichment of SUMOylated proteins from U-2 OS cells expressing His10-SUMO2 was confirmed by immunoblotting (Figure 5A bottom panel). This panel also shows accumulation of SUMOylated proteins in response to proteasome inhibition, particularly in lanes 8, 11 and 14. The top panel of this figure shows that SUMOylated CSB could be detected in response to UV treatment. In the absence of CSA, SUMOylated CSB accumulated to a higher extent at all three timepoints, compared to CSA wild-type cells. The reduction in SUMOylation due to the presence of CSA could not be reversed by blocking proteasomal degradation as shown in lanes 8, 11 and 14. In response to MG132 treatment, SUMO and ubiquitin are trapped on the targets that can be no longer be degraded and the pools of free SUMO and ubiquitin will concomitantly decrease. Due to these limited pools of free SUMO and ubiquitin, less SUMO and ubiquitin will be available for conjugation to new target proteins. As a result, the SUMOylation and ubiquitination levels of proteins that are not degraded by the proteasome will decrease. This appears to be the case for SUMOylated CSB in response to MG132 at 1 h and 6 h post UV. These results indicate that the CSA-CRL complex regulates the stability of SUMOylated CSB in response to DNA damage directly or indirectly in a proteasomal-independent manner.

CSA stimulates ubiquitination of RNA polymerase II but not CSB after UV irradiation

Following the observation that CSA influenced the destabilization of SUMOylated CSB, we tested whether CSA might target SUMOylated CSB for ubiquitination and would therefore act as a STUbL. To evaluate this, we investigated the influence of CSA and UV irradiation on the ubiquitination of CSB. CSA-Flag was reintroduced in the CS3BE cells described above and these cells were engineered to stably express His10-ubiquitin. To decrease background ubiquitination of CSB that could arise from misfolding of this 1493 amino acid long protein during protein synthesis since a significant percentage of newly synthesized proteins are misfolded[43,44], we treated the cells overnight with the translation inhibitor cycloheximide. We next irradiated the cells with UV light, lysed 2 h post-UV irradiation and purified ubiquitinated proteins. Efficient purification of ubiquitin and accumulation of ubiquitinated proteins in response to proteasome inhibition were confirmed by immunoblotting (Figure 5C, third panel). The absence of CSA in CS3BE and the presence of CSA in the rescued cells were also confirmed by immunoblotting (Figure 5C bottom panel). Next, we tested wether CSB ubiquitination was enhanced in the presence of of CSA and we confirmed that this was the case (Figure 5C top panel). However, CSA-dependent ubiquitination of CSB was already detectable in unirradiated cells (Figure 5C lanes 1-6) and was reduced rather than enhanced upon UV treatment (Figure 5C lanes 7-12). Inhibiting the proteasome did not result in an accumulation of ubiquitinated CSB although total ubiquitin conjugates increased as expected (Figure 5C). The destabilization of SUMOylated CSB can therefore not be explained by UV-induced CSA-dependent ubiquitination. Furthermore, ubiquitination of CSB does apparently not cause subsequent proteasomal degradation.

We next hypothesized that the observed UV- and CSA-dependent destabilization of SUMOylated CSB shown in Figure 5A, is an indirect effect of an ubiquitination event of another unknown protein. Therefore, we set out to identify possible UV-induced ubiquitination targets of CSA in an unbiased manner. We used CSA-deficient CS3BE cells stably expressing His10-ubiquitin with or without exogenous expression of CSA-Flag. Cells were stable isotope labelled by amino acids in cell culture (SILAC) as described in the upper panel of Figure 6A. Cells were treated in four different manners, including no UV irradiation, UV irradiation in combination with 1 h recovery, or 6 h recovery and 6 h recovery combined with proteasome inhibition. Differential ubiquitination of proteins was analysed by mass spectrometry for each of the four different treatments (Figure 6A). Ubiquitination of CSB was not detected in this screen. Most intriguingly, we identified the large RNAPII subunit, RPB1, as a differentially ubiquitinated protein 1 h after UV irradiation in a CSA-dependent manner. This ubiquitination of RPB1 was non-detectable after the 6 h recovery, but stabilized upon proteasome inhibition, indicating a CSA-dependent destabilization of RPB1 (Figure 6A, Table S4).

Subsequently, we carried out experiments to verify our proteomics data, using immunoblotting analysis of His10-ubiquitin-enriched fractions (Figure 6B). In the third panel of Figure 6B, His10-ubiquitin enrichment was confirmed in the stably expressing CS3BE cells as expected. The same panel shows that ubiquitin was stabilized by proteasome inhibition as expected. The bottom panel of Figure 6B confirms the presence of CSA-Flag in the rescued CS3BE cells. The second panel confirms the presence of elongating RPB1 (p-RPB1) in all samples. This is the relevant form of RPB1 in this context. Next, we asked wether p-RPB1 is a substrate for ubiquitination following UV irradiation, and whether that is dependent on CSA and leads to proteasomal degradation. This is shown in the top panel of the Figure. In CS3BE cells lacking His10-ubiquitin, no p-RBP1 is detected, showing correct

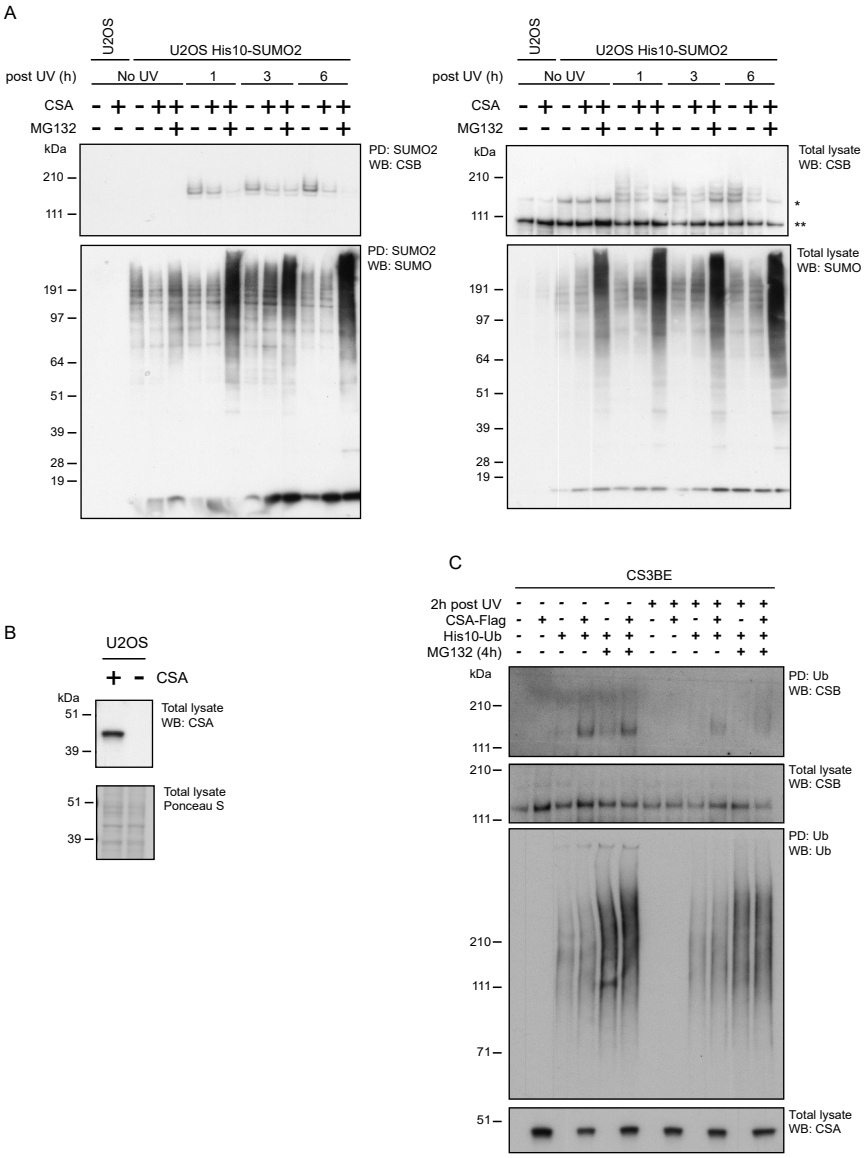

Figure 5. CSA destabilizes SUMOylated CSB. (**A**) U-2 OS WT and CSA-deficient cells stably expressing His10-SUMO2 were used to study whether CSA affects the SUMOylation of CSB. These cells were subjected to UV irradiation (20 J/m^2) and/or proteasomal inhibition (MG132) as indicated. Cells were lysed 1, 3, or 6 h after UV irradiation. Subsequently, SUMOylated proteins were purified from these lysates by Ni-NTA pulldown. SUMO-enriched fractions (PD) and total lysates were analysed by immunoblotting using antibodies against CSB or SUMO2/3. *marks full-length CSB; ** marks the CSB-piggyBac transposable element derived 3 fusion (CPFP). (**B**) Immunoblotting to confirm the absence of CSA in U-2 OS cells established by CRISPR-Cas9 targeting the CSA gene. (**C**) CSA-deficient CS3BE patient cells and a derivate cell line that was rescued by introducing CSA-Flag were used to study whether CSA affects ubiquitination of CSB. His10-ubiquitin was stably expressed in these cells as indicated and cells were treated overnight with cycloheximide to prevent new protein sythesis. The next day, cells were UV irradiated (20 J/m^2) and/or treated with MG132 as indicated. Ubiquitinated proteins were purified by His10-purification. Total lysates and ubiquitin-enriched (PD) fractions were analysed by immunoblotting using antibodies against CSB, CSA or Ub as indicated.

negative controls. Interestingly, ubiquitination p-RPB1 is only detected in response to UV damage. Cells expressing CSA have considerably more ubiquitinated p-RPB1. This is unlikely due to loading errors as shown in the second and the third panels of this figure. At 6 h post irradiation, the ubiquitination signal of p-RPB1 diminishes, presumably due to degradation of the ubiquitinated p-RPB1. This is supported by the results in lanes 9 and 10 in which the proteasomal inhibitor MG132 is present. In conclusion the results confirm our proteomics results that CSA regulates the ubiquitination of p-RPB1 in response to UV damage. In the absence of CSA, some ubiquitination of p-RPB1 in response to UV damage was still noticeable, indicating that UV-induced ubiquitination of elongating RPB1 in response to UV partly occurs in a CSA-independent manner.

Next, we carried out a similar experiment as described in Figure 6B, now using U-2 OS cells proficient or deficient for CSA (Figure 6C). This experiment confirms our results obtained in Figure 6A and B, strengthening the conclusion that CSA regulates the ubiquitination of p-RPB1 in response to UV damage. Using the samples shown in Figure 6C and staining them for RPB1 ubiquitination, we noticed that after a short recovery (1 h) upon UV irradiation, RPB1 was ubiquitinated in a CSA-dependent manner in U-2 OS cells but not subjected to proteasomal degradation as treatment with proteasome inhibitor did not result in an accumulation of ubiquitinated RPB1 (Figure 6C). However, after a longer recovery time of 6 h, proteasome inhibition stabilized ubiquitinated RPB1. Nevertheless, in the total lysate controls, the proteasome inhibitor does not rescue the levels of RPB1 and p-RPB1, indicating that proteasomal degradation of RPB1 at the 6 h timepoint is limited. Collectively, these results indicate that CSA is stimulating the ubiquitination of RNAPII either directly or indirectly upon UV irradiation, leading to proteasomal degradation of a subset of RNAPII only after a longer recovery upon the DNA damage.

DISCUSSION

Link between CSA, ubiquitinated RNAPII and SUMOylated CSB

Mutations in the *CSA* and *CSB* genes give rise to Cockayne Syndrome, a severe neurodegenerative and premature aging disorder that is associated with hypersensitivity to UV irradiation, primarily due to defects in TC-NER. CSA is the substrate recognition factor of an E3 Cullin ubiquitin ligase complex. However, it is currently unclear which proteins are targeted for CSA-dependent ubiquitination at sites of DNA damage. CSB has been suggested as a UV-specific target for CSA mediated ubiquitination and subsequent proteasomal degradation[45]. Although we observed an increase in CSB ubiquitination in a CSA-dependent manner, this was not induced and even slighly reduced in response to UV irradiation and ubiquitinated CSB was not stabilized in response to proteasome inhibition. Of note, the usage of tagged-ubiquitin constructs precludes the detection of potential linear ubiquitin chains on CSB. Nevertheless, in our hands it does not appear that CSB is a target for UV-dependent degradation via the CSA-CRL E3 ligase complex. However, we did find that the recruitment of this complex is responsible for the destabilization of SUMOylated CSB after UV. Our observation provides a novel link between CSB and CSA, but raises the question how CSA is regulating the destabilization of SUMOylated CSB.

A potential explanation for the destabilization of SUMOylated CSB by the CSA-CRL complex is the ubiquitination of other targets by this complex. We identified the RNAPII subunit RPB1 as a key target for the CSA complex. Ubiquitination of RPB1 directly or indirectly by the CSA complex could potentially induce the dissociation of CSB from chromatin and

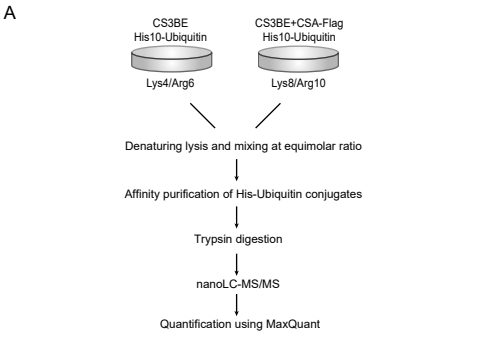

Experiment	Medium labeled	Heavy labeled	UV	Recovery	MG132
1	CS3BE	CS3BE + CSA-Flag	No UV	-	-
2	CS3BE	CS3BE + CSA-Flag	20 J/m^2	1 hour	-
3	CS3BE	CS3BE + CSA-Flag	20 J/m^2	6 hours	-
4	CS3BE	CS3BE + CSA-Flag	20 J/m^2	6 hours	+

	Normalized Log2 Ratio			
	Exp1	Exp2	Exp3	Exp4
RNA polymerase II, subunit RPB1	0	0.65	0	0.64

Figure 6. CSA stimulates ubiquitination of RNA polymerase II but not CSB in a UV-dependent manner. (**A**) CS3BE cells with or without ectopic expression of CSA-Flag and stably expressing His10-ubiquitin were SILAC labelled and subjected to UV irradiation (20 J/m^2) and/or treated with MG132 or were left untreated as indicated. Cells were lysed 1 h or 6 h after UV irradiation. Ubiquitinated proteins were purified by Ni-NTA pulldown. Eluted proteins were trypsinized and analysed by mass spectrometry. The table shows an overview of experimental conditions and the log2 medium/heavy ratios of the RNAPII subunit RPB1 in each experiment. (**B**) CS3BE cells with or without ectopic expression of CSA-Flag and stably expressing His10-ubiquitin were treated with UV irradiation (20 J/m^2) and MG132 where indicated and lysed after the indicated recovery times. Total lysates and ubiquitin-enriched fractions (PD) were analysed by immunoblotting using antibodies against p-RBP1 (S2/S5), His or CSA. (**C**) U-2 OS WT and CSA-deficient cells stably expressing His10-ubiquitin were subjected to UV irradiation (20 J/m^2) and/or proteasomal inhibition (MG132) or were left untreated as indicated. Cells were lysed 1, 3, or 6 h after UV irradiation. Ubiquitinated proteins were purified by Ni-NTA pulldown. Ubiquitin-enriched fractions and total lysates were analysed by immunoblotting using antibodies against RBP1, p-RBP1 (S2/S5) or ubiquitin. *residual p-RBP1 (S2/S5) signal in blot re-probed with ubiquitin antibody.

its translocation to the nucleoplasm where it can be deSUMOylated by SUMO-specific proteases (Figure 7). Intriguingly, RNAPII ubiquitination and degradation is believed to be a 'last-resort' response to DNA damage[46]. In contrast to CSB, we could observe CSA-dependent UV-induced ubiquitination of the RNAPII subunit RPB1. However, we could only observe a stabilization of the ubiquitinated RPB1 upon inhibition of the proteasome at a later timepoint (6 h) post-UV irradiation, indicating an ubiquitination event that does not immediately lead to degradation. Also we observed that there is a significant residual UV-induced ubiquitination of RNAPII in CS3BE cells lacking CSA, which indicates the presence of other ubiquitin E3 ligases targeting RNAPII. CSA-independent ubiquitination of RBP1 could be regulated by the E3 ligases NEDD4 and the Elongin A,B,C complex[47]. These E3 ligases play important roles at the early stage after UV irradiation, within 30 minutes and mediate K63-linked ubiquitin chains.

Intriguingly, it was previously found that CSB contains an ubiquitin binding domain (UbD) that is required for TC-NER[48]. If this observation is connected to our findings, CSA-dependent ubiquitination of RNAPII might provide a docking site for the UbD in CSB. Subsequent release, or degradation of ubiquitinated RNAPII might result in co-release or degradation of CSB. The UbD domain of CSB is not required for its SUMOylation[49]. Whether the UbD domain is required for the clearance of SUMOylated CSB is currently unclear. Follow-up projects could focus on the potential connection between CSB SUMOylation, its UbD domain and RNAPII ubiquitination. An alternative explanation for the observed effect would be that the degradation of other proteins is required for the destabilization of SUMOylated CSB.

SUMO group modification in response to UV

The SUMOylation of CSB was described in a previous publication, which reported lysine 205 as major SUMOylation site[49]. We could confirm this finding but additionally found a contribution of lysine 32 to SUMOylation of CSB. To evaluate the functional importance of K32 SUMOylation, we studied the recruitment of WT, the single mutants K205R and K32R and the 2KR CSB mutant to local UV lesions and observed that mutating both N-terminal lysines of CSB impaired the recruitment to the local UV-induced damage more effectively than the single mutation of K205, showing a functional contribution of K32 if K205 is not available for SUMOylation.

We could further confirm that SUMOylation and the two N-terminal SUMOylation sites in CSB contribute to RRS after UV damage. This is in line with the previous publication showing the effect of Ubc9 (SUMO E2 conjugating enzymes) knockdown on RRS[49]. Because CSB was the only TC-NER protein that we identified in our mass-spectrometry screen to be SUMOylated in response to UV, it is likely that CSB SUMOylation contributes to this effect. Interestingly, lesion recognition in GG-NER occurs via XPC, a well-known UV-regulated SUMO target that we confirmed in our screen[18-20]. Thus, both branches of NER involve lesion recognition factors that are regulated by SUMO.

Our results linking reduced levels of SUMOylated CSB to the presence of CSA are in contrast to this previous publication[49]. This could potentially be due to differences in SUMO-enrichment methodology between both studies. We prefer highly efficient enrichment of His10-tagged SUMOylated proteins using NiNTA beads, which is compatible with the use of strongly denaturing buffers to inactivate endogenous SUMO proteases, whereas the previously published study employed immunoprecipitation, necessitating the use of milder buffer conditions to prevent denaturation of the employed antibodies.

Although we did not identify any other obvious TC-NER proteins as UV-responsive SUMO

targets, we did identify dynamic SUMOylation in response to UV irradiation of proteins associated with transcription, like the TFIID basal transcription factor components TAF1, TAF5, TAF6 and TAF12. This observation suggests that the transcription response to elongation-blocking DNA lesions is in part controlled through SUMOylation. These results further highlight the SUMO group modification concept, where modification of a set of targets within a biological pathway is needed for stronger biological effects, as was observed in the context of DSB repair[50]. Our results indicate that SUMO co-regulates a considerably larger set of targets in response to UV irradiation compared to IR.

Model

Taken together we suggest a model wherein CSB is SUMOylated and recruited to UV lesion-stalled RNAPII. This association recruits the CSA-CRL complex to the site of damage, where it stimulates the ubiquitination of the RNAPII subunit, RPB1 in a direct or indirect manner. The activity of CSA initiates the release of SUMOylated CSB, but CSA does not act as a STUbL for SUMOylated CSB. Ubiquitinated RPB1 resides at the site of the lesion until the lesion is either repaired or in case repair failed, it would trigger the proteasomal degradation of RPB1. Our data fit well with initial observations in the field on reduced UV-induced ubiquitination of RPB1 in fibroblasts from CS patients[51]. Overall our results provide new insight in the cooperative signaling roles for SUMOylation and ubiquitination of TC-NER components. Whereas CSB is a prime SUMO2 target, the stability of SUMOylated CSB and the ubiquitination of RPB1 is dependent on CSA. Combined, these two small modifiers may contribute to RRS, presumably via efficient TC-NER and transcription restart in response to UV irradiation. Furthermore, we identified an extensive set of SUMOylated proteins in response to UV irradiation. Detailed functional analysis of these proteins will improve our understanding of the role of SUMO group modification in the cellular response to UV irradiation.

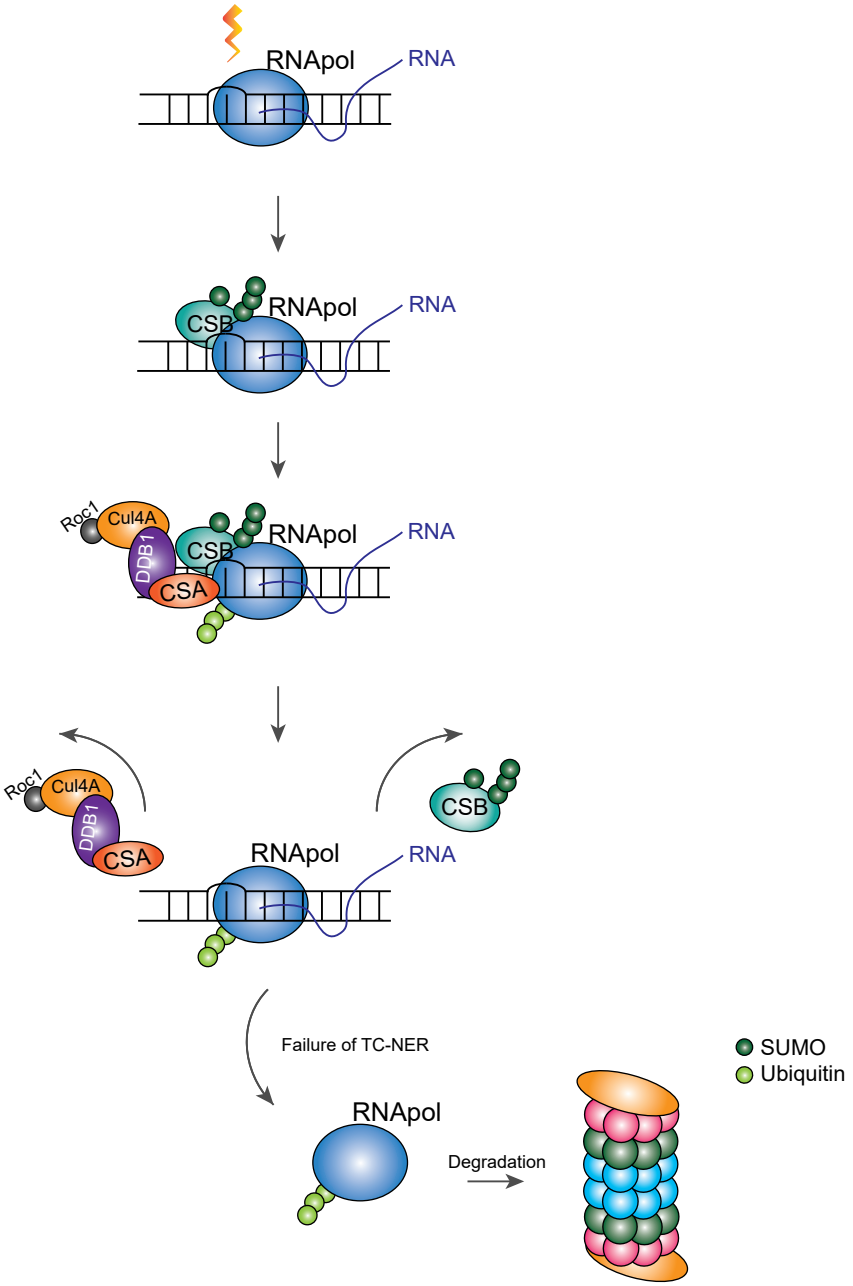

Figure 7. SUMO and ubiquitin cooperate during TC-NER.
The processing RNAPII is stalled upon encountering a DNA photolesion with helix distorting property, which is introduced by UV light, MMS or etoposide within an actively transcribed DNA region. In response to the stalled RNA polymerase, CSB is SUMOylated, recruited and stabilized at the lesion site. CSA is subsequently recruited to the site of damage and stimulates ubiquitination of RNAPII directly or indirectly. After a short recovery upon DNA damage, SUMOylated CSB is destabilized by the presence of CSA. The proteasomal degradation of ubiquitinated RNAPII is observed at a late stage (6 h) after UV irradiation, possibly related to failure of repair.

MATERIAL AND METHODS

Detailed information on antibodies, oligonucleotides, reagents and databases used can be found in Table S5.

Plasmids

Expression constructs for CSB K32R, K205R, 2KR and 5KR were generated by site-directed mutagenesis using the pDonR207-CSB wild-type (WT) plasmid as a template. Resulting CSB mutants and WT construct were cloned into pLX303 destination vector for lentiviral transduction (Addgene plasmid #25897), into pBabe-puro-GFP-DEST destination vector (kind gift of Dr. Marc Timmers, Freiburg, Germany) for retroviral transduction or into pDEST-EGFP-C1 destination vector for transient transfection, using Gateway cloning technology (Thermo Fisher Scientific). To create N-terminal CSB protein fragments, a cDNA encoding amino acids 1 to 341 of CSB was cloned into pDONR207. For bacterial expression of this CSB fragment, this construct was subsequently cloned into pDEST15 using Gateway cloning technology. Epitope-tagged CSA has been described previously[52].

Cell lines, SILAC labelling and generation of cell lines

U-2 OS, hTERT1 immortalized RPE1 cells and sv40 immortalized CS1AN, CS3BE and VH10 cells were cultured in Dulbecco's modified Eagle's medium supplemented with 10% FCS and 100 U/ml penicillin and 100 µg/ml streptomycin. For stable isotope labelling by amino acids in cell culture (SILAC), cells were essentially labelled as described before [53]. Briefly cells were grown in medium supplemented with [$^{12}C_6$, $^{14}N_4$] arginine (referred to as Arg0), [$^{13}C_6$, $^{14}N_4$] arginine (referred to as Arg6), [$^{13}C_6$, $^{15}N_4$] arginine (referred to as Arg10), [$^{12}C_6$, $^{14}N_2$] lysine (referred to as Lys0), [$^{2}H_4$, $^{13}C_6$, $^{14}N_2$] lysine (referred to as Lys4), [$^{13}C_6$, $^{15}N_2$] lysine (referred to as Lys8) as indicated.

U-2 OS cell lines stably expressing Flag-SUMO2, His10-SUMO2 or His10-ubiquitin were previously described[54,55]. U-2 OS His10-SUMO2-IRES-GFP cells expressing GFP-CSB WT and mutants were generated by infecting cells with retrovirus encoding the different pBabe-GFP-CSB constructs together with a Puromycin resistance gene. Cells were selected for GFP-CSB expression by culturing in medium supplemented with 1 µg/ml Puromycin. CS1AN cell lines co-expressing His10-SUMO2 and tagless CSB WT and mutants were generated by an initial round of infection of cells with lentivirus encoding a His10-SUMO2-IRES-puro construct and Puromycin selection (1 µg/ml) and a subsequent round of infection with lentivirus encoding the different pLX303-CSB mutant constructs. Cells were selected for CSB expression by culturing in medium supplemented with 5 µg/ml Blasticidin. CS1AN cells stably expressing EGFP-CSB WT or mutants were generated by transfecting cells with pDEST-EGFP-CSB constructs also encoding for a Neomycin resistance gene. Monoclonal cell cultures were selected with 400 µg/ml G418 (Neomycin) and based on EGFP expression.

U-2 OS Flp-In/T-REx cells, which were generated using the Flp-InTM/T-RExTM system (Thermo Fisher Scientific), were a gift of Daniel Durocher. These cells were co-transfected with pLV-U6g-PPB containing an antisense guide RNA targeting the CSA/ERCC8 gene (5-CCAGACTTCAAGTCACAAAGTTG-3) from the Sigma-Aldrich sgRNA library together with an expression vector encoding Cas9-2A-GFP (pX458; Addgene #48138). Transfected U-2 OS Flp-In/T-REx were selected on puromycin (1 µg/mL) for 3 days, plated at low density after which individual clones were isolated. Knockout of CSA in the isolated clones was verified by sequencing of genomic DNA by nested PCR using the following

primers: 5-CAGTCTGTGTCCAGTTTCTGTG-3, 5- CATATTTGTTATGTGTTTCTTTGAG-3, 5-GTACATACATACATACACATTTACCAATAC-3, and 5-CTGAGAAAAAATGTACCTAAATATTAAG-3, as well as by Western blot analysis (Rabbit α-CSA/ERCC8, EPR9237, Abcam 137033). The absence of Cas9 integration/stable expression was confirmed by western blot analysis (Mouse α-Cas9, 7A9-3A3, #14697, Cell Signaling Technology). CS3BE cells stably expressing His-CSA were generated by infecting cells with lentiviruses encoding CSA and the Blasticidin resistance gene. After infection, cells were selected for expression of CSA by culturing in medium supplemented with 5 µg/ml Blasticidin. RPE1 cell lines immortalized by hTERT1 and expressing inducible shRNA against UbA2/SAE2 were generated by infecting cells with lentiviruses encoding the different shRNA constructs and a Neomycin resistance cassette. Cells were selected for expression of the introduced construct by selection with 400 µg/ml G418.

For the induction of different DNA lesions 50 µM etoposide (Sigma Aldrich) was used in culture medium for 1 h, 0.02% Methyl methanesulfonate (MMS) (Sigma Aldrich) was used in culture medium for 1.5 h, 2 mM Hydroxyurea (HU) (Sigma Aldrich) was used in culture medium for 2 or 24 h. Cell were treated with 4 Gy of IR and 20 J/m^2 UV-C light and lysed after indicated recovery times. 100 µM 5,6-Dichlorobenzimidazole (DRB) (Sigma Aldrich) was used in culture medium for 3 h before UV irradiation. 2 µg/ml α-amanitin (HY-19610, MedChemExpress and A2263-1MG Sigma Aldrich) was used in culture medium for 24 h prior to UV irradiation.

Live imaging experiments, UV-C irradiation

Localisation studies of GFP-CSB were performed using UV-C (266 nm) laser-irradiation for local DNA damage infliction[33]. Briefly, a 2-mW pulsed (7.8 kHz) diode-pumped solid-state laser emitting at 266 nm (Rapp OptoElectronic) was connected to the confocal microscope Leica TCS SP5 AOBS with an Axiovert 200M housing adapted for UV by all-quartz optics. By focusing the UV–C laser inside cell nuclei without scanning, only a limited area within the nucleus (diffraction limited spot) was irradiated. Cells were imaged and irradiated through a 100×, 1.2 NA Ultrafluar quartz objective lens. Images obtained prior to and post UV-C laser irradiation were analysed using the LASAF software (Leica).

Purification of His10 conjugates using Ni-NTA beads

His10-ubiquitin conjugates and His10-SUMO2 conjugates were purified using Ni-NTA beads as previously described[25]. In brief, cells stably expressing His10-SUMO2 or His10-ubiquitin were lysed in 6 M guanidine-HCL pH 8.0. A small fraction of cells was separately lysed in SNTBS buffer (2% SDS, 1% N-P40, 50mM Tris pH 7.5, and 150mM NaCl) as input control. After sonication and addition of Imidazole (50 mM) and ß-mercaptoethanol (5 mM) lysates were incubated with pre-washed nickel-nitrilotriacetic acid- agarose beads (Ni-NTA)(Qiagen). After incubation, beads were washed subsequently with buffer 1-4. Wash Buffer 1: 6 M guanidine-HCL, 0.1 M Na_2HPO_4/NaH_2PO_4, pH 8.0, 0.0.1 M Tris-HCL pH 8.0, 10 mM imidazole pH 8.0, 5 mM ß-mercapthoethanol and 0.1% Triton X-100 (0.2% Triton X-100 for immunoblotting sample preparation). Wash Buffer 2: 8 M Urea, 0.1 M Na_2HPO_4/NaH_2PO_4, 0.01 M Tris-HCL pH 8.0, 10 mM imidazole pH 8.0, 5 mM ß-mercaptoethanol and 0.1% Triton X-100 (0.2% Triton X-100 for immunoblotting sample preparation). Wash Buffer 3: 8 M Urea, 0.1M Na_2HPO_4/NaH_2PO_4, 0.01 M Tris-HCL pH 6.3, 10 mM imidazole pH 7.0, 5 mM ß-mercaptoethanol and no Triton X-100 (0.2% Triton X-100 for immunoblotting sample preparation). Wash Buffer 4: 8 M Urea, 0.1 M Na_2HPO_4/NaH_2PO_4, 0.01 M Tris-HCL pH 6.3, 5

mM ß-mercaptoethanol and no Triton X-100 (0.2% Triton X-100 for immunoblotting sample preparation). Elution of sample was performed twice in one bead-volume of 7 M urea, 0.1 M Na_2HPO_4/NaH_2PO_4, 0.01 M Tris pH 7.0 and 500 mM imidazole pH 7.0.

Electrophoresis and immunoblotting
To visualize CSB and RPB1 by immunoblotting, either 6% Tris-Glycine gels or Novex 3-8% Tris-Acetate gradient gels (Thermo Fisher Scientific) were used for electrophoresis. To visualize other proteins, samples were separated on Novex 4-12% Bis-Tris gradient gels (Thermo Fisher Scientific) with MOPS buffer or via regular SDS-page using Tris-glycine gels. Separated proteins were transferred onto Amersham Protran Premium 0.45 NC Nitrocellulose blotting membrane (GE Healthcare) using a submarine system. For whole cell lysates, membranes were stained with Ponceau S (Sigma) as loading control. Membranes were blocked with 8% non-fat milk in PBS 0.05% Tween for 1 h, prior to primary antibody incubation.

RNA synthesis recovery assay
Two independent doxycycline (Dox)-inducible shRNAs against UbA2 and a non-targeted control shRNA[56] were stably expressed in RPE1 cells. Cells were seeded in 96 well plates, in which the knockdown was induced by Dox. Cells were irradiated with UV-C (10J/m^2), and incubated for the indicated time-periods (0–24 hours) to allow RNA synthesis recovery. RNA was labelled for 1 hour in medium supplemented with 1mM EU (Click-iT® RNA Alexa Fluor® 594 Imaging Kit, Life Technologies) according to the manufacturer's instructions. Imaging was performed on an Opera Phenix confocal High-Content Screening System (Perkin Elmer, Hamburg, Germany) equipped with solid state lasers. General nuclear staining (DAPI) and Alexa 594 were serially detected in 9 fields per well using a 20x air objective. Three independent experiments were analysed using a custom script in the Harmony 4.5 software (Perkin Elmer) in which nuclei were individually segmented based on the DAPI signal. RNA synthesis recovery was determined by measuring the mean Alexa 594 intensity of all nuclei per field.

Proteomics sample preparation and mass spectrometry
His10-purified samples were supplemented with ammonium biocarbonate (ABC) to 50 mM. Subsequently samples were reduced with 1 mM dithiothreitol (DTT) for 30 min and alkylated with 5mM chloroacatemide (CAA) for 30 min and once more reduced with 5 mM DTT for 30 min at room temperature. Proteins were digested with Lys C for 3 h in a 1:100 enzyme-to-protein ratio. Subsequently the peptides were diluted 4-fold with 50 mM ABC and trypsin digested overnight in a 1:100 enzyme-to-protein ratio.

Mass spectrometry
Samples were acidified and subsequently desalted and concentrated on triple-disc C18 reverse phase StageTips[57]. Peptides were eluted twice, with 40% and 60% acetonitrile (ACN) in 0.1% formic acid, respectively. Peptides were vacuum centrifuged until all liquid was evaporated and re-suspended in 0.1% formic acid. Peptides were analysed by mass spectrometry using a Q-Exactive Orbitrap (Thermo Fisher Scientific) coupled to an EASY-nLC system (Proxeon).

Processing of mass spectrometry data
MaxQuant (version 1.5.3.30) was used to analyse RAW data. The MaxQuant output protein

groups table was further analysed by Perseus software (version 1.5.3.1). Data were filtered by removing 'reverse identified', 'only identified by site' and 'potential contaminants'. LFQ intensities were Log2 transformed. The following groups were compiled: U-2 OS 1 h IR, U-2 OS 1 h UV, U-2 OS-His10SUMO mock treated, U-2 OS-His10-SUMO2 1 h IR, U-2 OS-His10-SUMO2 6 h IR, U-2 OS-His10-SUMO2 1 h UV, U-2 OS-His10-SUMO2 6 h UV from the three biological replicates.

Proteins groups that had at least 3 valid values in at least one group were selected for further analysis. Missing values were imputed using the Perseus software by normally distributed values with a 1.8 downshift (log2) and a randomized 0.3 width (log2) considering the whole matrix. Subsequently, two-sample t-tests were conducted between different experimental conditions (two-sided). A protein that at least in one His10-SUMO2 condition showed a log2 difference of >0.66 and a *p*-value of <0.05 compared with the U-2 OS parental control was selected as SUMO target protein. IR targets 1 h or 6 h post-IR needed a log2 difference of >0.66 and a *p*-value of <0.05 compared with His10-SUMO2 mock treated control and parental U-2 OS 1 h IR condition. UV targets 1 h or 6 h post-UV needed a log2 difference of >0.66 and a *p*-value of <0.05 compared with His10-SUMO2 mock treated control and parental U-2 OS 1 h IR condition.

Identification of proteins that bind to SUMOylated CSB

E. coli strain BL21 was co-transformed with a plasmid encoding the GST-CSB N-terminus (aa 1-341) and a plasmid encoding the SUMO2 machinery[34]. Expression of transgenes was induced by 0.5 mM IPTG at 25 °C overnight. Bacteria were harvested by centrifugation washed twice with icecold PBS before resuspending in PBS, 0.5 M NaCl, 1 mM PMSF and cOmplete™ mini protease inhibitor cocktail (Sigma). Cells were lysed by sonification and the addition of 10% Triton X-100. Lysates were cleared by centrifugation at 13,000 rcf and supernatant was incubated with glutathione Sepharose (GE Healthcare) for 2 h at 4 °C. After incubation, Sepharose was washed twice with PBS, 0.5 M NaCl,1 mM PMSF and cOmplete™, mini protease inhibitor cocktail (Sigma) and washed 3x with 50 mM Tris (pH 7.5), 0.5 M NaCl. Each sample was equally divided over 2 new reaction tubes and one half was treated with 10 µg of recombinant SENP2 overnight at 4 °C. Sepharose beads were washed 3x with 50 mM Tris (pH 7.5) and 0.5 M NaCl, then washed 2x with 50 mM Tris (pH 7.5), 150 mM NaCl, 0.5% NP-40, 1 mM $MgCl_2$, 20 mM NEM and cOmplete™, mini protease inhibitor cocktail (Sigma) before incubation with cell lysates.

For the preparation of the cell lysates, CS1AN cells were irradiated with 20J/m^2 UV-C light and lysed 1 h after UV treatment in lysis buffer (50 mM Tris (pH 7.5), 150 mM NaCl, 0.5% NP-40, 1 mM $MgCl_2$, 20 mM NEM and cOmplete™, mini protease inhibitor cocktail (Sigma)). Cells were sonicated and treated with 500 U/ml benzonase for 1 h at 4 °C. Cleared cell lysate was incubated with previously prepared glutathion Sepharose containing SUMOylated GST-CSB, de-SUMOylated GST-CSB or GST only for 2 h at 4 °C. After incubation, Sepharose beads were washed 4x with lysis buffer, subsequently 3x in 50 mM fresh ammonium bicarbonate (ABC) and bound proteins were trypsinized with 2 µg trypsin overnight at 37 °C.

Flag-SUMO2 and Flag-Ubiquitin immunoprecipitation

Flag-SUMO2 and Flag-Ubiquitin conjugates were enriched by anti-Flag immunoprecipitation as described previously[54].

Funding
This work was supported by the European Research Council (ERC) [310913 to A.C.O.V. and 340988 to W.V.], the Netherlands Organisation for Scientific Research (NWO) [Gravitation program CancerGenomiCs.nl to W.V. and ALWOP.143 to A.P., 855-01-074 to L.F.M.] and the NTC Netherlands Toxicogenomics Center [050-060-510 to L.F.M.], an LUMC research fellowship and NWO-VIDI grant (016.161.320) to M.S.L.

Acknowledgements

We thank Prof. Dr. Marc Timmers (Freiburg) for the pBabe-puro-GFP-DEST destination vector and Prof. Jesper V. Olsen (Copenhagen) for mass spectrometry support during the initial phase of the study.

Data availibility

The mass spectrometry proteomics data have been deposited to the ProteomeXchange Consortium via the PRIDE[58] partner repository with the dataset identifier PXD010609.

References

1. Hoeijmakers, J. H. DNA damage, aging, and cancer. *N Engl J Med* **361**, 1475-1485, (2009).
2. Ceccaldi, R., Rondinelli, B. and D'Andrea, A. D. Repair Pathway Choices and Consequences at the Double-Strand Break. *Trends Cell Biol* **26**, 52-64, (2016).
3. Thompson, L. H. Recognition, signaling, and repair of DNA double-strand breaks produced by ionizing radiation in mammalian cells: the molecular choreography. *Mutat Res* **751**, 158-246, (2012).
4. Frit, P., Barboule, N., Yuan, Y., Gomez, D. and Calsou, P. Alternative end-joining pathway(s): bricolage at DNA breaks. *DNA Repair (Amst)* **17**, 81-97, (2014).
5. Marteijn, J. A., Lans, H., Vermeulen, W. and Hoeijmakers, J. H. Understanding nucleotide excision repair and its roles in cancer and ageing. *Nat Rev Mol Cell Biol* **15**, 465-481, (2014).
6. Jackson, S. P. and Durocher, D. Regulation of DNA damage responses by ubiquitin and SUMO. *Mol. Cell* **49**, 795-807, (2013).
7. Flotho, A. and Melchior, F. Sumoylation: a regulatory protein modification in health and disease. *Annu. Rev. Biochem* **82**, 357-385, (2013).
8. Hickey, C. M., Wilson, N. R. and Hochstrasser, M. Function and regulation of SUMO proteases. *Nat. Rev. Mol. Cell Biol* **13**, 755-766, (2012).
9. Wang, L., Wansleeben, C., Zhao, S. *et al.* SUMO2 is essential while SUMO3 is dispensable for mouse embryonic development. *EMBO Rep* **15**, 878-885, (2014).
10. Hendriks, I. A. and Vertegaal, A. C. A comprehensive compilation of SUMO proteomics. *Nat. Rev. Mol. Cell Biol* **17**, 581-595, (2016).
11. Baba, D., Maita, N., Jee, J. G. *et al.* Crystal structure of thymine DNA glycosylase conjugated to SUMO-1. *Nature* **435**, 979-982, (2005).
12. Steinacher, R. and Schar, P. Functionality of human thymine DNA glycosylase requires SUMO-regulated changes in protein conformation. *Curr. Biol* **15**, 616-623, (2005).
13. Morris, J. R., Boutell, C., Keppler, M. *et al.* The SUMO modification pathway is involved in the BRCA1 response to genotoxic stress. *Nature* **462**, 886-890, (2009).
14. Hoege, C., Pfander, B., Moldovan, G. L., Pyrowolakis, G. and Jentsch, S. RAD6-dependent DNA repair is linked to modification of PCNA by ubiquitin and SUMO. *Nature* **419**, 135-141, (2002).
15. Bergink, S. and Jentsch, S. Principles of ubiquitin and SUMO modifications in DNA repair. *Nature* **458**, 461-467, (2009).
16. Galanty, Y., Belotserkovskaya, R., Coates, J. and Jackson, S. P. RNF4, a SUMO-targeted ubiquitin E3 ligase, promotes DNA double-strand break repair. *Genes Dev* **26**, 1179-1195, (2012).
17. Yin, Y., Seifert, A., Chua, J. S. *et al.* SUMO-targeted ubiquitin E3 ligase RNF4 is required for the response of human cells to DNA damage. *Genes Dev* **26**, 1196-1208, (2012).
18. Poulsen, S. L., Hansen, R. K., Wagner, S. A. *et al.* RNF111/Arkadia is a SUMO-targeted ubiquitin ligase that facilitates the DNA damage response. *J.Cell Biol.* **201**, 797-807, (2013).
19. Wang, Q. E., Zhu, Q., Wani, G. *et al.* DNA repair factor XPC is modified by SUMO-1 and ubiquitin following UV irradiation. *Nucleic Acids Res.* **33**, 4023-4034, (2005).
20. van Cuijk, L., van Belle, G. J., Turkyilmaz, Y. *et al.* SUMO and ubiquitin-dependent XPC exchange drives nucleotide excision repair. *Nat Commun* **6**, 7499, (2015).
21. Groisman, R., Kuraoka, I., Chevallier, O. *et al.* CSA-dependent degradation of CSB by the ubiquitin-proteasome pathway establishes a link between complementation factors of the Cockayne syndrome. *Genes Dev.* **20**, 1429-1434, (2006).
22. Schwertman, P., Lagarou, A., Dekkers, D. H. *et al.* UV-sensitive syndrome protein UVSSA recruits USP7 to regulate transcription-coupled repair. *Nat.Genet.* **44**, 598-602, (2012).
23. Zhang, X., Horibata, K., Saijo, M. *et al.* Mutations in UVSSA cause UV-sensitive syndrome and destabilize ERCC6 in transcription-coupled DNA repair. *Nat.Genet.* **44**, 593-597, (2012).
24. Nakazawa, Y., Sasaki, K., Mitsutake, N. *et al.* Mutations in UVSSA cause UV-sensitive syndrome and impair RNA polymerase IIo processing in transcription-coupled nucleotide-excision repair. *Nat.Genet.* **44**, 586-592, (2012).

25. Hendriks, I. A. and Vertegaal, A. C. Label-Free Identification and Quantification of SUMO Target Proteins. *Methods Mol Biol* **1475**, 171-193, (2016).
26. Hu, H., Yu, Z., Liu, Y. *et al.* The Aurora B kinase in Trypanosoma brucei undergoes post-translational modifications and is targeted to various subcellular locations through binding to TbCPC1. *Mol. Microbiol* **91**, 256-274, (2014).
27. Luo, K., Zhang, H., Wang, L., Yuan, J. and Lou, Z. Sumoylation of MDC1 is important for proper DNA damage response. *EMBO J* **31**, 3008-3019, (2012).
28. Rocha, J. C., Busatto, F. F., Guecheva, T. N. and Saffi, J. Role of nucleotide excision repair proteins in response to DNA damage induced by topoisomerase II inhibitors. *Mutat Res Rev Mutat Res* **768**, 68-77, (2016).
29. Kanamitsu, K. and Ikeda, S. Fission yeast homologs of human XPC and CSB, rhp41 and rhp26, are involved in transcription-coupled repair of methyl methanesulfonate-induced DNA damage. *Genes Genet. Syst* **86**, 83-91, (2011).
30. Bensaude, O. Inhibiting eukaryotic transcription: Which compound to choose? How to evaluate its activity? *Transcription* **2**, 103-108, (2011).
31. Mayne, L. V. and Lehmann, A. R. Failure of RNA synthesis to recover after UV irradiation: an early defect in cells from individuals with Cockayne's syndrome and xeroderma pigmentosum. *Cancer Res* **42**, 1473-1478, (1982).
32. Andrade-Lima, L. C., Veloso, A., Paulsen, M. T., Menck, C. F. and Ljungman, M. DNA repair and recovery of RNA synthesis following exposure to ultraviolet light are delayed in long genes. *Nucleic Acids Res* **43**, 2744-2756, (2015).
33. Dinant, C., de Jager, M., Essers, J. *et al.* Activation of multiple DNA repair pathways by sub-nuclear damage induction methods. *J Cell Sci* **120**, 2731-2740, (2007).
34. Uchimura, Y., Nakamura, M., Sugasawa, K., Nakao, M. and Saitoh, H. Overproduction of eukaryotic SUMO-1- and SUMO-2-conjugated proteins in Escherichia coli. *Anal. Biochem* **331**, 204-206, (2004).
35. Low, J. Y. and Nicholson, H. D. Emerging role of polymerase-1 and transcript release factor (PTRF/ Cavin-1) in health and disease. *Cell Tissue Res* **357**, 505-513, (2014).
36. Liu, L. and Pilch, P. F. PTRF/Cavin-1 promotes efficient ribosomal RNA transcription in response to metabolic challenges. *Elife* **5**, (2016).
37. Bradsher, J., Auriol, J., Proietti de, S. L. *et al.* CSB is a component of RNA pol I transcription. *Mol.Cell* **10**, 819-829, (2002).
38. Vogt, B. and Hofmann, K. Bioinformatical detection of recognition factors for ubiquitin and SUMO. *Methods Mol.Biol.* **832**, 249-261, (2012).
39. Nishida, C., Reinhard, P. and Linn, S. DNA repair synthesis in human fibroblasts requires DNA polymerase delta. *J Biol Chem* **263**, 501-510, (1988).
40. Araujo, S. J., Tirode, F., Coin, F. *et al.* Nucleotide excision repair of DNA with recombinant human proteins: definition of the minimal set of factors, active forms of TFIIH, and modulation by CAK. *Genes Dev* **14**, 349-359, (2000).
41. Kamiuchi, S., Saijo, M., Citterio, E. *et al.* Translocation of Cockayne syndrome group A protein to the nuclear matrix: possible relevance to transcription-coupled DNA repair. *Proc. Natl. Acad. Sci. U. S. A* **99**, 201-206, (2002).
42. Groisman, R., Polanowska, J., Kuraoka, I. *et al.* The ubiquitin ligase activity in the DDB2 and CSA complexes is differentially regulated by the COP9 signalosome in response to DNA damage. *Cell* **113**, 357-367, (2003).
43. Reits, E. A., Vos, J. C., Gromme, M. and Neefjes, J. The major substrates for TAP in vivo are derived from newly synthesized proteins. *Nature* **404**, 774-778, (2000).
44. Schubert, U., Anton, L. C., Gibbs, J. *et al.* Rapid degradation of a large fraction of newly synthesized proteins by proteasomes. *Nature* **404**, 770-774, (2000).
45. Groisman, R., Kuraoka, I., Chevallier, O. *et al.* CSA-dependent degradation of CSB by the ubiquitin-proteasome pathway establishes a link between complementation factors of the Cockayne syndrome. *Genes Dev* **20**, 1429-1434, (2006).
46. Wilson, M. D., Harreman, M. and Svejstrup, J. Q. Ubiquitylation and degradation of elongating RNA polymerase II: the last resort. *Biochim Biophys Acta* **1829**, 151-157, (2013).

47. Anindya, R., Aygun, O. and Svejstrup, J. Q. Damage-induced ubiquitylation of human RNA polymerase II by the ubiquitin ligase Nedd4, but not Cockayne syndrome proteins or BRCA1. *Mol. Cell* **28**, 386-397, (2007).
48. Anindya, R., Mari, P. O., Kristensen, U. *et al.* A ubiquitin-binding domain in Cockayne syndrome B required for transcription-coupled nucleotide excision repair. *Mol.Cell* **38**, 637-648, (2010).
49. Sin, Y., Tanaka, K. and Saijo, M. The C-terminal Region and SUMOylation of Cockayne Syndrome Group B Protein Play Critical Roles in Transcription-coupled Nucleotide Excision Repair. *J. Biol. Chem* **291**, 1387-1397, (2016).
50. Psakhye, I. and Jentsch, S. Protein group modification and synergy in the SUMO pathway as exemplified in DNA repair. *Cell* **151**, 807-820, (2012).
51. Bregman, D. B., Halaban, R., van Gool, A. J. *et al.* UV-induced ubiquitination of RNA polymerase II: a novel modification deficient in Cockayne syndrome cells. *Proc.Natl.Acad.Sci.U.S.A* **93**, 11586-11590, (1996).
52. Pines, A., Dijk, M., Makowski, M. *et al.* TRiC controls transcription resumption after UV damage by regulating Cockayne syndrome protein A. *Nat Commun* **9**, 1040, (2018).
53. Blagoev, B. and Mann, M. Quantitative proteomics to study mitogen-activated protein kinases. *Methods* **40**, 243-250, (2006).
54. Schimmel, J., Eifler, K., Sigurðsson, J. O. *et al.* Uncovering SUMOylation Dynamics during Cell-Cycle Progression Reveals FoxM1 as a Key Mitotic SUMO Target Protein. *Mol. Cell* **53**, 1053-1066, (2014).
55. Xiao, Z., Chang, J. G., Hendriks, I. A. *et al.* System-wide analysis of SUMOylation dynamics in response to replication stress reveals novel SUMO target proteins and acceptor lysines relevant for genome stability. *Mol. Cell Proteomics* **14**, 1419-1434, (2015).
56. Eifler, K., Cuijpers, S. A. G., Willemstein, E. *et al.* SUMO targets the APC/C to regulate transition from metaphase to anaphase. *Nat Commun* **9**, 1119, (2018).
57. Rappsilber, J., Mann, M. and Ishihama, Y. Protocol for micro-purification, enrichment, pre-fractionation and storage of peptides for proteomics using StageTips. *Nat. Protoc* **2**, 1896-1906, (2007).
58. Vizcaino, J. A., Csordas, A., del-Toro, N. *et al.* 2016 update of the PRIDE database and its related tools. *Nucleic Acids Res* **44**, D447-456, (2016).
59. Horibata, K., Saijo, M., Bay, M. N. *et al.* Mutant Cockayne syndrome group B protein inhibits repair of DNA topoisomerase I-DNA covalent complex. *Genes Cells* **16**, 101-114, (2011).

A

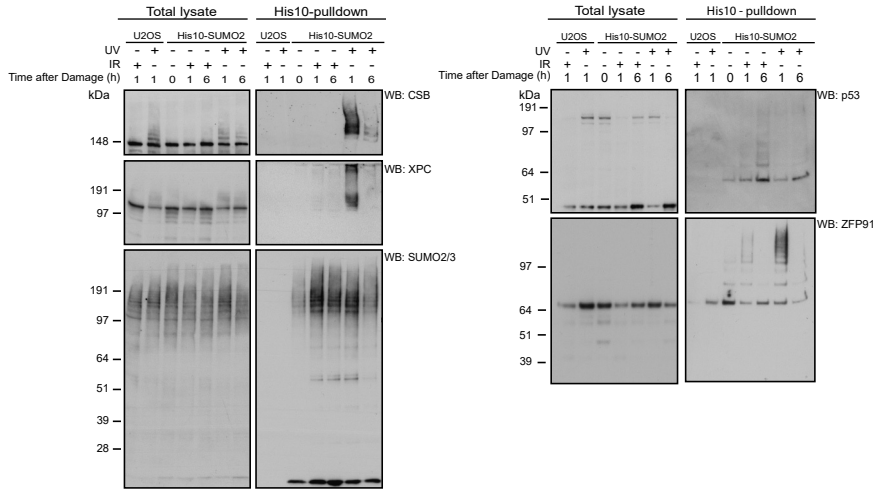

B

	Log2 fold change compared to mock treated control (proteomics)			
Protein	1h after IR	6h after IR	1h after UV	6h after UV
CSB	-0.33	-0.94	10	9.28
XPC	0.18	0.27	1.89	0.09
P53	0.32	0.73	-0.15	0.4
ZFP91	1.56	0.63	1.6	0.68

Figure S1. Validation of dynamic SUMOylation targets in response to IR- or UV-induced DNA damage.
(**A**) U-2 OS cells stably expressing His10-SUMO2 were either irradiated with 20 J/m2 UV-C light or 4 Gy IR. Cells were lysed after 1 h or 6 h recovery time following damage induction. SUMO2 conjugates were enriched by Ni-NTA pulldown. Total lysates and SUMO2-enriched fractions were analysed by immunoblotting using antibodies against CSB, XPC, p53, ZPF91 and SUMO2/3. (**B**) SUMOylation dynamics of CSB, XPC, p53 and ZFP91 (log2) in response to DNA damage as identified by quantitative mass spectrometry. U-2 OS cells stably expressing His10-SUMO2 were either irradiated with 20 J/m2 UV-C light or 4 Gy IR. Cells were lysed after 1 h or 6 h recovery time after damage induction. SUMO2 conjugates were enriched by Ni-NTA pulldown and identified by mass spectrometry.

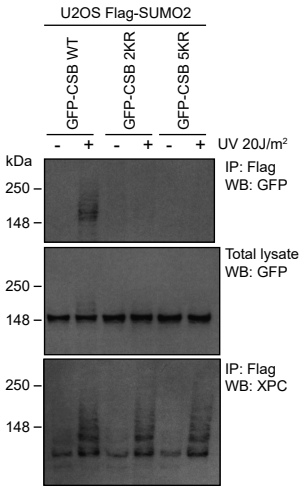

Figure S2. CSB 2KR and 5KR mutants are SUMOylation-deficient.
U-2 OS cells stably expressing Flag-SUMO2 were infected with retrovirus encoding either GFP-CSB wild type (WT) or GFP-CSB lacking the N-terminal lysines K32 and K205 (2KR) or GFP-CSB lacking all the SUMOylation consensus sites (5KR). Cells were lysed and SUMO2 conjugates were enriched by Flag-immunoprecipitation. Total lysates and SUMO2-enriched fractions (IP) were analysed by immunoblotting using antibodies against GFP or XPC.

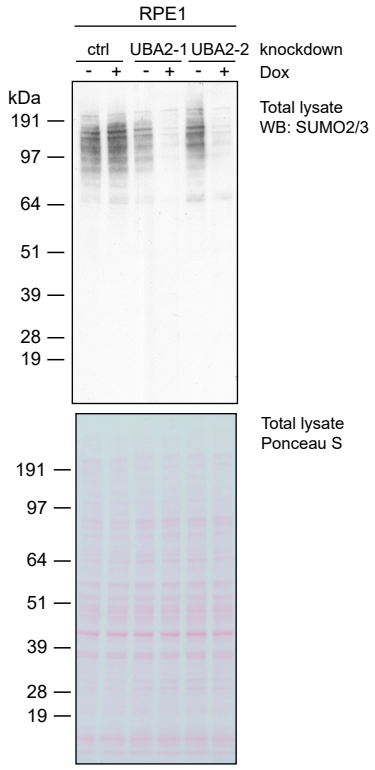

Figure S3. SUMO conjugates are decreased upon knockdown of UbA2.
Immunoblot analysis of RPE1 cells used in Figure 3A. RPE1 cells stably expressing either a (Dox)-inducible non-targeting shRNA (ctrl) or one of two (Dox)-inducible shRNA targeting the SUMO E1 activating enzyme subunit UbA2. Total lysates were analysed by immunoblotting using an antibody against SUMO2/3. A clear reduction in SUMO2/3 conjugates was observed after the depletion of UbA2. Ponceau S stain was used as loading control.

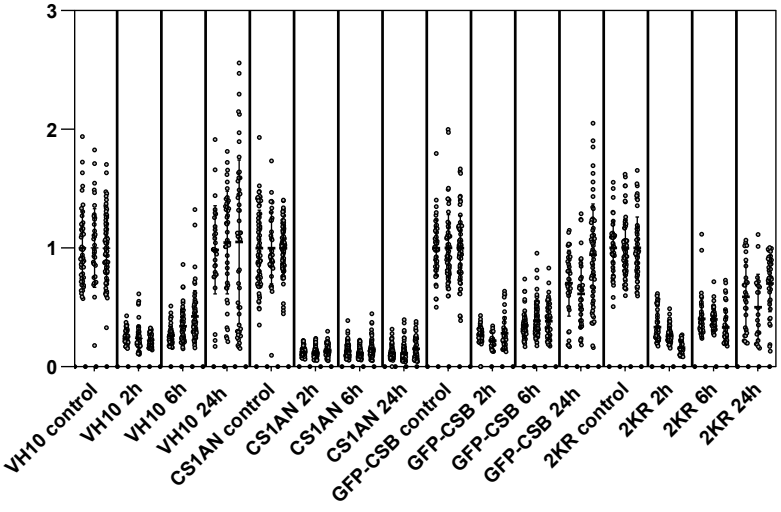

Figure S4. SUMOylation of CSB contributes to efficient transcription recovery after UV damage.
CSB-deficient patient cells (CS1AN) without rescue, or expressing GFP-tagged CSB wild-type or 2KR mutant (K32R, K205R) and VH10 cells were treated with 10 J/m2 UV. Relative RNA synthesis was measured by incorporation of EdU, before UV, and at 2, 6 and 24 h post-UV. All datapoints are shown. Error bars represent SD for each of three independent experiments.

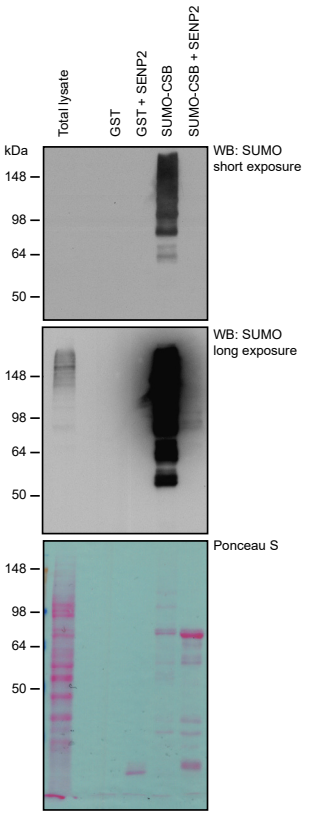

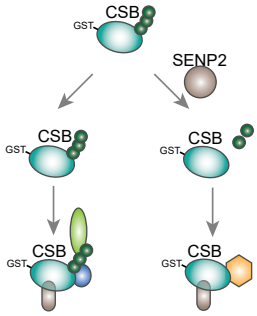

Figure S5. SUMOylation of CSB influences binding to RNA polymerase associated proteins.
Samples used in Figure 4 were analysed by immunoblotting against SUMO2/3. Analysis shows efficient deSUMOylation of SUMOylated CSB by SENP2.

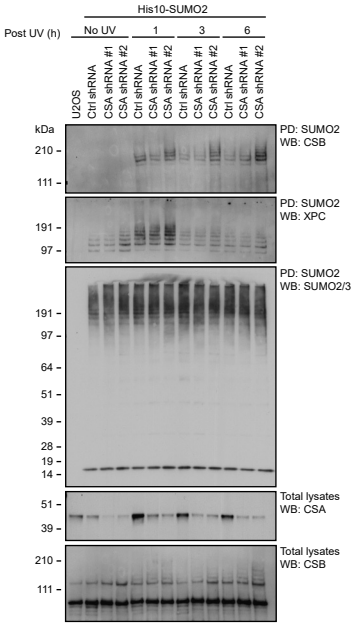

Figure S6. CSA knockdown stabilizes SUMOylated CSB post UV irradiation.
U-2 OS cells stably expressing His10-SUMO2 were transduced with either non-targeting shRNA (ctrl) or one of two independent shRNAs targeting CSA. Cells were left untreated or treated with UV irradiation and lysed at indicated time point post UV. SUMO2 conjugates were enriched by Ni-NTA purification and total lysates and SUMO2-enriched fractions (PD) were analysed by immunoblotting using antibodies against CSB, XPC, SUMO2/3, and CSA.

CHAPTER 6

General Discussion

Frauke Liebelt[1]

[1]Department of Cell and Chemical biology, Leiden University Medical Center, 2300 RC Leiden, The Netherlands.

Proteins are highly important components of the cell. Due to the fast, flexible and transient nature of post-translational protein modifications, such as SUMOylation, the cell can quickly react to extracellular or intracellular changes. SUMOylation plays an important role in systematic cellular changes such as the cell cycle, but is also pivotal for the adaptation to several stresses such as proteotoxic stress or DNA damage. The studies in this thesis investigate how SUMOylation is regulated and how SUMOylation can influence cellular processes. Mechanistic models and hypotheses derived from the data presented in this thesis are summarized and discussed in this chapter.

GROUP MODIFICATION VERSUS SELECTIVITY

The concept of group-modification describes that the biological function of SUMOylation often depends on multiple interactions between SUMOylated and SUMO-interaction motif (SIM)-containing proteins[1]. Therefore, the overall SUMOylation status of a protein complex matters more than the SUMOylation of a single subunit. It also implies that SUMOylation can have a certain degree of site-promiscuity, as for example demonstrated by the SUMOylation of the oncogenic transcription factor, c-Myc[2]. Since the proposal of group modification, seven years ago, researchers have delivered supporting data that SUMOylation often targets functionally or physically related proteins[3-5]. Mass spectrometry offers an ideal tool to study global SUMOylation events and detect clusters of proteins that are targeted by SUMO simultaneously. In this thesis, mass spectrometry was used to uncover SUMOylated proteins that are regulated by a HSF1-dependent mechanism upon heat shock (Chapter 3), by the poly-SUMO specific protease SENP6 (chapter 4) and in response to ultraviolet (UV)-induced or ionizing radiation (IR)-induced DNA damage (chapter 5). In all cases we identified clusters of highly interconnected proteins and protein complexes in which multiple subunits are modified by SUMO. STRING protein interaction analysis of the SUMOylated proteins that we identified to be regulated in a HSF1-dependent manner showed interconnected clusters of proteins involved thyroid hormone signalling, DNA replication or are components of the proteasome (Figure 1). The SUMO protease SENP6 also seems to regulate multiple clusters of proteins, including the constitutive centromere-associated network (CCAN), DNA damage response proteins, proteins involved in ribosomal RNA biogenesis and proteins that regulate DNA replication (Chapter 4, Figure 3). The classical concept of group- modification proposes multiple synergistic SUMO-SIM interactions, by which SUMOylation further stabilizes the interaction between proteins that already have affinity towards each other. Interestingly, in the case of the CCAN proteins, the opposite seems to be true. The SUMOylation of the CCAN proteins does not act as molecular glue but most probably marks the fraction of the CCAN proteins that are not assembled into the protein complex at the centromere and might even be the cause of the disassembly. Still, it is the highly interconnected group of proteins that is targeted for deSUMOylation by the protease SENP6. A possible and intriguing scenario could be that a balanced SUMOylation of the CCAN proteins is needed for the complex to assemble, with SENP6 carefully controlling SUMOylation levels.

In contrast to the group-regulation of the CCAN, it is less clear whether the SUMOylation of CSB upon UV-irradiation is part of a group-SUMOylation event or an isolated modification that functions independently. Although we did not identify UV-induced SUMOylation of obvious CSB-interaction partners, like CSA or RNA polymerase II, we cannot exclude the possibility of CSB being part of a SUMOylation-driven protein complex. For example, we observed the SUMOylation of multiple components of the transcription initiation factor TFIID upon

UV-induced DNA damage (Chapter 5, Figure 1). Both, TFIID and CSB, are associated with RNA polymerase II[6-8], therefore the SUMOylation of the TFIID components and CSB could potentially be connected in a group-like fashion. Not all SUMOylation events target protein groups and the SUMOylation of CSB could be an isolated modification event. Supporting a selective modification by SUMO, is the observation that an uncommonly large fraction of CSB is SUMOylated upon UV treatment, visible by the appearance of higher molecular weight species on the immunoblot without prior enrichment of SUMO conjugates (Chapter 5, Figure 2). Unfortunately, the precise mechanistic consequences of CSB SUMOylation remain elusive as will be elaborated on later within this chapter.

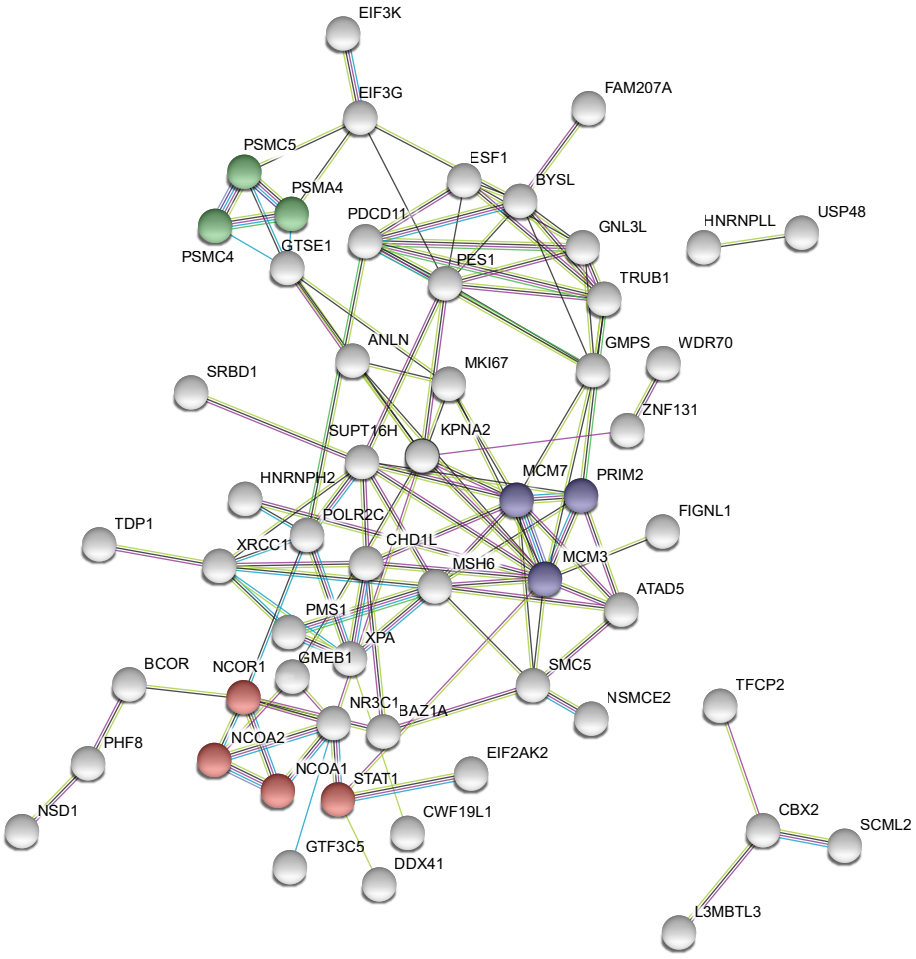

Figure 1. STRING protein-protein interaction network of HSF1-regulated SUMO substrates after heat shock. Each node represents a protein, red nodes indicate proteins involved in thyroid hormone signalling, blue nodes represent proteins involved in DNA replication and green nodes represent proteasome subunits. The edged represent interaction that are based on known interactions from curated databases (blue) or experimentally determined (magenta) or predicted interactions due to gene neighbourhood (green), gene fusions (red) or gene co-occurrence (dark blue). Other types of interactions identified by textmining (light green), co-expression (black) and homology (violet) are depicted as well.

HSF1-DEPENDENT DEGRADATION OF CO-MODIFIED PROTEINS

Proteostasis describes a cellular state in which the synthesis and degradation of proteins are in equilibrium. Proteostasis can be disturbed by an accumulation of denatured proteins due to extracellular stresses, such as heat stress, or genomic causes including the enhanced expression of oncogenes in cancers or expression of aggregation prone mutant proteins often associated with neurodegenerative diseases. The cell has evolved mechanisms to counteract such disturbances and to re-establish proteostasis. A well-studied mechanism to protect proteostasis is the heat-shock response, which is regulated by its master transcription factor heat shock factor 1 (HSF1). HSF1 is responsible for the transcription of proteins that assist directly in the recovery of proteostasis. A major group amongst the HSF1-induced proteins are the heat-shock proteins (HSPs), molecular chaperones that help refold or degrade denatured proteins, which accumulate due to proteotoxic insults such as increased temperature. In chapter 3, we show that SUMOylation and HSF1-controlled proteostasis are linked. Several publications have previously shown that global SUMOylation is induced in cells exposed to heat shock but decreases to normal levels when cells recover at lower temperatures. We show that this decrease of SUMOylation during the recovery of cells is dependent on the activity of HSF1 and the HSPs. This observation let us to speculate on the role of SUMOylation during the heat-shock response. We hypothesize that SUMOylation in concert with ubiquitination, both being able to quickly change properties of proteins, act as a first aid mechanism before HSF1 transcription is fully activated and HSPs are produced in high quantities to re-establish proteostasis. We propose that an unknown HSF1-mediated mechanism specifically targets proteins that are co-modified, by SUMOylation and ubiquitination, for proteasomal degradation. How and why are co-modified proteins degraded in an HSF1-dependent manner? The established co-modified protein is differentially regulated upon heat shock compared to proteins modified by either SUMO or ubiquitin alone, suggesting a distinct property of the co-modified protein. Ubiquitin most likely serves as signal for proteasomal degradation, but the property added by SUMOylation is less clear. Intriguingly, SUMO has been reported to solubilize proteins and is often used as solubility tag for protein purifications[9]. In Chapter 3, we demonstrate that either recombinant fusion of SUMO to a protein or SUMO conjugation increases the solubility of model target proteins in the in-vitro assay used. It is intriguing to think that the cell could exploit this property of SUMOylation in a similar fashion, by solubilizing proteins and making them more accessible to STUbLs, ubiquitination and degradation and therefore counteracting aggregation of unfolded proteins. In line with this theory and as reported in chapter 2, SUMOylation has been implicated to enhance solubility of the disease associated proteins in several neurodegenerative diseases such as the amyloid precursor protein (APP) in Alzheimer's disease or α-synuclein, which forms aggregates in Parkinson's disease[10,11].

Interestingly, several reports suggest that proteotoxic stress-induced transient aggregates can protect the ubiquitin-proteasome system (UPS) from being overwhelmed. Transient aggregates could prevent overload of the UPS system[12-17]. Another ubiquitin-like modifier, Nedd8 promoted the formation of these transient aggregates, which also contained sequestered ubiquitin and SUMO[18]. While Nedd8 stimulates a transient sequestration of proteins, many of which are already ubiquitinated, SUMO could possibly promote solubilisation at a later time point to increase accessibility when the UPS system is less occupied. This hypothesis would also open up a possible role for the HSF1-transcribed HSPs, as they would facilitate refolding and rescuing of proteins and therefore releasing pressure

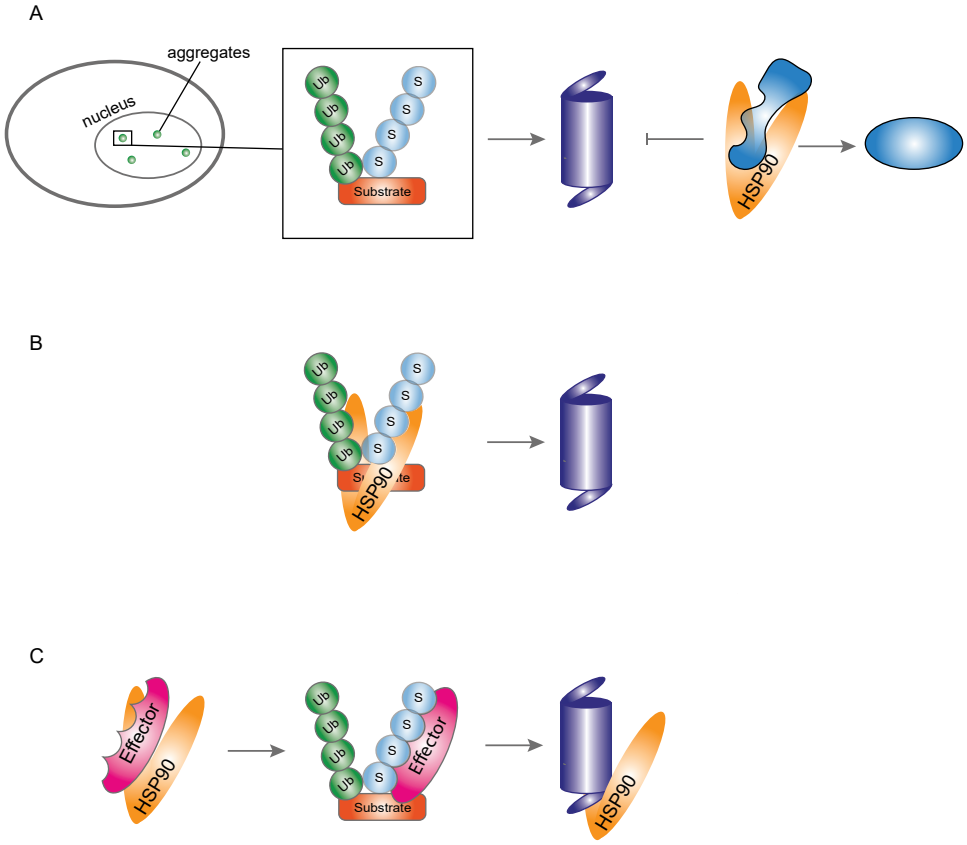

Figure 2. Hypotheses on how HSPs can contribute the proteasomal degradation of co-modified proteins. (A) Upon proteotoxic stress modified proteins are sequestered into nuclear aggregates to prevent overloading of the proteasome. HSP90 contributes to refolding and degradation of unfolded proteins, therefore releasing pressure on the proteasome. SUMO contributes to resolubilize proteins so that they can be targeted for degradation. (**B)** HSP90 selectively binds SUMOylated proteins due to the presence of SIMs and assists in delivery of the substrate to the proteasome. The substrate is marked for degradation by ubiquitin. **C** HSP90 stabilizes proteins which assist in the degradation of co-modified proteins, either proteasomal subunits or unknown SIM-containing effector proteins.

on the UPS and promoting the degradation of the previously sequestered PTM-modified proteins (Figure 2A). Another possibility for the observed HSF1-dependent degradation of co-modified proteins would be that SUMOylation stimulates binding of unidentified effector proteins, facilitating the delivery of the co-modified protein to the proteasome. The HSPs would be interesting effector protein candidates (Figure 2B). We showed that inhibition of HSP90 also prevented the degradation of the co-modified proteins. HSP90, one of the most prevalent molecular chaperones, is mostly reported to protect proteins from degradation rather than promote it, although the opposite was proposed in a few cases[19-21]. HSP90 also has multiple potential SUMO-interaction Motifs (SIMs) making it theoretically possible for it to recognize SUMOylated proteins. HSPs could also be indirectly involved by e.g. stabilizing the unidentified effector proteins that facilitate the degradation of the co-modified proteins (Figure 2C). For example, HSP90 can influence the stability of the proteasome itself[22].

Because global SUMOylation increases not only upon heat shock but also upon proteasomal inhibition and ethanol stress, it is not unlikely that SUMO conjugation fulfils a general role upon these stresses. Previous research already established unfolded proteins to be a common trigger for SUMOylation after inhibition of the proteasome by MG132 and heat shock. SUMOylation also seemed to occur on an overlapping pool of proteins[23], potentially representing proteins prone to unfolding. Insoluble protein inclusion that are induced by MG132 treatment, include SUMO, ubiquitin and HSPs, proposing that a link between the proteostasis network and SUMO conjugation is not limited to the response upon heat shock. Another interesting observation was that K63-linked ubiquitin chains accumulated on SUMOylated proteins upon prolonged treatment with MG132. These ubiquitin chains have been linked to the aggresome-autophagy pathway, which is activated when the capacity of chaperones and UPS is overwhelmed by the amount of misfolded proteins[24-26]. This opens up the possibility of co-modified proteins being additionally regulated by alternative degradation pathways during proteotoxic stress.
Unravelling this intriguing network between SUMOylation, other PTMs, HSPs and the UPS would be greatly beneficial for the development of new treatment options for diseases that are characterized by a disturbed proteostasis. Small molecule inhibitors for most of the players exist and are tested in different contexts and diseases, e.g. cancer, but potentially offer strong tools to be combined in the combat against Alzheimer's, Parkinson's or Huntington's disease.

SUMO CHAINS - DIFFERENT LINKAGE? DIFFERENT STRUCTURE? DIFFERENT EFFECTOR PROTEINS?

The increase of SUMO conjugation as reaction towards stresses is characterized by an increase of SUMO chains[4,27,28]. In the ubiquitin field, chain formation has been intensively studied in the last decade and different types of chains were shown to have different functions. Ubiquitin has seven internal lysines and each can be used as acceptor lysine for ubiquitination. Additionally, ubiquitin can be fused to the N-terminus of another ubiquitin, a phenomenon called linear ubiquitination. Each chain linkage has a set of linkage-specific proteins that can write, read and erase the ubiquitin chain.
Similar to ubiquitin, SUMO can also form polymers. It is believed that SUMO chains predominantly consist of SUMO2 and SUMO3, which both have eight internal lysine[29]. SUMO-SUMO linkages have been identified by mass spectrometry for most of the lysines[30]. Even SUMO1, which is proposed to play a limited role in SUMO chain formation, can be modified by SUMO2/3 at multiple positions. Lysine 11 of SUMO2 and SUMO3 is located in a SUMO consensus motif within their flexible N-termini and is thought to be the predominant site for polymerization[29]. The observation that different linkages can be identified in vivo, raises the possibility of an unexplored diversity of SUMO chain functions, including specific proteins that catalyse distinct chain linkages, recognize different chain structures and specifically target different chains for depolymerization, in other words unidentified writers, readers and erasers, similar to the ubiquitin system. In Chapter 4, we identify poly-SUMOylation targets that are regulated by the polySUMO specific protease, SENP6. We show that SENP6 knockdown leads to the SUMOylation of multiple components of the constitutive centromere-associated network (CCAN), which is the most chromatin-proximal group of proteins within the kinetochore. The accumulation of high-molecular weight species of the CCAN proteins upon SENP6 knockdown strongly suggests the formation of

SUMO chains. We observed that the depletion of SENP6 led to the failure of CCAN proteins to localize to the centromere. Previously, one CCAN subunit, CENP-I was already reported as target for deSUMOylation by SENP6. It was suggested that accumulation of SUMO chains on CENP-I, due to SENP6 depletion, let to the recruitment of the human StUbL RNF4 and the subsequent ubiquitination and proteasomal degradation of CENP-I, explaining the decreased accumulation of CENP-I foci at the centromere[31]. Although, we also observed reduced centromeric accumulation of other CCAN subunits, including CENP-A, CENP-T and CENP-W, at the centromere upon SENP6 knockdown (KD), the underlying cause of this observation seems to be independent of degradation and RNF4. Surprisingly, upon proteasomal inhibition we failed to observe an accumulation of the SUMOylated or the ubiquitinated forms of the CCAN proteins, including for CENP-I. Also, combined knockdown of RNF4 and SENP6 did not result in the expected stabilization of poly-SUMOylated CCAN proteins. These observations led us to believe that the CCAN proteins are not targeted for degradation in a RNF4-dependent manner and their reduced presence at the centromere upon SENP6 KD must be explained by an alternative mechanism. One possibility is that the bulky SUMO chain itself sterically hinders the CCAN proteins to assemble into the tight structure at the centromere. Inhibition of protein interaction by SUMOylation has been reported before and such obstructions would only be enhanced with increasing length of a SUMO polymer[32,33]. The accumulated SUMO polymer on the CCAN proteins could alternatively induce binding to unidentified SIM-containing proteins that prevent their assembly into the CCAN.
Which mechanism prevents the CCAN proteins to efficiently assemble at the centromere, is still to be determined, but the observation that they are not targeted by RNF4 raises the question of what distinguishes the poly-SUMOylated CCAN proteins from poly-SUMOylated proteins that are recognized by RNF4 and degraded, like PML or Mis18BP1[34-37]. Although, we identified the canonical K11-linked SUMO chain on the in vitro SUMOylated CENP-T, we cannot exclude the presence of different linkages nor can we guarantee that the in vitro approach mirrors the situation in vivo. Therefore, it would be interesting to investigate and compare SUMO chain linkage structure of the CCAN subunits and RNF4-targets upon SENP6 depletion in vivo. The recognition of specific chain linkages by STUbLs would be an intriguing explanation for the observed RNF4 specificity. The second human STUbL, RNF111, was shown to mediate K48-linked ubiquitin chains that facilitated degradation and K48-linked and K63-linked ubiquitin chains with non-degradative role[38-40]. These findings demonstrate that the fate of proteins can depend on which STUbL is recruited and which ubiquitin chain is assembled. Different SUMO chain linkages would be an intriguing explanation for differential signalling.

Interestingly, Gärtner et al, recently demonstrated that in addition to the canonical K11-linked SUMO chain the non-canonical K5- and K7-linked SUMO chains can also stimulate RNF4-dependent degradation of PML. Additionally, a RNF4-derived poly-SIM module could be used to purify non-canonical chains from heat shocked cells expressing a SUMO K11R mutant, demonstrating that RNF4 can recognize different chain-linkages[41]. Cells expressing SUMO2 K11Q, an acetylation mimic mutant, show an increased formation of K5- and K35-linked chains upon heat stress and may be able to compensate for the loss of the K11 chain. Also, mutational analysis the yeast Smt3 demonstrated no requirement of specific SUMO chain linkages[42]. These observations indicate at least a partial redundancy of SUMO chain linkages, but do not conclusively exclude distinct roles of different linkages.

SUMOYLATION REGULATES THE INNER KINETOCHORE

The centromere is a pivotal component of eukaryotic chromosomes and necessary for faithful cell division. It marks the position onto which the proteinaceous macromolecular structure of the kinetochore is assembled. The kinetochore forms the microtubule attachment site of the mitotic and meiotic spindle. Chromosomal segregation relies on these bipolar attachments as the sister chromatids are pulled apart during anaphase to ensure that the genetic material is equally divided between the two daughter cells. Most eukaryotes have regional centromeres, which are defined epigenetically by the presence of the histone H3 variant CENP-A. Notable exceptions are centromeres of some budding yeasts, including Saccharomyces cerevisiae, that are defined by specific DNA sequences and are collectively called point centromeres. CENP-A does not only mark the position of regional centromeres but is also necessary for the assembly of all kinetochore components[43-46]. During DNA replication CENP-A is equally divided between the sister chromatids and in human cells new CENP-A molecules are not deposited into the chromatin until G1 phase[47-49]. The incorporation of CENP-A during G1 phase is dependent on the Holliday junction recognition protein (HJURP) and the three subunit Mis18 complex, consisting of Mis18 binding protein 1 (Mis18BP1), Mis18α and Mis18β. CENP-A deposition is directed to sites of pre-existing centromeres by the direct interaction of Mis18BP1 and CENP-A with CENP-C, one of the components of the pre-existing centromere[50,51]. The deposition of CENP-A is additionally regulated by cyclin-dependent kinases (CDKs) and Polo-like kinase mediated phosphorylation events of CENP-A itself, HJURP and the Mis18 complex[52-55].

The constitutive centromere-associated network (CCAN) forms the most chromatin-proximal part of the kinetochore (also called inner kinetochore) and some of its components directly interact with CENP-A. The CCAN contains 16 subunits that can be divided into five subcomplexes, CENP-C, CENP-L-N complex, CENP-H-I-K-M complex, CENP-O-P-Q-U-R complex and CENP-T-W-S-X complex and their localization at the centromere is mostly cell cycle independent[43,56]. In Chapter 4, we describe that 11 of the 16 CCAN subunits are modified by SUMO chains upon knockdown of the polySUMO specific protease SENP6. Although one of the subunits, CENP-I, was identified to be regulated by SENP6 and SUMOylation in an earlier report we uncovered an unexpected and striking group-regulation of the CCAN[31]. SENP6 depletion was shown previously to result in a complete loss of CENP-I, CENP-H and CENP-O at the mitotic centromere[31]. Another recent report showed that SENP6 depletion affected the correct localization of CENP-A, which was mediated indirectly by the RNF4-dependent degradation of poly-SUMOylated Mis18BP1[37]. Our data confirms a reduced CENP-A accumulation at the centromere upon SENP6 depletion and additionally shows a decreased accumulation of CENP-T and CENP-W. Notable here is that whereas we failed to detect any SUMOylation of CENP-A upon SENP6 knockdown, supporting the previously reported indirect regulation by SENP6, the polySUMOylated forms of most of the CCAN proteins highly increased. This observation indicates that the CCAN proteins are directly regulated by SENP6. The recruitment of all CCAN proteins depend on CENP-A but vice versa CENP-C, CENP-N and CENP-I can influence the positioning of CENP-A to the centromeric chromatin[50,51,56-58]. Further CCAN assembly does not follow a linear hierarchy but depends on a complicated network of dynamic interactions between the subcomplexes, CENP-A and centromeric DNA[59,60]. It is therefore difficult to conclusively identify the underlying cause of the reduced centromere accumulation of the CCAN proteins upon SENP6 knockdown. Double knockdown of RNF4 and SENP6 was reported to result in a substantial rescue of the SENP6

depletion phenotype, demonstrating a clear involvement of RNF4-dependent regulation[37]. However, we demonstrate that the polySUMOylated CCAN proteins are not regulated by RNF4. Therefore, a combination of the RNF4-mediated processes, like the degradation of Mis18BP1, and a poly-SUMO-induced sterical restriction of the CCAN proteins is a possible scenario. Whatever the mechanism, it has become clear that the deSUMOylation of proteins plays an important role in the regulation of the CCAN assembly. Future studies will also have to investigate why these proteins are SUMOylated in the first place.

CSB SUMOYLATION MIGHT INFLUENCE PROTEIN INTERACTIONS

In chapter 5 we identified CSB as the most dynamically SUMOylated target upon UV-induced DNA damage. We show that CSB SUMOylation is dependent on transcription and that other DNA lesions, possibly interfering with the progression of elongating RNA polymerase, also cause CSB SUMOylation. Also, we observed reduced efficiency of recruitment and/or retention of SUMO-deficient CSB at the lesion site, suggesting altered binding properties of CSB to other proteins or to the chromatin. A few protein interactions seemed to be influenced by the SUMOylation of CSB (Chapter, Figure 4). For example, two subunits of the polymerase-associated factor (Paf) 1 complex, Paf1 and Leo1, showed enhanced binding to the SUMOylated CSB N-terminus. The Paf1 complex influences multiple steps of RNA polymerase II (RNAPII) transcription, including promotor-proximal pausing, elongation and termination. The functionality of the Paf1 complex is multifaced and can have positive as well as negative influence on transcription levels[61]. A connection between CSB and Paf1 complex has not been reported before and it would be highly interesting to study this interaction in the context of the fate of stalled RNA polymerase II upon transcription-obstructing DNA lesion. Interestingly, we also identified Pol I and transcript release factor (PTRF) to preferentially bind SUMOylated CSB. PTRF regulates the termination of RNA polymerase I transcription[62,63]. Therefore, our findings link the SUMOylation of CSB to regulatory processes of both, RNA polymerase I and II. Proteins that were identified binding preferentially to unmodified CSB included the proliferating cell nuclear antigen (PCNA), which recruits DNA polymerases for the gap filling step during NER, and PolR2H, a subunit of RNA polymerase I, II and III. The significance of these interactions and the role of SUMOylation need to be further evaluated but these findings indicate a possible new layer of PTM regulation during transcription-coupled nucleotide excision repair.

BALANCE BETWEEN INHIBITION AND STIMULATION

SUMOylation has evolved as important regulator of many nuclear processes, some of which have been investigated in this thesis, including proteostasis[64,65], cell cycle control[66] and DNA damage[67]. The SUMOylation pathway is essential and mouse embryos lacking the SUMO E2 conjugating enzyme Ubc9 die at the early implantation stage[68]. Knockdown of Ubc9 or the SUMO E1 activating enzyme subunit SAE1 in human cells, led to a severe reduction of cell proliferation without affecting any specific cell cycle phase[69,70], demonstrating the importance of SUMOylation for each cell cycle phase. Cancer cells, as being highly proliferative, especially depend on SUMOylation[71,72]. This is reflected by the finding that components of the SUMO conjugation cycle are upregulated in many cancers, and drugs targeting the SUMO machinery to block SUMOylation are currently under investigation as anti-cancer treatments[66]. For example, the SUMO E1 conjugating enzyme inhibitor ginkgolic

acid was demonstrated to be effective in Notch-driven breast cancer cells[73,74] and a recently developed potent and selective SAE1 inhibitor demonstrated reduced proliferation of multiple cancer cell lines, by causing mitotic defects [75]. In chapter 4, we show that depletion of SENP6 leads to reduced proliferation with a subtle but reproducible G2-M arrest. SENP6 is essential for cell survival and mitotic progression[31,76,77]. Similar to the overexpression of SUMO conjugation enzymes, the overexpression of deSUMOylation enzymes has been connected to multiple cancers, demonstrating that the equilibrium of SUMOylation is important for cell viability[66]. Tipping the scale towards one or the other direction could be a promising strategy against cancer cell proliferation since cancer cells appear to be especially dependent on SUMOylation. As discussed in chapter 2 and 3, SUMO can have a potentially beneficial role during cellular stresses and neurodegenerative diseases. Inhibition of SUMO proteases could be a potential strategy to increase the neuroprotective role of SUMOylation or in cases where SUMO was shown to have a disadvantageous effect, inhibitors like the SAE1 inhibitor could be of great interest. In conclusion, SUMO affects multiple cellular pathways and hundreds of proteins and consequences of SUMOylation or deSUMOylation inhibition are difficult to predict and have to be carefully investigated in the context of the particular subjective.

References

1. Jentsch, S. and Psakhye, I. Control of nuclear activities by substrate-selective and protein-group SUMOylation. Annu. Rev. Genet 47, 167-186, (2013).
2. Gonzalez-Prieto, R., Cuijpers, S. A., Kumar, R., Hendriks, I. A. and Vertegaal, A. C. c-Myc is targeted to the proteasome for degradation in a SUMOylation-dependent manner, regulated by PIAS1, SENP7 and RNF4. Cell Cycle 14, 1859-1872, (2015).
3. Psakhye, I. and Jentsch, S. Protein group modification and synergy in the SUMO pathway as exemplified in DNA repair. Cell 151, 807-820, (2012).
4. Hendriks, I. A., D'Souza, R. C., Yang, B. et al. Uncovering global SUMOylation signaling networks in a site-specific manner. Nat. Struct. Mol. Biol 21, 927-936, (2014).
5. Johnson, E. S. and Blobel, G. Cell cycle-regulated attachment of the ubiquitin-related protein SUMO to the yeast septins. J. Cell Biol 147, 981-994, (1999).
6. van Gool, A. J., Citterio, E., Rademakers, S. et al. The Cockayne syndrome B protein, involved in transcription-coupled DNA repair, resides in an RNA polymerase II-containing complex. The EMBO journal 16, 5955-5965, (1997).
7. Tantin, D., Kansal, A. and Carey, M. Recruitment of the putative transcription-repair coupling factor CSB/ERCC6 to RNA polymerase II elongation complexes. Mol. Cell Biol 17, 6803-6814, (1997).
8. Thomas, M. C. and Chiang, C. M. The general transcription machinery and general cofactors. Critical reviews in biochemistry and molecular biology 41, 105-178, (2006).
9. Kuo, D., Nie, M. and Courey, A. J. SUMO as a solubility tag and in vivo cleavage of SUMO fusion proteins with Ulp1. Methods Mol. Biol 1177, 71-80, (2014).
10. Zhang, Y. Q. and Sarge, K. D. Sumoylation of amyloid precursor protein negatively regulates Abeta aggregate levels. Biochem. Biophys. Res. Commun 374, 673-678, (2008).
11. Krumova, P., Meulmeester, E., Garrido, M. et al. Sumoylation inhibits alpha-synuclein aggregation and toxicity. J. Cell Biol 194, 49-60, (2011).
12. Deriziotis, P., Andre, R., Smith, D. M. et al. Misfolded PrP impairs the UPS by interaction with the 20S proteasome and inhibition of substrate entry. The EMBO journal 30, 3065-3077, (2011).
13. Lindersson, E. K., Hojrup, P., Gai, W. P. et al. alpha-Synuclein filaments bind the transcriptional regulator HMGB-1. Neuroreport 15, 2735-2739, (2004).
14. Bennett, E. J., Bence, N. F., Jayakumar, R. and Kopito, R. R. Global impairment of the ubiquitin-proteasome system by nuclear or cytoplasmic protein aggregates precedes inclusion body formation. Molecular cell 17, 351-365, (2005).
15. Kim, Y. E., Hosp, F., Frottin, F. et al. Soluble Oligomers of PolyQ-Expanded Huntingtin Target a Multiplicity of Key Cellular Factors. Molecular cell 63, 951-964, (2016).
16. Schipper-Krom, S., Juenemann, K. and Reits, E. A. The Ubiquitin-Proteasome System in Huntington's Disease: Are Proteasomes Impaired, Initiators of Disease, or Coming to the Rescue? Biochemistry research international 2012, 837015, (2012).
17. Treusch, S., Cyr, D. M. and Lindquist, S. Amyloid deposits: protection against toxic protein species? Cell cycle 8, 1668-1674, (2009).
18. Maghames, C. M., Lobato-Gil, S., Perrin, A. et al. NEDDylation promotes nuclear protein aggregation and protects the Ubiquitin Proteasome System upon proteotoxic stress. Nature communications 9, 4376, (2018).
19. Whittier, J. E., Xiong, Y., Rechsteiner, M. C. and Squier, T. C. Hsp90 enhances degradation of oxidized calmodulin by the 20 S proteasome. The Journal of biological chemistry 279, 46135-46142, (2004).
20. Goasduff, T. and Cederbaum, A. I. CYP2E1 degradation by in vitro reconstituted systems: role of the molecular chaperone hsp90. Archives of biochemistry and biophysics 379, 321-330, (2000).
21. Sha, L., Wang, X., Li, J. et al. Pharmacologic inhibition of Hsp90 to prevent GLT-1 degradation as an effective therapy for epilepsy. The Journal of experimental medicine 214, 547-563, (2017).
22. Imai, J., Maruya, M., Yashiroda, H., Yahara, I. and Tanaka, K. The molecular chaperone Hsp90 plays a role in the assembly and maintenance of the 26S proteasome. The EMBO journal 22, 3557-3567, (2003).
23. Tatham, M. H., Matic, I., Mann, M. and Hay, R. T. Comparative proteomic analysis identifies a role for SUMO in protein quality control. Sci. Signal 4, rs4, (2011).

24. Kopito, R. R. Aggresomes, inclusion bodies and protein aggregation. Trends Cell Biol 10, 524-530, (2000).
25. Iwata, A., Riley, B. E., Johnston, J. A. and Kopito, R. R. HDAC6 and microtubules are required for autophagic degradation of aggregated huntingtin. The Journal of biological chemistry 280, 40282-40292, (2005).
26. Olzmann, J. A. and Chin, L. S. Parkin-mediated K63-linked polyubiquitination: a signal for targeting misfolded proteins to the aggresome-autophagy pathway. Autophagy 4, 85-87, (2008).
27. Saitoh, H. and Hinchey, J. Functional heterogeneity of small ubiquitin-related protein modifiers SUMO-1 versus SUMO-2/3. J. Biol. Chem 275, 6252-6258, (2000).
28. Golebiowski, F., Matic, I., Tatham, M. H. et al. System-wide changes to SUMO modifications in response to heat shock. Sci. Signal 2, ra24, (2009).
29. Tatham, M. H., Jaffray, E., Vaughan, O. A. et al. Polymeric chains of SUMO-2 and SUMO-3 are conjugated to protein substrates by SAE1/SAE2 and Ubc9. J. Biol. Chem 276, 35368-35374, (2001).
30. Hendriks, I. A. and Vertegaal, A. C. A comprehensive compilation of SUMO proteomics. Nat. Rev. Mol. Cell Biol 17, 581-595, (2016).
31. Mukhopadhyay, D., Arnaoutov, A. and Dasso, M. The SUMO protease SENP6 is essential for inner kinetochore assembly. J. Cell Biol 188, 681-692, (2010).
32. Moldovan, G. L., Pfander, B. and Jentsch, S. PCNA controls establishment of sister chromatid cohesion during S phase. Mol. Cell 23, 723-732, (2006).
33. Liu, X., Chen, W., Wang, Q., Li, L. and Wang, C. Negative regulation of TLR inflammatory signaling by the SUMO-deconjugating enzyme SENP6. PLoS Pathog 9, e1003480, (2013).
34. Tatham, M. H., Geoffroy, M. C., Shen, L. et al. RNF4 is a poly-SUMO-specific E3 ubiquitin ligase required for arsenic-induced PML degradation. Nat. Cell Biol 10, 538-546, (2008).
35. Weisshaar, S. R., Keusekotten, K., Krause, A. et al. Arsenic trioxide stimulates SUMO-2/3 modification leading to RNF4-dependent proteolytic targeting of PML. FEBS Lett 582, 3174-3178, (2008).
36. Cuijpers, S. A. G., Willemstein, E. and Vertegaal, A. C. O. Converging Small Ubiquitin-like Modifier (SUMO) and Ubiquitin Signaling: Improved Methodology Identifies Co-modified Target Proteins. Mol Cell Proteomics 16, 2281-2295, (2017).
37. Fu, H., Liu, N., Dong, Q. et al. SENP6-mediated M18BP1 deSUMOylation regulates CENP-A centromeric localization. Cell Res 29, 254-257, (2019).
38. Poulsen, S. L., Hansen, R. K., Wagner, S. A. et al. RNF111/Arkadia is a SUMO-targeted ubiquitin ligase that facilitates the DNA damage response. J. Cell Biol 201, 797-807, (2013).
39. Sun, H. and Hunter, T. Poly-small ubiquitin-like modifier (PolySUMO)-binding proteins identified through a string search. J. Biol. Chem 287, 42071-42083, (2012).
40. McIntosh, D. J., Walters, T. S., Arinze, I. J. and Davis, J. Arkadia (RING Finger Protein 111) Mediates Sumoylation-Dependent Stabilization of Nrf2 Through K48-Linked Ubiquitination. Cellular physiology and biochemistry : international journal of experimental cellular physiology, biochemistry, and pharmacology 46, 418-430, (2018).
41. Gartner, A., Wagner, K., Holper, S. et al. Acetylation of SUMO2 at lysine 11 favors the formation of non-canonical SUMO chains. EMBO reports 19, (2018).
42. Newman, H. A., Meluh, P. B., Lu, J. et al. A high throughput mutagenic analysis of yeast sumo structure and function. PLoS genetics 13, e1006612, (2017).
43. Musacchio, A. and Desai, A. A Molecular View of Kinetochore Assembly and Function. Biology 6, (2017).
44. Fachinetti, D., Folco, H. D., Nechemia-Arbely, Y. et al. A two-step mechanism for epigenetic specification of centromere identity and function. Nature cell biology 15, 1056-1066, (2013).
45. Liu, S. T., Rattner, J. B., Jablonski, S. A. and Yen, T. J. Mapping the assembly pathways that specify formation of the trilaminar kinetochore plates in human cells. The Journal of cell biology 175, 41-53, (2006).
46. Regnier, V., Vagnarelli, P., Fukagawa, T. et al. CENP-A is required for accurate chromosome segregation and sustained kinetochore association of BubR1. Molecular and cellular biology 25, 3967-3981, (2005).
47. Falk, S. J., Guo, L. Y., Sekulic, N. et al. Chromosomes. CENP-C reshapes and stabilizes CENP-A nucleosomes at the centromere. Science 348, 699-703, (2015).
48. Jansen, L. E., Black, B. E., Foltz, D. R. and Cleveland, D. W. Propagation of centromeric chromatin requires exit from mitosis. The Journal of cell biology 176, 795-805, (2007).

49. Bodor, D. L., Valente, L. P., Mata, J. F., Black, B. E. and Jansen, L. E. Assembly in G1 phase and long-term stability are unique intrinsic features of CENP-A nucleosomes. Molecular biology of the cell 24, 923-932, (2013).
50. Dambacher, S., Deng, W., Hahn, M. et al. CENP-C facilitates the recruitment of M18BP1 to centromeric chromatin. Nucleus 3, 101-110, (2012).
51. Moree, B., Meyer, C. B., Fuller, C. J. and Straight, A. F. CENP-C recruits M18BP1 to centromeres to promote CENP-A chromatin assembly. The Journal of cell biology 194, 855-871, (2011).
52. McKinley, K. L. and Cheeseman, I. M. Polo-like kinase 1 licenses CENP-A deposition at centromeres. Cell 158, 397-411, (2014).
53. Silva, M. C., Bodor, D. L., Stellfox, M. E. et al. Cdk activity couples epigenetic centromere inheritance to cell cycle progression. Developmental cell 22, 52-63, (2012).
54. Muller, S., Montes de Oca, R., Lacoste, N. et al. Phosphorylation and DNA binding of HJURP determine its centromeric recruitment and function in CenH3(CENP-A) loading. Cell reports 8, 190-203, (2014).
55. Yu, Z., Zhou, X., Wang, W. et al. Dynamic phosphorylation of CENP-A at Ser68 orchestrates its cell-cycle-dependent deposition at centromeres. Developmental cell 32, 68-81, (2015).
56. McKinley, K. L. and Cheeseman, I. M. The molecular basis for centromere identity and function. Nat Rev Mol Cell Biol 17, 16-29, (2016).
57. Carroll, C. W., Milks, K. J. and Straight, A. F. Dual recognition of CENP-A nucleosomes is required for centromere assembly. The Journal of cell biology 189, 1143-1155, (2010).
58. Carroll, C. W., Silva, M. C., Godek, K. M., Jansen, L. E. and Straight, A. F. Centromere assembly requires the direct recognition of CENP-A nucleosomes by CENP-N. Nature cell biology 11, 896-902, (2009).
59. McKinley, K. L., Sekulic, N., Guo, L. Y. et al. The CENP-L-N Complex Forms a Critical Node in an Integrated Meshwork of Interactions at the Centromere-Kinetochore Interface. Mol Cell 60, 886-898, (2015).
60. Nagpal, H., Hori, T., Furukawa, A. et al. Dynamic changes in CCAN organization through CENP-C during cell-cycle progression. Molecular biology of the cell 26, 3768-3776, (2015).
61. Van Oss, S. B., Cucinotta, C. E. and Arndt, K. M. Emerging Insights into the Roles of the Paf1 Complex in Gene Regulation. Trends Biochem Sci 42, 788-798, (2017).
62. Low, J. Y. and Nicholson, H. D. Emerging role of polymerase-1 and transcript release factor (PTRF/ Cavin-1) in health and disease. Cell Tissue Res 357, 505-513, (2014).
63. Liu, L. and Pilch, P. F. PTRF/Cavin-1 promotes efficient ribosomal RNA transcription in response to metabolic challenges. Elife 5, (2016).
64. Liebelt, F. and Vertegaal, A. C. Ubiquitin-dependent and independent roles of SUMO in proteostasis. Am. J. Physiol Cell Physiol 311, C284-C296, (2016).
65. Liebelt, F., Sebastian, R. M., Moore, C. L. et al. SUMOylation and the HSF1-Regulated Chaperone Network Converge to Promote Proteostasis in Response to Heat Shock. Cell reports 26, 236-249 e234, (2019).
66. Eifler, K. and Vertegaal, A. C. SUMOylation-Mediated Regulation of Cell Cycle Progression and Cancer. Trends Biochem. Sci 40, 779-793, (2015).
67. Jackson, S. P. and Durocher, D. Regulation of DNA damage responses by ubiquitin and SUMO. Mol. Cell 49, 795-807, (2013).
68. Nacerddine, K., Lehembre, F., Bhaumik, M. et al. The SUMO pathway is essential for nuclear integrity and chromosome segregation in mice. Dev. Cell 9, 769-779, (2005).
69. Neyret-Kahn, H., Benhamed, M., Ye, T. et al. Sumoylation at chromatin governs coordinated repression of a transcriptional program essential for cell growth and proliferation. Genome Res 23, 1563-1579, (2013).
70. Schimmel, J., Eifler, K., Sigurðsson, J. O. et al. Uncovering SUMOylation Dynamics during Cell-Cycle Progression Reveals FoxM1 as a Key Mitotic SUMO Target Protein. Mol. Cell 53, 1053-1066, (2014).
71. Liu, X., Xu, Y., Pang, Z. et al. Knockdown of SUMO-activating enzyme subunit 2 (SAE2) suppresses cancer malignancy and enhances chemotherapy sensitivity in small cell lung cancer. J. Hematol. Oncol 8, 67, (2015).
72. He, X., Riceberg, J., Pulukuri, S. M. et al. Characterization of the loss of SUMO pathway function on cancer cells and tumor proliferation. PLoS One 10, e0123882, (2015).
73. Fukuda, I., Ito, A., Hirai, G. et al. Ginkgolic acid inhibits protein SUMOylation by blocking formation of the E1-SUMO intermediate. Chem. Biol 16, 133-140, (2009).
74. Licciardello, M. P., Mullner, M. K., Durnberger, G. et al. NOTCH1 activation in breast cancer confers sensitivity to inhibition of SUMOylation. Oncogene doi: 10.1038/onc.2014.319, (2014).

75. He, X., Riceberg, J., Soucy, T. et al. Probing the roles of SUMOylation in cancer cell biology by using a selective SAE inhibitor. Nat Chem Biol 13, 1164-1171, (2017).
76. Hattersley, N., Shen, L., Jaffray, E. G. and Hay, R. T. The SUMO protease SENP6 is a direct regulator of PML nuclear bodies. Mol. Biol. Cell 22, 78-90, (2011).
77. Hart, T., Chandrashekhar, M., Aregger, M. et al. High-Resolution CRISPR Screens Reveal Fitness Genes and Genotype-Specific Cancer Liabilities. Cell 163, 1515-1526, (2015).

6

GENERAL DISCUSSION

APPENDIX &

NEDERLANDSE SAMENVATTING

Eiwitten zijn de werkers van de cel. Ons DNA codeert voor minimaal 20.000 (geschat tot 100.000) verschillende eiwitten met verschillende functies in de cel. Alle eiwitten bestaan uit een combinatie van 20 verschillende moleculaire bouwstenen, de aminozuren. Door deze verschillende combinaties heeft ieder eiwit een unieke structuur en functie.
De functie van eiwitten is dynamisch en kan afhankelijk van de toestand van de cel, ook na de synthese van het eiwit kortstondig veranderd worden, vaak door een verandering van de structuur. Deze verandering noemt men post-translationele modificaties (PTM). SUMOylering en *ubiquitinering*, twee van vele verschillenden PTMs, worden in dit proefschrift nader onderzocht. De mechanismen van deze twee processen lijken op elkaar en bestaan uit het binden van de kleine eiwitten ubiquitine en SUMO (Small Ubiquitin-like MOdifier) aan één of meerdere lysines (een aminozuur) die zich in de sequentie van het doeleiwit bevinden. Door structurele veranderingen kan de functie van het doeleiwit beïnvloed worden en deze functieverandering is sterk afhankelijk van het doeleiwit en het modificerende eiwit. Bijvoorbeeld, de ubiquitinering van eiwitten leidt in veel gevallen tot een gereguleerde degradatie. Maar ubiquitinering en SUMOylering kunnen ook andere functionele consequenties hebben, bijvoorbeeld een verandering van bindingsplekken welke de interactie met andere eiwitten kan stimuleren of tegen kan houden. Om te begrijpen waarom eiwitten met SUMO gemarkeerd worden, helpt het om de identiteit van deze eiwitten te kennen. In dit proefschrift is hiervoor een eerder ontwikkelde techniek gebruikt om eerst geSUMOyleerde eiwitten uit de cel te isoleren en deze in vervolg te identificeren met massa spectrometrie. Elk hoofdstuk begint met de identificatie van geSUMOyleerde eiwitten onder bepaalde omstandigheden om vervolgens de functionele consequenties van deze modificaties te achterhalen.

Hoofdstuk 1 biedt een uitgebreide introductie over PTMs en SUMOylering, de betrokkene enzymen en de, voor dit proefschift, relevante biologische processen. Het biedt een basiskennis die aan de onderzoeksresultaten in hoofdstuk 3, 4 en 5 te gronde liggen.
Proteostase is het evenwicht tussen de synthese, het vouwen, het transporteren en de afbraak van eiwitten. **Hoofdstuk 2** biedt een samenvatting van bestaande literatuur over hoe SUMOylering onafhankelijk, of in samenwerking met ubiquitinering betrokken is bij de regulatie van proteostase.

In **hoofdstuk 3** vragen wij waarom de SUMOylering van honderden eiwitten toeneemt als cellen aan hoge temperaturen blootgesteld worden. Verhoogde temperaturen kunnen ertoe leiden dat eiwitten ontvouwen, ook denaturatie genoemd, en daardoor hun functie verliezen. Om dit te voorkomen, en de overlevingskansen van de cel te vergroten, reageert de cel met de hitteschok respons. Dit proces leidt tot de expressie van eiwitten die gedenatureerde eiwitten kunnen beschermen, hervouwen of ervoor zorgen dat beschadigde eiwitten gecontroleerd worden afgebroken. Onze resultaten tonen aan dat de SUMOylering van vele eiwitten langer aanhoudt als de hitteschok respons en het proteostase netwerk niet functioneel zijn. Verder laten we zien dat vele geSUMOyleerde eiwitten ook geubiquitineerd zijn en dat de SUMOylering waarschijnlijk bijdraagt aan de oplosbaarheid en de toegankelijkheid van deze eiwitten. Dit voorkomt dat ontvouwen eiwitten aggregaten vormen die moeilijk op te lossen zijn voor de cel. Zo ondersteunt de SUMOylering van eiwitten na een hitteschok het herstellen van proteostase.

Hoofdstuk 4 beschrijft de identificatie van geSUMOylerde eiwitten, die door de SUMO-protease SENP6 gereguleerd zijn. Het SUMO-eiwit kan zichzelf SUMOyleren en daardoor ontstaan SUMO-kettingen die doeleiwitten kunnen markeren. De functie van SUMO-kettingen is in tegenstelling tot ubiquitine-kettingen weinig onderzocht. Tot nu toe zijn SUMO-kettingen voornamelijk bekend als indirect signaal voor de degradatie van het doeleiwit. Een belangrijk eiwit in dit proces is de ubiquitine ligase RNF4. RNF4 heeft drie naast-elkaar liggende bindingplekken voor SUMO, en conjugeert daardoor ubiquitine gericht op eiwitten die met SUMO-kettingen gemarkeerd zijn. SUMO-proteasen kunnen SUMO van gemarkeerde eiwitten verwijderen en de twee SUMO-proteasen SENP6 en SENP7 doen dit specifiek voor SUMO-kettingen. De SUMOylering van SENP6- en SENP7-gereguleerde eiwitten is kortstondig en zijn daardoor onder normale omstandigheden moeilijk te detecteren. Om deze eiwitten alsnog te kunnen identificeren hebben we de expressie van SENP6 in de cel gereduceerd. Dit leidde tot een accumulatie van met SUMO-kettingen gemodificeerde eiwitten die we met behulp van massa spectrometrie konden identificeren. Wij ontdekten dat meerdere leden van het Constitutive-Centromer-Associated Network (CCAN), een belangrijk centromeer eiwitcomplex, door SUMO-kettingen gemodificeerd zijn en deze door SENP6 gereguleerd worden. Niet verwijderde SUMO-kettingen voorkomen een correcte lokalisatie van de CCAN-eiwitten, maar leiden niet tot een RNF4-afhankelijke degradatie. Wij stellen voor dat geSUMOyleerde CCAN-eiwitten door sterische hinder niet in staat zijn om een correct eiwitcomplex op het centromeer te vormen. SENP6 zorgt ervoor dat het complex kan ontstaan, de integriteit van het centromeer gewaarborgd is en bevorderd daardoor een correcte celdeling.

SUMOylering is belangrijk in vele cellulaire processen, zo ook bij het repareren van DNA schade. Ons DNA, dat in elke cel te vinden is, is altijd in gevaar om beschadigd te worden. De cel heeft meerdere mechanismen om DNA schade te repareren. Bijvoorbeeld kan DNA schade geïnduceerd door ultraviolet licht (UV) door nucleotide-excision repair (NER) herstelt worden. In **hoofdstuk 5** gaan wij op zoek naar eiwitten die geSUMOyleerd worden nadat DNA schade is toegebracht, door cellen te behandeld met UV straling of ioniserende straling (IR). Meerdere eiwitten werden geïdentificeerd en één eiwit vertoonde de hoogste SUMOylering na UV straling en werd gekozen voor vervolg onderzoek: cockayne syndrome B (CSB). CSB is een belangrijk eiwit in NER en mutaties in CSB die het verlies van CSB-functie als gevolg hebben, zijn verantwoordelijk voor de verouderingsziekte Cockayne Syndroom. Wij tonen aan dat SUMOylering van CSB geen essentiële rol speelt tijdens NER, maar wel bijdraagt aan de efficiëntie van het mechanisme. Ook laten wij zien dat CSA, een ander belangrijk eiwit in NER, de stabiliteit van geSUMOyleerd CSB kan beïnvloeden. Deze invloed is indirect, en is mogelijk een consequentie van de invloed van CSA op RNA polymerase 2, ook een belangrijk eiwit in NER. Vervolg experimenten zijn nodig om dit proces beter te kunnen begrijpen, de rol van CSB-SUMOylering te achterhalen en het samenspel van CSB en de andere betrokkenen eiwitten te analyseren.

Hoofdstuk 6 neemt een kritische kijk op de experimentele data en bespreekt hoe de data in de overige literatuur past. Hypothetische modellen, die op basis van de experimentele data in dit proefschrift opgebouwd zijn, worden behandeld en bediscussieerd. Verder onderzoek moet aantonen of deze modellen de werkelijkheid weerspiegelen.

DEUTSCHE ZUSAMMENFASSUNG

Proteine sind die Arbeiter der Zelle. Unsere DNA codiert für minimal 20 000 verschiedene Proteine mit unterschiedlichen Funktionen in der Zelle. Unterschiedliche Kombinationen aus 20 verschiedenen molekularen Bausteinen, den Aminosäuren, geben jedem Protein eine einzigartige Struktur und Funktion.
Proteinfunktionen sind nicht statisch und können je nach Gebrauch, auch nach der Synthese des Proteins, vorübergehend verändert werden, oft durch Veränderungen ihrer Struktur. Diese Alterationen nennt man Posttranslationale Protein Modifikationen. SUMOylierung und Ubiquitinierung, zwei von vielen verschiedenen Posttranslationalen Protein Modifikationen werden in dieser Dissertation näher behandelt. Der Mechanismus dieser zwei Prozesse ähnelt sich und besteht aus der Bindung der kleinen Proteine Ubiquitin oder SUMO (Small-Ubiquitin like Modifier) an ein oder mehrere Lysine (Aminosäuren) die sich in der Sequenz des Zielproteins befinden. Durch diese strukturellen Veränderung kann die Funktion des Zielproteins beeinflusst werden. Das Resultat ist jedoch stark abhängig von dem Zielprotein und dem Modifikationsprotein. Zum Beispiel ist Ubiquitinierung häufig beschrieben im Zusammenhang mit dem geregelten Abbruch von Proteinen. Allerdings kann Ubiquitinierung und SUMOylierung auch andere Konsequenzen haben, wie zum Beispiel die Veränderung von Proteinbindungsstellen zur Förderung oder zur Hemmung von Interaktionen mit anderen Proteinen oder Biomolekülen. Um zu verstehen, warum Proteine von SUMO markiert werden, bedarf es der Identifizierung der Zielproteine. Um dies zu tun, habe ich validierte Techniken benutzt um erst SUMO markierte Proteine aus Zellen zu isolieren und danach mit Hilfe von Massenspektrometrie zu identifizieren. Jedes Kapitel beginnt mit der systemweiten Identifizierung von SUMO Zielproteinen unter bestimmten Konditionen um anschließend herauszufinden, welche Proteinfunktionen dadurch verändert werden.

In **Kapitel 1** meiner Dissertation biete ich dem Leser eine ausführliche Einleitung zu dem Prozess der SUMOylierung, den beteiligten Enzymen und die, für diese Dissertation relevanten, biologischen zellularen Prozesse. Dieses Kapitel bietet eine Wissensgrundlage für die Forschungsergebnisse, die in den Kapiteln 3, 4 und 5 beschrieben sind.

Eine detaillierte Rezension über bestehende Literatur, die den Schnittpunkt zwischen SUMOylierung, Ubiquitinierung und Proteostasis thematisiert, befindet sich in **Kapitel 2** und bietet zusätzliche Hintergrundinformationen für die Forschungsergebnisse in Kapitel 3.

In **Kapitel 3** stellen wir die Frage, warum die SUMOylierung von hunderten Proteinen zunimmt, wenn Zellen hohen Temperaturen ausgesetzt sind. Erhöhte Temperaturen können zu einer Entfaltung, auch Denaturierung genannt, der Proteine führen mit der Konsequenz eines Funktionsverlustes. Um dies zu verhindern und um ihre Überlebenschancen zu vergrößern, reagiert die Zelle mit dem Prozess der Hitzeschutzantwort. Dieser Prozess führt unter anderem zu der Expression von Hitzeschockproteinen, die dazu beitragen die Denaturierung zu verhindern und den geregelte Abbruch geschädigter Proteine zu fördern. Unsere Ergebnisse zeigen, dass viele Proteine anhaltend SUMOyliert bleiben, wenn der Prozess der Hitzeschutzantwort außer Kraft gesetzt wird. Wir zeigen, dass Proteine die gleichzeitig mit SUMO und Ubiquitin markiert sind, effizienter abgebaut werden und implizieren mit weiteren Resultaten, dass SUMOylierung die Löslichkeit und Zugänglichkeit von Proteinen erhöht. Damit unterstützt die globale SUMOylierung nach einem Hitzeschock den Abbruch und die Regulierung denaturierter Proteine, bis Hitzeschockproteine diese Aufgabe übernehmen können.

Kapitel 4 beschreibt die Identifizierung von SUMOylierten Proteinen, die von der SUMO protease SENP6 reguliert sind. Das SUMO Protein kann sich selbst modifizieren und bildet sogenannte SUMO-Ketten mit denen Zielproteine markiert werden können. Die Funktion dieser SUMO-Ketten ist im Vergleich zu Ubiquitin-Ketten wenig erforscht. Bisher werden SUMO-Ketten hauptsächlich als indirektes Signal zum Proteinabbruch betrachtet. Ein wichtiges Protein in diesem Prozess ist die Ubiquitin-Ligase RNF4. RNF4 hat drei nebeneinanderliegende Bindungsstellen für SUMO und konjungiert deshalb Ubiquitin gezielt an mit SUMO-Ketten markierten Proteinen. SUMO-Proteasen können SUMO von markierten Proteinen abspalten und zwei dieser SUMO-Proteasen, SENP6 und SENP7, spalten gezielt SUMO-Ketten von Proteinen und können dadurch deren Abbruch verhindern. Die SUMOylierung von SENP6- und SENP7-regulierten Proteinen ist kurzlebig und schwer zu identifizieren. Um diese kurzlebigen SUMOylierten Proteine erforschen zu können, haben wir die Expression von SENP6 in der Zelle stark reduziert. Mit Hilfe von Massenspektrometrie konnten wir ungefähr 180 Proteine identifizieren die von SUMO-Ketten und von SENP6 reguliert werden. Darunter befanden sich mehrere Mitglieder des Constitutive-Centromer-Associated Netzwerkes (CCAN), einem Protein Komplex der eine wichtige Rolle für die Integrität von Centromeren spielt. Unsere Resultate implizieren, dass die Akkumulation von SUMO-Ketten an den CCAN Proteinen ihre korrekte Lokalisation verhindert, allerdings nicht zu einem Abbruch der Proteine führt. Wir spekulieren, dass die SUMO-Ketten nicht durch RNF4 erkannt werden sondern sterisch die Formation des CCAN Komplexes verhindert. SENP6 wird benötigt, um die Bildung des Komplexes zu ermöglichen, die Integrität der Centromere zu sichern und einen fehlerfreien Zellzyklus zu fördern.

SUMOylierung ist wichtig in vielen zellularen Prozessen und spielt unter anderem eine wichtige Rolle in DNA-Reparaturmechanismen. DNA, die sich in jeder unserer Zellen befindet, ist ständig in Gefahr beschädigt zu werden z.B. durch Ultaviolettstrahlung (UV-Strahlung). UV-Strahlung verursacht DNA-Schäden die durch den Nukleotidexzisionsreparatur Mechanismus rückgängig gemacht werden kann. In **Kapitel 5** beschreiben wir die SUMOylierung von Cockayne-Syndrome B (CSB), die durch UV-Strahlung induziert wird. CSB ist ein wichtiges Protein für die Nukleotidexzisionsreparatur. Wir zeigen, dass die SUMOylierung von CSB keine essenzielle Rolle spielt, allerdings die Effizienz der Nukleotidexzisionsreparatur beeinflussen kann. Des Weiteren zeigen wir, dass Cockayne Sydrome A (CSA), ein zweites Protein, welches an der Reparatur von UV-induzierten DNA-Schäden beteiligt ist, die Stabilität von SUMOylierten CSB indirekt beeinflusst. Wir spekulieren, dass CSA die Degradierung von RNA-polymerase 2, einem dritten essenziellen Protein für die Nukleotidexzisionsreparatur, direkt oder indirekt fördert und dadurch auch die Stabilität des SUMOylierten CSBs beeinflusst.

Das **Kapitel 6** setzt sich kritisch mit den experimentellen Resultaten auseinander und bietet eine Einordung der Resultate in die bestehende Literatur. Auch bietet dieses Kapitel, auf den in dieser Dissertation besprochenen Observationen aufgebaute, hypothetische Modelle, die in der Zukunft durch das Forschungsfeld experimentell untersucht werden können.

CURRICULUM VITAE

Frauke Liebelt was born on the 23rd of September 1987 in Bad Kreuznach, Germany, where she also completed her secondary school education. She undertook her undergraduate studies in 2008 at the University of Leiden, The Netherlands, and was awarded a BSc in Biology in 2011. She subsequently attained a post-graduate Molecular and Cellular Biosciences MSc qualification at the Leiden University in 2013. As part of this qualification, Frauke gained research experience in the laboratory of Dr. Anne-Marie Cleton-Jansen, Department of Pathology, at the Leiden University Medical Center, studying Loss of heterozygosity, amplification and mutations in candidate tumor suppressor genes in osteosarcoma. She performed a second research internship with Prof. Dr. Kirsten Lauber at the Department of Radiation Oncology, Ludwig-Maximilian University, Munich, Germany, where she studied the role of SECURIN and P53 in the radio-sensitizing effect of the novel HSP90 inhibitor NW457. Subsequently, Frauke carried out her doctoral research in the laboratory of Prof. Dr. Alfred Vertegaal at Leiden University Medical Center. Here, she studied the role of the small ubiquitin-like modifier (SUMO) in various cellular processes. In 2019, Frauke joined the group of Prof. Dr. Andrew Jackson at the Institute for Genetics and Molecular Medicine, University of Edinburgh, United Kingdom.

LIST OF PUBLICATIONS

F. Liebelt, J. Schimmel, M. Verlaan- de Vries, E. Kleemann, M. E. van Royen, Y. van der Weegen, M. S. Luijsterburg, L. H. Mullenders, A. Pines, W. Vermeulen, A. C. O. Vertegaal **(2019)** Transcription-Coupled Nucleotide Excision Repair is Coordinated by Ubiquitin and SUMO in Response to Ultraviolet Irradiation. *Accepted for publication at Nucleic Acid Research*

F. Liebelt, N. S. Jansen, S. Kumar, E. Gracheva, M. Verlaan- de Vries, E. Willemstein, A. C. O. Vertegaal **(2019)** The Poly-SUMO2/3 protease SENP6 enables the assembly of the constitutive centromere-associated network by group de SUMOylation. *Nat Commun. 10 (1): 3987.*

F. Liebelt*, R. M. Sebastian*, C. L. Moore, M. P. C. Mulder, H. Ovaa, A. C. O. Vertegaal, M. D. Shoulders **(2019)** SUMOylation and the HSF1-Regulated Chaperon Network Converge to Promote Proteostasis in Response to Heat Shock. *Cell Rep. 26(1): 236-249.*

M. C. P. Mulder, R. Merkx, K. F. Witting, D. S. Hameed, D. El Atmioui, L. Lelieveld, **F. Liebelt**,. J. Neefjes, I. Berlin, A. C. O. Vertegaal, H. Ovaa **(2018)** – Total chemical synthesis of SUMO and SUMO-based Probes for profiling the activity of SUMO-specific Proteases. *Angew Chem Int Ed Engl. 57(29):8958-8962.*

D. G. P. Van Ijzendoorn*, Z. Forghany*, **F. Liebelt**, A. C. O. Vertegaal, A. G. Jochemsen, J. V. M. G. Bovee, K. Szuhai, D. A. Baker **(2017)** Functional analyses of human vascular tumor FOS variant identify a novel degradation mechanism and link to tumorigenesis. *J Biol Chem. 292(52): 21282-21290.*

F. Liebelt and A. C. O. Vertegaal **(2016)** Ubiquitin-dependent and independent roles of SUMO in proteostasis. *Am J Physiol Cell Physiol. 311(2):C283-96.*

*both authors contributed equally to this work

ACKNOWLEDGEMENTS

Finally, it's done! Six years after I started this adventure, I am at the finish line. I have learned a lot during these years, most about myself. I am thankful for everybody who stood beside me through the Ups and Downs of my PhD student life. Of course, this thesis would have never had happened without the help of a lot of people.

First of all, I want to thank Alfred for his guidance as my direct supervisor and promotor. Thank you for giving me the opportunity to do my doctoral research in your lab and to learn about SUMO. During the years, I appreciated that your door was (literally) always open for me. I thank you for giving me the space I needed to develop my independency and to give me the freedom to follow up on my own ideas.

I also want to thank Peter. During our (half)-yearly progress meetings, you always listened with interest and inspired with ideas. Your kind words after my department-wide presentations were always much appreciated.

Likewise, I want to thank my guidance committee, AG and David, for attending my progress meetings, always having valuable points of critique and offering support whenever needed.

I would also like to thank the rest of the department of Chemical Cell Biology for all your support, gezelligheid and inspriration. Joop, Willem, Lennard, Annelies, Karien, Julia, Vera, Amiet, Tobias, Timo, Stuart, Aat, Leonie, Georg, Danielle and David thank you for being awesome colleagues.

Renier and Zhary, you were not only colleagues but dear friends, hopefully for years to come, thank you so much for everything.

A big 'thank you!' goes out to all the fellow past and present SUMO wrestlers, Joost, Ivo, Karo, Aleks, Minnie, Eka, Oezge, Jessie, Tamara, Sumit, Fredrik, Daniel, Edwin, Matty, Román and Sabine, who I had the pleasure working with side by side. You were always there for support, discussion and a drink after work. Also, I want to thank Nicolette and Esra for giving me the chance to gain experience in supervising and for contributing valuable data to my projects. I think you have a bright future ahead of you.

Minnie (Zhenyu), you just started a few months before me and it was a pleasure getting to know you and Emilie, I dearly hope that we meet again at some point in life. Matty, jij hebt met mij gestreden voor het CSB project, gelukkig met een mooi resultaat. Jij bent er altijd voor me geweest, je hebt me ondersteunt en altijd aangemoedigd om door te gaan. Je positiviteit en kijk op de wereld is pure inspiratie. Roman, you have been with me from the beginning and even though I was annoyed by you for most of the time, you are so special to me. Not only as colleague, but also as friend and former neighbour. We danced at each other's weddings (more at yours, though!) and we shared many drinks over scientific discussions (mainly, me asking you for help).

Sabine, Sabine, mijn paranymph. Wow, wat hebben wij samen doorgemaakt. Met jou heb ik gelachen en gehuild. Soms had ik het moeilijk met jou naast me maar zonder jou had het nooit gekund. Nu ben ik blij dat wij gewoon vrienden kunnen zijn en hoop dat onze vriendschap nog lang gaat voortduren. Dank je voor al je steun, begrip en voor je vriendschap.

Liebe Babsi, danke, dass du immer ein offenes Ohr für mich und das richtige zu sagen hattest und dass du mein soziales Leben ausserhalb des Labors warst.

Auch vielen Dank an meinen fellow Biologen Deutschen Felix für viele Gespräche über die Wissenschaft und anderes. Wir schaffen das!

Corrie, Jan, Hanneke, Pieter, Marieke en Ruben harstikke bedankt voor alle lieve woorden en steun en dat ik altijd bij jullie even kon doorademen.

Mama, Papa, Andreas, Sandra, Felix, Kyra, Noah, Lea und Opa vielen Dank für eure Unterstützung, für euer offenes Ohr und für euer Verständnis. Vielen Dank für die tausend Skype Gespräche, fürs aufheitern und anfeuern. Vielen Dank, dass ich immer wenn ich Zuhause bin meine Seele bei euch baumeln lassen kann, dass ihr mich verpfelgt und aufpeppelt. Ohne euch hätte ich das wirklich nie geschafft! Dies ist auch euer Verdienst.

Mijn lieve man, Maarten, jij bent mijn rots (eigenlijk meer mijn gebergte). Zonder het te weten begonnen we op de dezelfde dag met onze PhD in dezelfde afdeling. Pas een jaar later kwamen we elkaar voor het eerst tegen en wat was dit voor een geluk. Jij hebt me altijd gesteund en je vaak op de tweede plaats gezet terwijl je het zelf ook moeilijk hebt gehad. Hiervoor ben ik ontzettend dankbaar. Samen hebben we de laatste jaren gevochten en hebben het nu bijna gehaald. Heel erg bedankt dat je er bent.